

# IL NUOVO CIMENTO

ORGANO DELLA SOCIETÀ ITALIANA DI FISICA  
SOTTO GLI AUSPICI DEL CONSIGLIO NAZIONALE DELLE RICERCHE

VOL. IX, N. 5

Serie decima

1° Settembre 1958

## Interactions and Decays of $K^-$ -mesons.

### III. Analysis of the Stars in Flight.

Y. EISENBERG (\*), W. KOCH, E. LOHRMANN (+), M. NIKOLIĆ (×),  
M. SCHNEEBERGER and H. WINZELER

*Physikalisches Institut der Universität Bern*

(ricevuto il 31 Marzo 1958)

**Summary.** — 415 interactions of  $K^-$ -mesons in flight with complex nuclei of the nuclear emulsion have been analyzed. Comparing the derived results with those obtained by ALVAREZ *et al.* from  $K^-$ -free proton absorptions at rest, we must conclude that there is a significantly higher fraction of  $\Lambda$ -hyperons produced directly through the reaction  $K^- + N \rightarrow \Lambda + \pi$ , for our stars in flight (average kinetic energy of the interacting  $K$ -mesons 86 MeV), than it must be expected if one transfers the ALVAREZ results to compound nuclei assuming isotopic spin conservation. If the fraction of directly produced  $\Lambda$ 's increases with increasing  $K^-$ -energy, one could expect also a real increase in the direct  $\Lambda$ -production in the  $K^-$ -absorptions « at rest » in the nuclear emulsion, because of the Fermi-motion of the nucleons. Other topics which are discussed in the present work are the energy spectrum and absorption probabilities of the pions and  $\Sigma$ -hyperons and also the relative number of hyperfragments observed per  $\Lambda$ -hyperon produced.

### 1. — Introduction.

It is the aim of a detailed investigation as presented in this paper, to study the behaviour of negative  $K$ -particles undergoing strong interactions in nuclear emulsions. Naturally the nuclear composition of the emulsion is not simple

(\*) On leave of absence from the Weizmann Institute, Rehovoth.

(+) Also from the Institut für Kernphysik, Frankfurt-Main.

(×) On leave of absence from the Institute of Nuclear Sciences, Boris Kidrich, Belgrade.

as compared with liquid hydrogen, used in bubble chamber experiments (1). But actually, as we shall see later, the complexity of the nuclear emulsion is not so disadvantageous as it seems at first sight. Since only the nucleus-compound contains neutrons, experiments with nuclei offer quite a lot of possibilities for checks, and in fact the comparison of the hydrogen bubble chamber data with results obtained from interactions on nuclei enables us, at least in principle, to draw important conclusions about the behaviour of the entire  $K^-$ -nucleon system.

The two main transition groups of the  $K^-$ -nucleon (\*) interaction system are,

$$\begin{array}{lcl} (a) & K^- + N \rightarrow \Sigma + \pi & \text{consisting} \\ & & \text{of the} \\ (b) & K^- + N \rightarrow \Lambda + \pi & \text{processes} \end{array} \left\{ \begin{array}{ll} K^- + p \rightarrow \Sigma^+ + \pi^- & (a) \\ \phantom{K^- + p} \phantom{\rightarrow} \phantom{\Sigma} + \pi^+ & (a) \\ \phantom{K^- + p} \phantom{\rightarrow} \phantom{\Sigma}^0 + \pi^0 & (a) \\ \phantom{K^- + p} \phantom{\rightarrow} \phantom{\Sigma}^0 + \pi^0 & (b) \\ K^- + n \rightarrow \Lambda^0 + \pi^- & (b) \\ \phantom{K^- + n} \phantom{\rightarrow} \phantom{\Lambda}^0 + \pi^- & (a) \\ \phantom{K^- + n} \phantom{\rightarrow} \phantom{\Lambda}^- + \pi^0 & (a) \end{array} \right.$$

The cross-sections for (a) and (b) can in general be energy-dependent. In other words, a change in the relative momentum between the  $K^-$  and the nucleon will possibly alter  $\sigma_\Sigma$  and  $\sigma_\Lambda$ . If the  $\Sigma$  for instance, is preferentially produced in an S-state, the  $\Lambda$  in a P-state, one could expect more directly produced  $\Lambda$ 's with increasing energy of the K. Such a possibility must be taken into account in the analysis. The reaction rates of processes (a) and (b) are known for zero relative momentum from the Alvarez experiments on free protons. If one assumes charge independence in strong interactions of strange particles (2), one can predict the interaction ratios also for neutrons for zero relative K-nucleon momentum. But in the nucleus protons and neutrons have a Fermi momentum, and if  $\sigma_\Sigma$  and  $\sigma_\Lambda$  are energy dependent, this might already change the ratios (a) and (b). So one has to be careful with the direct use of the hydrogen bubble chamber data of  $K^-$ -proton absorptions at rest for the calculation of production ratios for the compound nucleus even if the  $K^-$  is absorbed «at rest». This was already pointed out in ref. (3).

(1) L. W. ALVAREZ, H. BRADNER, P. FALK-VAIRANT, J. D. GOW, A. H. ROSENFELD, F. T. SOLMITZ and R. D. TRIPP: *Nuovo Cimento*, **5**, 1026 (1957); L. W. ALVAREZ, H. BRADNER, P. FALK-VAIRANT, J. D. GOW, A. H. ROSENFELD, F. T. SOLMITZ and R. D. TRIPP: *Proceedings of the Seventh Rochester Conference* (1957).

(\*) Two nucleon reactions will be neglected in this work. See footnote, page 761.

(2) J. J. SAKURAI: *Phys. Rev.*, **107**, 908 (1957).

(3) J. HORNOSTEL and G. T. ZORN: *Observation and Analysis of  $K^-$ -Interactions*, Brookhaven National Laboratory, preprint (1957).



In fact, the results which will be presented in this paper are in striking disagreement with the predictions deduced from Alvarez' experiment. In particular, the  $\pi^+/\pi^-$ -ratio in our experiment is about  $\sim 0.12$ , whereas the value deduced from the ALVAREZ data is  $\sim 0.67$ ! The large negative excess of pions produced in the interactions of fast  $K^-$ -mesons must be explained by assuming a substantial direct production of  $\Lambda$ -hyperons (process (b) above).

The specific question, which we shall treat in this paper (Interactions and Decays III), for the stars in flight, and in a forthcoming paper (Interactions and Decays IV) for the stars at rest, is, whether and how the cross-sections for the processes (a) and (b) change with energy.

An important practical point is, how to distinguish between the individual reactions mentioned above, since neutral particles cannot be seen in the emulsion. Assuming charge independence, one can answer this question statistically by determining the electric charges of the emerging  $\pi$ 's and  $\Sigma$ 's. Some experimental parameters, which can be used, for instance, are the ratios,

$$N^{\text{emitted}}(\pi^+)/N^{\text{emitted}}(\pi^-) \quad \text{from the stars in flight,}$$

$$N^{\text{emitted}}(\Sigma^+)/N^{\text{emitted}}(\Sigma^-) \quad \text{from the stars in flight,}$$

$$N'(\Sigma^+)/N'(\Sigma^-) \quad \text{from } K^- \text{-free proton absorptions in flight.}$$

The whole problem is more complex with nuclei than with pure hydrogen, since the  $\pi$ 's and  $\Sigma$ 's can suffer inelastic scatterings and reabsorptions inside the nucleus in which they are produced, or deflections at the nuclear boundary. To help clearing up these problems the experimental energy distribution of the emerging  $\pi$ 's in the laboratory-system is compared with a theoretical spectrum, which takes into account, roughly, inelastic scatterings and absorptions of the pions inside the nucleus.

The energy spectrum of  $\pi$ 's from «clean» events, where no stable charged particles are emitted, can be compared with the energy spectrum of all other  $\pi$ 's and the branching ratios of the different kinds of «clean» events can also be analysed. One might get from this analysis indications whether the clean events coming from interactions on light nuclei are preferentially due to «peripheral» interactions, or whether the elementary process takes place with equal probabilities in every region inside the nucleus.

The energy spectrum of the  $\Sigma$ 's can also be compared with a theoretical spectrum.

In the following sections we show in detail how we approached successively these problems, from the experimental and the theoretical points of view.

In Sect. 2 the experimental procedure and direct experimental results concerning «observation values» are reported.

Sect. 3 contains the detailed discussion of the experimental results, the possible systematic errors and a collection of the « emission values ».

In Sect. 4 we describe basic aspects of the analysis.

In Sect. 5 the analysis of the interactions in flight is performed and numerical results are given.

In Sect. 6 the final conclusions are summarized.

## 2. — Experimental procedure.

The experimental set-up, methods and general results were described in part I <sup>(4)</sup>. The foregoing part II <sup>(5)</sup> dealt with results obtained by an extensive investigation of the decays. It contained in particular the classification of the one-prong  $\pi$ -events into « real decays » and « decay-like stars ». The latter number is of interest for this part (see Sect. 5'4).

This work is restricted to the detailed analysis of 415 interactions of negative K-mesons in flight on complex nuclei. They were obtained from a total  $K^-$  path of 112 m. The kinetic energy of the K-mesons considered in this work ranged from about 5 to 150 MeV. Every black and grey track emerging from the interactions was followed, either to its end inside the stack (99.5%), or to the point where the particle left the stack. In addition we had a total of 90 thin (and sometimes grey or even black) tracks which were due to charged pions. Each pion track which according to ionization measurements could be expected to end inside the stack of  $(10 \times 15 \times 17)$  cm<sup>3</sup> was followed twice independently. In this way we were able to determine the electric charge and exact rest-range of 49 pions. The kinetic energy  $T$  of further 15 pions could be determined with good reliability by ionization measurements, since they had kinetic energies less than 100 MeV. These tracks were followed to the point where the pions either left the stack with smaller energy or made interactions in flight. The percentage of positive and negative pions in each energy interval among these 15 cases was assumed to be the same as in the rest of 49 events with  $T < 100$  MeV. The remaining 26 pions were fast (corresponding to more than 100 MeV energy, according to ionization measurements).

<sup>(4)</sup> E. LOHRMANN, M. NIKOLIĆ, M. SCHNEEBERGER, P. WALOSCHEK and H. WINZELER: *Nuovo Cimento*, **7**, 163 (1958).

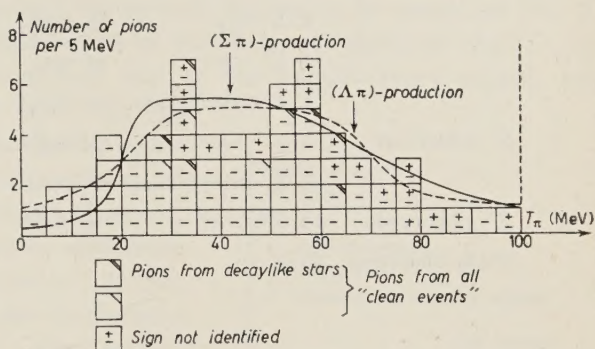
<sup>(5)</sup> Y. EISENBERG, W. KOCH, E. LOHRMANN, M. NIKOLIĆ, M. SCHNEEBERGER and H. WINZELER: *Nuovo Cimento*, **8**, 663 (1958).



The energy spectrum of the 64 pions with energies smaller than 100 MeV is shown in Fig. 1. The electric charge of the pions is also given in this figure. The mean energy of these particles is essentially low. The angular distribution of the pion emission was also measured and shows no marked anisotropies.

The ratio  $\pi^+/\pi^-$  from all stopped cases is 4/45. The corrected ratio from all pions with  $T < 100$  MeV becomes,

$$6/58.$$



This result will be discussed in the next sections.

Fig. 1. — Observed and theoretical pion energy spectrum.

We wish now to present the separation of the « double star »-events, namely events where one of the secondary particles makes another interaction in the emulsion block and the connecting track is so short, that it cannot be iden-

TABLE I. —  $K^-$ -reemissions.

Primary energy $T_1$ (MeV)	Secondary energy $T_2$ (MeV)	$\Delta T/T_1$	Scattering angle	Number of prongs besides the reemitted $K^-$
129	22	0.83	$59^\circ$	4 short, black
112	23	0.79	$57^\circ$	1 proton of 73 MeV
86	45	0.47	$106^\circ$	4 short, black
45	29	0.40	$149^\circ$	0
73	46	0.37	$13^\circ$	3 short, black
87	48	0.45	$25^\circ$	3 short. black
85	26	0.58	$158^\circ$	0
118	109	0.08	$55^\circ$	2 short, black
54	7	0.87	$33^\circ$	2 short, black

TABLE II. - Observed hyperons.

$\Sigma^+$ observed:	4 $\Sigma^+ \rightarrow p$	at rest
	2 $\Sigma^+ \rightarrow p$	in flight
	1 $\Sigma^+ \rightarrow \pi^+$	at rest
	1 $\Sigma^+$ -interaction	in flight (see Appendix)
$\Sigma^-$ observed:	3 $\Sigma^- \rightarrow \pi^-$	in flight ( $\pi^-$ stars)
	3 $\Sigma^-$ -interactions	at rest with more than 1 prong
$\Sigma^\pm$ observed:	12 $\Sigma^\pm \rightarrow \pi^\pm$	in flight
Total observed: 26 $\Sigma$		

tified. These events could be due to  $\pi$ -mesons, hyperfragments,  $\Sigma$ -hyperons,  $K^-$ -re-emissions and nucleonic secondary interactions.

Fig. 1 is rather complete in the sense that it contains very probably all charged pions which are emitted. From the shape of the pion energy spectrum

TABLE III. - Summary of emulsion data for prong distribution of  $\Sigma^-$ -capture stars.  $\Sigma^-$ -hyperons were produced by  $K^-$ -free-proton absorption.

Number of events	Number of prongs					Remarks
	0	1	2	3	4	
	6	1	1	2		collected in <sup>(6)</sup>
	1		1			<sup>(7)</sup>
	2	1	1			<sup>(4)</sup>

it can be seen that the number of low energy pions is small and thus they should practically not contribute to the number of « double stars ».

Table I gives the details of the 9  $K^-$ -re-emissions (their number altered quite a lot compared with the value given in Table III of part I).

<sup>(6)</sup> F. C. GILBERT and R. S. WHITE: *K<sup>-</sup>-Meson Captures by Bound Neutrons*, University of California, UCRL-4966 (1957); F. C. GILBERT, C. E. VIOLET and R. S. WHITE: *Phys. Rev.*, **107**, 228 (1957).

<sup>(7)</sup> R. G. GLASSER, N. SEEMAN and G. A. SNOW: *Nuovo Cimento*, **7**, 142 (1958).



Considering the energy distribution of the re-emitted  $K$ 's, one can see that there is no reason to assume a higher number of very short re-emitted  $K$ 's, which might have escaped a direct identification.

The next step was to separate the excited fragments by means of Fig. 2, which shows the frequency distribution of the distances down to about  $1\text{ }\mu\text{m}$  between the primary and secondary star of the «double-star» events, the secondary star of which had more than one prong. (There is a clear accumulation below  $40\text{ }\mu\text{m}$ ). Regarding the energy spectra of pions,  $K$ -mesons and  $\Sigma$ -hyperons observed, these particles are not expected to contribute appreciably to the events below  $40\text{ }\mu\text{m}$ . Therefore we consider all these short-range events as excited fragments. Two hyper-fragment tracks observed are longer than  $40\text{ }\mu\text{m}$ , so that the total number of hyper-fragments is 17.

We observed 26 certain  $\Sigma$ 's. In Table II the details of these hyperons are listed. Correcting for the fact that we only took into account those  $\Sigma^-$ -absorptions at rest, which had two or more prongs (longer than  $2\div 3$  grains), we got a total of 33 «observed» (\*)  $\Sigma$ -hyperons. This correction was taken from the average prong distribution of 16 certain  $\Sigma^-$ -absorptions at rest. In all these 16 cases the  $\Sigma^-$  was produced in  $K^-$ -free proton absorptions. Table III lists the 16 events, which we used for the correction. The ratio of (2 or more)-prong stars to (one or zero)-prong stars is  $5/11$ .

Among the 33 hyperons were 12  $\Sigma$ - $\pi$ -decays in flight, the sign of which could not be determined. Thus we had to derive how many of the 12  $\Sigma$ - $\pi$ -decays in flight were positively and how many negatively charged in order to get the total number of  $\Sigma^+$  and  $\Sigma^-$  observed. We did this by assuming the ratio  $\Sigma_p^+/\Sigma_{\pi}^+$  to be about 1<sup>(8)</sup>, by using the information listed in Table II and the known lifetimes of the  $\Sigma^-$  and the  $\Sigma^+$ . Thus the observed number of hyperons becomes,

$$N^{\text{observed}}(\Sigma^+) = 12,$$

$$N^{\text{observed}}(\Sigma^-) = 21.$$

The energy distribution of the  $\Sigma$ -hyperons is shown in Fig. 3.

(\*) As will be seen in the next section, in accordance with our terminology, the number of «emitted» hyperons is a bit larger than the observed number.

(8) W. F. FRY, J. SCHNEPS, G. A. SNOW, M. S. SWAMI and D. C. WOLD: *Phys. Rev.*, **107**, 257 (1957).

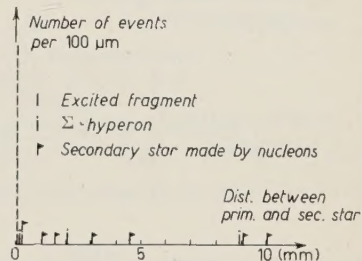


Fig. 2. — Distance-distribution of «double» star events.

TABLE IV.

*Observation values from 415 interactions in flight of  $K^-$ -mesons on complex nuclei.*

	$T_K < 90 \text{ MeV}$ $\bar{T}_K = 59 \text{ MeV}$	$T_K > 90 \text{ MeV}$ $\bar{T}_K = 113 \text{ MeV}$	$T_K = 0 \div 150 \text{ MeV}$ $\bar{T}_K = 86 \text{ MeV}$
No. of stars with « stable » prongs only	116	129	245
Number of star with pions $\left\{ \begin{array}{l} \pi^+ (*) \\ \pi^- (*) \\ \pi^\pm \end{array} \right.$	3 ( $T_\pi < 100$ )	3 ( $T_\pi < 100$ )	6 ( $T_\pi < 100 \text{ MeV}$ )
	38 ( $T_\pi < 100$ )	20 ( $T_\pi < 100$ )	58 ( $T_\pi < 100 \text{ MeV}$ )
	13 ( $T_\pi > 100$ )	13 ( $T_\pi > 100$ )	26 ( $T_\pi > 100 \text{ MeV}$ )
Total	54	36	90
No. of stars with $\Sigma$	16	17	33
No of stars with Ex. Frag.	7	10	17
No. of $K^-$ -re-emissions (+)	7	3	10
$K^-$ -« stops » (x)	20	11	31
Total No. of stars in flight (°)	214	201	415
Track length scanned	53 m	59 m	112 m
% charged $\pi$ 's per star	25.2	17.9	21.7
% charged $\Sigma$ 's per star	7.5	8.5	7.9
% Ex. Frag.'s	3.3	5.0	4.0
% re-emitted $K$ 's	3.3	1.5	2.4
Mean free path for inter-action.	24.8 cm	29.4 cm	27.0 cm

(\*) The pions with  $T_\pi < 100 \text{ MeV}$ , which left the stack or made interactions in flight, are already distributed at both charges by means of Fig. 1 (see text).

(+) An additive correction of 1  $K^-$ -re-emission is included here, owing to 16%  $K^-$ 's from  $K^-$ -captures at rest.

(x) 5 events are subtracted here. They are supposed to belong to interactions on free protons with no charged secondaries.

(°) Without the  $K^-$ -free-proton interactions.



We finish now the separation of emitted particles by considering the 7 not identified double stars statistically. As could be deduced from the experimental rest-range distribution of the protons of the stars in flight, we should expect more than 10 nucleon-produced secondary stars, with at least 2 prongs. So we believe that these 7 secondary stars were produced by protons.

During the analysis of the stars in flight 3 rare or curious events were found. Since their investigation is not in the general frame of this work we discuss them in the appendix.

The stable-prong distribution (pion track not counted as prong) of the 79 pion emitting stars (not including stars having also a charged  $\Sigma$  or a hyperfragment) is shown in Fig. 4. The number of 16 decay-like stars (with no « stable » prongs) was deduced from careful investigations

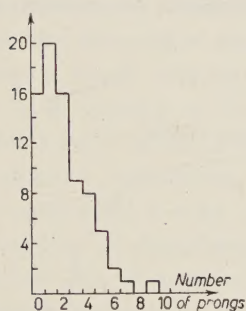


Fig. 4. - « Stable » prong distribution of 79 pion emitting stars where no hyperon was observed.

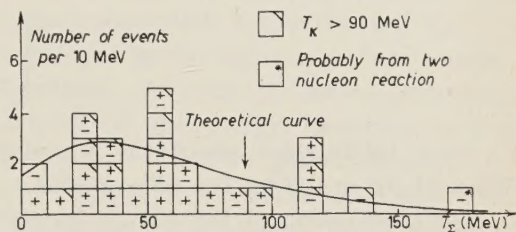


Fig. 3. - Energy distribution of the  $\Sigma$ -hyperon.

of the decays and the decay-like stars (as already mentioned, see parts I and II). The number 16 fits the overall shape, a result, which can be taken as an independent test for the procedure applied there. As will be shown in the next sections, Fig. 4 helps us to investigate the  $K^-$ -disappearances with no visible prongs, the so called « stops » in flight.

Table IV on page 752 shows general « observation values » for the two energy intervals  $(0 \div 90)$  MeV and  $(90 \div 150)$  MeV, and for the average of the whole interval  $(0 \div 150)$  MeV.

### 3. - Detailed discussion of the experimental results.

In order to deduce the number of pions and  $\Sigma$ -hyperons emitted from the  $K^-$ -stars from the number of such particles which were actually observed, several corrections are necessary. They will be treated in this section. In particular it will be shown, that the large fraction of  $\pi^-$  as compared with the  $\pi^+$  is not changed, when passing from the observed values to the values of emission.

3'1.1. Pion energy spectrum. — The elementary reactions, which produce charged pions are the following

$$\begin{aligned} K^- + p &\rightarrow \begin{cases} \pi^+ + \Sigma^- \\ \pi^- + \Sigma^+ \end{cases} \\ K^- + n &\rightarrow \begin{cases} \pi^- + \Sigma^0 \\ \pi^- + \Lambda^0. \end{cases} \end{aligned}$$

Some information about the abundance of the above reactions can be obtained by analysing the pion events.

The observation of the energy distribution of the pions presents at least in principle a possibility to determine the ratio of  $\Sigma$ - to  $\Lambda$ -hyperon production in the elementary  $K^-$ -absorption. For comparison with experiments the spectrum of  $\pi$ -mesons at production inside the nucleus has been calculated by various authors (<sup>6</sup>) for  $K^-$ -captures at rest, using the statistical model. We have extended these calculations to  $K^-$ -interactions in flight, using the same method as described in refs. (<sup>6,9</sup>). Fig. 5 shows, for example, the energy distri-

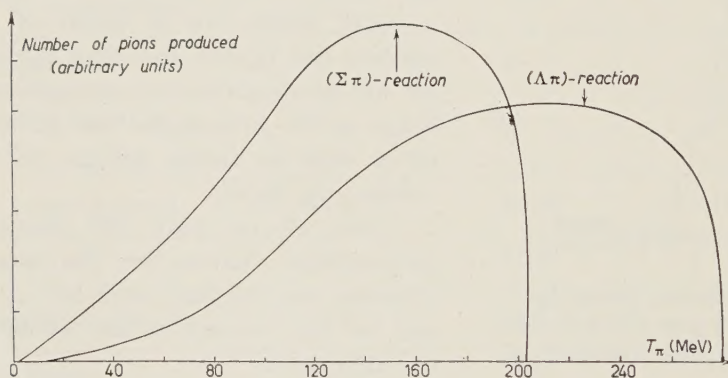


Fig. 5. — Calculated energy distribution of pions inside the nucleus at production by 110 MeV  $K^-$ -mesons.

bution of  $\pi$ -mesons at production inside the nucleus by 110 MeV  $K^-$ -mesons. The distribution of  $\pi$ -mesons produced together with a  $\Sigma$ -hyperon and those produced together with a  $\Lambda$ -hyperon are plotted separately. A determination of the ratio between the reactions  $(\Sigma\pi)$  and  $(\Lambda\pi)$  would now be possible by noting, that at a  $K^-$ -energy of 110 MeV about 45% of the  $\pi$ -mesons from

(<sup>9</sup>) R. H. CAPPS: *Phys. Rev.*, **107**, 239 (1957).



the  $(\Lambda\pi)$ -reaction have energies exceeding the maximum allowed value for the  $(\Sigma\pi)$ -reaction.

These considerations, however, apply only to  $\pi$ -mesons at production inside the nucleus. For comparison with experiments one needs the energy distribution outside the nucleus. To calculate it from the internal energy spectrum, a number of corrections must be applied, for example for the effect of the Coulomb field, the energy dependance of the pion absorption coefficient and for the influence of inelastic scattering. The inelastic scattering is expected to introduce the greatest distortions of the spectrum, and only this point is discussed here. The influence of inelastic scattering on the energy spectrum cannot be accurately calculated at present. We have tried to get an estimate by using the data compiled by BLAU and CAULTON<sup>(10)</sup> on the inelastic scattering of  $\pi$ -mesons in nuclear emulsions in the energy interval from 70 to 500 MeV. In this work the probability of inelastic scattering is compared with the absorption probability. Now, for our stars, the probability of a  $\pi$ -meson to be absorbed inside the nucleus is known (see Sect. 4). If one assumes, that the ratio of absorptions to inelastic scattering in our stars is the same as that given by Blau and Caulton, then the *number* of inelastic scatterings can be calculated from the known number of absorptions. The exact energy dependence of the absorption and of inelastic scattering are not known. So one can get only a rough estimate.

At a  $K^-$ -energy of 50 MeV for instance, about 60% of the  $\Sigma\pi$ -mesons and about 80% of the  $\Lambda\pi$ -mesons which are not absorbed should have undergone inelastic scatterings. Thus the influence of inelastic scattering on the energy spectrum is very great. (Compare for instance Figs. 1 and 7).

According to measurements made by GOLDBABER<sup>(11)</sup>, MORRISH<sup>(12)</sup>, FRY<sup>(13)</sup> and BLAU and CAULTON<sup>(10)</sup> in nuclear emulsions, the *energy distribution* of inelastically scattered  $\pi$ -mesons depends only slightly on the primary  $\pi$ -energy; a large fraction of mesons have energies  $< 100$  MeV after inelastic scattering. Using these energy distributions and the number of inelastically scattered  $\pi$ -mesons at various energies, we calculated the energy distribution of  $\pi$ -mesons from  $K^-$ -stars outside the nucleus, for  $\pi$ -energies  $< 100$  MeV. As is to be expected, there is no great difference between the energies of the  $\pi$ -mesons from the reactions  $(\Sigma\pi)$  and  $(\Lambda\pi)$ . The energy spectrum found below 100 MeV is in good agreement with the calculated curve, Fig. 1. Experimental and theoretical data of Fig. 1 represent an average over all stars in flight. The shape of the spectrum is very different from the uncorrected one of Fig. 5.

---

<sup>(10)</sup> M. BLAU and M. CAULTON: *Phys. Rev.*, **96**, 150 (1954).

<sup>(11)</sup> G. GOLDBABER and S. GOLDBABER: *Phys. Rev.*, **91**, 467 (1953).

<sup>(12)</sup> A. H. MORRISH: *Phil. Mag.*, **45**, 47 (1954).

<sup>(13)</sup> W. F. FRY: *Phys. Rev.*, **93**, 845 (1954).

The number of  $\pi$ -mesons with an energy  $> 100$  MeV is relatively small. These facts show that the observed energy distribution of  $\pi$ -mesons from the stars in flight is greatly influenced by inelastic scattering and that no accurate conclusions about the ratio of  $\Lambda$ - to  $\Sigma$ -production can be drawn from it.

**3.1.2. Pion sign-fraction.** — If charge independence holds in the  $K^-$ -nucleon interaction, the «sign-fraction», *i.e.* the number  $N(+)$  to the number  $N(-)$  gives some information on the relative frequencies of the elementary reactions (1)-(7), (see Sect. 4). For the derivation of the emission sign-fractions from the *observed* sign-fractions and of the *production* sign-fractions  $N(+)/N(-)$  from the *emission* sign-fractions  $N(+)/N(-)$  one must assume something about the absorption probabilities of  $\pi^+$  and  $\pi^-$  inside the nucleus. We have assumed that they are approximately equal. This is suggested by charge independence if the nucleus is self-conjugate and is supported a posteriori, as we shall see later, by the good overall consistency of the derived results.

64 of our 90 observed charged pions had energies  $< 100$  MeV. The charge of most of them could be determined. However the charge of the 26 pions with an energy  $> 100$  MeV could not be determined. In the following we give some estimate for the sign-fraction of these 26 mesons. A difficulty arises here from the fact that the inelastic scattering of  $\pi^+$  and  $\pi^-$  in the energy interval between 100 and 250 MeV is possibly not exactly equal, as is suggested by measurements on  $\pi$ -mesons of about 110 MeV made by FERRARI *et al.* <sup>(14)</sup>. For lack of more experimental evidence, we cannot calculate exactly the number of  $\pi^+$  among the 26 pions with more than 100 MeV, but we can give narrow absolute limits

The scanty experimental knowledge on inelastic scattering and absorption of  $\pi^+$ -mesons above 100 MeV allows only an estimate for the upper limit of the number of  $\pi^+$  above 100 MeV. By using the data on  $\pi^-$  inelastic scattering <sup>(6)</sup> and on  $\pi^+$  inelastic scattering below 100 MeV <sup>(14,15)</sup>, one can show by means of conservative extrapolation that at least 50% of the  $\pi^+$  escaping the nucleus should have undergone inelastic scattering. In the same way, and using also the calculated energy spectrum at production, one expects that at most 25% of the inelastically scattered  $\pi^-$  have energies exceeding 100 MeV, (averaged over all stars in flight).

Summing up the inelastically scattered and directly escaping  $\pi^-$ -mesons with more than 100 MeV, we get that their number is at most 50% of the

<sup>(14)</sup> G. FERRARI, L. FERRETTI, R. GESSAROLI, E. MANARESI, E. PEDRETTI, G. PUPPI, G. QUARENI, A. RANZI, A. STANGHELLINI and S. STANTIĆ: *Proceedings of the 1955 Pisa Conference*, in *Suppl. Nuovo Cimento*, **4**, 914 (1956).

<sup>(15)</sup> G. PUPPI: *Suppl. Nuovo Cimento*, **11**, 438 (1954).



total number of  $\pi^+$  emitted. Therefore the number of  $\pi^+$ -mesons with an energy  $> 100$  MeV is at most about the number of  $\pi^+$  below 100 MeV. We conclude that the total number of  $\pi^+$  emitted is smaller than 12, and assume as a reliable number:

$$N^{\text{emitted}}(\pi^+) = 10,$$

$$N^{\text{emitted}}(\pi^-) = 80.$$

Before deducing from this number the numbers of  $\pi^+$  and  $\pi^-$  produced, we have to mention two other effects. First, we have up to now neglected charge exchange scattering. It can however be shown, that for pure  $T^{\frac{1}{2}}$ -scattering in a self-conjugate nucleus the influence of charge exchange scattering increases the emitted sign fraction, that means, that correcting for charge exchange, the produced sign-fraction would become smaller <sup>(15)</sup>. Secondly the Coulomb effect would also tend to increase the  $+/-$  ratio observed. The charge exchange scattering is probably small since we have not seen any  $\Sigma^-\pi^-$  pairs emitted from a single star. Therefore we can safely conclude that the produced  $+/-$  ratio is very probably 10/80

3.2. *The  $\Sigma$ -hyperons.* - While, because of the surprisingly small number of emitted  $\pi^+$ , the behavior of the  $\pi$ -mesons in the emission processes was discussed in detail, we report for the hyperons only the main consequences of the calculations.

3.2.1.  *$\Sigma$ -hyperon energy spectrum.* - As for the  $\pi$ -mesons, the energy distribution of the  $\Sigma$ -hyperons produced by  $K^-$ -meson captures at rest have been calculated by various authors <sup>(6,9)</sup>. The method of calculation is explained in ref. <sup>(9)</sup>. By the same method we calculated the energy spectrum of  $\Sigma$ -hyperons produced in the reaction  $K^- + N \rightarrow \Sigma + \pi$  by  $K^-$ -mesons in flight (most important assumption: production isotropy in the CM-system). As an ex-

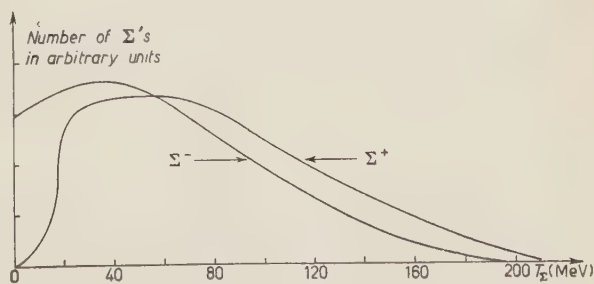


Fig. 6. - Calculated energy distribution of  $\Sigma^-$ 's and  $\Sigma^+$ 's outside the nucleus produced by 110 MeV  $K^-$ -mesons.

<sup>(15)</sup> M. KOSHIBA: *Nuovo Cimento*, **4**, 357 (1956).

ample the energy distribution of positively and negatively charged  $\Sigma$ 's outside the nucleus produced by 110 MeV  $K^-$ -mesons are shown in Fig. 6.

Such curves should be compared with the experimental data. To get statistically more significant results, we combined the data from all stars in flight. In the same way the theoretical spectra were properly averaged over the  $K^-$ -energies. Both positively and negatively charged hyperons were included together. It was furthermore assumed, that the absorption probability of  $\Sigma$ 's inside the nucleus does not depend on their energy. Fig. 3 shows the comparison of calculated and measured energy distributions of all hyperons emerging from the stars in flight. The mean kinetic  $K^-$ -energy is 86 MeV.

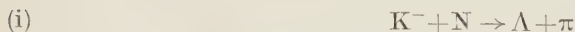
**3.2.2.  $\Sigma$ -hyperon sign-fraction.** — The calculated energy distributions can be used to determine the influence of the Coulomb field on the transmission probability of positive and negative hyperons through the nuclear boundary. Since these probabilities are different, the sign-fractions of production and emission must be different, even if the absorption probability of positive and negative hyperons inside the nucleus is about the same.

To correct for this effect, we used the transmission factors calculated by CAPPS (\*) together with the calculated energy distributions. Averaging over the energy distribution of the  $\Sigma^-$ 's one obtains a 12% reduction for the number of  $\Sigma^-$  which are emitted. With this we get:

$$N^{\text{emitted}}(\Sigma^+) = 12 ,$$

$$N^{\text{emitted}}(\Sigma^-) = 23 (*) .$$

**3.3. Energy distribution of  $\Lambda$ -hyperons.** — For the discussion of hyperfragments (see Sect. 5.5) we need the energy distribution of all  $\Lambda$ 's. The energy distribution of  $\Lambda$ -hyperons coming from the reaction



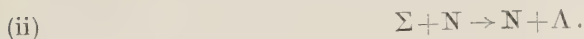
inside the nucleus was calculated in the same manner as the  $\Sigma$ -spectra. The resulting distribution for  $\Lambda$ 's inside the nucleus is shown in Figs. 7 and 8. It corresponds to a  $K^-$ -energy of 0 and 110 MeV respectively.

---

(\*) Although the 12%  $\Sigma^-$ -correction does not really contribute to the *emission*, we apply this correction here. The relations of the following section will then become simpler.



A further source of  $\Lambda$ -hyperons is the reaction



For  $K^-$ -captures at rest more  $\Lambda$ 's are expected to come from reaction (ii). (See later). For our stars in flight, we estimate that reaction (ii) contributes about 50% of all  $\Lambda$ 's produced inside the nucleus (see Sect. 5). We have therefore also calculated the energy distribution of  $\Lambda$ 's coming from reaction (ii). The cross-section of reaction (ii) was assumed to be energy independent. Curves calculated for various  $\Sigma$ -energies were added according to the calculated  $\Sigma$ -spectrum inside the nucleus. The resulting energy distribution of  $\Lambda$ 's from reaction (ii) obtained in this way, is given in Figs. 7 and 8 for stars induced by  $K^-$ -mesons of 0 and 110 MeV respectively.

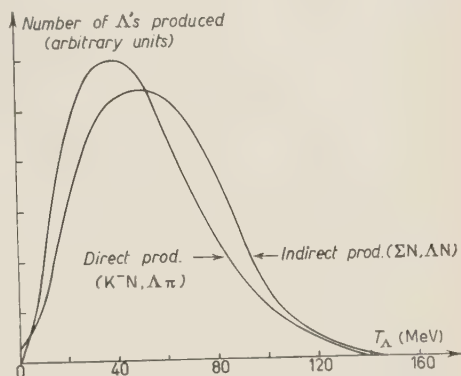


Fig. 7. —  $\Lambda$ -production spectra inside the nucleus at 0 MeV  $K^-$ -energy.

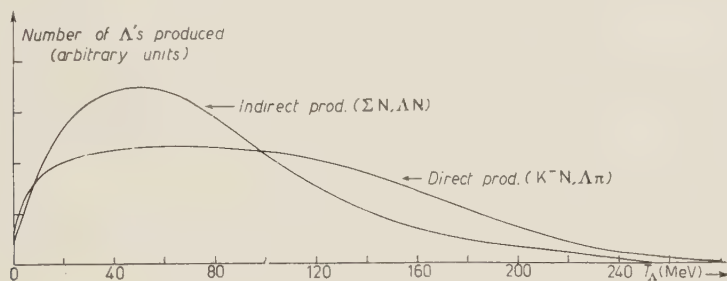


Fig. 8. —  $\Lambda$ -production spectra inside the nucleus at 110 MeV  $K^-$ -energy.

3.4.  $\Sigma$ -sign fraction from  $K^-$ -free-proton absorptions in flight. — An unbiased sign-fraction of  $\Sigma$ -hyperons produced on protons can be obtained from the absorptions of  $K^-$  at flight by free protons. Table V is a compilation of the few events in which the sign of the  $\Sigma$  was published up to now. It yields  $N'(\Sigma^+) = 6$  and  $N'(\Sigma^-) = 6$ . The mean kinetic  $K^-$ -energy considered in these events is substantially lower than in our case, but, because of our small statistics these events had to be included. Adding our proton-like events  $N_5$  and  $N_6$  (see Table VI below), we conclude that the total  $K^-$ -p absorption in flight yields 12  $\Sigma^+$  and 8  $\Sigma^-$ .

TABLE V. —  $K^-$ -absorptions in flight on free protons, where the sign of the hyperons was published.

Laboratory	Number of hyperons	
	$\Sigma^+$	$\Sigma$
(7)	$4 \left\{ \begin{array}{c} 15 \\ 25 \\ 57 \\ 75 \end{array} \text{ MeV} \right\}$	$2 \left\{ \begin{array}{c} 16 \\ 14 \end{array} \text{ MeV} \right\}$
(17)	—	$2 \{ ? \}$
(4)	$2 \left\{ \begin{array}{c} 110 \\ 20 \end{array} \text{ MeV} \right\}$	$2 \left\{ \begin{array}{c} 30 \\ 55 \end{array} \text{ MeV} \right\}$

The numbers in parentheses are the kinetic energies of the corresponding  $K^-$ -mesons.

TABLE VI.

	Emission values from all stars (+)	Emission values ${}^0N_i$ from the « clean » events
Stars emitting no $\Sigma$ and no $\pi$	$N_0(0\pi, 0\Sigma) = 288$	${}^0N_0 = 31$ (×) (stops)
Stars emitting no $\Sigma$ but a $\pi^+$	$N_1(\pi^+, 0\Sigma) = 8$	${}^0N_1 + {}^0N_2 = 16$  (decaylike stars)
Stars emitting no $\Sigma$ but a $\pi^-$	$N_2(\pi^-, 0\Sigma) = 74$	
Stars emitting a $\Sigma^+$ and no $\pi$	$N_3(0\pi, \Sigma^+) = 6$	${}^0N_3 + {}^0N_4 = 3$
Stars emitting a $\Sigma^-$ and no $\pi$	$N_4(0\pi, \Sigma^-) = 21$	
Stars emitting a $\Sigma^-$ and a $\pi^+$	$N_5(\pi^+, \Sigma^-) = 2$	${}^0N_5 + {}^0N_6 = 5$
Stars emitting a $\Sigma^+$ and a $\pi^-$	$N_6(\pi^-, \Sigma^+) = 6$	

(+) Apparent charge exchange events (see Sect. 3.1) were not observed, and  $K^-$ -re-emissions are not included.

(×) 5  $K^-$ -free proton events leading to  $(\Lambda, \Sigma^0 + \pi^0)$  and  $(K^0 + n)$  are already subtracted, see Sect. 4 and 5.

(17) W. H. BARKAS, W. F. DUDZIAK, P. C. GILES, H. H. HECKMAN, F. V. INMAN, C. J. MASON, N. A. NICKELS and F. M. SMITH: *Phys. Rev.*, **105**, 1417 (1957).



3.5. *Summary of  $\pi$ -meson and  $\Sigma$ -hyperon experimental results.* - We summarize briefly what we could deduce directly from the experimental data presented in this section and in the foregoing section. From the observed quantities we got the following values of emission:

$$N^{\text{em.}}(\pi^+) = 16,$$

$$N^{\text{em.}}(\pi^-) = 80,$$

$$N^{\text{em.}}(\Sigma^+) = 12,$$

$$N^{\text{em.}}(\Sigma^-) = 23 (*),$$

and the following combined emission data (Table VI).

#### 4. - Fundamental aspects of the analysis.

4.1. *Relations between the emitted and produced numbers of particles.* - The fundamental processes of production, as already mentioned in the introduction are (+)

$$(1) \quad K^- + p \rightarrow \Sigma^- + \pi^+,$$

$$(2) \quad \Sigma^+ + \pi^-,$$

$$(3) \quad \Sigma^0 + \pi^0,$$

$$(4) \quad \Lambda^0 + \pi^0,$$

$$(5) \quad K^- + n \rightarrow \Sigma^- + \pi^0,$$

$$(6) \quad \Sigma^0 + \pi^-,$$

$$(7) \quad \Lambda^0 + \pi^-.$$

The abundances of these 7 individual reactions are a priori not known. They can, however, be directly connected with the 6 emission values  $N_1-N_6$

(\*) 12% corresponding to the Coulomb correction are already included here.

(-)  $K^-$ -re-emissions, the two nucleon reactions, and  $K^-$ -charge exchanges, leading to  $K^0$ -re-emissions are neglected. The influence of the two nucleon reactions on the present results is small and will be discussed in our next publication.

which are listed in Sect. 3.5, Table VI, if one uses  $A(\pi)$  and  $A(\Sigma)$ , the probabilities, respectively of a pion and a  $\Sigma$ -hyperon to be re-absorbed in the nucleus in which it was produced:

$$N(\pi^+, 0\Sigma) = N_1 = (1)[1 - A(\pi)]A(\Sigma),$$

$$N(\pi^-, 0\Sigma) = N_2 = [(2)A(\Sigma) + (6) + (7)][1 - A(\pi)],$$

$$N(0\pi, \Sigma^+) = N_3 = (2)[1 - A(\Sigma)]A(\pi),$$

$$N(0\pi, \Sigma^-) = N_4 = [(1)A(\pi) + (5)][1 - A(\Sigma)],$$

$$N(\pi^+, \Sigma^-) = N_5 = (1)[1 - A(\Sigma)][1 - A(\pi)],$$

$$N(\pi^-, \Sigma^+) = N_6 = (2)[1 - A(\Sigma)][1 - A(\pi)] \quad (*) .$$

The  $N_i$ 's are the normalized emission values  $\sum_1^6 N_i + N_0(0\pi, 0\Sigma) = 1$  of Table VI and the numbers in brackets (1)-(7) are the normalized reaction rates written above.

The independent unknowns are, for instance, (2)-(7),  $A(\pi)$  and  $A(\Sigma)$ , 8 together, and we have only 6 independent equations (+). It will be shown in the

(\*)  $A(\pi_\Lambda) = A(\pi_\Sigma)$  is assumed.

(+) In principle the relations  $N_1$ - $N_6$  enable us to get directly the following unknowns,

$$A_\pi: \quad \frac{1 - A_\pi}{A_\pi} = N_6/N_3,$$

$$A_\Sigma: \quad \frac{1 - A_\Sigma}{A_\Sigma} = N_5/N_1,$$

$$(1): \quad (1) = \frac{N_1}{(1 - A_\pi) A_\Sigma}, \quad \text{For } A(\pi), A(\Sigma) \text{ we also use } A_\pi, A_\Sigma -$$

$$(2): \quad (2) = N_3/(1 - A_\Sigma)A_\pi,$$

$$(5): \quad (5) = \frac{N_4}{1 - A_\Sigma} - (1) A_\pi,$$

$$(6) + (7): \quad \{(6) + (7)\} = \frac{N_2}{1 - A_\pi} - (2) A_\Sigma,$$

$$(3) + (4): \quad \{(3) + (4)\} = 1 - [(1) + (2) + (5) + (6) + (7)]$$

but owing to the poor statistics, we apply another way to get the reaction rates in the case of stars in flight.



next sub-section how the reaction rates (1)-(7) can be reduced to 3 unknowns. Then we shall have 5 independent unknowns and 6 independent equations,  $N_1-N_6$ . So we have a possibility to check the method applied.

As one can see, the ratio  $N_5/N_6$  does not depend upon  $A(\pi)$  and  $A(\Sigma)$ . Improving the statistics, one can therefore combine these numbers directly with those obtained from the  $K^-$ -free-proton absorptions, in other words, one can add the apparent  $K^-$ -bound proton absorptions (see Sect. 3'4) to the free-proton absorptions.

4'2. *Isotopic spin considerations.* — If the  $K^-$ -nucleon interaction is charge independent (the total isotopic spin  $T$  is then a good quantum number of the system) some simple relations among the various reaction rates can be derived. This was already shown by GASIOROWICZ <sup>(18)</sup>; KOSHIBA <sup>(16)</sup> especially discussed the charge exchange of  $\pi$ -mesons. Because of the completeness and of the importance of these considerations for the analysis, it seems reasonable to us to describe here briefly the principal steps of the calculations.

According to the Gell-Mann theory <sup>(19,20)</sup>, the  $K^-$ , the  $\Sigma$  and the  $\Lambda$  have the isotopic spins  $\frac{1}{2}$ , 1 and 0 respectively. Thus, the  $K^-$ -nucleon system can be in an isotopic spin state  $T=1$  and in a state  $T=0$ . Using the Clebsch-Gordon coefficient  $(j_1, j_2, m_1, m_2 | j_1, j_2, j, m)$  for the representation of the « particles »  $(m_1, m_2)$ -eigenstates in terms of isotopic spin eigenstates, we obtain:

$$(a) \quad \begin{cases} (K^-p) = \frac{1}{\sqrt{2}} (0, 0) + \frac{1}{\sqrt{2}} (1, 0), \\ (K^-n) = 1 \cdot (1, -1). \end{cases}$$

The isotopic spin eigenfunctions at the right are denoted by their  $(T, T_3)$  value.

Similary, the  $(\Sigma\pi)$  and the  $(\Lambda\pi)$  systems can be written as in Table (b).

By inspecting the set of equations (a) and (b) one interesting feature becomes obvious: the  $T=1$  state cannot have any  $(\pi^0 + \Sigma^0)$  production, but since the experiment shows  $(\pi^0 + \Sigma^0)$ -production <sup>(1)</sup>, the  $K^-$ -proton interaction cannot take place in a pure  $T=1$  state.

<sup>(18)</sup> G. GASIOROWICZ: *Isotopic Spin Consideration in  $K^-$  Interactions with Nuclear Matter*, University of California, UCRL-3074 (1955).

<sup>(19)</sup> M. GELL-MANN and A. PAIS: *Proceedings 1954 Glasgow Conference on Nuclear and Meson Physics* (London-New York, 1955).

<sup>(20)</sup> T. NAKANO and K. NISHIJIMA: *Prog. Theor. Phys., Japan*, **10**, 581 (1953).

(b)	$(\pi^+ \Sigma^-) =$	$+(1/\sqrt{3})(0, 0)$	$+(1/\sqrt{2})(1, 0)$	$+(1/\sqrt{6})(2, 0)$
	$(\pi^- \Sigma^+) =$	$+(1/\sqrt{3})(0, 0)$	$-(1/\sqrt{2})(1, 0)$	$+(1/\sqrt{6})(2, 0)$
	$(\pi^0 \Sigma^0) =$	$-(1/\sqrt{3})(0, 0)$		$+(\sqrt{2/3})(2, 0)$
	$(\pi^0 \Lambda^0) =$		$1 \cdot (1, 0)$	
	$(\pi^0 \Sigma^-) =$		$(1/\sqrt{2})(1, -1)$	$+(1/\sqrt{2})(2, -1)$
	$(\pi^- \Sigma^0) =$		$-(1/\sqrt{2})(1, -1)$	$+(1/\sqrt{2})(2, -1)$
	$(\pi^- \Lambda^0) =$		$1 \cdot (1, -1)$	

With the help of (a) and (b) and by assuming  $T$  to be a good quantum number, one can write down the matrix elements and the reaction rates for all the different  $K^-$ -nucleon reactions. The results are summarized in Table VII.

TABLE VII.

Reaction	Matrix element	Reaction rates ( $\sim \sigma$ )
a) (1) $K^- + p \rightarrow \Sigma^- + \pi^+$	$\frac{1}{2}M_1 + (1/\sqrt{6})M_0$	$r^2 + \frac{2}{3} + 2\sqrt{\frac{2}{3}}r \cos \varphi$
(2) $\Sigma^+ + \pi^-$	$-\frac{1}{2}M_1 + (1/\sqrt{6})M_0$	$r^2 + \frac{2}{3} - 2\sqrt{\frac{2}{3}}r \cos \varphi$
(3) $\Sigma^0 + \pi^0$	$-(1/\sqrt{6})M_0$	$\frac{2}{3}$
(4) $\Lambda^0 + \pi^0$	$(1/\sqrt{2})M_{1\Lambda}$	$2r_\Lambda^2$
b) (5) $K^- + n \rightarrow \Sigma^- + \pi^0$	$(1/\sqrt{2})M_1$	$2r^2$
(6) $\Sigma^0 + \pi^-$	$-(1/\sqrt{2})M_1$	$2r^2$
(7) $\Lambda^0 + \pi^-$	$M_{1\Lambda}$	$4r_\Lambda^2$



The matrix element notation in the table is as follows:

$$\begin{aligned} M_0 &= \langle T=0 | H^\Sigma \text{ interact} | T=0 \rangle, \\ M_1 &= \langle T=1 | H^\Sigma \text{ interact} | T=1 \rangle, \\ M_{1\Lambda} &= \langle T=1 | H^\Lambda \text{ interact} | T=1 \rangle. \end{aligned}$$

For the analysis it is convenient to write down the ratios between the various matrix elements. We shall therefore define (see, for instance, <sup>(1)</sup>).

$$M_1/M_0 = r \exp[i\varphi] \quad \text{and} \quad |M_{1\Lambda}/M_0| = r_\Lambda,$$

$r$  and  $r_\Lambda$  are real numbers. The reaction rates in Table VII are given in terms of  $r_\Lambda$ ,  $r$  and  $\cos \varphi$ . The 5 unknowns in the 6 equations  $N_1$ - $N_6$  of Sect. 4.1 are:  $A(\pi)$ ,  $A(\Sigma)$ ,  $r_\Lambda$ ,  $r$  and  $\cos \varphi$ .

The  $(r_\Lambda, r, \cos \varphi)$  set obtained from the isotopic spin analysis has a straightforward interpretation only when the  $K$ -nucleon interaction takes place in an  $S$  angular momentum state. This is probably not the case, neither in the interactions at rest <sup>(21)</sup>, nor in the interactions in flight. Nevertheless one can, formally at least, by redefining the matrix elements (\*), apply the isotopic spin analysis and get the energy dependence of the ratio between the various matrix elements.

4.3. *Prong-distribution aspects, the «clean» events.* — If one uses the sign-fractions only from those stars which were selected according to a special «stable»-prong number criteria, one must in principle be able to get additional information, since the re-absorption or emission of pions and hyperons from nuclei is strongly influencing the number of observed prongs.

Following this idea one can analyse the «clean» events. The clean events are  $K^-$ -interactions from which no stable charged particles escape. (For the stars in flight their numbers  $^0N_i$  are given in Sect. 3.5, Table VI). They consist of  $K^-$ -stops, ( $K^-$ 's for the stars at rest), decay-like stars, (stars with one

<sup>(21)</sup> R. H. DALITZ: *The Strong Interactions of Strange Particles*, Brookhaven Lectures (1957).

(\*) For example, if  $S$  and  $P$  states are present, one could define:

$$\frac{M_1^S + M_1^P}{M_0^S + M_0^P} = r \exp[i\varphi]$$

and similarly:

$$r_\Lambda = \frac{M_{1\Lambda}^S + M_{1\Lambda}^P}{M_0^S + M_0^P}.$$

$\pi$ -prong only), stars emitting a  $\Sigma$  only, and stars emitting  $(\pi + \Sigma)$  only. The equations  $N_1$ - $N_6$  of Sect. 4.1 together with the reaction rates of Table VII enable us to calculate  $A(\pi)$ ,  $A(\Sigma)$ ,  $r_\Lambda$ ,  $r$  and  $\cos \varphi$ . (1)-(7) can therefore be considered as known and can be used for this analysis. Although for our stars in flight the small and uncertain number of clean events does not justify a very detailed investigation, it seems to us of some importance to perform this analysis. For the capture stars at rest, which are treated in a forthcoming paper, the statistics will be more comprehensive and these considerations will become more meaningful.

Let  $a$  and  $e$  be the probabilities that a particle, when absorbed inside the nucleus or emitted from it respectively, does not produce a visible excitation prong. Then, to the clean interactions from which only, for instance, a  $\Sigma^-$  escapes, contribute the following reactions:

$$\left. \begin{array}{l} (1) \rightarrow \Sigma_{\text{emitted}}^- \text{ and } \pi_{\text{absorbed}}^+ \\ (5) \rightarrow \Sigma_{\text{emitted}}^- \text{ and } \pi_{\text{absorbed}}^0 \\ \Sigma_{\text{emitted}}^- \text{ and } \pi_{\text{emitted}}^0 \end{array} \right\} \begin{array}{l} \text{without emis-} \\ \text{sion of stable} \\ \text{prongs} \end{array}$$

and the reaction from which only a  $\Sigma^+$  escapes is due to

$$(2) \rightarrow \Sigma_{\text{emitted}}^+ \text{ and } \pi_{\text{absorbed}}^-.$$

Thus we get for the number of clean events, where only a  $\Sigma$ -hyperon is emitted, the following expression,

$$\begin{aligned} (\alpha) \quad {}^0N_3 + {}^0N_4 = (1 - A_\Sigma) \cdot \{a_\pi e_\Sigma A_\pi [(1) + (5)] + (5)(1 - A_\pi) e_\pi e_\Sigma\} + \\ + (1 - A_\Sigma) \cdot (2) \cdot A_\pi a_\pi e_\Sigma. \end{aligned}$$

Analogously one gets from the number of clean events, where pion and  $\Sigma$  escape,

$$(\beta) \quad e_\pi e_\Sigma (N_5 + N_6) = {}^0N_5 + {}^0N_6 = \{(1) + (2)\} (1 - A_\pi) (1 - A_\Sigma) e_\pi e_\Sigma.$$

From these two equations  $e_\pi e_\Sigma$  and  $a_\pi e_\Sigma$  can be calculated (\*).

(\*) Presuming that the observation of a  $\pi$  and a  $\Sigma$  without any other prong is not biased in the sense that the corresponding absorptions all have taken place on the surface of the nucleus or on light nuclei. The energy distribution of the corresponding  $\pi$ -mesons suggests that there is no strong bias, see in Fig. 1 the  $\pi$ 's from clean events.



The processes which contribute to the decay-like stars from which only one charged pion is emitted are

$$(1) \rightarrow \Sigma_{ab}^- \text{ and } \pi_{em}^+,$$

$$(2) \rightarrow \Sigma_{ab}^+ \text{ and } \pi_{em}^-,$$

$$(6) \rightarrow \Sigma_{ab}^0 \text{ and } \pi_{em}^-,$$

$$\Sigma_{em}^0 \text{ and } \pi_{em}^-,$$

$$(7) \rightarrow \Lambda_{em}^0 \text{ and } \pi_{em}^-,$$

$$\Lambda_{ab}^0 \text{ and } \pi_{em}^-,$$

and we get from the decay-like stars the relations

$$(\gamma) \quad {}^0N_1 = N_1 e_\pi a_\Sigma = (1)(1 - A_\pi) A_\Sigma e_\pi a_\Sigma,$$

$$(\delta) \quad {}^0N_2 = (1 - A_\pi) e_\pi \{ [(2) + (6)] A_\Sigma a_\Sigma + (6)(1 - A_\Sigma) e_\Sigma + (7)[A_\Lambda a_\Lambda + (1 - A_\Lambda) e_\Lambda] \}.$$

Since it is the purpose of this whole investigation to predict the number of stops from the residual number of clean events, we give now the bit more voluminous equation for the number of stops caused by complex nuclei (\*)

$${}^0N_0 =$$

$$\begin{aligned} &= (1) [ \quad \quad \quad + A_\pi A_\Sigma a_\pi a_\Sigma \quad \quad \quad ] + \\ &+ (2) [ \quad \quad \quad + A_\pi A_\Sigma a_\pi a_\Sigma \quad \quad \quad ] + \\ &+ (3) [(1 - A_\pi)(1 - A_\Sigma) e_\pi e_\Sigma + A_\pi A_\Sigma a_\pi a_\Sigma + (1 - A_\Sigma) A_\pi a_\pi e_\Sigma + (1 - A_\pi) A_\Sigma e_\pi a_\Sigma] + \\ &+ (4) [(1 - A_\pi)(1 - A_\Lambda) e_\pi e_\Lambda + A_\pi A_\Lambda a_\pi a_\Lambda + A_\pi (1 - A_\Lambda) a_\pi e_\Lambda + (1 - A_\pi) A_\Lambda e_\pi a_\Lambda] + \\ &(\varepsilon) + (5) [ \quad \quad \quad + A_\pi A_\Sigma a_\pi a_\Sigma \quad \quad \quad + (1 - A_\pi) A_\Sigma e_\pi a_\Sigma ] + \\ &+ (6) [ \quad \quad \quad + A_\pi A_\Sigma a_\pi a_\Sigma + A_\pi (1 - A_\Sigma) a_\pi e_\Sigma \quad \quad \quad ] + \\ &+ (7) [ \quad \quad \quad + A_\pi A_\Lambda a_\pi a_\Lambda + A_\pi (1 - A_\Lambda) a_\pi e_\Lambda \quad \quad \quad ] + \\ &+ (K^- \text{-charge exchanges on compound nuclei, which are associated with a} \\ &\quad \text{clean re-emission of the } K^0). \end{aligned}$$

Generally we have 6 unknowns, namely,

$$e_\pi, \quad a_\pi, \quad e_\Sigma, \quad a_\Sigma, \quad \{A_\Lambda a_\Lambda + (1 - A_\Lambda) e_\Lambda\},$$

and the percentage of « clean »  $K^0$ -re-emissions.

(\*) The  $K^-$ -interactions on free protons which lead to stops are already subtracted by using  $r_\Lambda$ ,  $r$ ,  $\cos \varphi$  and the  $K^-$ -free-proton interactions which lead to charged  $\Sigma$ 's.

Since there are only 5 equations:  $(\alpha)$ ,  $(\beta)$ ,  $(\gamma)$ ,  $(\delta)$  and  $(\epsilon)$ , one must deduce at least one parameter from other experiments.

Unfortunately our experimental data do not allow a statistically significant analysis along the lines indicated in this section. With better statistics one might be able to approach the question, whether the branching ratios (1)-(7), which were calculated under the assumption of conservation of isotopic spin in strong interactions of strange particles, are self-consistent.

## 5. - Analysis of the interactions in flight.

5.1. *The reaction rates and absorption probabilities.* - We shall now attempt to get a set of values for  $A(\pi)$ ,  $A(\Sigma)$ ,  $r$ ,  $r_\Lambda$ ,  $\cos \varphi$  and (1)-(7) defined in Sects. 4'1 and 4'2. First one has to modify the relations between the reaction rates (1)-(7) and  $r$ ,  $r_\Lambda$ ,  $\cos \varphi$  of Table VII, Sect. 4'2, obtained from isotopic spin calculations for the self-conjugate nucleus. Taking into account the 20% neutron excess in the average emulsion nucleus, the  $K^-$ -neutron reactions are multiplied by a factor of 1.2 (\*). Using the corrected reaction rates (as function of the  $r$ 's and  $\cos \varphi$ ), the relations between the emission values  $N^{\text{em}}(\pi^-)$ ,  $N^{\text{em}}(\pi^-)$ ,  $N^{\text{em}}(\Sigma^+)$  and  $N^{\text{em}}(\Sigma^-)$  which have been discussed in Sect. 3, and the  $A$ 's,  $r$ 's and  $\cos \varphi$  can be written by means of equations  $N_1$ - $N_6$  Sect. 4'1.

While we discussed in Sect. 3 the sign-fractions  $+/-$ , in future it will be more convenient to consider the normalized difference ratio

$$2 \cdot \{N(-) - N(+)\} / \{N(-) + N(+)\}.$$

Applying the equations of Sects. 4'1 and 4'2 (with correction for 20% neutron excess), one gets

$$(\alpha) \quad \begin{cases} c_1 = 2 \frac{N_2 + N_6 - N_1 - N_3}{N_1 + N_2 + N_5 + N_6} = \frac{4.8r_\Lambda^2 + 2.4r^2 - 4\sqrt{\frac{2}{3}}r \cos \varphi}{2.4r_\Lambda^2 + 2.2r^2 + \frac{2}{3}}, \\ c_2 = 2 \frac{N_4 + N_5 - N_3 - N_6}{N_3 + N_4 + N_5 + N_6} = \frac{2.4r^2 + 4\sqrt{\frac{2}{3}}r \cos \varphi}{2.2r^2 + \frac{2}{3}}, \\ c_3 = 2 \frac{N_5 + N_5' - N_6 - N_6'}{N_5 + N_5' + N_6 + N_6'} = \frac{4\sqrt{\frac{2}{3}}r \cos \varphi}{r^2 + \frac{2}{3}}. \quad (+) \end{cases}$$

(\*) This correction factor of 1.2 should be used only if the  $K^-$ -nucleon interaction is taking place uniformly throughout the nucleus. According to Sects. 3, 4 (footnote) and 6 we have reasons to believe that this is indeed the case for the  $K^-$ -interactions in flight.

(+) As already mentioned in Sect. 3'4 and 4'1 we added here the  $K^-$ -free proton absorption numbers  $N'$ .

Experimentally we have obtained (see Sect. 3)

$$c_1 = 1.56 \pm 0.13 ,$$

$$c_2 = 0.65 \pm 0.31 ,$$

$$c_3 = -0.4 \pm 0.4 .$$

The absorption probabilities  $A(\pi)$  and  $A(\Sigma)$  can also be calculated from equations  $N_1$ - $N_6$ . (This is trivially the ratio of emission and production).

$$(\beta) \quad \begin{cases} 1 - A(\pi) = \frac{N_1 + N_2 + N_5 + N_6}{(1) + (2) + (6) + (7)} , \\ 1 - A(\Sigma) = \frac{N_3 + N_4 + N_5 + N_6}{(1) + (2) + (5)} . \end{cases}$$

Tables for the expressions on the right side of eq. (z) were calculated for all possible values of  $r_\Lambda$ ,  $r$  and  $\cos \varphi$ .

With the help of these tables a set of values for  $r_\Lambda$ ,  $r$  and  $\cos \varphi$  was obtained, namely:

$$r_\Lambda \approx 1 ,$$

$$r \approx 1 ,$$

$$\cos \varphi \approx -0.2 .$$

The sensitivity of the results obtained to the choice of the set  $(r_\Lambda, r, \cos \varphi)$  is illustrated in Table VIII. (For the explanation of  $c_4$  see next sub-sections).

By using the relations  $(\beta)$  above we get

$$A(\pi) = 0.67 \pm 0.07 ,$$

$$A(\Sigma) = 0.77 \pm 0.14 .$$

It should be remarked that since almost all K-nucleon absorptions produce pions,  $A(\pi)$  is practically independent of the set  $(r_\Lambda, r, \cos \varphi)$ .  $A(\Sigma)$  on the other hand, depends, in principle, on the choice of the matrix elements. However, unless an extremely unreasonable choice of  $r_\Lambda$ ,  $r$  and  $\cos \varphi$  is made,  $A(\Sigma)$  practically remains constant (see Table VIII). By comparing the present  $A(\Sigma)$  with the one obtained for the super-sigma stars, one can get an idea about the energy dependence of the  $\Sigma$ -hyperon capture probability. The value for  $A(\pi)$  from the stars in flight is larger than for the  $K^-$ -capture stars



TABLE VIII. — Reaction rates and absorption probabilities in percent for different sets of  $r_\Lambda$ ,  $r$  and  $\cos \varphi$ .

Reaction rates	$r_\Lambda$	0.5	0.5	1.5	1.5	1.0	1.0	1.0	1.5	2.0
	$r$	0.5	1.5	0.5	1.5	1.0	1.0	0.8	1.5	2.0
	$\cos \varphi$	—0.5	0.0	0.0	0.0	—0.2	—0.3	—0.2	—0.3	—0.3
(1)	$r^2 + \frac{2}{3} + 2\sqrt{\frac{2}{3}}r \cos \varphi$	9.4	15.5	4.8	8.9	8.5	7.5	8.0	6.7	6.6
(2)	$r^2 - \frac{2}{3} - 2\sqrt{\frac{2}{3}}r \cos \varphi$	24.5	15.5	4.8	8.9	12.8	13.8	11.9	11.2	10.0
(3)	$\frac{2}{3}$	12.3	3.5	3.5	2.0	4.3	4.3	5.1	2.0	1.2
(4)	$2r_\Lambda^2$	9.4	2.6	23.7	13.8	12.8	12.8	15.2	13.8	14.2
(5)	$2.4r^2$	11.1	28.3	3.2	16.6	15.4	15.4	11.6	16.6	17.0
(6)	$2.4r^2$	11.1	28.3	3.2	16.6	15.4	15.4	11.6	16.6	17.0
(7)	$4.8r_\Lambda^2$	22.2	6.3	56.8	33.2	30.8	30.8	36.6	33.1	34.0
	$A(\pi)$	67	66	68	68	67	68	68	68	68
	$A(\Sigma)$	81	86	33	76	77	78	75	77	76
	$\Lambda_{\text{prod}} \%$	31.5	8.9	60.3	46.9	43.6	43.6	51.7	46.9	48.2
	$\Sigma_{\text{prod}} \%$	68.5	91.1	39.7	53.1	56.4	56.4	48.3	53.1	51.8
	$\sum_1^4 \left( \frac{C_i^{\text{exp}} - C_i^{\text{calc.}}}{\Delta C_i} \right)^2$ ( $\Delta C_i = \text{stand. dev.}$ )	9.8	100	5.2	2.6	0.34	0.93	0.57	1.2	1.8

at rest <sup>(8)</sup>. This could be due to the increase of the absorption cross-section for pions with increasing energy <sup>(22,23)</sup>.

In order to confirm the values obtained for  $r_\Lambda$ ,  $r$  and  $\cos \varphi$ , we required some consistency checks which will be described now.

<sup>(22)</sup> A. E. IGNATENKO: *Proceedings of the CERN Symposium on High Energy Accelerators and Pion Physics* (1956), Vol. 2, pag. 313.

<sup>(23)</sup> S. J. LINDENBAUM: *Annual Review of Nuclear Science*, 7, 317 (1957).

5.2. *Very fast pions.* — The values of  $r_\Lambda$  and  $r$  suggest that for the stars in flight direct  $\Lambda$ -production occurs with appreciable frequency. One would thus expect a big number of high-energy pions, which were produced together with the  $\Lambda$ . However, mainly by the influence of inelastic scattering, this number is expected to be greatly reduced (see Sect. 3'1.1). In 11 cases where the pions had less than  $10^\circ$  dip the energy of the pions was determined.

In 2 cases the energy of the pions was so high, that they could not be produced together with a  $\Sigma$ . This number is compatible with the values of  $r_\Lambda$  and  $r$  given in Sect. 5'1.

5.3.  *$\Lambda$ -production on neutrons.* — As already mentioned in Sect. 4'1 the equation system  $N_1$ - $N_6$  opens the possibility for a check, since there are 5 unknowns and 6 equations. In principle one could calculate the  $A$ 's,  $r$ 's and  $\cos \varphi$  from 5 of these equations and take the remaining equation as a check. But for statistical reasons and regarding the symmetry of the equation system, we applied mixtures of  $N_1$ - $N_6$  to calculate the 5 unknowns. So one has to find now a good «test-mixture». For physical reasons this quantity should be most sensitive to the  $\Lambda$ -production. Since according to Table VIII with a  $(r, r_\Lambda, \cos \varphi)$ -set of  $(1, 1, -0.2)$  more than  $\frac{1}{2}$  of all negative  $\pi$ -mesons should be produced in the  $K^-n \rightarrow \Lambda\pi^-$ -reaction, a sensitive quantity which can be formed is:

$$c_4 = (N_1 + N_5 + N_6)/N_2 = 16/74 = 0.22 \pm 0.05 = \frac{(1) + (2) - (2) A(\Sigma)}{(6) + (7) + (2) A(\Sigma)}.$$

More than 50% of the denominator is contributed by  $\Lambda$ -production. The fraction is similar to the sign-fraction  $+/-$  of pions, but is not identical with it, and is statistically more significant. It is more sensitive to the choice of the set  $(r_\Lambda, r, \cos \varphi)$  than the other three fractions used in Sect. 5'1 and is in good agreement with the values of  $r_\Lambda$ ,  $r$  and  $\cos \varphi$  found.

Actually, the major difference in the reaction rates corresponding to the set  $(1, 1, -0.2)$  as compared with the set  $(2, 2, -0.3)$  is the ratio  $\Lambda^0\pi^0/\Sigma^0\pi^0$ , which turns out to be about 3 in the first case and about 14 in the second case. It is to be hoped that, when Alvarez-type experiments are performed, using  $K^-$  in flight, a more definite set of  $(r_\Lambda, r, \cos \varphi)$  will be obtained.

It should be noted that  $\cos \varphi$  is negative. Physically this means, that more  $\Sigma^-$  than  $\Sigma^+$  are produced in the interactions of fast  $K^-$ -mesons with protons, as compared with a reversed situation for the interactions of  $K^-$  at rest on free protons.

It must be emphasized, that our conclusion of a negative  $\cos \varphi$  does not depend only upon the  $\Sigma^+$ -hyperon excess in  $K^-$  proton-absorptions, which is statistically not very reliable. Attempts to fit  $c_1$  and  $c_2$  with positive  $\cos \varphi$

necessarily lead to a small  $r$  and a very large  $r_\Lambda/r$  ratio  $(r_\Lambda/r)^2 = 20$  which would be completely inconsistent with the rest of the experimental data presented in this section.

5.4. *Clean events.* — Because of the small number of clean events, we cannot calculate the unknowns of Sect. 4.3 by means of eqs. ( $\alpha$ )-( $\varepsilon$ ). Therefore we apply a rough consistency check in the following manner. Adding up all clean events, we get the relation

$$(\alpha) \quad {}^0N_{\text{total}} = \{(1 - A_\pi)e_\pi + A_\pi a_\pi\} \cdot \{(4) + (7)\} \cdot [(1 - A_\Lambda)e_\Lambda + A_\Lambda a_\Lambda] + \\ + [(1) + (2) + (3) + (5) + (6)] \cdot [(1 - A_\Sigma)e_\Sigma + A_\Sigma a_\Sigma],$$

and adding  ${}^0N_1$ ,  ${}^0N_2$ ,  ${}^0N_5$  and  ${}^0N_6$  we get

$$(\beta) \quad {}^0N_1 + {}^0N_2 + {}^0N_5 + {}^0N_6 = \{(1 - A_\pi)e_\pi\} \cdot \\ \cdot \{[(1) + (2) + (6)] \cdot [(1 - A_\Sigma)e_\Sigma + A_\Sigma a_\Sigma] + (7)[(1 - A_\Lambda)e_\Lambda + A_\Lambda a_\Lambda]\},$$

and our check is now given by the task to get by reasonable assumptions for  $e_\pi$ ,  $a_\pi$ ,  $e_\Sigma$  and  $a_\Sigma$  (\*) agreement with the experimental values for both equations.

Experiments with fast pions in nuclear emulsions <sup>(15)</sup>, indicate that about 20% of the negative pions disappear in flight, producing no visible prongs (-). We take therefore

$$a_\pi = 0.2.$$

Observations of  $\Sigma^-$ -captures at rest <sup>(24,25)</sup> showed that about 50% of the stars are  $\rho$ -events. Since the  $\Sigma$ 's emitted from the stars in flight are not very energetic ( $T \approx 20$  MeV), the value

$$a_\Sigma = 0.5.$$

is used

In order to estimate  $e_\pi$  we regard the average energy loss of the emitted pions inside the nucleus. It is about 100 MeV. As can be taken from interactions of protons and pions of this energy with emulsion nuclei <sup>(26,27)</sup>, the

(\*) We make the very rough assumption that  $a_{\Sigma^-} = a_{\Sigma^+}$ , which is certainly not correct.

(+) We did not take into account the difference between  $\pi^+$  and  $\pi^-$ , because our number of  $\pi^+$  is very small.

<sup>(24)</sup> W. H. BARKAS: *Proceedings of the Seventh Rochester Conference* (1957).

<sup>(25)</sup> N. N. BISWAS and M. CECCARELLI: *Nuovo Cimento*, **8**, 599 (1958).

<sup>(26)</sup> R. E. MARSHAK: *Meson Physics* (New York, 1952).

<sup>(27)</sup> S. JANNELLI and F. MEZZANARES: *Nuovo Cimento*, **5**, 380 (1957).



corresponding zero prong ratio is about 35%. Thus we use

$$e_{\pi} = 0.35.$$

With respect to  $e_{\Sigma}$  we argue as follows: the energy distribution of the emitted  $\Sigma$ 's was calculated disregarding inelastic scattering, and in spite of this approximation the agreement between the calculated and measured distribution is good. This means that the influence of inelastic scattering on the energy distribution of  $\Sigma$ -hyperons probably is not very great. Therefore we took

$$e_{\Sigma} = 0.8.$$

Inserting these values and the reaction rates deduced from the set (1, 1, -0.2) for  $(r_{\Lambda}, r, \cos \varphi)$  and using eqs. ( $\alpha$ ) and ( $\beta$ ) one gets agreement for the predicted and observed numbers of clean events.

5.5. *Absorption of  $\Lambda$ -hyperons.* - We have shown in Sect. 3.3 that the average energy of the  $\Lambda$ -hyperons, produced either directly or through the absorption of  $\Sigma$ -hyperons, is about 85 MeV in our experiment. It is, naturally, interesting to obtain experimentally the number of hyperfragments produced per  $\Lambda$  produced, as a function of the  $\Lambda$ -kinetic energy. In other words, knowing the  $\Lambda$  trapping probability as a function of the  $\Lambda$  energy may lead to a better understanding of the entire hyperfragment production process.

We have observed 17 hyperfragments (see Sect. 2). According to the reaction rates presented in Sect. 5.1, the number of directly produced  $\Lambda$ 's is  $\sim 175$  and another  $\sim 180$   $\Lambda$ 's were formed in the target nucleus by re-absorptions of  $\Sigma$ -hyperons. Thus there are 4.8% hyperfragments observed per  $\Lambda$  produced for the stars in flight. Results obtained from absorptions of  $K^-$  at rest in nuclear emulsions (\*) indicate that the corresponding number of hyperfragments in this case is 6.6%.

The difference between the stars in flight and at rest, although not statistically significant, can probably be explained with the help of Figs. 7 and 8, which show the energy distribution of directly and indirectly produced  $\Lambda$ 's. The fraction of  $\Lambda$ 's with low energy is greater for the stars at rest than for the  $K^-$ -stars in flight (mean  $\Lambda$ -energy 85 MeV). This can be taken as an indication that the  $\Lambda$ -trapping probability decreases with increasing  $\Lambda$ -energy.

5.6. *Visible energy.* - The visible energy analysis will be published in a separate paper. The preliminary results fit the main conclusions which were drawn here. In particular it indicates that a considerable number of  $\Lambda$ -hyperons are trapped inside the nucleus (<sup>28</sup>), without production of a visible hyperfragment.

(<sup>28</sup>) M. SCHNEEBERGER: to be published.

## 6. — Final discussion and conclusions.

Table IV Sect. 2 gives the over all view of the experimental results. The average kinetic energy of the interacting  $K^-$ -mesons is 86 MeV and the considered energy interval ranged from about 5 to 150 MeV.

The energy spectrum of the emitted  $\pi^-$ -mesons is dominated by the influence of inelastic scattering, see Fig. in Sect. 2 and Sect. 3, and this should at least approximately be valid also for  $\pi^-$ -mesons. The influence of inelastic scattering is especially strong on the faster pions and this leads to difficulties in getting fast pions from the  $(\Lambda\pi)$ -reaction.

For the  $\Sigma$ -hyperons the comparison between the observed and the calculated energy spectrum was performed, neglecting in the calculations inelastic scatterings and a possible anisotropy of production in the CM-system. In spite of this, we found good agreement between the experiment and the Monte Carlo calculation.

By comparing the results obtained in this experiment to those obtained by the analysis of the super sigma stars <sup>(29,8)</sup> one gets an idea about the energy dependence of the absorption probabilities of the various particles: pions,  $\Sigma$ -hyperons and  $\Lambda$ -hyperons. The absorption of  $\Lambda$ -hyperons is proportional to the number of hyperfragments observed per  $\Lambda$  produced.

In our experiment we did not observe many «two-nucleon» reactions:



Thus approximately each  $K^-$ -absorption should yield a pion, and the  $A(\pi)$  value obtained in this experiment could be compared with the value obtained in the analysis of  $K^-$  captures at rest in nuclear emulsions. The absorption probability for the pions — assuming equal probabilities of absorption for  $\pi^+$  and  $\pi^-$  — seems to rise with increasing  $K^-$ -energy, and therefore also with the increase in the average pion energy. This might be explained partially as a geometrical effect but would also very well agree with the fact that the pion absorption cross-section in heavy nuclei increases with energy <sup>(22,23)</sup>. The predominance of the latter effect is supported by the experimental indication that the energy distribution of the emitted pions from the «clean» events is about the same as the energy distribution of the pions from all stars. Thus the pions from the clean events are scattered in the same manner as the other pions, and this supports the assumption that — at least for the other stars in flight — the interaction takes place uniformly over all the regions of the nucleus. The analysis of the clean events (Sect. 4'3

<sup>(29)</sup> C. DILWORTH: *Proceedings of the Seventh Rochester Conference* (1957) and *Geneva Conference*, July 1958. Also: *Bern Emulsion group results on  $K^-$  absorptions at rest*, to be published soon.

and Sect. 5.4), is statistically very poor, but is not in contradiction with this assumption.

The absorption probabilities of the  $\Sigma$  and  $\Lambda$  hyperons can be calculated only when the fraction of  $\Sigma$  and  $\Lambda$  hyperons present in the nucleus is known (\*). Thus the discussion of the energy dependence of  $A(\Sigma)$  and of the number of hyperfragments per  $\Lambda$  produced (directly and indirectly) will be postponed until the reaction rates for the super-sigma stars will be determined. We wish only to remark that we have reasons to believe that  $A(\Sigma)$  seems to increase with increasing  $\Sigma$  energy and that the fraction of hyperfragments per  $\Lambda$  produced decreases with increasing  $\Lambda$  energy.

The analysis of the branching ratios for the different reactions of  $\Lambda$ - and  $\Sigma$ -production (1)-(7) Sect. 4.1 leads us to draw the following conclusions:

Comparing our results obtained from interactions of  $K^-$ -mesons in flight (with an average relative  $K^-$ -nucleon momentum in the CM-system of  $\sim 380$  MeV/c) on complex nuclei of the emulsion with the results obtained by ALVAREZ *et al.* (1) from interactions of  $K^-$ -mesons at rest with zero relative momentum on hydrogen, see Table IX, — and presuming charge independence for strong interactions by strange particles — we must conclude that there is a significant rise in the direct  $\Lambda$ -production with increasing relative momentum of the interacting  $K^-$ -nucleon system.

The detection of very fast pions which energetically could not correspond to an associated  $(\Sigma\pi)$ -production in the elementary  $K$ -nucleon reaction, and the overall consistency of the observed data with the calculated reaction rates support this result. The charge exchange of the pions inside the nucleus would only enlarge the effect, and no apparent example of a charge exchange, for instance the emission of only a  $\pi^-$  and a  $\Sigma^-$  was observed.

We wish to emphasize again that our conclusion that the extraordinarily low  $\pi^+/\pi^-$  ratio observed in our experiment must be explained by a large direct  $\Lambda\pi$ -reaction, depends essentially upon two assumptions: (1) charge independence, (2) approximately equal absorption probabilities for  $\pi^+$  and  $\pi^-$ -mesons. Our  $\pi^+/\pi^-$  ratio would be compatible with Alvarez' results, if, for example, the absorption probability of  $\pi^-$  in our energy region were  $\sim 65\%$  and that of  $\pi^+ \sim 95\%$ .

Another interesting result is, that in the interaction of  $K^-$  in flight the sign of  $\cos \varphi$  is very probably negative, contrary to a positive  $\cos \varphi$  in the absorption of  $K^-$  at rest by free protons (see Table IX). Physically this means, that in the elementary  $K^-$ -proton absorption more  $\Sigma^+$  than  $\Sigma^-$  are produced as the relative  $K^-$ -proton momentum increases.

(\*) The integral absorption probabilities  $A(\pi^+)$  and  $A(\pi^-)$  can be different, even if  $\pi^+$  and  $\pi^-$  of the same energy are absorbed approximately equally, since  $\pi^+$  and  $\pi^-$  are produced with different average energies. This effect however would probably tend to lower the numbers of  $\pi^-$ -emitted.



TABLE IX. — Comparison between the results obtained in the present experiment and those observed by ALVAREZ *et al.*

Reaction		Reaction rates in percent	
		Present experiment $P_{\text{rel}}^{\text{CM}} = 380 \text{ MeV/c}$	ALVAREZ <i>et al.</i> (*) $P_{\text{rel}}^{\text{CM}} = 0 \text{ MeV/c}$
(1)	$K^- + p \rightarrow \Sigma^- + \pi^+$	8.5	28.6
(2)	$\Sigma^+ + \pi^-$	12.8	14.7
(3)	$\Sigma^0 + \pi^0$	4.3	15.5
(4)	$\Lambda^0 + \pi^0$	12.8	3.5
(5)	$K^- + n \rightarrow \Sigma^- + \pi^0$	15.4	14.6
(6)	$\Sigma^0 + \pi^-$	15.4	14.6
(7)	$\Lambda^0 + \pi^-$	30.8	8.5
Matrix elements (ratios)	$r$	1	0.51
	$r_{\Lambda}$	1	0.28
	$\cos \varphi$	-0.2	+0.36
	$r^2/r_{\Lambda}^2$	1	3.4
% $\Sigma$ -production		56	88
% $\Lambda$ -production		44	12

(\*) Note that in the Alvarez experiment only  $K^-$ -proton reactions were measured. However, assuming charge independence, the neutron reaction rates for 0 relative  $K^-$ -n momentum can be determined. The 20% neutron excess correction was introduced in the above table so that a direct comparison between Alvarez' results and ours can be made.

If the increase in the elementary  $\Lambda$ -production is directly correlated to an angular momentum change, it could be already appreciable for the  $K^-$ -capture stars at rest in nuclear emulsions <sup>(3)</sup>, because of the average relative  $K$ -nucleon Fermi momentum of about 115 MeV/c in the CM-system. Thus one will have the matrix elements for 3 different relative  $K$ -nucleon momenta. It is hoped that perhaps some conclusions concerning the matrix elements in the various angular momentum and isotopic spin states could be drawn, when still more data become available.

The increase in the  $\Lambda$ -production is also able to explain the difficulties mentioned by other authors (<sup>29,6</sup>), in transferring directly the Alvarez-results to the  $K^-$ -captures «at rest» in the emulsions. Naturally this does not exclude the possibility of the formation of  $\Sigma$ -compounds in the nucleus (<sup>6</sup>). These points must be treated in more detail for the stars at rest, where one has the advantages of lower average pion-production energy and of vanishing  $K^0$ -re-emission from  $K^-$ -charge exchanges.

Finally it should be remarked that the  $\Lambda$ -production increase is contrary to simple phase-space considerations. The relative phase-space ( $\Lambda/\Sigma$ ) available to the  $(\Lambda\pi)$ -reaction at the  $K^-$ -free proton interactions at rest is bigger than in the interactions in flight. Thus, since the  $\Lambda$ - and  $\Sigma$ -hyperons probably have the same spin (<sup>30</sup>), this increase in the direct  $\Lambda$ -production could be due to a different coupling. Perhaps the  $\Lambda$ - and  $\Sigma$ -hyperons might have different parities (\*).

\* \* \*

We are very indebted to Drs. L. JAUNEAU, E. J. LOFGREN and M. TEUCHER. They arranged the exposure in Berkeley. Without their generous co-operation this experiment would not have been possible.

We express our sincere thanks to Prof. F. G. HOUTERMANS for his continuous interest in this investigation and Prof. CH. PEYROU especially for his useful suggestions and for the many stimulating discussions during all the phases of this work.

Our thanks are also due to Profs. G. BERNARDINI and A. DE SHALIT for interesting discussions.

Our scanning team did efficient work. We are grateful to Mrs. B. ALBRECHT, E. KOCH, CH. PLUMETTAZ, T. RIESEN, I. RITSCHARD and S. SCHILT. Mrs. B. ALBRECHT and CH. PLUMETTAZ made precise measurements for us.

One of us (E.L.) thanks Prof. R. E. SCHOPPER for his interest in this work. Our further thanks are due to the Schweizer Nationalfonds for financial help.

## APPENDIX

We discuss here the 3 events which were already mentioned in Sect. 2.

The one is a  $\Sigma^-$ -hyperon with very high kinetic energy (175 MeV, see also Fig. 2). The kinetic energy of the  $K^-$ -meson, which produces the parent star is 70 MeV. Thus, from energy and momentum-balance arguments, this is very probably an example of a  $K^-$ -two-nucleon reaction.

(<sup>30</sup>) F. EISLER, R. PLANO, A. PRODELL, N. SAMIOS, M. SCHWARTZ, J. STEINBERGER, P. BASSI, V. BORELLI, P. FRANZINI, I. MANNELLI, R. SANTANGELO, V. SILVESTRI, G. L. BROWN, D. A. GLASER and C. GRAVES: *Nuovo Cimento*, **7**, 222 (1958).

(\*) If parity is conserved in that kind of interaction.

The second event is a disappearance in flight of a particle of hyperonic mass ( $M = 2300 \pm 200$ , according to the change in ionization). From the disappearance point  $B$  with which a blob is associated, a  $\pi^+$  is emitted. This event is clearly not consistent with the kinematics of the  $\Sigma^+$ -decay. The  $\pi^-$  is emitted in the forward direction and is relatively slow.  $T_\pi = 32$  MeV. This energy follows both from ionization measurements and from the rest-range. It comes to rest and undergoes the usual decay. Since from the parent star  $A$ , a negative pion is emitted, the disappearing particle should be assumed to be a  $\Sigma^+$ -hyperon. It has kinetic energy of 52 MeV. A drawing of it is shown in Fig. 9).

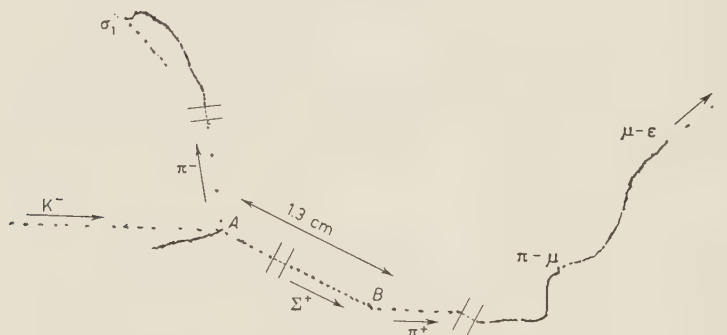


Fig. 9.

One possible explanation of this event, the process  $\Sigma^+ + n \rightarrow \pi^+ + \Lambda^0 + n$  can be ruled out because of energy conservation arguments. Another explanation would be, that the event represents a decay where the  $\pi^+$ -meson undergoes a single deflection within the first fraction of a micron. This would have escaped observation. We wish to mention another possibility, namely the production of a short range excited fragment. One can assume that the  $\Sigma^+$  produced an excited fragment, the  $\Lambda$  of which undergoes the neutral decay and the  $\pi^0$  makes a charge exchange inside the fragment.

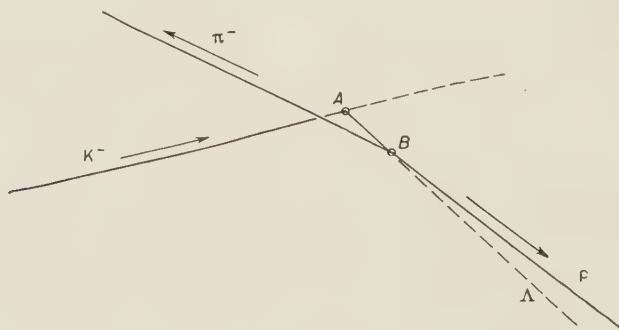


Fig. 10.

A drawing of the last in the series of rare events is shown in Fig. 10. A  $K^-$  produces a «stop» in flight  $A$ . In the immediate neighbourhood of the



$K^-$ -track disappearance point  $B$  a  $\Lambda$ -decay is observed. (Distance about 23  $\mu$ m). It could be shown that the line of flight of the  $K^-$  and that of the  $\Lambda$  intersect within narrow limits. Thus both events must be provided with one explanation, and can be interpreted as a  $K^-$ -absorption in flight leading to no charged prong, but giving rise to a  $\Lambda$ -emission. The emission angle of the  $\Lambda$  with respect to the  $K^-$ -direction of flight is  $60^\circ$ .  $T_K$  is 69 MeV and  $T_\Lambda = 89$  MeV. This event is not compatible with the kinematics of the reaction

$$K^- + p \rightarrow \Lambda + \pi^0$$

or

$$K^- + p \rightarrow \Sigma^0 + \pi^0$$

on a free proton. It must be due to a  $K^-$ -absorption by a complex nucleus.

#### RIASSUNTO (\*)

Si sono analizzate 415 interazioni in volo di mesoni  $K^-$  con nuclei complessi dell'emulsione nucleare. Confrontando i nostri risultati con quelli ottenuti da ALVAREZ dagli assorbimenti a riposo  $K^-$ -protoni liberi si deve concludere che si ha una significativa maggior frazione di iperoni  $\Lambda$  prodotti direttamente dalla reazione  $K^- + N \rightarrow \Lambda + \pi$  per le nostre stelle in volo (energia cinetica media dei mesoni interagenti 86 MeV) di quanto non ci si debba aspettare trasferendo i risultati di ALVAREZ ai nuclei composti, nell'ipotesi della conservazione dello spin isotopico. Se la frazione dei  $\Lambda$  prodotti direttamente crescesse con l'aumento dell'energia dei  $K^-$ , ci si dovrebbe attendere anche un aumento reale della produzione diretta dei  $\Lambda$  negli assorbimenti a « riposo » dei  $K^-$  nell'emulsione nucleare, a causa del moto di Fermi dei nucleoni. Altri argomenti trattati nel presente lavoro sono lo spettro energetico e le probabilità di assorbimento dei pioni e degli iperoni  $\Sigma$ , nonché il numero relativo di iperframmenti osservati per iperone  $\Lambda$  prodotto.

---

(\*) Traduzione a cura della Redazione.

## Energetic Heavy Fragments Emitted from Nuclear Stars.

S. NAKAGAWA, E. TAMAI and S. NOMOTO (\*)

*Department of Physics, Rikkyo (St. Paul's) University  
Ikebukuro, Tokyo, Japan*

(ricevuto l'11 Aprile 1958)

**Summary.** — The authors have investigated the heavy nuclear fragments ( $Z \geq 3$ ) emitted in the cosmic ray stars of heavy nuclei (Ag, Br) in emulsion by the method of charge determination which was carried out by measuring their track width. It was found that a majority of the fragments were ejected by the nuclear evaporation process, but that also there was a small number of the energetic fragments ( $Z \geq 3$ ) not explained by this process. In the present paper are described these energetic ones emitted in the stars (due to Ag or Br nuclei) induced by 6.2 GeV protons from the Bevatron. The charge distribution, angular distribution, and energy spectra of those particles were determined. The angular distribution shows strong collimations in the direction of the primary, and significantly differs from that of the evaporated (slow) fragments. The charge distribution gives an exponential decrease with increase in the charge and is similar in form to that of the evaporation process. It seems that the energetic fragments may not be produced by the evaporation process nor by the direct knock-on processes by the primary. It is probable that they may be ejected as the result of intense local heating near the surface of the nucleus during the process of nuclear cascade.

### 1. — Introduction.

Several investigators <sup>(1-5)</sup> have observed among the heavy nuclear fragments ejected from the nuclear stars produced by cosmic rays or accelerator beams, those with kinetic energies much greater than that which can be ac-

(\*) Now at Japan Atomic Energy Research Institute.

(1) S. O. C. SØRENSEN: *Phil. Mag.*, **42**, 325 (1951).

(2) D. D. PERKINS: *Proc. Roy. Soc., A* **203**, 399 (1950).

(3) B. A. MUNIR: *Phil. Mag.*, **1**, 355 (1956).

(4) S. J. GOLDSACK, W. O. LOCK and B. A. MUIR: *Phil. Mag.*, **2**, 149 (1957).

(5) O. V. LOZHKIN and N. A. PERFILOV: *Žu. Èksper. Teor. Fiz.*, **3**, 913 (1956).

counted for in terms of the electrostatic repulsion of the residual nucleus. The angular distribution of these particles has a peak in the forward direction, and is very different from that of slower fragments due to the evaporation process. It was noted that the emission of such energetic heavy fragments, the aggregate of nucleons from the nucleus, is itself very interesting, and suggests the existence of a long range force which agglomerates several nucleons and is responsible for fragment emission.

The authors have also found energetic heavy fragments in determining the charges of prongs from the stars produced by cosmic rays by the method of track width measurement<sup>(6,7)</sup>. In this paper a further investigation was made of these high energy fragments using the same method of charge determination. However, in the case of cosmic ray stars, the incident particle energy usually can not be accurately measured, so in this case the observations were made using nuclear plates irradiated by the 6.2 GeV proton beam with the help of the Bevatron Group. The charge, energy, and angular distributions of these particles ( $Z \geq 3$ ) are described, and the features of emission types different from evaporated fragments are examined.

## 2. — Experimental Procedure.

The experiments were carried out on the stacks of G-5 pellicle emulsions, 600  $\mu\text{m}$  thick (3 in.  $\times$  3 in.), irradiated by protons with energy of 6.2 GeV from the Bevatron at Berkeley and exposed to cosmic rays at high altitude. The beam intensity of the Bevatron was of the order of  $10^5$  protons per square cm per pulse and the exposure was for one pulse. The beam was allowed to pass through the plates parallel to one edge and in the plane of the emulsion so that almost horizontal proton tracks were obtained. As it is difficult to identify the stars due to light nuclei in the emulsion, only the stars due to Ag and Br were measured, by selecting those which had more than 8 prongs (grey tracks + black tracks). As was described in previous papers<sup>(6,7)</sup>, the charges of heavy fragments were determined by measuring the mean width of the end portion of their tracks with dip angles less than  $12.5^\circ$  before processing the emulsions.

In some cases the following methods of measurement were also used:

- (i)  $\delta$ -ray counting,
- (ii) thin-down length.

<sup>(6)</sup> S. NAKAGAWA, E. TAMAI, H. HUZITA and K. OKUDAIRA: *Journ. Phys. Soc. Japan*, **12**, 747 (1957).

<sup>(7)</sup> S. NAKAGAWA, E. TAMAI, H. HUZITA and K. OKUDAIRA: *Journ. Phys. Soc. Japan*, **11**, 191 (1956).

### 3. - Experimental results.

3'1. *Separation of energetic heavy fragments from slow fragments.* - About 1400 stars (with  $> 8$  prongs) were examined in an emulsion irradiated by the 6.2 GeV proton beam, and 143 measurable heavy fragments ( $Z \geq 3$ ) ejected from these stars were observed. Table I gives the ratios of the number of the Li fragments emitted in the forward direction to those emitted backward with respect to the proton beam for several energy regions. It shows that the Li fragments

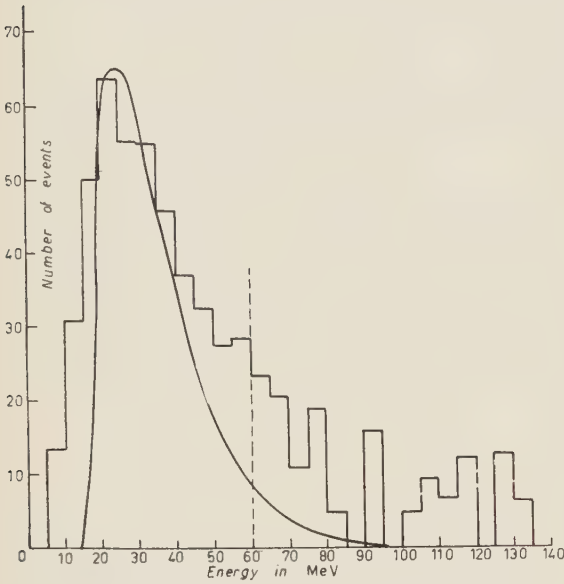


Fig. 1. - Energy distribution of the Li fragments observed in 1400 stars with 9 or more prongs.

TABLE I.

Energy region (MeV)	Forward	Backward
5 - 15	2	8
15 - 25	12	13
25 - 35	15	9
35 - 45	12	6
45 - 60	9	10
60 - 70	7	2
70 - 80	6	0
80 - 100	4	0
100 - 120	6	0



of low energies (kinetic energy  $< 60$  MeV) are emitted isotropically, while the energetic ones ( $\geq 60$  MeV) are favored in the forward direction. In our previous paper <sup>(6)</sup> it was reported that the slower fragments are emitted due to the evaporation process, so the fast fragments might be due to a different type of process. Fig. 1 and Fig. 2 show the energy spectra of Li and Be fragments, respectively. The solid curves in these figures represent the distribution of evaporated particles, so the figures indicate certainly the existence of a fast group. These fast

particles can probably be separated from the slower ones, at a kinetic energy of about 10 MeV per nucleon. The properties of this so-called fast group were examined.

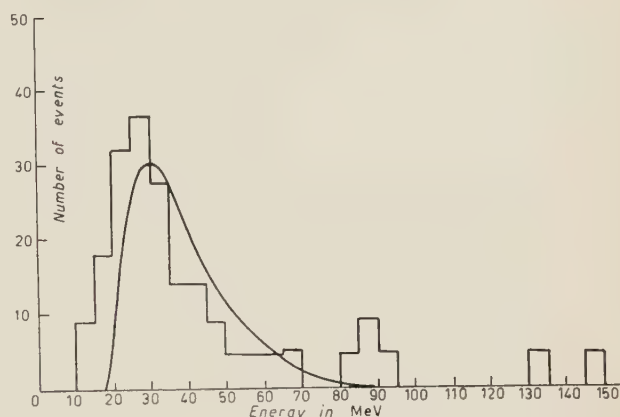


Fig. 2. — Energy distribution of the Be fragments in 1400 stars with 9 or more prongs.

3'2. *Angular distribution of fast fragments.* — By means of the above criterion, 80 fast heavy fragments ( $Z \geq 3$ ) were observed in about 5000 stars

produced by the Bevatron beam, and their angular distributions were observed. The incident particles could be easily distinguished in the nuclear plates exposed to the accelerator beam. In our case, the plates were exposed to the incident protons so as to be parallel to the emulsion surface, and the dip angles of the measurable fragments were less than  $12.5^\circ$ , since a projected angle between the track of a heavy fragment and the direction of motion of the incident particle approximately indicates a true angle. Fig. 3 gives the angular

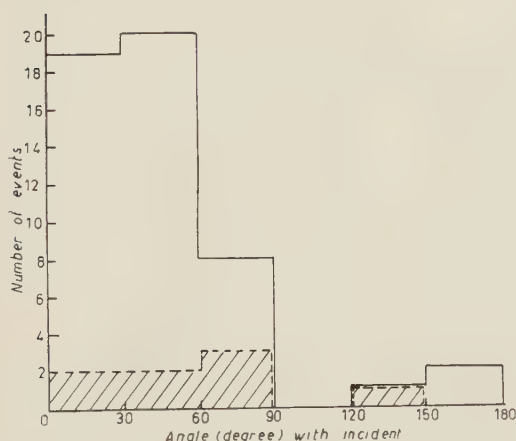


Fig. 3. — Angular distribution of fast Li fragments. The shaded area shows the angular distribution obtained from cosmic ray data.

distribution of fast Li fragments, and Fig. 4 that of fast fragments of charge  $Z \geq 4$ . In both figures, collimations appear in the direction of the primary, and this fact is a distinct discrepancy in the angular distribution of slow fragments.

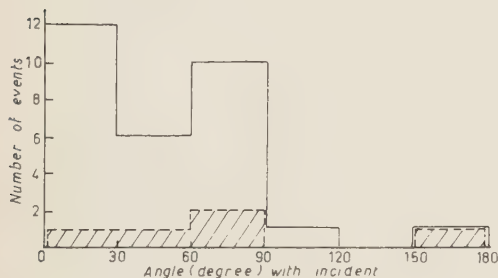


Fig. 4. — Angular distribution of fast fragments of charge  $Z \geq 4$ . The shaded area shows the angular distribution obtained from cosmic ray data.

The ratios of the number of particles in the forward and backward directions with respect to the incident protons for the Li group and the group of charge  $Z \geq 4$  are equal to 47 to 3 and 28 to 2, respectively. These ratios were obtained in the laboratory system. The shaded areas in Fig. 3 and Fig. 4 show the angular distribution of fast fragments emitted from cosmic ray stars. Distinct anisotropy is also shown in this case.

**3.3. Charge distribution of fast fragments.** — The charge distribution was investigated in 80 fast heavy fragments ( $Z \geq 3$ ). The number of fragments for charge  $Z$  is shown in Table II. These frequencies were corrected for:

- (i) geometrical loss of long tracks out of the emulsion layer,
- (ii) restriction in dip angle ( $\theta \leq 12.5^\circ$ ), and
- (iii) location of star in the emulsion,

on the assumption that the distribution of tracks is isotropic in the forward hemisphere with respect to the proton beam. This assumption was based on the angular distributions shown in Sect. 3.2 and seems to be approximately correct. The corrected frequency of fast heavy fragments ( $Z \geq 3$ ) is about 0.05 per star, and this value corresponds to 10% of the frequency of slow

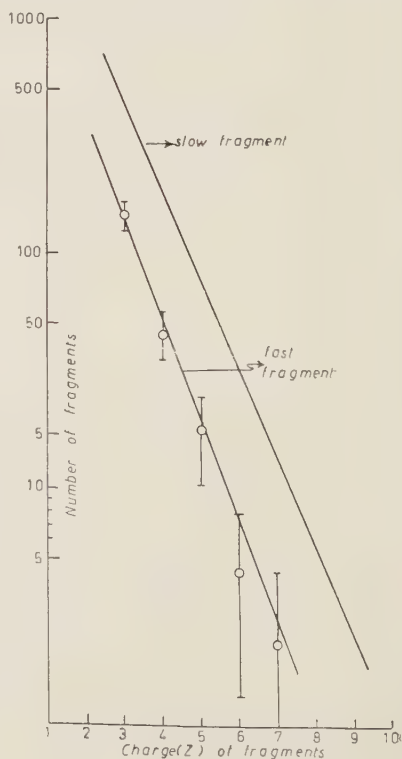


Fig. 5. — Charge distributions of fast and slow heavy fragments.

heavy fragments (<sup>6</sup>). Fig. 5 shows the charge distributions of fast fragments and also slow fragments described in the previous paper (<sup>6</sup>). The two curves seem to be similar in form, and show an exponential decrease with increasing charge  $Z$ , although the statistical errors are large in the region of the higher charges. This decrease may be approximately represented by the following formula:

$$F \propto \exp [-Z],$$

where  $F$  is the frequency of the fast heavy fragment of charge  $Z$ .

TABLE II.

Charge ( $Z$ )	3	4	5	6	7	8
Observed frequency	50	19	6	2	1	2
Corrected frequency	$144.7 \pm 20.5$	$45.5 \pm 10.4$	$17.5 \pm 7.2$	$4.55 \pm 3.2$	$2.27 \pm 2.27$	$5.22 \pm 3.68$

3.4. *Energy distribution of fast fragments.* — The energies of the fast heavy fragments were obtained by measuring the ranges of their tracks in emulsion.

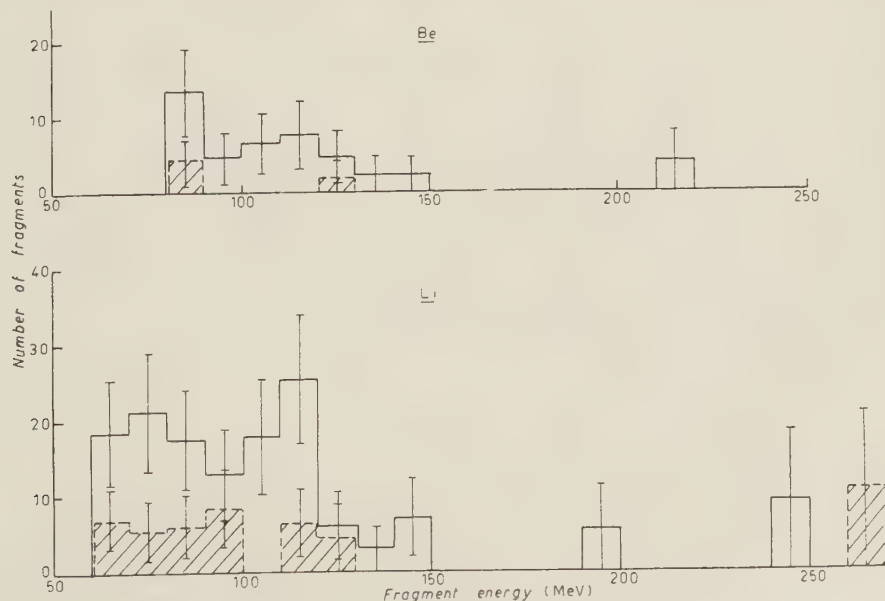


Fig. 6. — Energy distribution of fast fragments of  $Z = 3, 4$ .

Although an ambiguity exists in the application of the range energy relationship<sup>(\*)</sup> (the mass number of the fragment was taken as  $A = 2Z$ ), such uncertainty of energies of the fragments does not appreciably change the energy distribution.

Fig. 6 and Fig. 7 show the energy distributions of the fast fragments for the charge  $Z=3, 4, 5, 6, 7$  and  $8$ . In these figures, the shaded areas represent the data of fast fragments produced in the cosmic ray stars. From these figures, it is found that the energy region of fast fragments ( $Z \geq 3$ ) extends from 60 MeV to 250 MeV, and their average energy is about 120 MeV.

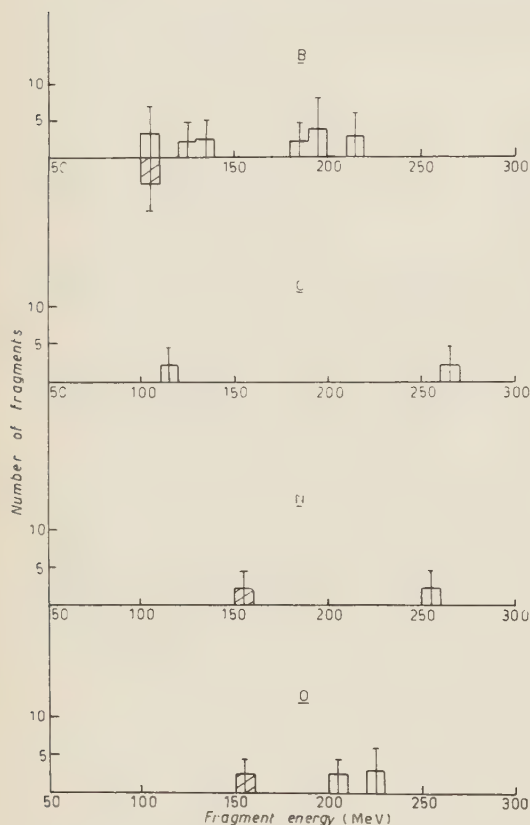


Fig. 7. — Energy distribution of fast fragments of  $Z = 5, 6, 7, 8$ .

**3.5. Characteristics of the stars associated with the emission of fast fragments.** — Out of a total number of 5 000 stars with prongs  $\geq 9$ , 73 stars were found from which fast fragments with charge  $Z \geq 3$  emerge. Of these, six stars emit simultaneously two or three fast fragments.

Using the following criteria<sup>(\*)</sup>, the tracks of particles emitted from stars are divided into three groups according to their grain density as compared with minimum grain density  $g_{\min}$ :

- (i) « Thin » tracks,  $g_{\min} \leq g \leq 1.4g_{\min}$  (shower particles),
- (ii) « Grey » tracks,  $1.4g_{\min} < g < 6.8g_{\min}$ ,
- (iii) « Black » tracks,  $g > 6.8g_{\min}$ .

(\*) C. M. G. LATTES, G. P. S. OCCHIALINI and C. F. POWELL: *Proc. Phys. Soc.*, **61**, 173 (1948).

(\*) J. G. WILSON: *Progress in Cosmic Ray Physics*, I (Amsterdam, 1952), p. 6.



The numbers of the « grey » and « black » tracks from a star are represented by the symbol  $N_g$  and  $N_b$ , respectively, and the number of shower particles

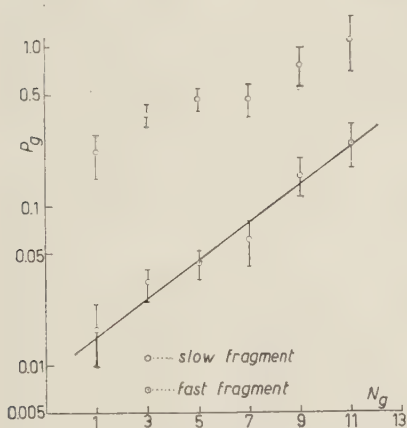


Fig. 8. — Probability of the ejection of a fast fragment as a function of  $N_g$ .

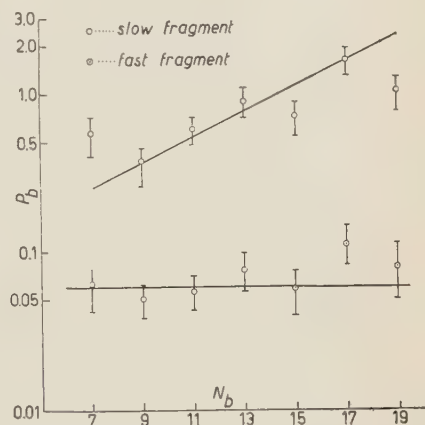


Fig. 9. — Probability of the ejection of a fast fragment as a function of  $N_b$ .

by  $n_s$ . The probability,  $P_g$ , that a star with a given  $N_g$  has an associated fast heavy fragment ( $Z \geq 3$ ) is shown in Fig. 8, and for the sake of a comparison,  $P_g$  for the emission of slow fragments is also given in this figure. Fig. 8 indicates clearly a linear rise in the emission probability of fast fragments with increase in  $N_g$ , while such a tendency is hardly seen in the case of slow fragments. Fig. 9 represents the emission probability  $P_b$  of heavy fragments from a star with a given  $N_b$ . It appears that  $P_b$  for the slow group rises with increase in  $N_b$ , while  $P_b$  for the fast group seems to be independent of  $N_b$ . The emission probability  $P_s$  versus  $n_s$  is given in Fig. 10. From this figure, it is evident that  $P_s$  has no connection with the  $n_s$  in either the slow or fast case.

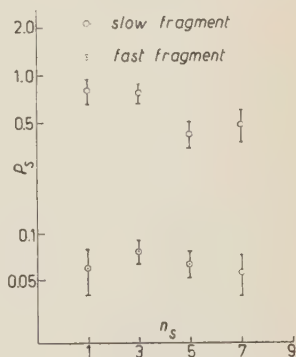


Fig. 10. — Probability of the ejection of a fast fragment as a function of  $n_s$ .

#### 4. — Discussion and conclusion.

The results of the analysis of fast heavy fragments may be summarized as follows:

a) The emission probability of fast heavy fragments ( $Z \geq 3$ ) amounts to 0.05 in the interaction of 6.2 GeV protons with heavy nuclei in the emulsion.

b) The charge distribution shows an exponential decrease with an increase in the charge  $Z$ .

c) The angular distribution is highly anisotropic and shows a collimation in the direction of the primary.

d) Their energies lie all in the interval from 60 MeV to 250 MeV and do not show any dependence on their charge. Their average energy is about 120 MeV.

e) The emission probability rises with an increase in  $N_g$ , but indicates no strong connection with  $N_b$  and  $n_s$ .

f) No evidence was found of instability of the fast fragments, such as a secondary electron from the end of a track or a hammer track due to  $^8\text{Li}$ .

As mentioned before in a previous paper (<sup>6</sup>), slow fragments are emitted by the evaporation process. The above features of fast fragments are quite different from those of evaporated particles, and another type of emission mechanism may be considered. First, there is the possibility of the emission of a fast fragment in a direct « knock-on » collision of the primary proton with an aggregate of nucleons in a heavy nucleus. Assuming the collision between a free proton and a free aggregate, the relationship of the kinetic energy  $E_f$  of a fast fragment to  $\theta$ , the angle which it makes with respect to the primary, is represented by the following formula,

$$E_f = E_p \cdot \frac{2m_p M_f (\gamma + 1) \cos^2 \theta}{(m_p \gamma + M_f)^2 - m_p^2 (\gamma^2 - 1) \cos^2 \theta}, \quad \gamma = \frac{1}{\sqrt{1 - \beta^2}},$$

where  $M_f$  is the mass of a fast fragment and  $m_p$  that of an incident proton.  $E_f$  versus  $E_p = 6.2$  GeV is shown in Fig. 11 and there is no dependence of the fast fragment energy on  $\theta$  in our experimental data. As SÖRENSEN (<sup>1</sup>) suggested, it seems that the majority of the fast fragments can not have been ejected as a result of a direct collision with the primary proton. Thus it appears more reasonable to assume that most of the fast fragments have been emitted by interactions with secondary nucleons or  $\pi$ -mesons in the nuclear cascade process. This hypothesis is supported by the result (c) mentioned above, that is, the emission probability of fast fragments rises with an increase in  $N_g$ , because the cascade particles produce grey tracks in the emulsion. In addition to this, according to cosmic ray data (<sup>10</sup>) the average energy of the grey track appears to be almost independent of primary energy, and is about

(<sup>10</sup>) U. CAMERINI, J. H. DAVIES, P. H. FOWLER, C. FRANZINETTI, W. O. LOCK, D. H. PERKINS and G. YEKUTIELI: *Phil. Mag.*, **42**, 1241 (1951).

150 MeV; and this value seems to be comparable to the average energy of the fast fragment in the present experiments. Also, the angular distribution of grey particles with respect to the primary shows collimation in the direction of the primary <sup>(10)</sup>. This fact is in agreement with the observations on fast fragments.

Recently radiochemical studies of a wide variety of products resulting from the bombardment of medium and heavy elements have been reported <sup>(11,12)</sup>. At several GeV the mechanism of fragmentation is thought to be important. In particular, the fragmentation is considered as proceeding by knock-on cascades which break numbers of neighbouring nucleon-nucleon bonds and thus produce considerable local disturbances in the nucleus. Our observed fast fragments seem to be well explained by this fragmentation mechanism.

However, the fact that the heavy fragments—the aggregates of nucleons with either low or high energies—are emitted from the nucleus suggests that there is a tendency for some nucleons to agglomerate and to form a cluster in the nucleus, at least in the highly excited states. Our measured charge distribution of emitted fragments shows an exponential decrease with increasing charge  $Z$ . This condition seems to resemble somewhat the relative abundance of nuclei in the system represented by the «grand ensemble» in the equilibrium theory <sup>(13,14)</sup>, but the data are not sufficient to discuss it at length. Further work has now been undertaken to investigate this problem, in particular with regard to the evaporation process.

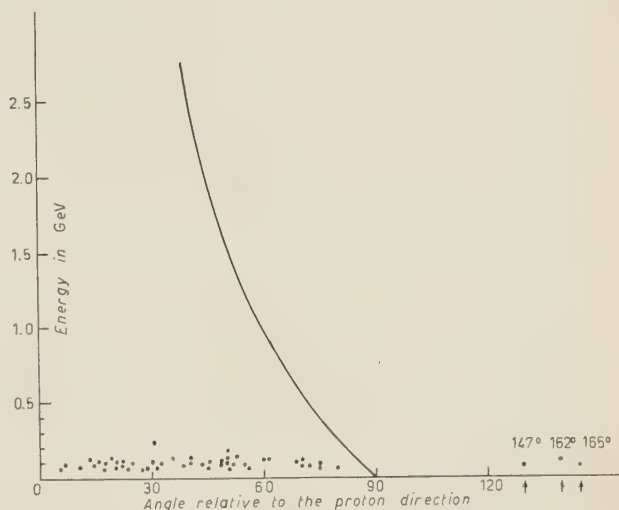


Fig. 11. — Dependence of the energy of the fast fragment with  $Z=3$  on the angle with the direction of the 6.2 GeV proton beam. (The curve is calculated from the formula for elastic scattering for a proton energy of 6.2 GeV).

<sup>(11)</sup> R. WOLFGANG, E. W. BAKER, A. A. CARETTO, J. B. CUMMING, G. FRIEDLANDER and J. HUDIS: *Phys. Rev.*, **103**, 304 (1956).

<sup>(12)</sup> N. T. PORILE and T. SUGARMAN: *Phys. Rev.*, **107**, 1422 (1957).

<sup>(13)</sup> R. A. ALPHER and R. C. HERMAN: *Rev. Mod. Phys.*, **22**, 153 (1950).

<sup>(14)</sup> D. TER HAAR: *Elements of Statistical Mechanics* (New York), p. 311.

\* \* \*

We should like to express our sincere thanks to Professor E. J. LOFGREN and the members of the Radiation Laboratory at Berkeley, California, who made the exposure of the nuclear plates possible; to Mr. K. OKUDAIRA and Mr. M. ODA for helpful discussions; to Miss N. KUROKI and Miss K. KAWAZOE for their assistance with the scanning. The present work has been supported in part by the Scientific Research Fund from the Ministry of Education of Japan.

---

#### RIASSUNTO (\*)

Col metodo della determinazione della carica applicato con la misurazione della larghezza delle tracce, gli autori hanno studiato i frammenti nucleari pesanti ( $Z \geq 3$ ) emessi nelle stelle dei raggi cosmici da nuclei pesanti (Ag, Br) nell'emulsione. Si è trovato che la maggioranza dei frammenti sono emessi nel processo di evaporazione nucleare, ma anche che resta un piccolo numero di frammenti con  $Z \geq 3$  non attribuibili a quel processo. Nel presente lavoro si descrivono i frammenti con  $Z \geq 3$  emessi nelle stelle (da nuclei di Ag o Br) provocate dai protoni di 6.2 GeV del Bevatrone. Si sono determinati la distribuzione della carica, la distribuzione angolare e gli spettri d'energia di tali particelle. La distribuzione angolare mostra forte collimazione nella direzione del primario e differisce significativamente da quella dei frammenti (lenti) evaporati. La distribuzione della carica mostra una diminuzione esponenziale con l'aumento della carica ed è simile nella forma a quella del processo di evaporazione. Sembra che i frammenti dotati di alta energia non possano esser prodotti nè nel processo di evaporazione nè nei processi di knock-on diretti del primario. È probabile che siano emessi per effetto dell'intenso riscaldamento totale vicino alla superficie del nucleo durante il processo della cascata nucleare.

---

(\*) Traduzione a cura della Redazione.



## Dynamics of an Elastic Ellipsoid.

R. K. OSBORN and E. D. KLEMA

*University of Michigan - Ann Arbor, Michigan*

(ricevuto il 9 Maggio 1958)

**Summary.** — The present investigation is an attempt to provide a dynamical basis for the kinematical scheme employed previously for the empirical correlation of certain nuclear data. The primary purpose of this paper is the delineation of the dynamical system itself. Particular attention is paid to the following points: 1) The basic assumptions required for the specification of the system. These may be divided roughly into two groups, those employed in the definition of the independent degrees of freedom chosen for the description of the system and those required for at least partial characterization of relevant potentials. The former are of principal importance in the formulation of the kinetic energy operators appropriate to the choice of degrees of freedom and are dealt with in detail. The latter, being less germane to the purpose of this paper, are treated more or less summarily. 2) The detailed development of the kinetic energy of this model. It is carried out without approximation; i.e., the formulation of this aspect of the physical implications of the model is quite rigorous. Calculations within the model must ultimately, of course, require resort to approximation. 3) The physical significance of two different representations employable for partial diagonalization of the Hamiltonian. 4) The close kinematical connection between the system considered herein and the hydrodynamical model. 5) The extent to which the dynamical system incorporates the kinematical scheme previously used for data correlation. Directions of feasible, and perhaps fruitful, generalization are indicated with the suggestion of possibly significant implications for the description of nuclear collective behavior in regions in which neither purely vibrational nor purely rotational characteristics are to be expected.

### 1. — Introduction.

In previous papers, hereafter referred to as I <sup>(1)</sup>, II <sup>(2)</sup>, III <sup>(3)</sup> and IV <sup>(4)</sup>, attempts have been made to exploit the kinematics of the extreme single-

(<sup>1</sup>) R. K. OSBORN and E. D. KLEMA: *Phys. Rev.*, **100**, 822 (1955).

(<sup>2</sup>) E. D. KLEMA and R. K. OSBORN: *Phys. Rev.*, **103**, 833 (1956).

(<sup>3</sup>) R. K. OSBORN and E. D. KLEMA: *Nucl. Phys.*, **2**, 454 (1956/57).

(<sup>4</sup>) E. D. KLEMA and R. K. OSBORN: *Nucl. Phys.*, **3**, 571 (1957).

particle model coupled to a rigidly rotating core for purposes of correlating a relatively wide range of nuclear data. In that work no effort was devoted to validating the model within the context of a dynamical scheme. In fact, precisely the contrary view was adopted; namely that the empirical correlations themselves might lead to sufficient insight into the interrelationships among the few dynamical parameters invoked for the purpose of exhibiting the correlations to suggest an appropriate direction in which to proceed in the search for such a dynamical scheme.

It is the purpose of this paper to present the detailed development of a dynamical model which is characterized by the following points of interest:

a) The basic physical assumptions required to limit the number of degrees of freedom of a complex system to a small set for detailed consideration may be clearly and simply stated in both intuitive and analytical terms. Furthermore, since it is these assumptions which essentially define the degrees of freedom singled out for close examination, it follows that these degrees of freedom and their corresponding dynamical variables are also clearly interpretable.

b) Given the basic assumptions which delineate the physical object to which the model corresponds, the subsequent analysis proceeds rigorously. In particular, the kinetic energy operator to be employed in the dynamical description of the core oscillations is obtained without recourse to a small oscillation approximation. Thus in this instance also it is possible to place the burden of success or failure directly upon the model itself; *i.e.* the difficulty is avoided of assessing to what extent a given area of disagreement between prediction and experiment is model-dependent and to what extent dependent solely upon mathematical approximations invoked *within* the model.

c) Because the severest assumptions employed herein are restricted essentially to the description of the core itself, the transition from the weak to strong coupling situations as one moves away from closed major shell configurations must in some sense be internal to the model; and, because of point b), must also be readily observable, at least in principle.

d) In the model employed herein it is assumed that the odd particle of an odd- $A$  nucleus *does not* share in the *constraints* employed to define the collective behavior of the core. Of course the odd particle is presumed to interact (and strongly) with the core via an assumed potential which, for purposes of maintaining mathematical rigor in the analysis, has been chosen to be an appropriate modification<sup>(5)</sup> of the harmonic oscillator potential. Furthermore, it is shown below that the kinematics of the core-plus-particle

(5) S. G. NILSSON: *Dan. Mat. Fys. Medd.*, **29**, no. 16 (1955).

coupling as developed in the context of the hydrodynamical model <sup>(6)</sup> is identical to that exhibited herein, thus rendering some interpretative generalizations <sup>(7)</sup> of the hydrodynamical model somewhat obscure. In fact, the close kinematical correspondence of the present model and the hydrodynamical model makes possible direct comparison between them which is, in our opinion, illuminating.

Sect. 2 of this paper presents the detailed physical and analytical description of the model itself as well as the derivation of the corresponding Hamiltonian implied by the model. Sect. 3 is devoted to an examination of the physical significance and the operator representatives of various relevant dynamical variables. In this connection also considerable attention is given to different representations appropriate for partial diagonalization of the Hamiltonian. Further, in this section a detailed comparison with the hydrodynamical model is presented. Sect. 4 contains an evaluation of the extent to which the dynamics of the present model incorporates the kinematical scheme previously resorted to, and hence also the empirical correlations previously observed. Sect. 5 consists of a summarizing discussion.

## 2. — The hamiltonian.

In order to achieve minimal complexity consonant with analytical rigor we take as our model of a nucleus the following set of assumptions:

1) A nucleus for which both  $A$  and  $Z$  are even is presumed to be completely characterizable in terms of the four dynamical variables;  $\theta_1, \theta_2, \theta_3$ , and  $\gamma$ : the three Euler angles required to locate the principal axes of the body relative to a space-fixed co-ordinate system with origin at the center of mass, and the shape variable  $\gamma$ , which is defined to be the ratio of the semi-axis along the symmetry axis of an axially-symmetric ellipsoid to the radius of the sphere from which the ellipsoid was obtained by a volume-preserving deformation. It is further supposed that only a certain fraction of the uniformly distributed nuclear matter participates in the collective behavior of the nucleus, and that this fraction is measured by the parameter  $k$ , previously defined in II and IV. It should be pointed out that the restriction to axially symmetric systems is adopted not because the asymmetric system cannot be handled with the same analytic thoroughness as the symmetric one, but rather because it is felt that the additional complexity entailed in the analysis of the asymmetric case would tend more to obscure than to clarify the specific issues to be dealt with

<sup>(6)</sup> A. BOHR: *Dan. Mat. Fys. Medd.*, **26**, no. 14 (1952).

<sup>(7)</sup> A. K. KERMAN: *Dan. Mat. Fys. Medd.*, **30**, no. 15 (1956).

herein. Thus we set aside the discussion of the asymmetric case for future consideration.

2) A nucleus for which  $A$  is odd is presumed to be completely characterizable in terms of the same degrees of freedom as above plus three positional co-ordinates,  $X_1$ ,  $X_2$  and  $X_3$ , of the odd particle *measured relative to the space-fixed* co-ordinate axes,  $e_1$ ,  $e_2$ , and  $e_3$ . Of course this odd particle also has the degree of freedom appropriate to a particle with intrinsic spin one-half. It is further presumed that the particle energy is dependent upon a spin-orbit interaction and an « orbit-orbit interaction » <sup>(5)</sup> so chosen that for a spherical core the conventional level structure <sup>(8)</sup> is realized, and an oscillator potential which has an anharmonicity consonant with the symmetry of the core.

Clearly we may obtain the Hamiltonian for either case 1) or 2) by obtaining it first for case 1), then simply adjoining a particle Hamiltonian which requires special attention only in the development of the interaction energy. We therefore devote our attention initially to the dynamical description of the variables  $\theta_i$  and  $\gamma$  which are purported to characterize the collective behavior of the  $A-1=A_c$  particles that comprise the core of an odd- $A$  nucleus.

To this end we define  $y_k^\sigma$  to be the  $k$ -th component of the position vector of the  $\sigma$ -th particle *measured* relative to the  $e$  (space-fixed) basis. Then, assuming that the masses of all nucleons are the same, the core kinetic energy is

$$(1) \quad T_c = \frac{m}{2} \sum_{\sigma=1}^{A_c} \sum_{k=1}^3 (\dot{y}_k^\sigma)^2.$$

We now transform from a space to a body description of the positions of the core nucleons according to the rotation  $R(\theta_i) = R(\theta_3)R(\theta_2)R(\theta_1)$ ; where  $R(\theta_1)$  is a positive rotation through  $\theta_1$  about the space  $e_3$ -axis,  $R(\theta_2)$  is a second rotation about the new  $e$ -axis, and  $R(\theta_3)$  is a third rotation through  $\theta_3$  about the ultimate  $e_3$ -axis. Thus

$$(2) \quad t_1) \quad y_k^{\sigma'} = \sum_j R_{kj}(\theta_i) y_j^\sigma.$$

The angles  $\theta_i$  are to be defined by the constraints,

$$(3) \quad c_1) \quad \sum_{\sigma=1}^{A_c} y_k^{\sigma'} y_j^{\sigma'} = \sum_{\sigma=1}^{A_c} \sum_{l=1}^3 \sum_{m=1}^3 R_{kl} y_l^\sigma R_{jm} y_m^\sigma = 0 \quad \text{if } k \neq j.$$

We now perform a second, stretching, transformation such that if the core nucleon distribution has prolate shape, then each particle has its 3-component so shrunk and its 1 and 2-components so stretched that in terms of these last

<sup>(8)</sup> M. GOEPPERT-MAYER and J. H. D. JENSEN: *Elementary Theory of Nuclear Shell Structure* (New York, 1955).



co-ordinates the distribution appears spherical; *i.e.*

$$(4) \quad t_2) \quad y_k^{\sigma''} = \sum_j S_{kj} y_j^{\sigma'},$$

where

$$(5) \quad S = \begin{pmatrix} \gamma^{\frac{1}{2}} & 0 & 0 \\ 0 & \gamma^{\frac{1}{2}} & 0 \\ 0 & 0 & \gamma^{-1} \end{pmatrix}.$$

The variable  $\gamma$  is to be determined by the constraints

$$(6) \quad c_2) \quad \sum_{\sigma=1}^{A_c} (y_1^{\sigma''})^2 = \sum_{\sigma=1}^{A_c} (y_2^{\sigma''})^2 = \sum_{\sigma=1}^{A_c} (y_3^{\sigma''})^2 = \frac{1}{5} k A_c R_0^2,$$

where  $R_0$  is the radius of the undeformed core and  $k$  is the mass-fraction parameter which measures the fraction of the uniformly distributed nuclear mass which participates in collective behavior.

It is perhaps worthwhile to point out here that if the stretching transformation ( $t_2$ ) is generalized according to

$$(7) \quad S = \begin{pmatrix} \alpha^{-1} & 0 & 0 \\ 0 & \beta^{-1} & 0 \\ 0 & 0 & \gamma^{-1} \end{pmatrix},$$

where  $\alpha$ ,  $\beta$ , and  $\gamma$  are the ratios of the 1, 2, and 3 semi-axes of an ellipsoid to the radius of the sphere which represents the equilibrium shape of the core, then the analysis of more general core oscillations may be carried through in complete analogy to the treatment that follows for the simpler case of axially symmetric, volume-preserving oscillations.

The remaining degrees of freedom associated with the  $A_c$  nucleons of the core satisfy the constraints (not all independent),

$$(8) \quad c_3) \quad \dot{y}_k^{\sigma''} = 0 \quad \text{for all } k \text{ and all } \sigma.$$

These last constraints merely assert that the only motion the core nucleons experience relative to the co-ordinate system fixed along the principal axes of the body is that characterized by the time rate of change of  $\gamma$ .

One may invert the transformations to obtain

$$(9) \quad y_k^{\sigma} = \sum_{l,j} R_{kl}^T S_{lj}^{-1} y_j^{\sigma''},$$

and

$$(10) \quad \hat{y}_k^{\sigma} = \sum_{i=1}^3 \hat{\theta}_i \sum_{lj} \frac{\partial R_{kl}^T}{\partial \theta_i} S_{ij}^{-1} y_j^{\sigma} + \hat{\gamma} \sum_{lj} R_{kl}^T \frac{\partial S_{ij}^{-1}}{\partial \gamma} y_j^{\sigma}.$$

It is now a straightforward task to obtain the kinetic energy of the  $A_c$  nucleons of the core (or nucleus) in terms of the time derivatives of the variables  $\theta_i$  and  $\gamma$  in the form

$$(11) \quad 2T_c = \sum_{\mu\nu} g_{\mu\nu} \hat{q}^{\mu} \hat{q}^{\nu},$$

where we have defined

$$(\theta_1, \theta_2, \theta_3, \gamma) \equiv (q^1, q^2, q^3, q^4),$$

and where the « metric » tensor  $g_{\mu\nu}$  may be exhibited as the matrix

$$(12) \quad (g_{\mu\nu}) = \begin{pmatrix} A_1 \sin^2 \theta_2 + A_3 \cos^2 \theta_2 & 0 & A_3 \cos \theta_2 & 0 \\ 0 & A_1 & 0 & 0 \\ A_3 \cos \theta_2 & 0 & A_3 & 0 \\ 0 & 0 & 0 & \frac{A_s (2\gamma^3 + 1)}{4\gamma^3} \end{pmatrix}.$$

The quantities  $A_1$  and  $A_3$  are simply the moments of inertia of the spheroid about its 1 and 3-axes, respectively, *i.e.*

$$(13) \quad \begin{cases} A_1 = A_s \frac{\gamma^3 + 1}{2\gamma}, \\ A_3 = A_s \gamma^{-1}, \end{cases}$$

where  $A_s$  is the moment of inertia of a sphere of the same volume. The « element of volume » in this « metric » is

$$(14) \quad [A(g)]^{\frac{1}{2}} = [\det(g_{\mu\nu})]^{\frac{1}{2}} = \frac{A_s^2 (\gamma^3 + 1)(2\gamma^3 + 1)^{\frac{1}{2}}}{4\gamma^3} \sin \theta_2.$$

Finally, if  $g^{\mu\nu}$  is defined by

$$\sum_{\nu} g^{\mu\nu} g_{\nu\sigma} = \delta_{\mu\sigma},$$

then an appropriate, hermitian, kinetic energy operator may be obtained according to

$$(15) \quad T_c \rightarrow -\frac{\hbar^2}{2[A(g)]^{\frac{1}{2}}} \frac{\partial}{\partial q^{\mu}} \left( [A(g)]^{\frac{1}{2}} g^{\mu\nu} \frac{\partial}{\partial q^{\nu}} \right).$$

This expression may be most conveniently exhibited as

$$(16) \quad \left\{ \begin{array}{l} T_c = T(\theta, \gamma) + T(\gamma), \\ T(\theta, \gamma) = \frac{\hbar^2 \mathcal{L}^2}{2A_1} + \left( \frac{1}{A_3} - \frac{1}{A_1} \right) \frac{\hbar^2 \mathcal{L}_3'^2}{2}, \\ T(\gamma) = -\frac{2\hbar^2}{A_s} \frac{\gamma^3}{(\gamma^3 + 1)(2\gamma^3 + 1)^{\frac{1}{2}}} \frac{\partial}{\partial \gamma} \left( \frac{\gamma^3 + 1}{(2\gamma^3 + 1)^{\frac{1}{2}}} \frac{\partial}{\partial \gamma} \right). \end{array} \right.$$

The body components of the angular momentum operator,  $\mathcal{L}'_k$ , and its space components  $(^s)\mathcal{L}_k$ , are

$$\mathcal{L}'_k = -i \sum_j \Omega'_{kj} \frac{\partial}{\partial \theta_j},$$

$$(^s)\mathcal{L}_k = -i \sum_j \Omega_{kj} \frac{\partial}{\partial \theta_j},$$

$$(17) \quad \left\{ \begin{array}{l} \Omega = \begin{pmatrix} -\frac{\cos \theta_1 \cos \theta_2}{\sin \theta_2} & -\sin \theta_1 & \frac{\cos \theta_1}{\sin \theta_2} \\ -\frac{\sin \theta_1 \cos \theta_2}{\sin \theta_2} & \cos \theta_1 & \frac{\sin \theta_2}{\sin \theta_1} \\ 1 & 0 & 0 \end{pmatrix}, \\ \Omega' = \begin{pmatrix} -\frac{\cos \theta_3}{\sin \theta_2} & \sin \theta_3 & \frac{\cos \theta_3 \cos \theta_2}{\sin \theta_2} \\ \frac{\sin \theta_3}{\sin \theta_2} & \cos \theta_3 & -\frac{\sin \theta_3 \cos \theta_2}{\sin \theta_2} \\ 0 & 0 & 1 \end{pmatrix}. \end{array} \right.$$

These formulae for the operator representatives of the six angular momentum components are obtained most directly by performing infinitesimal rotations of the body about the six corresponding axes.

In order to complete the dynamical description of the collective behavior of the  $A_c$  nucleons comprising the core (excepting its dependence upon an interaction with an extra-core nucleon, if there is one), it is necessary to add a potential,  $V(\gamma)$ , which is presumed to depend only upon the shape of the core. Since it is not our purpose in this paper to enter into a detailed exam-

(<sup>9</sup>) H. NIELSEN: *Rev. Mod. Phys.*, **20**, 90 (1951).

ination of the nature of the core oscillations, but rather merely to exhibit a model which incorporates explicitly the kinematics previously invoked for purposes of empirical correlation of data and which further embraces implicitly a dynamical description of some of the parameters in terms of which the data were correlated, we eschew further consideration here of this potential energy.

However, it is necessary that the energy of interaction between the core and the extra-core nucleon be explicitly formulated. To this end (and in accordance with our comments above) we assume an oscillator potential of such a form that, in the rotating system,

$$(18) \quad V = \frac{m\omega^2}{2} \left[ \gamma(x_1'^2 + x_2'^2) + \frac{1}{\gamma^2} x_3'^2 \right].$$

Thus, in terms of the space co-ordinates of the particle, one has

$$(19) \quad \begin{cases} V &= V(\mathbf{x}, \gamma) + V(\mathbf{x}) + V(\mathbf{x}, \gamma, \theta), \\ V(\mathbf{x}) &= \frac{m\omega^2}{2} (\mathbf{x})^2, \\ V(\mathbf{x}, \gamma) &= \frac{m\omega^2}{2} (\mathbf{x})^2 \frac{(\gamma-1)^2(2\gamma+1)}{3\gamma^2}, \\ V(\mathbf{x}, \gamma, \theta) &= -\frac{m\omega^2}{2} (\mathbf{x})^2 \frac{\gamma^3-1}{3\gamma^2} 4 \left( \frac{\pi}{5} \right)^{\frac{1}{2}} \sum_m Y_2^m(\hat{\mathbf{x}}) D_{m,0}^2(\theta), \end{cases}$$

where  $(\mathbf{x})^2 = x_1^2 + x_2^2 + x_3^2$  and  $D_{m,0}^2(\theta)$  is that irreducible representation of the rotation group, defined in terms of the Euler angles previously discussed, which corresponds to a rotation from the space-fixed system to the body system.

Now, recalling the earlier comments about the assumed nature of the purely particle part of the system Hamiltonian, we may exhibit the complete Hamiltonian for the system as

$$(20) \quad \begin{cases} H &= H(\gamma) + H(\mathbf{x}) + H(\gamma, \theta) + H(\gamma, \mathbf{x}) + H(\gamma, \theta, \mathbf{x}), \\ H(\gamma) &= -\frac{2\hbar^2}{A_s} \frac{\gamma^3}{(\gamma^3+1)(2\gamma^3+1)^{\frac{1}{2}}} \frac{\partial}{\partial \gamma} \left( \frac{\gamma^3+1}{(2\gamma^3+1)^{\frac{1}{2}}} \frac{\partial}{\partial \gamma} \right) + V(\gamma), \\ H(\mathbf{x}) &= \frac{p^2}{2m} + \frac{m\omega^2}{2} (\mathbf{x})^2 - \hbar^2 \mathbf{DS} \cdot \mathbf{L} - \hbar^2 C L^2, \\ H(\gamma, \theta) &= \frac{\hbar^2 \mathcal{L}^2}{2A_1} + \left( \frac{1}{A_3} - \frac{1}{A_1} \right) \frac{\hbar^2 \mathcal{L}_3'^2}{2}, \\ H(\gamma, \mathbf{x}) &= \frac{m\omega^2}{2} (\mathbf{x})^2 \frac{(\gamma-1)^2(2\gamma+1)}{3\gamma^2}, \\ H(\gamma, \theta, \mathbf{x}) &= -\frac{m\omega^2}{2} (\mathbf{x})^2 \frac{\gamma^3-1}{3\gamma^2} 4 \left( \frac{\pi}{5} \right)^{\frac{1}{2}} \sum_m Y_2^m(\hat{\mathbf{x}}) D_{m,0}^2(\theta). \end{cases}$$



### 3. - Representations for partial diagonalization of $H$ .

It is perhaps obvious that the wave functions employed in the earlier empirical studies will serve here as one set of appropriate angular momentum wave functions for the partial diagonalization of the Hamiltonian derived above. However, both for the sake of completeness and because the question of the choice of representation is crucial to the comparison of the present model and the hydrodynamical model, we shall reconstruct the state vectors and re-examine their meaning in some detail.

We concern ourselves first with the kinematical part of the state vectors which describes the angular momenta of the system as coupled in a particular way. First, observing that  $\mathcal{F}^2 = (\mathcal{L} + \mathbf{J})^2$  and  $\mathcal{F}_3 = \mathcal{L}_3 + J_3$  commute with the total Hamiltonian (as they must) and that  $L^2$ ,  $J^2$ ,  $\mathcal{L}^2$ ,  $S^2$ , and  $L'_3$  commute with all parts of the Hamiltonian except  $H(\gamma, \theta, \mathbf{x})$ , we take as an initial choice of representation one which corresponds to the coupling scheme,

$$(21) \quad \begin{cases} \mathbf{L} + \mathbf{S} = \mathbf{J}, \\ \mathbf{J} + \mathcal{L} = \mathcal{F}, \end{cases}$$

and which diagonalizes the above operators.

If we define  $\chi_s^r$  by

$$(22) \quad \begin{cases} S^2 \chi_s^r = s(s+1) \chi_s^r, \\ S_z \chi_s^r = \tau \chi_s^r, \end{cases}$$

then

$$\chi_{jl}^m = \sum_{\tau} C(\tfrac{1}{2}lj; \tau m - \tau) Y_l^m(\hat{\mathbf{x}}) \chi_{\frac{1}{2}}^{\tau}$$

diagonalizes  $L^2$ ,  $S^2$  (with eigenvalue  $\frac{3}{4}$ ),  $J^2$  and  $J_z$ . Then since  $D_{MK}^{\lambda*}(\theta)$ , where

$$(23) \quad \begin{cases} D_{MK}^{\lambda}(\theta) = \exp[-iM\theta_1] d_{MK}^{\lambda}(\theta_2) \exp[-iK\theta_3], \\ d_{MK}^{\lambda}(\theta_2) = \sum_{s=0}^{\lambda-K} N_{MK}^{\lambda}(s) \left(\cos \frac{\theta_2}{2}\right)^{2\lambda-2s+M-K} \left(\sin \frac{\theta_2}{2}\right)^{K-M+2s}, \\ \text{and} \\ N_{MK}^{\lambda}(s) = (-1)^s \frac{[(\lambda+K)! (\lambda-K)! (\lambda+M)! (\lambda-M)!]^{\frac{1}{2}}}{(\lambda+M-s)! (\lambda-K-s)! (K-M+s)! s!}, \end{cases}$$

diagonalizes  $\mathcal{L}^2$ ,  $\mathcal{L}_3$  and  $\mathcal{L}'_3$  the function

$$\Psi_{I\lambda j l}^{MK} = \sum_m C(j\lambda I; m M - m) \chi_{jl}^m D_{M-m, K}^{\lambda*}$$

diagonalizes the specified operators with corresponding eigenvalues:

$$(24) \quad \left\{ \begin{array}{l} \mathcal{F}^2 \sim I(I+1) \\ \mathcal{F}_3 \sim M \\ \mathcal{L}^2 \sim \lambda(\lambda+1) \\ \mathcal{L}'_3 \sim K \\ J^2 \sim j(j+1) \\ L^2 \sim l(l+1) \\ S^2 \sim 3/4. \end{array} \right.$$

Note particularly that the particle functions depend upon particle co-ordinates *measured* relative to space-fixed axes and that  $D_{MK}^\lambda(\theta)$  corresponds to that rotation which takes the space system into the body system in accordance with the Euler rotations previously described. The function  $\Psi$  is not yet normalized. Adding the normalization, we adopt the following notation:

$$(25) \quad |IM\lambda j l K\rangle = \left(\frac{2\lambda+1}{8\pi^2}\right)^{\frac{1}{2}} \Psi_{I\lambda j l}^{MK}.$$

Because of the axial symmetry assumed for the core, it is clear that the system is invariant under a  $180^\circ$  rotation of the core about any axis through the center of mass contained in the body  $xy$ -plane. Such an operation is *like* a parity operation for the axially symmetric system for which the  $xy$ -plane is a plane of symmetry and has the effect on  $D^\lambda$  of

$$(26) \quad D_{MK}^\lambda \rightarrow (-1)^{\lambda+K} D_{M,-K}^\lambda.$$

Hence if we define  $\Pi$  to be the parity operator for the system as a whole and define its effect on  $D^\lambda$  to be as indicated in equation (26), then

$$(27) \quad \Pi |IM\lambda j l K\rangle = (-1)^{l+\lambda+K} |IM\lambda j l -K\rangle.$$

Since  $[H, \Pi] = 0$ , these eigenfunctions will not be suitable without additional symmetrization of states unless our consideration is restricted to those states which correspond to  $K=0$ ; *i.e.*, those states which represent core rotations about an axis perpendicular to the body symmetry axis. As the empirical studies undertaken previously suggest that such a restriction is valid, we shall adhere to it here. Hence we take for the kinematical part of our wave functions

$$(28) \quad |IM\lambda j l\rangle \equiv |IM\lambda j l 0\rangle,$$

which are now also eigenfunctions of system parity.

If we now adjoin to these states the functions <sup>(5)</sup>

$$(29) \quad \mathcal{F}_{nl}(R) = g_{nl} R^l \exp[-R^2/2] F(-n, l + \frac{3}{2}; R^2),$$

where  $F$  is a confluent hypergeometric function,  $g_{nl}$  is a normalizing constant,  $n$  is a positive integer or zero, and  $R = (m\omega/\hbar)^{\frac{1}{2}}x$ , and define

$$(30) \quad |IM\lambda jln\rangle \equiv \mathcal{F}_{nl} |IM\lambda jl\rangle,$$

then

$$(31) \quad \begin{cases} H(\mathbf{x}) |IM\lambda jln\rangle = \mathcal{E}_{njl} |IM\lambda jln\rangle, \\ \mathcal{E}_{njl} = \hbar\omega \left(2n + l + \frac{3}{2}\right) - \hbar^2 \frac{D}{2} \left[ j(j+1) - l(l+1) - \frac{3}{4} \right] - \hbar^2 Cl(l+1). \end{cases}$$

As was shown by NILSSEN <sup>(5)</sup>, the parameters  $C$  and  $D$  may be adjusted so that  $\mathcal{E}_{njl}$  reproduces the conventional level structure of the extreme single-particle model quite satisfactorily.

Finally it is necessary to give some consideration to functions defined in the space of  $\gamma$  which may be employed in the description of the characteristic oscillator states of the core. Since we wish to avoid detail here, we proceed quite formally. We simply assume the existence of a complete set of functions,  $\{\varphi_\nu(\gamma)\}$ , which have the properties

$$(32) \quad \begin{cases} H(\gamma)\varphi_\nu = \mathcal{E}_\nu \varphi_\nu, \\ \langle \nu | \nu' \rangle \equiv \int_0^\infty \varphi_\nu^\dagger \varphi_{\nu'} \frac{(\gamma^3 + 1)(2\gamma^3 + 1)^{\frac{1}{2}}}{\gamma^3} d\gamma = \delta_{\nu\nu'}. \end{cases}$$

The construction of a representation is then completed if we define

$$(33) \quad |IM\lambda jln\rangle \equiv \varphi_\nu |IM\lambda jln\rangle.$$

Of course now only  $H(\mathbf{x})$  and  $H(\gamma)$  are diagonalized by the representation. It is nevertheless relevant to present the matrix elements of the total Hamiltonian in this representation, as it was essentially this one that was used in the earlier empirical work. These matrix elements are

$$(34) \quad \begin{aligned} \langle IM\lambda jln\rangle |H| IM\lambda' j'l'n'\nu' \rangle &= (\mathcal{E}_{njl} + \mathcal{E}_\nu) \delta_{\lambda\lambda'} \delta_{jj'} \delta_{ll'} \delta_{nn'} \delta_{\nu\nu'} + \\ &+ \langle \nu | \frac{\hbar^2 \lambda(\lambda+1)}{2A_1} | \nu' \rangle \delta_{\lambda\lambda'} \delta_{jj'} \delta_{ll'} \delta_{nn'} + \\ &+ \varepsilon \frac{\hbar\omega}{2} \langle nl | R^2 | n'l' \rangle \langle \nu | \frac{(\gamma-1)^2(2\gamma+1)}{3\gamma^2} | \nu' \rangle \delta_{\lambda\lambda'} \delta_{jj'} \delta_{ll'} - \\ &- \varepsilon \frac{\hbar\omega}{2} \langle nl | R^2 | n'l' \rangle \langle \nu | \frac{\gamma^3-1}{3\gamma^2} | \nu' \rangle (4) \left( \frac{\pi}{5} \right)^{\frac{1}{2}} (jl \| 2 \| j'l') [(2j+1)(2\lambda'+1)]^{\frac{1}{2}}, \\ &(\text{times})(-1)^{j-j'} C(\lambda'2\lambda; 00) W(jj'\lambda\lambda'; 2I), \end{aligned}$$

where

$$(35) \quad (jl \| 2 \| j'l') = (-1)^{j'+l'-\frac{1}{2}} \left( \frac{5}{4\pi} \right)^{\frac{1}{2}} [(2l'+1)(2j'+1)]^{\frac{1}{2}} C(l'2l; 00) W(ljl'j'; \frac{1}{2}2),$$

and  $W$  is a Racah coefficient.

The factor  $\varepsilon$  appearing in the last two terms, which represent the energy of the interaction between the particle and the core oscillations and the particle and both the core oscillations and rotations, respectively, assumes the value  $-1$  if the particle levels characterized by  $(jl)$  and  $(j'l')$  contain no core particles, and is  $+1$  if these particle levels contain  $(2j-1)$  and  $(2j'-1)$  core particles, respectively. For configurations other than those characterizable as either a single particle or a single hole, these matrix elements cannot be so simply expressed. However, since it is our purpose here solely to delineate a model in the simplest possible terms, we shall not, in this paper, give any attention to those cases in which the odd particle must be conceived of as belonging to a multiple-particle or multiple-hole configuration.

Since in this section we are primarily concerned with the illumination, in qualitative terms, of the physical significance of the model itself, we shall reserve until the next section detailed examination of the matrix elements exhibited in equation (34). Instead, we turn our attention to the construction of an alternative representation in terms of which the connection between the present and the hydrodynamical <sup>(6)</sup> model is manifest.

Because the new representation now contemplated and the one employed above in equation (34) differ somewhat in their « parity » properties, it is convenient to return to the general angular momentum representation in equation (25) for purposes of explicitly exhibiting the unitary connection between the two. Though the eigenfunction (25) is not an eigenfunction of  $\Pi$ , a simple linear combination is; *i.e.*,

$$(36) \quad |IM\lambda j l K\rangle_s = 2^{-\frac{1}{2}} [|IM\lambda j l K\rangle + (-1)^{\lambda+K} |IM\lambda j l - K\rangle],$$

is an eigenfunction of  $\Pi$  with eigenvalues  $(-1)^l$ . Consider now the new representation generated according to the unitary transformation

$$(37) \quad |IMm j l K\rangle_s = \sum_{\lambda} (-1)^{j-m} C(j l \lambda; m, -K-m) |IM\lambda j l K\rangle_s.$$

Though the function  $|IMm j l K\rangle_s$  is defined entirely in terms of variables measured relative to a space-fixed co-ordinate system, it is readily shown (as has previously been remarked in I) that it is simply a member of the representation employed by BOHR and MOTTELSON <sup>(10)</sup> in their study of the implications of the hydrodynamical model. This correspondence may be ex-

<sup>(10)</sup> A. BOHR and B. R. MOTTELSON: *Mat. Fys. Medd. Dan. Vid. Selsk.*, **27**, no. 16 (1953).



hibited explicitly in two alternative ways; one being to rotate the particle co-ordinates from space to body-fixed axes (as was done in I), the other to examine the matrix elements of the operator representatives of diverse dynamical variables in the representation given by equation (37). We choose the latter, since by this method the physical content of the representation is most directly displayed.

We note first that the states  $|IMmjK\rangle_s$  (or  $|IMmjKnv\rangle_s$ , obtained by simply adjoining the particle-radial and core-oscillation functions,  $\mathcal{F}_{nl}$  and  $\varphi_\nu$ , respectively), correspond to the same general angular momentum coupling scheme as did the one previously discussed; *i.e.*, equation (21). Second, these states diagonalize—with corresponding eigenvalues—the same operators as did the previous representation (see equations (24)), with the exception of  $\mathcal{L}^2$ . And third, the constant of the motion which characterizes this latter representation, in contradistinction to  $\mathcal{L}^2$ , which characterized the former, is the magnitude of the *projection* of the single particle total angular momentum,  $\mathbf{J}$ , upon the moving symmetry axis of the body. Explicitly, we have (in terms of operators defined relative to the space axes)

$$(38) \quad J_0(e')^2 |IMmjKnv\rangle_s = m^2 |IMmjKnv\rangle_s,$$

where  $J_0(e') = \sum_\mu J_\mu(e) D_{\mu 0}^1$ .

The vector  $\mathbf{J}$  rotates according to  $D^1$  provided it is expressed in the « spherical » basis related to the Cartesian basis by

$$(39) \quad \mathbf{e}_s = A \mathbf{e}_c; \quad A = \begin{pmatrix} -2^{-\frac{1}{2}} & -i2^{-\frac{1}{2}} & 0 \\ 0 & 0 & 1 \\ 2^{-\frac{1}{2}} & -i2^{-\frac{1}{2}} & 0 \end{pmatrix}.$$

Finally, the matrix elements of  $H$  in this representation are (for states characterized by  $K=0$ ),

$$(40) \quad \begin{aligned} \langle IMmjlnv | H | IMm'j'l'n'v' \rangle = & (\mathcal{E}_{njl} + \mathcal{E}_\nu) \delta_{mm'} \delta_{jj'} \delta_{ll'} \delta_{nn'} \delta_{vv'} + \\ & + \langle \nu | \frac{\hbar^2}{2A_1} | \nu' \rangle [\{I(I+1) + j(j+1)\} \delta_{mm'} - \\ & - 2\{I(I+1)j|j+1\}^{\frac{1}{2}} \{C(j|j; m', m-m')C(I|I; m', m-m') + \\ & + (-1)^{j-l}C(j|j; -m', m+m')C(I|I; -m', m+m')\}] \delta_{jj'} \delta_{ll'} \delta_{nn'} + \\ & + \varepsilon \frac{\hbar\omega}{2} \langle nl | R^2 | n'l' \rangle \langle \nu | \frac{(\gamma-1)^2(2\gamma+1)}{3\gamma^2} | \nu' \rangle \delta_{jj'} \delta_{ll'} \delta_{mm'} - \\ & - \varepsilon \frac{\hbar\omega}{2} \langle nl | R^2 | n'l' \rangle \langle \nu | \frac{\gamma^3-1}{3\gamma^2} | \nu' \rangle (4) \left(\frac{\pi}{5}\right)^{\frac{1}{2}} (jl \| 2 \| j'l'), \\ & (\text{times}) [C(j'2j; m0) \delta_{mm'} + (-1)^{j'-l} C(j'2j; m0) \delta_{m,-m'}]. \end{aligned}$$

The more familiar diagonal elements of  $H$  in this representation are

$$\begin{aligned}
 (41) \quad \langle IMmjlnv | H | IMmjlnv \rangle = & \mathcal{E}_{njl} + \mathcal{E}_v + \langle v | \frac{\hbar^2}{2A_1} | v \rangle \cdot \\
 & \cdot \left[ I(I+1) + j(j+1) - 2m^2 + (-1)^{j+l+1} \left( j + \frac{1}{2} \right) \left( I + \frac{1}{2} \right) \delta_{m, \frac{1}{2}} \right] + \\
 & + \varepsilon \frac{\hbar\omega}{2} \left( 2n + l + \frac{3}{2} \right) \langle v | \frac{(\gamma-1)^2(2\gamma+1)}{3\gamma^2} | v \rangle + \\
 & + \varepsilon \frac{\hbar\omega}{2} \left( 2n + l + \frac{3}{2} \right) \langle v | \frac{\gamma^3-1}{3\gamma^2} | v \rangle \frac{3m^2 - j(j+1)}{2j(j+1)}.
 \end{aligned}$$

It is seen that, except for factors which depend explicitly upon the details of the description of the core oscillations, these matrix elements are identical to those discussed extensively by BOHR and MOTTELSON<sup>(10)</sup> and by NILSSON<sup>(5)</sup> in their examination of nuclear dynamics in the context of the hydrodynamical model in the strong coupling limit.

Thus, since the two representations are connected by a unitary transformation corresponding to an angular momentum recoupling, it is clear that predictions and/or correlations based upon the hydrodynamical model and the present one will differ only to the extent that these models treat the details of the core oscillations in quite different ways (a substantial difference as was suggested by II and IV). It is furthermore apparent that since the two models correspond as they do and since the present one was derived with the explicit proviso that the particle co-ordinates were not to be regarded as sharing in the constraints defining the collective variables descriptive of the core, the thorny issues surrounding the treatment of constrained degrees of freedom are germane to neither—at least to the level of development of both as discussed herein. Finally, in view of the above, it would seem not only not necessary but perhaps not even desirable to construe the analysis of collective nuclear behavior in terms of an analogy to molecular theory.

#### 4. — Dynamical implications of the hamiltonian.

We turn now to a detailed, qualitative consideration of the extent to which the previous empirical correlations are embraced by the dynamics of the model as presently constituted. However, one of the first points which should be raised and discussed is concerned not so much with the correlations themselves as with an implication provided by the kinematical scheme employed for the purpose of establishing the correlations. This implication was (and is) that not only did all of the two-component states chosen to correlate nuclear ground-

state magnetic and quadrupole moments correspond to system states in which the core exhibited some degree of rotational excitation, but actually all of the nuclei characterized by a single-particle configuration with  $j = l - \frac{1}{2}$  and  $I > \frac{3}{2}$  were represented by states for which the core angular momentum was considered to be a constant of the motion—and not zero. Since the energy of a free rotator increases with increasing angular momentum, it was difficult to visualize from the non-dynamical arguments previously advanced how (if at all) the coupling of that rotator to another system exhibiting angular momentum of its own might lead to an actual lowering of the *total system energy* for non-zero core angular momentum, even though the *purely rotational energy* of the core did increase. Of course, the observation of precisely this possibility: *i.e.*, the lowering of the system energy in spite of an increase in the rotational energy of the rotator, is implicit in diverse analyses<sup>(6-10)</sup> of the hydrodynamical model. Here, for the kinematically equivalent model, it is exhibited explicitly.

It is necessary that this point be examined in some detail, and it is particularly relevant that it be examined in the context of the earlier empirical analysis. To this end it is first observed that an appropriate wave function to represent nuclear ground states for nuclei presumed representable by the above Hamiltonian (this qualification is a reminder that the Hamiltonian employed herein—derived in terms of the explicit assumption of axially-symmetric oscillations—cannot be expected to be adequate except for nuclei in regions in which a simple rotational excitation spectrum is observed) may be exhibited as

$$(42) \quad \Psi = \sum_{\lambda j l n v} a_{\lambda j l n v} |IM\lambda j l n v\rangle,$$

where the  $a$ 's are the eigenvectors of the matrix, (34). Of course, the sum runs over *either* even *or* odd  $l$  since the parity of the component states is  $(-1)^l$ . The representation employed for purposes of empirical correlation is then obtained by the specialization:

$$(43) \quad \Psi \rightarrow (1 - a^2)^{\frac{1}{2}} |IM\lambda j l n v\rangle + a |IM\lambda' j' l' n' v\rangle.$$

This specialization is undoubtedly an oversimplification; nevertheless the contribution to the system energy from that part of the particle-core interaction which is non-zero only if the core angular momentum is non-zero, is negative in applicable cases. More explicitly, the energy of the system in the above state is

$$(44) \quad E = (1 - a^2) \langle IM\lambda j l n v | H | IM\lambda j l n v \rangle + a^2 \langle IM\lambda' j' l' n' v | H | IM\lambda' j' l' n' v \rangle + 2a(1 - a^2)^{\frac{1}{2}} \langle IM\lambda j l n v | H | IM\lambda' j' l' n' v \rangle.$$

For those two-component states which correspond to the admixture of different core angular momenta rather than single-particle configurations and for which  $I=j$ , (44) may be exhibited in the form

$$\begin{aligned}
 (45) \quad E = \bar{\epsilon}_{njl} + \bar{\epsilon}_v + (1-a^2)\langle v | \frac{\hbar^2 \lambda(\lambda+1)}{2A_1} | v \rangle + a^2 \langle v | \frac{\hbar^2 \lambda'(\lambda'+1)}{2A_1} | v \rangle + \\
 + \varepsilon \frac{\hbar\omega}{2} \left( 2n+l+\frac{3}{2} \right) \langle v | \frac{(\gamma-1)^2(2\gamma+1)}{3\gamma^2} | v \rangle + \\
 + \varepsilon \frac{\hbar\omega}{2} \left( 2n+l+\frac{3}{2} \right) \langle v | \frac{\gamma^3-1}{3\gamma^2} | v \rangle \frac{2I+3}{2I} [(1-a^2)P_s(II, \lambda\lambda) + \\
 + a^2 P_s(II, \lambda'\lambda') + 2a(1-a^2)^{\frac{1}{2}} P_s(II, \lambda\lambda')] .
 \end{aligned}$$

The expression in brackets in the last term is defined in equation (11) of III to be  $(Q-Q_p)/Q_0 \approx Q/Q_0$ , where  $Q$  is the observed nuclear quadrupole moment and

$$(46) \quad Q_0 = \frac{2}{5} ZeR_0^2 \left( \frac{\gamma^3-1}{\gamma} \right),$$

is the corresponding «static» moment. In the development of the magnetic-quadrupole moment correlations in III, the principle of the similarity of static and dynamic shapes was adopted—thus essentially requiring that only those states were acceptable for which  $Q/Q_0 > 0$ . Thus the sign of the last term of (45) is always negative in these cases; since for a particle configuration  $\varepsilon = +1$  and  $\gamma^3 < 1$ , and for a hole configuration  $\varepsilon = -1$  and  $\gamma^3 > 1$ . Therefore, it is seen that in these cases states of non-zero core angular momentum may well be preferred in the instance of a non-spherically symmetric core if the magnitude of the last term of (45) is greater than the «free rotator» contribution (terms 3 and 4 of (45)).

The situation cannot be so simply illustrated analytically for the  $j=l-\frac{1}{2}$  nuclei, since in these cases the particle-oscillator-rotator interaction cannot be shown to be so simply related to the expression for the quadrupole moment. However, the same general qualitative conclusions may be drawn here also, as indicated by the calculations presented in Table I. In order to strengthen the suggestion that non-zero core angular momentum might be expected in nuclear ground states, we have included in the table a comparison of the contributions to the system energy from the «rotator» with those from the particle-core interaction.

An interesting point, clearly visible in (45) and hastily passed over above, should receive some emphasis here. If, for purposes of illustration, one adopts the assumption that

$$(47) \quad \langle v | f(\gamma) | v \rangle \simeq f(\gamma_0),$$



TABLE I. — *Ground-state energies of the listed nuclei.*

The terms are given in the order in which they appear in Equations (34), (44). The values of  $\gamma$  used are those given in Sect. 4. The «rotator» energies (third term) are taken from Sect. 4 and are given in MeV. The entries for  $^{175}\text{Lu}$  are based on the recently-measured energy of the first excited state of  $^{174}\text{Yb}$  given by J. W. MIHELICH,

B. HARMATZ and T. H. HANDLEY (to be published in *Phys. Rev.*).

$^{187}\text{Re}$	$E = 0.8762(\mathcal{E}_{njl} + \mathcal{E}_v + 0.124 - 0.641\hbar\omega - 0.196 \hbar\omega)$ $+ 0.1238(\mathcal{E}_{njl} + \mathcal{E}_v + 0.413 - 0.641\hbar\omega + 0.196 \hbar\omega)$ $+ 0.6588(-0.305 \hbar\omega)$
$^{191}\text{Ir}$	$E = 0.8182(\mathcal{E}_{njl} + \mathcal{E}_v - 0.308\hbar\omega)$ $+ 0.1818(\mathcal{E}_{njl} + \mathcal{E}_v + 0.186 - 0.308\hbar\omega)$ $+ 0.7714(-0.339 \hbar\omega)$
$^{193}\text{Ir}$	$E = 0.8864(\mathcal{E}_{njl} + \mathcal{E}_v - 0.332\hbar\omega)$ $+ 0.1136(\mathcal{E}_{njl} + \mathcal{E}_v + 0.20574 - 0.332\hbar\omega)$ $+ 0.6348(-0.351 \hbar\omega)$
$^{173}\text{Yb}$	$E = 0.5678(\mathcal{E}_{njl} + \mathcal{E}_v + 0.0787 - 1.04 \hbar\omega + 0.113 \hbar\omega)$ $+ 0.4322(\mathcal{E}_{njl} + \mathcal{E}_v + 0.262 - 1.04 \hbar\omega + 0.289 \hbar\omega)$ $+ 0.9907(-0.335 \hbar\omega)$
$^{153}\text{Eu}$	$E = 0.8398(\mathcal{E}_{njl} + \mathcal{E}_v + 0.122 - 1.08 \hbar\omega + 0.106 \hbar\omega)$ $+ 0.1602(\mathcal{E}_{njl} + \mathcal{E}_v + 0.122 - 1.08 \hbar\omega - 0.254 \hbar\omega)$ $+ 0.7335(-0.136 \hbar\omega)$
$^{165}\text{Ho}$	$E = 0.4483(\mathcal{E}_{njl} + \mathcal{E}_v + 0.073 - 1.07 \hbar\omega - 0.336 \hbar\omega)$ $+ 0.5517(\mathcal{E}_{njl} + \mathcal{E}_v + 0.073 - 1.07 \hbar\omega - 0.429 \hbar\omega)$ $+ 0.9948(-0.0281\hbar\omega)$
$^{175}\text{Lu}$	$E = 0.5828(\mathcal{E}_{njl} + \mathcal{E}_v + 0.0766 - 0.803\hbar\omega - 0.292 \hbar\omega)$ $+ 0.4172(\mathcal{E}_{njl} + \mathcal{E}_v + 0.0766 - 0.803\hbar\omega - 0.372 \hbar\omega)$ $+ 0.9862(-0.0244\hbar\omega)$
$^{181}\text{Ta}$	$E = 0.8586(\mathcal{E}_{njl} + \mathcal{E}_v + 0.0933 - 0.758\hbar\omega - 0.284 \hbar\omega)$ $+ 0.1414(\mathcal{E}_{njl} + \mathcal{E}_v + 0.0933 - 0.758\hbar\omega - 0.362 \hbar\omega)$ $+ 0.6968(-0.0237\hbar\omega)$

where  $\gamma_0$  is the shape parameter appropriate to describe the mean distortion in the ground state—and therefore corresponds to the shape parameters empirically determined in II, III, and IV, it follows that

$$(48) \quad \frac{\langle v | \frac{(\gamma-1)^2(2\gamma+1)}{3\gamma^2} | v \rangle}{\langle v | \frac{\gamma^3-1}{3\gamma^2} | v \rangle} \rightarrow \begin{cases} 0 & \text{as } \gamma_0 \rightarrow 1, \\ 2 & \text{as } \gamma_0 \rightarrow \infty. \end{cases}$$

Hence for small distortion; i.e.,  $\gamma_0 \sim 1$ , the interaction energy is dominated

by the nucleon-oscillator-rotator term which, for the states we have chosen and have examined in detail, always provides a negative contribution to the system energy. Thus in these instances there is apparently no marked preference for either hole or particle nucleonic configurations, although the correspondence between nucleonic «hole» configurations and prolate core shapes on the one hand and «particle» configurations with oblate core shapes on the other is clearly preferred. Conversely, for large distortions the nucleon-oscillator term predominates in the interaction. But the sign of the energy contribution that this term makes to the system energy is either positive or negative depending upon whether the nucleon is in a particle or hole configuration. Thus it is implied that large distortions and hole configurations should go together, as indeed they apparently do. The close connection between shape and magnitude of distortion exhibited by the fact that highly-distorted cores are presumably prolate cannot be observed in the present analysis. This connection can only be displayed subsequent to a detailed examination of the oscillator part of the Hamiltonian,  $H(\gamma)$ .

We turn now to specific consideration of the previously formulated empirical correlations in the light of the dynamical scheme presently under discussion. The magnetic moment analysis, I, rested almost entirely upon a purely kinematical basis (which appears here intact), with the exception of its dependence upon the amplitudes of the states chosen to describe the system. These amplitudes were the principal empirical parameters upon which the correlations were hung; and are, of course, ultimately to be determined in terms of complete dynamical knowledge of the system. In particular, the assumption in effect that all amplitudes except two were zero must be regarded as a considerable over-simplification. It is to be noted, however, that these two-component states are energy-favored in the cases for which system energies were calculated. Thus, though these states can hardly be regarded as dynamically preferred in the sense of minimizing the energy, the suggestion previously advanced that the two components chosen might in some sense predominate in the true ground state seems still valid. In particular, the  $I = \frac{3}{2}$  nuclei are generally quite reasonably characterized by the simple admixture of the two core angular momentum states,  $\lambda = 0$  and 2, and an invariant nucleon configuration. Some estimates of the ratios of the amplitudes of the  $\lambda = 2$  state to the  $\lambda = 0$  state to be expected from the diagonalization of (45) after invoking (47) agree favorably with the ratios obtained empirically in I.

This observation is also implicit in the work of BOHR and MOTTELSON<sup>(10)</sup> for their (symmetrized) state for the  $I = \frac{3}{2}$  nuclei bears the following correspondence to the two-component core state admixture: (see equations (36) and (37))

$$\begin{aligned}
 (49) \quad \left| \frac{3}{2} M \frac{3}{2} \frac{3}{2} 10 \right\rangle_s &= 2^{\frac{1}{2}} \sum_{\lambda} C\left(\frac{3}{2} \frac{3}{2} \lambda; \frac{3}{2}, -\frac{3}{2}\right) \left| \frac{3}{2} M \lambda \frac{3}{2} 10 \right\rangle = \\
 &= 2^{-\frac{1}{2}} \left| \frac{3}{2} M 0 \frac{3}{2} 10 \right\rangle + 2^{-\frac{1}{2}} \left| \frac{3}{2} M 2 \frac{3}{2} 10 \right\rangle .
 \end{aligned}$$

Thus the single state  $|\frac{3}{2} M \frac{3}{2} 70\rangle$  in the  $m$ -representation corresponds, in the  $\lambda$ -representation, to an effectively pure particle state plus a state of core angular momentum  $\lambda=2$  with an amplitude of 0.707. This value for the amplitude of the admixed state is in fair agreement with those required to fit the magnetic moment data for the cases with  $j=l+\frac{1}{2}$ , but consistently large for the cases with  $j=l-\frac{1}{2}$  (see III).

The empirical analysis of quadrupole moments given in III required the introduction of a dynamical parameter to characterize core shapes. The parameter  $\gamma$  introduced for this purpose now emerges from the dynamics with exactly the same physical significance as originally intended. The numerical analysis of functions of  $\gamma$  appearing in II, III, and IV, must, however, be interpreted in the light of the assumption exhibited in equation (47). It is interesting to observe that the assertion employed in III that the static and dynamic shapes of the core should be either both prolate or both oblate—invoked in that instance largely arbitrarily, though suggested by an analysis of MOSZKOWSKI and TOWNES<sup>(11)</sup>, now receives energetic substantiation.

One aspect of III now requires some revision; namely, that in the calculations of the estimates of  $\gamma$  from quadrupole moment measurements, the extra-core nucleon was always regarded as being in a particle configuration. This was justified on the ground that, in the main, the nucleonic contribution to the quadrupole moment is small compared to the core contribution, and the distinction between particles and holes at that stage would be unobservable from the empirical point of view. However, for consistency with the model as presently constituted, such a distinction should be made.

The effort in II and IV was directed mainly toward attempting to establish a connection between the data on the first-excited states of even-even nuclei (the energies of these states and the transition probabilities connecting them to the ground states) and that on the neighboring odd- $A$  nuclei obtained by adding a nucleon to the even-even nucleus under consideration. The connection was to be established via the previously conceived shape parameter,  $\gamma$ , and a new empirical parameter,  $k$ , invoked in II to take account of the fact that only a fraction of the core mass presumably participates in the collective motion.

The dynamical considerations thus far developed offer little further insight into the matter of this connection, except for the fact that there is as yet no demonstrable dynamical inconsistency. That this situation obtains is certainly not surprising, since additional illumination of this issue must depend sensitively upon—among other things—a more thoroughgoing analysis of the level structures of the even-even nuclei. Such an analysis would presumably require the development of the kinetic energy operator for the asymmetric oscillator

(11) S. A. MOSZKOWSKI and C. H. TOWNES: *Phys. Rev.*, **93**, 306 (1954).

as well as the determination of the explicit functional dependence of the potential energy upon the shape variable  $\gamma$ . These issues have been deferred until later. Furthermore, it is probably not to be expected that any such oversimplified approach to nuclear dynamics as inheres in a scheme which couples the extremes of pure particle behavior with that of pure collective behavior should reveal much insight into the fundamental physical significance of the mass-fraction parameter  $k$  which is essentially a link between the extremes and which partakes of both. This parameter enters the present dynamical model—still empirically—simply as one of the factors which make up the constraints that define the kind of collective behavior under consideration herein.

## 5. — Discussion.

It is desirable that a few main points be reviewed in summary.

The dynamical scheme under present discussion—embodied in the hamiltonian of equation (20)—seems to us to be based upon assumptions which, however realistic, are relatively unambiguous. In particular, the not inconsiderable uncertainty attaching to the quantum mechanical description of constrained dynamical variables is here completely avoided by adopting the assumption that the degrees of freedom of the odd nucleon in the odd- $A$  nucleus are characterizable by independent, unconstrained position and spin variables. Nor does this assumption, in itself, in any fundamental way compromise the model. Especially, this assumption does not imply anything in particular about the presence or absence of a strong-coupling situation. Since the constraint concept is mainly useful as a device for extracting in a systematic and reproducible way a limited set of variables of presumed dominant significance out of a welter of many variables; *i.e.*, a device for defining the core collective variables, for example; but is never a *necessary* concept, it would seem that when feasible its use should be avoided. In other words, it would appear that there is no *a priori* restriction against the simple assertion that a set of independent variables with which to attempt to describe the dynamical behaviour of an odd- $A$  nucleus is the set employed herein. Once the assertion of independence is advanced, there can be no question of constraint. It should be pointed out in fact that, since the origin of the possibly translating but non-rotating co-ordinate system fixed in the body was defined to be at the center of mass, of the core, the particle does not even share in the center-of-mass constraint. This does imply, of course, that the kinetic energy must include the terms arising from translational motion,

$$(50) \quad T_{Tr} = \frac{mA}{2} \sum_{k=1}^3 (\dot{X}_k)^2 + m \sum_{k=1}^3 \dot{X}_k \dot{x}_k,$$



where the  $x_k$  are the positional co-ordinates of the extra-core nucleon measured relative to the center of mass of the core, and the  $X_k$  are the position co-ordinates of the center of mass of the core, measured relative to a laboratory co-ordinate system.

A second, somewhat precautionary, point is that the kinematical equivalence of the hydrodynamical model and the present one assures considerable *formal* similarity in the descriptions they provide of the level structures of odd- $A$  nuclei. This similarity is modified, of course, by fundamental differences in the assumed nature of the core oscillations. It is further largely obscured by the adoption of two-component ground states to facilitate ground-state data correlations. It does not seem feasible to attempt a description of the excited states of the odd- $A$  nuclei in the same simple terms that have proved fruitful (we feel) for ground states.

Finally, it would seem desirable that at least two generalizations of the present development be undertaken. The first, and perhaps less immediately significant of these (while simultaneously more embroiled in subtlety), is modification of the evaluation of the matrix elements of the particle-core interaction to account for nucleonic configurations other than single holes or particles. The second is the explicit formulation of the kinetic and potential energy operators for the completely asymmetric ellipsoidal oscillations, and their attempted diagonalization. This development is essential to the illumination of some issues merely posed herein—such as the matter of the connection between large core distortions and prolate core shapes, for example. It is further desirable in that quite possibly some information might be forthcoming concerning the manner in which the low-lying « collective » energy level structure varies from rotational to oscillational character as one proceeds from a consideration of nuclei in the middle of major shells to those near the ends of the shells. That such a transition should occur is at least suggested by the nature of the explicit dependence of the magnitude of the rotational level spacing upon the mass-fraction parameter  $k$ . Near the ends of shells this spacing becomes large, and it is reasonable to expect that in these regions the rotational and vibrational spacings will be of the same order of magnitude. More explicitly, in the middle of shells the level sequence in the order of increasing energy for even-even nuclei may be characterized in terms of the quantum numbers,  $(\lambda\nu)$ , as  $(00) \rightarrow (20) \rightarrow (40)$ , etc. However, in the transition region one might expect a sequence something like  $(00) \rightarrow (01) \rightarrow (20) \rightarrow (21)$  etc. Because of the unlikelihood of inducing or observing a transition  $(00) \rightleftharpoons (01)$ , it is clear that the observable level-spin sequence would here be 0, 2, 2, with an observed level spacing which does not obviously follow a simple rule; but, nevertheless, a rule which is theoretically accessible (within the context of the present model) upon formulation and solution of the more general rotator-oscillator problem. As mentioned above, the *formulation* of this problem is

straightforward as far as the kinetic energy part of the Hamiltonian is concerned—the principal uncertainty resides in the treatment of the potential energy.

\* \* \*

It is a pleasure to acknowledge our deep indebtedness to G. R. SATCHLER for the many hours of stimulating and clarifying discussion which he so freely gave.

#### RIASSUNTO (\*)

La presente ricerca è un tentativo di fornire una base dinamica allo schema cinematico precedentemente adottato per la correlazione empirica di alcuni dati nucleari. Scopo principale del presente lavoro è il tracciamento del sistema dinamico stesso. Si presta particolare attenzione ai seguenti punti: 1) Le ipotesi basi richieste per la specificazione del sistema. Queste possono dividersi grosso modo in due gruppi; quelle impiegate per la definizione dei gradi di libertà indipendenti scelti per la descrizione del sistema e quelle richieste per una almeno parziale caratterizzazione dei potenziali rilevanti. Le prime sono di primaria importanza nella formulazione degli operatori dell'energia cinetica appropriati alla scelta dei gradi di libertà e se ne tratta in dettaglio. Le seconde essendo meno attinenti allo scopo del presente lavoro sono trattate più o meno sommariamente. 2) Lo sviluppo dettagliato dell'energia cinetica di questo modello. Si esegue senza approssimazione; cioè la formulazione di questo aspetto delle conseguenze fisiche del modello è del tutto rigorosa. I calcoli nell'ambito del modello debbono in ultima analisi, naturalmente ricorrere ad approssimazioni. 3) Il significato fisico di due differenti rappresentazioni utilizzabili per la parziale diagonalizzazione dell'hamiltoniana. 4) La stretta connessione cinematica tra il sistema qui considerato e il modello idrodinamico. 5) L'ampiezza con la quale il sistema dinamico assorbe lo schema cinematico precedentemente usato per la correlazione dei dati. Si danno suggerimenti per possibili, e forse fruttuose, generalizzazioni con l'esposizione di conseguenze che possono essere significative per la descrizione del comportamento nucleare collettivo in regioni nelle quali non ci si può attendere un comportamento nè puramente vibrazionale nè puramente rotazionale.

(\*) Traduzione a cura della Redazione.

## Interaction of Negative K Mesons with Protons (\*).

G. ASCOLI, R. D. HILL and T. S. YOON

*Physics Department, University of Illinois - Urbana, Illinois*

(ricevuto il 13 Maggio 1958)

**Summary.** — Ten events of elastic and four events of inelastic scattering of  $K^-$ -particles by free protons in nuclear emulsions have been observed in the K-particle energy range from 5 to 70 MeV. These data when added to those from other laboratories are consistent with an  $s$ -wave interaction between the negative K particle and proton at low K-particle energies. A preliminary investigation of the evidence for isotopic spin states 0 and 1 is also made.

### 1. — Introduction.

Preliminary summaries <sup>(1,2)</sup> of the interactions of negative K-particles with hydrogen, both in bubble chambers and nuclear emulsions have already been given. More detailed data from many laboratories <sup>(3,4)</sup>, are now beginning to appear in the literature. In this note we wish to add our events to the

(\*) Assisted by a joint contract of the U.S. Office of Naval Research and the U.S. Atomic Energy Commission.

<sup>(1)</sup> M. CECCARELLI: *Report on Rochester Conference* (1957).

<sup>(2)</sup> A. H. ROSENFELD: *Report on Rochester Conference* (1957).

<sup>(3)</sup> F. C. GILBERT, C. E. VIOLET and R. S. WHITE: *Phys. Rev.*, **103**, 1825 (1956).

<sup>(4)</sup> L. W. ALVAREZ, H. BRADNER, P. FALK-VAIRANT, J. D. GOW, A. H. ROSENFELD, F. T. SOLMITZ and R. D. TRIPP: *U.C.R.L.*-3775.

<sup>(5)</sup> W. ALLES, N. N. BISWAS, M. CECCARELLI and J. CRUSSARD: *Nuovo Cimento*, **6**, 571 (1957).

<sup>(6)</sup> R. G. GLASSER, N. SEEMAN and G. A. SNOW: *Nuovo Cimento*, **7**, 142 (1958).

<sup>(7)</sup> E. LOHRMANN, M. NIKOLIĆ, M. SCHNEEBERGER, P. WALOSCHKE and H. WINZELER: *Nuovo Cimento*, **7**, 163 (1958).

<sup>(8)</sup> J. HORNBOSTEL and G. T. ZORN: *Phys. Rev.* (in press).

general body of data on elastic and inelastic scatters of  $K^-$ -particles on free protons.

## 2. - Experiment and observations.

Two stacks of water-soaked emulsions were exposed to the bevatron beam of  $(300 \pm 10)$  MeV/c  $K^-$ -particles. The preparation and processing of these emulsions has already been described <sup>(9)</sup>. The emulsions were scanned in the customary manner for K-particles entering the leading edge of the stack. A careful search for coplanar interaction events with two outgoing prongs was then carried out by along-the-track scanning.

In the two stacks, 803 and 1068  $K^-$ -particle tracks were observed. In the first stack, all K-particles were followed to their ends either at rest or to their points of interaction or decay in flight. In this stack, the energies of the K-particles at their point of initial observation were between 60 and 65 MeV. In the second stack, it has unfortunately not been possible to complete the along-the-track scanning beyond the plate in which each K-particle track was initially observed. However, out of the 1068 K-particles found, 102 have been followed to their ends at rest in the plate in which they were initially found. In this stack, the initial energies of the K-particles which ended were between 70 and 75 MeV. The mean range of the remainder of tracks, either to their points of interaction or to their emergence from the plate, was 23.2 mm in our water-soaked emulsion.

The results of the analysis of 10 elastic  $K^-$ -p interactions and of 4  $K^-$ -p absorptions are given in Tables I and II.

TABLE I. - *Elastic  $K^-$ -p interactions.*

Event	$T_K$ (Lab.) (MeV)	$\theta_{KK'}$ (CM) (degrees)
I- 1	58.8	55°
I- 2	26.2	85°
I- 3	52.6	68°
I- 4	43.8	57°
I- 5	54.1	78°
I- 6	31.5	41°
I- 7	46.9	92°
I- 8	45.4	129°
I- 9	40.3	142°
I-10	71.7°	155°

<sup>(9)</sup> G. ASCOLI, R. D. HILL and T. S. YOON: *Nuovo Cimento*, 565 (1958).



TABLE II. — *Inelastic K<sup>-</sup>-p interactions.*

Event	$T_K$ (Lab) (MeV)	$\theta_{K\pi}$ (CM) (degrees)	Products
I-11	45.8	32°	$\Sigma^- \rightarrow \rho$
I-12	14.5	24°	$\Sigma^- \rightarrow \text{star}$
I-13	34.8	14°	$\Sigma^- \rightarrow \text{star}$
I-14	48.7	113°	$\Sigma^\pm \rightarrow \pi^\pm \text{ flight}$

### 3. — Summary of available scattering data.

A histogram of the cumulative K<sup>-</sup>-particle track lengths in nuclear emulsion, given in terms of g/cm<sup>2</sup> of hydrogen traversed, is shown in Fig. 1 as a function of K-particle energy for four laboratories. All four laboratories (Bern, Wash-

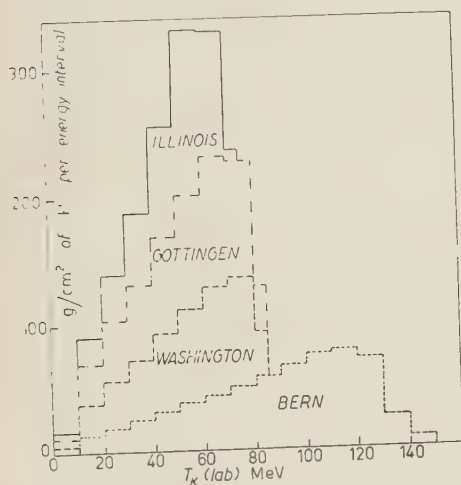


Fig. 1. — Cumulative histogram of K<sup>-</sup>-particle track lengths in emulsion. The histogram adds together measurements from four laboratories: Bern<sup>(7)</sup>, Washington<sup>(6)</sup>, Göttingen<sup>(5)</sup> and Illinois (present paper).

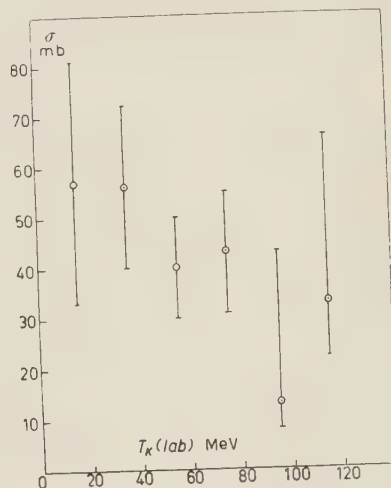


Fig. 2. — Elastic K<sup>-</sup>-p scattering cross-section as a function of K-particle laboratory kinetic energy. Width of energy bin for each point is 20 MeV. Statistical errors were obtained by the procedure described in Table III.

ington, Göttingen and Illinois) have studied comparable amounts of track but in somewhat different energy ranges. The Bern exposure was performed with the earlier un-enriched 435 MeV/c K<sup>-</sup> bevatron beam. The other three exposures were made with the later separated 300 MeV/c K<sup>-</sup>-particle beam.

Some slight difficulty was encountered in collecting together the information required for an analysis of the scattering data. Histograms of track

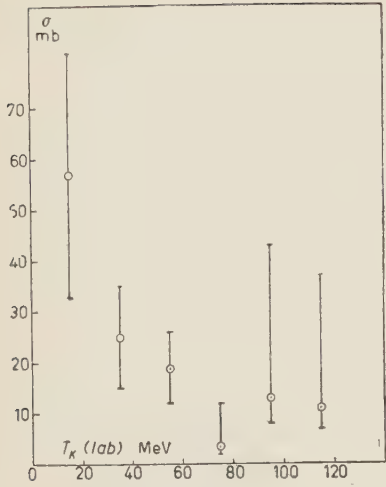


Fig. 3. — Inelastic K<sup>-</sup>p scattering cross-section as a function of K-particle laboratory kinetic energy.

and inelastic scattering cross-sections as a function of K-particle laboratory kinetic energy are shown in Figs. 2 and 3, respectively.

lengths from the Washington and Göttingen groups were not published, and the histograms shown in Fig. 1 for these groups were inferred from their published values of mean K-particle energies, total track lengths scanned and numbers of tracks interacting and ending in flight. The histograms of the Bern and Illinois groups were taken directly from experiment. The hydrogen content used for converting track lengths in normal G5 emulsion to mass per unit area of hydrogen was 0.0534 g/cm<sup>3</sup> and, for our wet G5 emulsion was 0.0929 g/cm<sup>3</sup>.

The numbers of elastic and inelastic scattering events observed by all groups together are collected in Tables III and IV, respectively, and histograms of the elastic

TABLE III. — Summary of elastics K<sup>-</sup>p scattering events.

Energy interval (MeV-Lab)	5 ÷ 25	25 ÷ 45	45 ÷ 65	65 ÷ 85	85 ÷ 105	105 ÷ 125
Numbers of events ± √N	6 ± 2.5	13 ± 3.6	15 ± 3.9	13 ± 3.6	1 <sup>+2.4</sup> <sub>-0.4</sub> (*)	3 <sup>+3</sup> <sub>-1</sub> (*)
g/cm <sup>2</sup> of Hydrogen	175	384	622	501	132	150
σ (mb)	57 ± 24	56 ± 16	40 ± 10	43 ± 12	13 <sup>+30</sup> <sub>-5</sub>	33 <sup>+33</sup> <sub>-11</sub>

(\*) For very small values of N, the average expectation value of N, calculated from a Poisson distribution, is N+1 and the RMS deviation from N+1 is √N+1.

TABLE IV. — Summary of inelastic K<sup>-</sup>p scattering events.

Energy interval (MeV-Lab)	5 ÷ 25	25 ÷ 45	45 ÷ 65	65 ÷ 85	85 ÷ 105	105 ÷ 125
Numbers of events ± √N	6 ± 2.5	6 ± 2.5	7 ± 2.7	1 <sup>+2.4</sup> <sub>-0.4</sub> (*)	1 <sup>+2.4</sup> <sub>-0.4</sub> (*)	1 <sup>-2.4</sup> <sub>-0.4</sub> (*)
g/cm <sup>2</sup> of Hydrogen	175	384	622	501	132	150
σ (mb)	57 ± 24	25 ± 10	19 ± 7	3.3 <sup>+8</sup> <sub>-1.3</sub>	13 <sup>+30</sup> <sub>-</sub>	11 <sup>+26</sup> <sub>-4</sub>

(\*) For very small values of N, the average expectation value of N, calculated from a Poisson distribution, is N+1 and the RMS deviation from N+1 is √N+1.

#### 4. - Discussion (\*).

The suggestion of a decrease in the elastic  $K^-p$  scattering cross-section with increasing K-particle energy has already been made by the Bern group (7). Our data also suggest this behavior, but because of the scarcity of events above 60 MeV we believe that this decrease cannot be statistically substantiated at this stage.

The evidence for a decrease in the inelastic  $K^-p$  scattering cross-section with increasing K-particle energy appears to be fairly sound. This has already been pointed out by the Washington group (6) who suggested the possibility of a dependence of the cross-section on the inverse first power of the  $K^-$ -particle velocity.

In order to separate out known energy-dependent factors from the matrix elements for the cross-sections of the following scattering processes:

$$K^- + p^+ \rightarrow K^- + p^+ \quad (\text{elastic}),$$

and

$$K^- + p^+ \rightarrow \Sigma^\pm + \pi^\mp \quad (\text{inelastic}),$$

we write

$$\sigma_{\text{el}} \sim |M_{\text{el}}|^2 / U^2,$$

and

$$\sigma_{\text{inel}} \sim p_\pi |M_{\text{inel}}|^2 / p_K U^2,$$

where  $U$  is the total energy of the reacting particles, including their rest energies, in the CM system; and  $p_\pi$  and  $p_K$  are the momenta of the pion and K-particle, respectively, in the CM system. The factors multiplying the matrix elements arise from the densities of final states per incident particle flux, and from the annihilation and creation operators in the elastic and inelastic processes.

For the elastic reaction,  $1/U^2$  varies very little over the K-particle energy range studied; but because of the exoergic character of the inelastic process, the  $(1/U^2) \cdot (p_\pi/p_K)$  factor has large values at low K-particle energies and varies as approximately  $1/p_K$ . If we divide the observed elastic and inelastic cross-section values by the dimensionless factors  $(M_K + M_p)^2/U^2$  and  $p_\pi(M_K + M_p)^2/p_K U^2$ , respectively, we obtain the modified cross-sections shown in Figs. 4 and 5 as a function of K-particle energy. While these values suggest a small and similar decrease in the modified elastic and inelastic cross-sections,

(\*) For our approach to this discussion we are greatly indebted to our colleagues: Drs. J. D. JACKSON, D. G. RAVENHALL and H. W. WYLD, who also have a note on this subject, in press.

or matrix elements, the experimental results are not accurate enough to draw a statistically significant conclusion other than that the cross-sections certainly do not increase strongly with K-particle energy. On this basis therefore the most likely possibility is that the negative K-particle and proton interact in an  $s$  state.

The data collected from all sources (<sup>5-7,9</sup>), on angular distributions of elastic

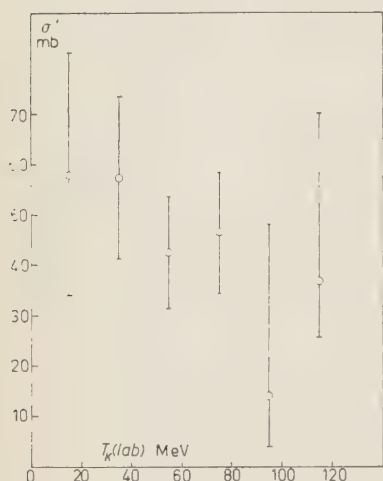


Fig. 4. — Modified elastic  $K^-$ -p scattering cross-sections  $\sigma' = \sigma(U/(M_K + M_p))^2$ .

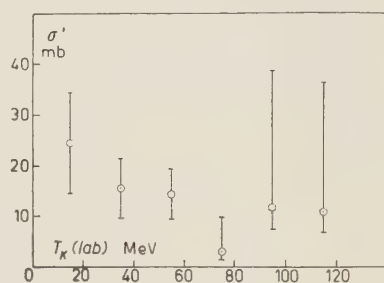


Fig. 5. — Modified inelastic  $K^-$ -p scattering cross-sections  $\sigma' = \sigma(p_K/p_\pi) \cdot (U/(M_K + M_p))^2$ .

and inelastic scattering are shown in Figs. 6 and 7. These data are clearly consistent with isotropy. However, because of the limited number of events, the inelastic scattering angular distribution is also consistent with a large degree of anisotropy. If the angular distributions are in fact isotropic, this would suggest that the interaction of the  $s$  wave predominates.

In the following analysis it will be shown that if the  $s$ -wave interaction

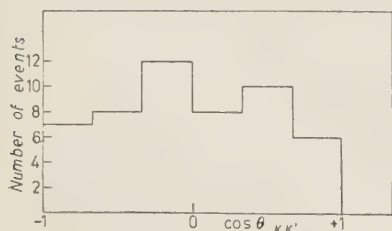


Fig. 6. — Angular distribution of  $K^-$ -p elastic scattering. Angle  $\theta_{KK'}$  is between the incoming K- and outgoing K-particles in the center of mass system. A distribution function:  $1 + 2A \cos \theta + B(3 \cos^2 \theta - 1)$  fitted to the histogram yields:  $A = -0.06 \pm 0.4$  and  $B = -0.05 \pm 0.2$ .

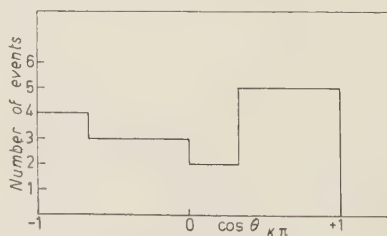


Fig. 7. — Angular distribution of  $K^-$ -p inelastic scattering. Angle  $\theta_{K\pi}$  is between the incoming K-particle and the outgoing  $\pi$ -meson in the center of mass system. A distribution function  $1 + 2A \cos \theta + B(3 \cos^2 \theta - 1)$  fitted to the histogram yields:  $A = 0.1 \pm 0.2$  and  $B = 0.3 \pm 0.3$ .



predominates, then the experimental data on the variation of cross-sections with  $\bar{K}$ -particle energy can probably be interpreted as indicating contributions from the two  $s$ -waves of isotopic spins 0 and 1 in the ordinary  $K^- + p^+ \rightarrow K^- + p^+$  scattering. The amount of interference cannot be determined from the data, but it probably could be obtained if accurate information on either charge exchange  $K^- + p \rightarrow \bar{K}^0 + n$  scattering  $K^- + n \rightarrow K^- + n$  scattering were available.

For interaction in  $s$  waves only the cross-sections would be given by:

$$\begin{aligned} K^- + p &\rightarrow K^- + p & \sigma_{el} &= (\pi/4k^2) |2 - \eta_0 - \eta_1|^2 \\ K^- + p &\rightarrow \bar{K}^0 + n & \sigma_{ex} &= (\pi/4k^2) |\eta_1 - \eta_0|^2, \\ K^- + p &\rightarrow Y_0^\pm + \pi^\mp & \sigma_{abs} &= (\pi/2k^2) \{ (1 - |\eta_0|^2) + (1 - |\eta_1|^2) \}, \\ K^- + p &\rightarrow \Sigma^\pm + \pi^\mp & \sigma_{inel} &= (\pi/2k^2) \{ \frac{2}{3}(1 - |\eta_0|^2) + (1 - |\eta_1|^2)(1 - f_\Lambda) \}, \end{aligned}$$

where  $k$  ( $=1/\lambda$ ) is the wave number of the  $K$ -particle in the CM system of  $K^-$  and proton,  $\eta_{0,1} = \exp [2i\delta_{0,1}]$  are the amplitudes of the outgoing  $T=0, 1$   $s$  waves (normalized to unit incident flux in both  $T=0$  and  $T=1$  waves so that  $|\eta_{0,1}|^2 \leq 1$ ), and  $f_\Lambda$  is the fraction of  $T=1$  absorption leading to  $\Lambda^0 + \pi^0$  production. Note that  $\sigma_{inel}$  is that part of  $\sigma_{abs}$  which is observable in emulsion experiments.

At the outset one can investigate the limitations on the cross-section imposed by the optical theorem. These limitations are rather severe if interaction in only one isotopic spin state is present, since the observed elastic scattering is accompanied by an equal amount of charge exchange scattering. The following inequality is then obtained if the elastic scattering is isotropic:

$$\sigma_{abs} + 2\sigma_{el} \leq \sqrt{4\pi\lambda^2} \sigma_{el}.$$

Table V shows the observed number of inelastic scattering events (column 7) compared with the maximum possible number of inelastic events (columns 5 and 6) calculated from this inequality and from the observed number of elastic scattering events. Only in the lowest  $K$ -particle energy interval does the observed number of events satisfy the inequality. In the other five energy intervals, the observed numbers of events lie consistently above the anticipated maximum numbers deduced from the elastic scattering events. It appears, therefore, that the observations are rather inconsistent with either pure  $T=0$  or pure  $T=1$   $s$ -wave interaction.

In order to see whether the observations are consistent with possible mixtures of  $T=0$  and  $T=1$  isotopic spin states of pure  $s$ -wave interactions we have tried to determine how well the elastic and inelastic cross-sections could be fitted if one assumes the simplest possible energy dependence of the complex

phase shifts, viz,

$$k \cot \delta_{0,1} = 1/a_{0,1} ,$$

where the  $a_{0,1}$  are complex constants which are independent of K-particle energy over the intervals studied.

TABLE V. — *Maximum K<sup>-</sup>p inelastic scattering for pure isotopic spin states, as compared with observed cross-section.*

$T_K$ (Lab) (MeV)	$k$ (a) ( $10^{13}$ cm <sup>-1</sup> )	$N_0$ (b)	$N_{el}$ (observed)	$N_{inel}$ (max) ( $T=0$ only) (Calc) (c)	$N_{inel}$ (max) ( $T=1$ only) (Calc) (d)	$N_{inel}$ (ob- served)
5 ÷ 25	0.40	40.3	6	6.7	$10 \times (1 - f_{\Lambda})$	6
25 ÷ 45	0.62	38.0	13	3.6	$5.4 \times \gg$	6
45 ÷ 65	0.77	39.1	15	2.8	$4.2 \times \gg$	7
65 ÷ 85	0.90	22.9	13	-1.1 (e)	$-1.6 \times \gg$	1
85 ÷ 105	1.03	4.7	1	0.7	$1.0 \times \gg$	1
105 ÷ 125	1.12	4.5	3	-0.8	$-1.2 \times \gg$	1

- (a) CM wave numbers of K particles at mean energy of interval:  $k=1/\lambda$ .  
(b)  $N_0 = 2\pi\lambda^2 \times$  (number of protons traversed by K particles/cm<sup>2</sup>).  
(c)  $N_{inel}(\text{max}) = \frac{3}{2} \{ \sqrt{2N_0N_{el}} - 2N_{el} \}$  for  $T=0$  only and for isotropic elastic scattering.  
(d)  $N_{inel}(\text{max}) = (1 - f_{\Lambda}) \{ \sqrt{2N_0N_{el}} - 2N_{el} \}$  for  $T=1$  only and for isotropic elastic scattering.  
(e) Negative number means that the number of elastic events exceeds the maximum allowable number,  $N_0/2$ , for  $s$ -wave interaction in one, and one only, isotopic spin state.

Figs. 8 and 9 show four examples of calculated  $s$ -wave cross-sections for different amounts of  $T=0$  and  $T=1$  state mixing. In each example an arbitrary choice was made to reduce the number of adjustable parameters from four to two, and the values of these two parameters were adjusted to give the best overall fit to the observed data.

It will be seen from these curves that a variation of the ratio of the two ampli-

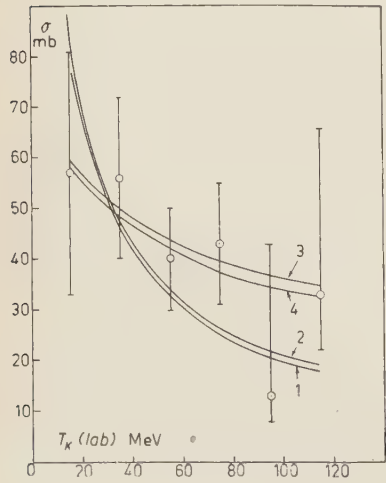
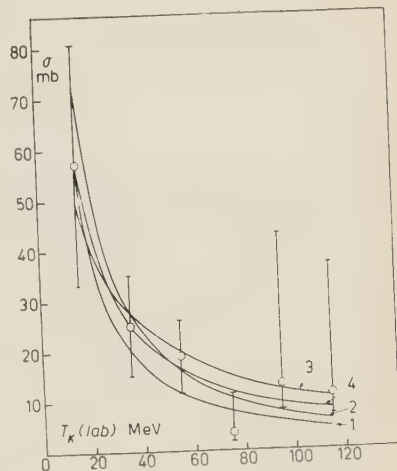


Fig. 8. — Calculated  $s$ -wave elastic scattering, compared with observed cross-sections, as function of K-particle energy. (1) Interaction in  $T=0$  state only:  $a_0=5i$ ,  $a_1=0$ . (2) Interaction in  $T=1$  state only:  $a_0=0$ ,  $a_1=\pm 2.8 + 3.2i$ . (3) Interaction in mixed  $T=0$  and  $T=1$  states, with maximum constructive interference:  $a_0=a_1=\pm 0.74 + 0.26i$ . (4) Interaction in mixed  $T=0$  and  $T=1$  states:  $a_0=\pm 0.63 + 1.4i$ ,  $a_1=\pm 0.63$ . Units of  $a_{0,1}$  are  $10^{-13}$  cm.

tudes of the  $T=0$  and  $T=1$   $s$ -waves over a considerable range has relatively little effect on the magnitudes of the cross-sections. We conclude, therefore, that little can be inferred from the data at this stage about even the approximate amount of  $T=0$  and  $T=1$  states entering into the  $K^-p$  interaction at low  $K$ -particle energies.

Fig. 9. — Calculated  $s$ -wave inelastic scattering, compared with observed cross-sections, as function of  $K$ -particle energy. (1), (2), (3), (4), as for Fig. 8.



\* \* \*

We wish to acknowledge our indebtedness to the Radiation Laboratory of the University of California, and especially to Drs. E. J. LOFGREN, W. H. BARKAS, W. F. DUDZLAK and their collaborators for making possible the  $K$ -particle exposures. We also wish to thank our scanners, Noreen CHRISTY, Beverley GROCE and Maria STOPPINI for their excellent and painstaking work.

#### RIASSUNTO (\*)

Fra le particelle  $K$  d'energia da 5 a 70 MeV si sono osservati 10 eventi di scattering elastico e 4 di scattering anelastico di  $K^-$  sui protoni liberi di emulsioni nucleari. Questi dati, aggiunti a quelli di altri laboratori sono compatibili con un'interazione di onde  $s$  tra i  $K$  negativi e i protoni a basse energie dei  $K$ . Si esegue anche un esame preliminare dei dati per gli stati di spin isotopico 0 e 1.

(\*) Traduzione a cura della Redazione.

## Strong Coupling Nucleon's Propagator.

L. M. GARRIDO

*Junta de Energia Nuclear - Madrid*

(ricevuto il 13 Maggio 1958)

**Summary.** — We present a method to approximate a solution to the equation of the propagator of the stationary nucleon strongly coupled to the pion field. As an example we apply the procedure to the well known case of neutral pions. Work on the same continues.

### 1. — Introduction.

Two functional differential equations in terms of arbitrary external fields which define the propagators of the nucleon and meson fields in interaction have been given by SCHWINGER <sup>(1)</sup>. Only the neutral scalar theory without recoil is soluble exactly and its propagator can be given in a closed form <sup>(2)</sup>.

We plan to treat the recoilless nucleon and limit ourselves, for simplicity reasons, to the purely charged meson field. The coupled non-linear functional equations that result are approximated and reduced to a single linear equation by assuming that the meson propagator is a given function of co-ordinates independent of the meson field as it was done by EDWARDS and PEIERLS <sup>(3)</sup>.

If our formalism has any physical sense, no matter how complicated our equations are and for reasonably strong interactions, there must be conditions under which the fields are uncoupled and the corresponding equations solved. Otherwise we would not see in Nature the particles as free.

For the strong coupling treatment these conditions are obtained by means of unitary transformations that diagonalize the largest terms, those which contain the coupling constant.

We start with the neutral case.

<sup>(1)</sup> J. S. SCHWINGER: *Proc. Nat. Acad. Sci., Wash.*, **37**, 452 (1951).

<sup>(2)</sup> S. I. TOMONAGA: *Progr. Theor. Phys.*, **1** (1946).

<sup>(3)</sup> S. F. EDWARDS and E. R. PEIERLS: *Proc. Roy. Soc., A* **224**, 24 (1954).



## 2. - Neutral pions.

The equation for the propagator  $G$  of the recoilless nucleon coupled to non-charged pions is reduced to the following linear one

$$(1) \quad \left\{ i \frac{\partial}{\partial t} + m - g\varphi(t) + ig \int dt'' \Delta(t, t'') \frac{\delta}{\delta\varphi(t'')} \right\} G(t, t'; \varphi) = \delta(t - t'),$$

where the notation  $G(t, t'; \varphi)$  indicates that it is a function of  $t, t'$  and a functional of the arbitrary meson field  $\varphi$ .

The function  $\Delta(t, t')$  is solution of the one dimensional equation

$$(2) \quad \left( \frac{d^2}{dt^2} + \kappa^2 \right) \Delta(t, t') = \delta(t - t').$$

However the meson momenta may be quite easily introduced <sup>(3)</sup>.

To start with we want to remark that the nucleon's mass «  $m$  » may be eliminated by writing

$$G(t, t'; \varphi) = \exp [im(t - t')] S(t, t'; \varphi),$$

since the new unknown  $S(t, t'; \varphi)$  satisfies an equation similar to (1)

$$(3) \quad \left\{ i \frac{\partial}{\partial t} - g\varphi(t) + ig \int dt'' \Delta(t, t'') \frac{\delta}{\delta\varphi(t'')} \right\} S(t, t'; \varphi) = \delta(t - t').$$

To solve this equation we assume that

$$S(t, t'; \varphi) = \theta(t, t') \exp \left[ \left\{ \int_{t'}^t \chi(t''; \varphi) dt'' \right\} \right],$$

where  $\chi(t''; \varphi)$  is an arbitrary function of  $t''$  and a functional of  $\varphi$ .

We substitute expression (4) into equation (3) and require

$$(5) \quad \left( i \frac{\partial}{\partial t} - g\varphi(t) + ig \int dt'' \Delta(t, t'') \frac{\delta}{\delta\varphi(t'')} \right) \exp \left[ \int_{t'}^t \chi(t''; \varphi) dt'' \right] = 0,$$

$$i\chi(t; \varphi) - g\varphi(t) + ig \int dt'' \Delta(t, t'') \frac{\delta\chi(t'', \varphi)}{\delta\varphi(t'')} = 0.$$

We are left with

$$i \exp \left[ \int_{t'}^t \chi(t''; \varphi) dt'' \right] \frac{\partial}{\partial t} \theta(t, t') = \delta(t - t'),$$

which is equivalent to

$$(6) \quad i \frac{\partial}{\partial t} \theta(t, t') = \delta(t - t'),$$

i.e.  $\theta(t, t')$  is proportional to the step function.

To solve equation (5) it is sufficient to take

$$(7) \quad \chi(t) = -ig\varphi(t) + ig^2 \int \Delta(t, t'') dt'',$$

an expression with which we have found in closed form the propagator for the neutral pion field.

### 3. - Charged mesons.

It has been observed that in the strong coupling the isobaric spin becomes almost fixed in a direction, around which it oscillates giving origin to the terms in  $g^{-2}$ . Therefore we should generate a rotation of isospin to the fixed direction: such rotation will produce the desired diagonalization.

After the elimination of the nucleon's mass by means of the same relation as used before in the neutral case, we will have the following equation for the charged case propagator  $G_c(t, t'; \varphi)$

$$(8) \quad G_c(t, t'; \varphi) = \exp [i m (t - t')] S_c(t, t'; \varphi).$$

and

$$(9) \quad \left\{ i \frac{\partial}{\partial t} - g\tau_j \varphi_j(t) + ig\tau_j \int dt'' \Delta(t, t'') \frac{\delta}{\delta \varphi_j(t'')} \right\} S_c(t, t'; \varphi) = \delta(t - t'), \quad j = 1, 2,$$

an equation that can be converted into

$$(10) \quad \left\{ i \frac{\partial}{\partial t} - \tau_3 \frac{\dot{\omega}(t)}{2} + g\tau_1 \left[ \varphi_1(t) - i \int dt'' \Delta(t, t'') \frac{\delta}{\delta \varphi_1(t'')} \right]^2 \right\} S(t, t'; \varphi) = \delta(t - t'),$$

$$(11) \quad S'_c(t, t'; \varphi) = R^{-1} S_c(t, t'; \varphi) R$$

by means of the rotation  $R$  in isobaric space defined by

$$(12) \quad \begin{cases} R = \exp \left[ \frac{i}{2} \tau_3 \omega(t) \right] \\ \omega(t) = \operatorname{tg}^{-1} \frac{\varphi_2(t) - i \int dt'' \Delta(t, t'') (\delta / \delta \varphi_2(t''))}{\varphi_1(t) - i \int dt'' \Delta(t, t'') (\delta / \delta \varphi_1(t''))} \end{cases}$$

Evidently we can, if we need, apply further rotations until the derivative  $\dot{\omega}(t)$  of the angle becomes sufficiently small. We stop now at the first approximation so as to not complicate the exposition.

If  $(\dot{\omega}t)$  is small the diagonalized equation is

$$(13) \quad \left\{ i \frac{\partial}{\partial t} + g \sqrt{\left( \varphi_1(t) - i \int dt'' \Delta(t, t'') \frac{\delta}{\delta \varphi_j(t'')} \right)^2} \right\} S'_e(t, t'; \varphi) = \delta(t - t'),$$

where we have set  $\tau_1 = 1$ . Similarly we could have written  $\tau_1 = -1$  obtaining a different solution.

It is equation (13), or any other more approximate equation obtained with the use of further rotations, that we solve assuming that

$$(14) \quad S'_e(t, t'; \varphi) = \theta(t, t') \exp \left\{ \left[ \int_{t'}^t \chi_c(t''; \varphi) dt'' \right] \right\},$$

where  $\theta(t, t')$  is defined by (6).

The equation for  $\chi_c(t; \varphi)$  is

$$(15) \quad i\chi_c(t; \varphi) + g \sqrt{\left[ \varphi_j(t) - i \int dt'' \Delta(t, t'') \frac{\delta \chi_c(t''; \varphi)}{\delta \varphi_j(t'')} - i \int dt'' \Delta(t, t'') \frac{\delta}{\delta \varphi_j(t'')} \right]^2} = 0.$$

The functional equation (15) may be solved approximately by extracting the largest contribution under the radical which comes from  $\delta \chi_c / \delta \varphi_j$  and is proportional to the coupling constant,  $g$ . Then we expand the radical in descending powers of  $g$  up to a term consistent with the approximation made in (13).

We would like to remark that in the evaluation of propagator we don't have to apply a unitary transformation that translates the value of the pion field by a term proportional to the self-field as it is done treating the strongly coupled hamiltonian. This is so because the propagators are an attempt to take into account at once all the virtual processes associated with a given real process.

#### RIASSUNTO (\*)

Si presenta un metodo per ottenere una soluzione approssimata dell'equazione del propagatore del nucleone stazionario fortemente accoppiato col campo pionico. A titolo d'esempio si applica il procedimento al ben noto caso dei pioni neutri. Le ricerche sull'argomento continuano.

(\*) Traduzione a cura della Redazione.

## Angular Distributions in Strange Particles Two Body-Decays (\*).

M. JACOB

*Brookhaven National Laboratory - Upton, New York*

(ricevuto il 14 Maggio 1958)

**Summary.** — General considerations are developed for the decay of a particle into two particles of arbitrary spins and some formulae are derived. The formalism introduced suits easily parity non conserving decays. The results obtained are applied to the  $K_{\mu 2}$  decay and a numerical calculation is carried out in the special case of spin 2; the polarization of the emitted  $\mu$ -meson is also discussed.

### 1. — Introduction.

Recent experiments have shown a large anisotropy in the angular distribution of the decay products of the  $\Lambda^0$  <sup>(1)</sup>. This phenomenon is a direct consequence of parity and charge conjugation non-conservation in weak interactions <sup>(2,3)</sup>. It is therefore expected to be a general feature of the weak decay of polarized strange particles. Though the computation of the actual angular distribution would involve the interaction Hamiltonian which is yet unknown, it is however possible to express it in terms of a small number of parameters and limitations can be obtained. Such inequalities have already

---

(\*) Work performed under the auspices of the U.S. Atomic Energy Commission.

<sup>(1)</sup> F. S. CRAWFORD, Jr. *et al.*: *Phys. Rev.*, **108**, 1102 (1957); F. EISLER *et al.*: *Phys. Rev.*, **108**, 1353 (1957).

<sup>(2)</sup> T. D. LEE, J. STEINBERGER, G. FEINBERG, D. K. KALIR and C. N. YANG: *Phys. Rev.*, **106**, 1367 (1957).

<sup>(3)</sup> R. GATTO: *Phys. Rev.*, **108**, 1103 (1957); T. D. LEE, R. OEHME and C. N. YANG: *Phys. Rev.*, **106**, 340 (1957).



been proposed for the determination of the  $\Lambda^0$  spin <sup>(4)</sup>. The parameters introduced may be also used to discuss the polarization of the emitted particles.

## 2. - General formalism and results.

The initial particle is considered in its rest system and is first supposed to be in a sharp spin state  $J$ ,  $Jz = M$ . In view of the possible relativistic nature of the two emitted particles, the simplest method to construct states of relative motion is by superposition of plane wave states with definite helicities. In the center-of mass system the two daughter particles have respectively momentum  $\mathbf{p}$  and  $-\mathbf{p}$ . The plane wave states may be labelled by means of  $\mathbf{p}$  and an index  $\lambda$ , when  $\lambda$  is the component of angular momentum along  $\mathbf{p}$ . In particular we indicate by  $\psi_\lambda$  a state with a given  $\lambda$  and with  $\mathbf{p}$  parallel to the  $z$  axis. The magnitude of  $\mathbf{p}$  need not be specified since it will be a constant throughout. States of definite angular momentum  $J$  and  $Jz = M$  can be constructed by applying rotations  $R_{\alpha\beta\gamma}$  to  $\psi_\lambda$  and integrating over the Euler angles  $\alpha\beta\gamma$  with a suitable amplitude, function of  $\alpha\beta\gamma$ . The procedure is well known <sup>(5)</sup>. One finds

$$(1) \quad \psi'_M = \sum_{\lambda} c_{\lambda} \psi'_{M\lambda}.$$

There are as many linearly independent states as possible values for  $\lambda$ . They are respectively found to be

$$(2) \quad \psi'_{M\lambda} = \frac{2J+1}{4\pi} \int D_{M\lambda}^{J*}(\varphi, \theta, 0) R_{\varphi, \theta, 0} \psi_{\lambda} d\Omega,$$

where  $D'_{MM'}(\alpha\beta\gamma)$  is the customary representation matrix of  $R_{\alpha\beta\gamma}$ , the integration is to be performed over the whole sphere and  $d\Omega = \sin \theta d\theta d\varphi$ . The state  $R_{\varphi, \theta, 0} \psi_{\lambda}$  is a plane wave state in the direction specified by the polar angles  $\theta$  and  $\varphi$  and has a norm independent of  $\theta$  and  $\varphi$ .

The asymptotic form of the wave function can then be calculated and the emission probability in the direction  $\theta\varphi$  is found to be

$$(3) \quad W(\theta, \varphi) d\Omega = \frac{2J+1}{4\pi} \sum_{\lambda} |c_{\lambda}|^2 |D_{M\lambda}^J(\varphi, \theta, 0)|^2 d\Omega,$$

where the normalization  $\sum_{\lambda} |c_{\lambda}|^2 = 1$  is assumed. The emission probabilities with each value of  $\lambda$  are then clearly separated.

<sup>(4)</sup> T. D. LEE and C. N. YANG: *Phys. Rev.*, **109**, 1755 (1958).

<sup>(5)</sup> E. P. WIGNER: *Gruppentheorie*, Ch. XII, Eq. (2) and (3).

If the initial particle is not in a state of definite  $M$ , the result is supposed to be averaged over the azimuthal angles and only the diagonal elements  $P_M$  of the density matrix need to be considered. They are such that

$$\sum_M p_M = 1.$$

The quantization axis will be chosen normal to the production plane. The quantities involved in (3) can be calculated by means of the Clebsch Gordon series and the angular distribution finally obtained reads

$$(4) \quad W(\theta q) d\Omega = \frac{2J-1}{4\pi} \sum_M (-1)^M P_M \sum_L (J, J, M, -M | J, J, L, 0) \cdot \sum_{\lambda} (-1)^{-\lambda} |c_{\lambda}|^2 (J, J, \lambda, -\lambda | J, J, L, 0) P_L(\cos \theta) d\Omega,$$

where  $L$  runs from 0 to  $2J$ . The bracket symbol used are the standard Clebsch-Gordan coefficients.  $P_L(\cos \theta)$  is the Legendre polynomial of order  $L$ .

If the initial particle is non-polarized the angular distribution will be isotropic. The emitted particles will be however in general longitudinally polarized. The resultant longitudinal polarization is easily obtained from (2) thanks to the orthogonality properties of the  $D_{MM'}(\alpha\beta\gamma)$  matrices and is equal to

$$(5) \quad \sum_{\lambda} \lambda |c_{\lambda}|^2.$$

This is also the longitudinal polarization averaged over all angles obtained when the initial particle is polarized. In this case an « Up-Down » asymmetry may be observed. The angular anisotropy is then often expressed by means of the average value of  $\cos \theta$ , and (4) allows the determination of limits for this parameter. This average value reads.

$$(6) \quad \langle \cos \theta \rangle = \frac{2J+1}{3} \cdot \sum_M (-1)^M P_M(J, J, M, -M | JJ10) \sum_{\lambda} (-1)^{-\lambda} |c_{\lambda}|^2 (J, J, \lambda, -\lambda | JJ10).$$

The Clebsch-Gordan coefficients involved have very simple expressions and we obtain

$$\langle \cos \theta \rangle = \frac{1}{J(J+1)} (\sum_M M \cdot P_M) (\sum_{\lambda} \lambda |c_{\lambda}|^2),$$

or

$$(7) \quad \langle \cos \theta \rangle = \frac{\langle Sp \rangle \langle J_z \rangle}{J(J+1)},$$

where  $\langle J_z \rangle$  is the expectation value of the  $z$  component of the spin of the initial particle and  $\langle Sp \rangle$  is the expectation value of the longitudinal component of the total spin of the two decay particles. The maximum of the absolute values of these two quantities are respectively  $J$  and  $S$  (if  $S \leq J$ ), where  $S$  is the total spin of the two emitted particles. The limits obtained for  $\langle \cos \theta \rangle$  then read

$$(8) \quad -\frac{S}{(J+1)} \leq \langle \cos \theta \rangle \leq \frac{S}{(J+1)} \quad \text{if } S \leq J,$$

the maximum value of  $\langle Sp \rangle$  is however  $J$  so that in any case

$$(9) \quad -\frac{J}{J+1} \leq \langle \cos \theta \rangle \leq \frac{J}{J+1};$$

if  $S = \frac{1}{2}$ , (8) gives the result already obtained for the  $\Lambda^0$  decay (<sup>4</sup>).

### 3. - Application to the $K_{\mu 2}$ decay.

3.1. *Angular distribution of the emitted  $\mu$ -meson.* - Although the spin of the K-meson is now believed to be zero, it is desirable to discuss a few more experiments with other possibilities in mind. To this end the results so far obtained are applied to the most probable decay mode

$$K^+ \rightarrow \mu^+ + \nu.$$

We assume that only left handed neutrinos occur (two component theory). There are only two possible states,  $\lambda = 0$  if the  $\mu$ -meson is left handed and  $\lambda = 1$  if it is right handed. We first suppose that the K-meson is in a sharp spin state  $J_z = M$ . The final state is given by (1) namely

$$(10) \quad \psi_M^J = A\psi_{M0}^J + B\psi_{M1}^J$$

and (4) then takes the reduced form

$$(11) \quad W(\theta\varphi) d\Omega = \frac{2J+1}{4\pi} \sum_M (-1)^M P_M \sum_L (J, J, M, -M | J, J, L, 0) \cdot \\ \cdot [ |A|^2 (J, J, 0, 0 | J, J, L, 0) - |B|^2 (J, J, 1, -1 | J, J, L, 0) ] P_L(\cos \theta) d\Omega,$$

where  $|A|^2 + |B|^2 = 1$  is assumed.

Since the spin of the K-meson is known to be even a numerical calculation has been made for  $J=2$ . The emission probability is a sum of two terms corresponding to the two possible helicity states of the  $\mu$ -meson ( $\lambda=0$  or  $1$ ).

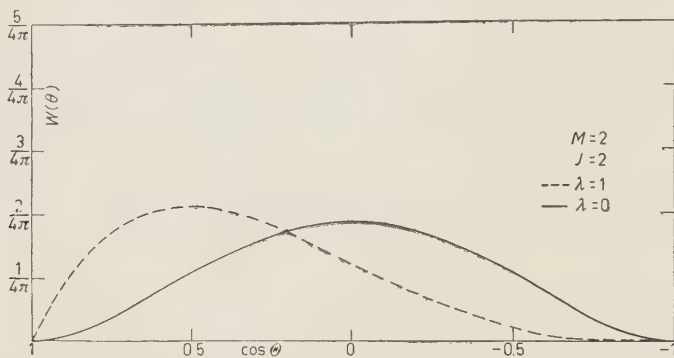


Fig. 1.

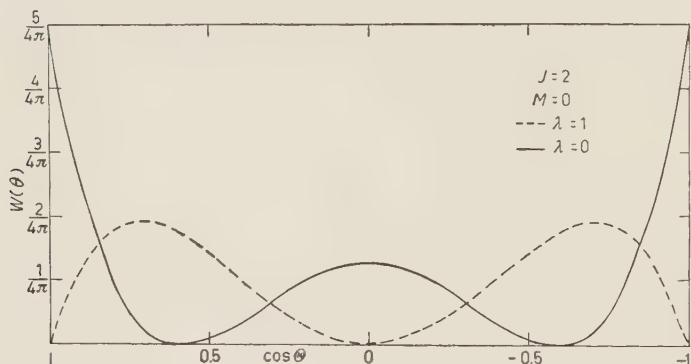


Fig. 2.

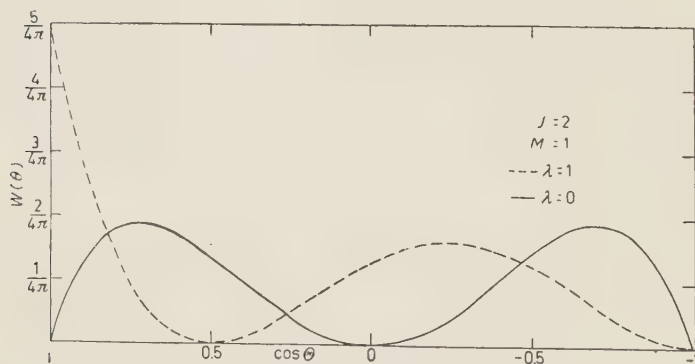


Fig. 3.

Figures 1, 2, 3 provide a plot of the normalized angular distributions per unit solid angle corresponding to the different possible substates  $(M, \lambda)$ . They can be used to discuss any angular distribution or longitudinal polarization measurements in term of 5 parameters, 4 describing the polarization of the initial K-meson, 1 describing the helicity state of the  $\mu$ -meson.



The angular distributions referring to these two states are separately computed for each of the K-meson spin substates  $M = 2, 1, 0$ . The corresponding normalized curves are given in Fig. 1 to 3. The curves for  $M = -1, -2$  (or those for the  $K^-$ -meson decay in which a right handed neutrino is presumably emitted) are obtained by reversing the sign of  $\cos \theta$ .

3.2. *Polarization of the emitted  $\mu$ -meson.* — The two helicity states do not interfere in the emission probability and the angular distribution curves given can be used to discuss a longitudinal polarization measurement.

The expectation value of the longitudinal polarization of the  $\mu$ -meson in the direction  $\theta\varphi$ ,  $\frac{1}{2}\langle\sigma_p\rangle_{\theta,\varphi}$ , reads

$$(12) \quad \frac{1}{2}\langle\sigma_p\rangle_{\theta\varphi} = \frac{-1}{2W(\theta,\varphi)} \frac{2J+1}{4\pi} \sum_M (-1)^M p_M \sum_L (J, J, M, -M | J J L 0) \cdot \\ \cdot [ |A|^2(J, J, 0, 0 | J J L 0) + |B|^2(J, J, 1, -1 | J J L 0) ] P_L(\cos \theta).$$

The experimental results so far obtained <sup>(6)</sup> are in agreement with those obtained for the  $\pi\mu$  decay for which the  $\mu$ -meson emitted is completely longitudinally polarized (2 component theory). For a non-zero K-meson spin this would mean that

$$(13) \quad |A|^2 \gg |B|^2.$$

However, the experimental set-up used selects  $\mu$ -mesons emitted in only one particular direction with respect to an axis normal to the production plane. The result obtained could then also be interpreted without the assumption (13) if the  $p_M$  are such that for the particular direction chosen the pertinent emission probability is negligible.

A possible check of the simultaneous presence of the  $A$  and  $B$  terms would be to measure an effect depending on their cross product. Such an effect could be observed by means of a transverse polarization measurement.

For each value of  $M$ , the asymptotic angular part of the wave function obtained from (2) reads

$$(14) \quad \psi'_M(\theta\varphi) = \sqrt{\frac{2J+1}{4\pi}} (A D_{M0}^{J*}(\varphi, \theta, 0) \chi'_L + B D_{M1}^{J*}(\varphi, \theta, 0) \chi'_R),$$

where  $\chi'$  is the neutrino spinor (left handed state).  $\chi_L$  and  $\chi_R$  are the  $\mu$ -meson spinors corresponding respectively to a left handed and a right handed state.

<sup>(6)</sup> C. A. COOMBS *et al.*: *Phys. Rev.*, **108**, 1348 (1957).

They can be written, ( $c=1$ )

$$(15) \quad \chi_L = \frac{1}{\sqrt{1 + p^2/(E+m)^2}} \begin{pmatrix} \frac{p}{E+m} u_L \\ u_L \end{pmatrix},$$

$$(16) \quad \chi_R = \frac{1}{\sqrt{1 + p^2/(E+m)^2}} \begin{pmatrix} -\frac{p}{E+m} u_R \\ u_R \end{pmatrix}$$

where

$$u_L = \begin{pmatrix} -\sin \frac{\theta}{2} & e^{-i\frac{\varphi}{2}} \\ \cos \frac{\theta}{2} & e^{i\frac{\varphi}{2}} \end{pmatrix}, \quad u_R = \begin{pmatrix} \cos \frac{\theta}{2} & e^{-i\frac{\varphi}{2}} \\ \sin \frac{\theta}{2} & e^{i\frac{\varphi}{2}} \end{pmatrix}.$$

The expectation value of any component of the  $\mu$ -meson spin, observed in a direction  $\theta\varphi$  can then be easily calculated.

The  $z$  axis and the momentum of the  $\mu$ -meson (in the rest system of the  $K$ -meson) define a particular plane. The spin component on an axis of this plane directly perpendicular to the momentum will be called the transverse component. Its expectation value,  $\frac{1}{2}\langle\sigma_t\rangle_{\theta\varphi}$  is found to be

$$(17) \quad \frac{1}{2}\langle\sigma_t\rangle_{\theta\varphi} = -\frac{m}{2E} \frac{AB^*D_{M_0}^{J*}(\varphi, \theta, 0)D_{M_1}^J(\varphi, \theta, 0) + BA^*D_{M_1}^{J*}(\varphi, \theta, 0)D_{M_0}^J(\varphi, \theta, 0)}{|A|^2|D_{M_0}^J(\varphi, \theta, 0)|^2 + |B|^2|D_{M_1}^J(\varphi, \theta, 0)|^2},$$

when  $m$  and  $E$  are the rest mass and total energy of the  $\mu$ -meson expressed in the same unit. This expression can be extended to the case when the  $K$ -meson is not in a state of definite  $M$  but the density matrix is nevertheless diagonal. The procedure is identical to the one already developed. One finds

$$(18) \quad \frac{1}{2}\langle\sigma_t\rangle_{\theta\varphi} = \frac{m}{2E} \frac{(AB^* + BA^*) \sum_M (-1)^M p_M \sum_L (J, J, M, -M | J, J, L, 0)(J, J, 1, 0 | J, J, L, 1) \sqrt{4\pi/(2L+1)} \mathcal{P}'_L(\theta)}{\sum_M (-1)^M p_M \sum_L (J, J, M, -M | J, J, L, 0) [ |A|^2 (J, J, 0, 0 | J, J, L, 0) - |B|^2 (J, J, 1, -1 | J, J, L, 0) ] P_L(\cos \theta)},$$

where the  $\mathcal{P}_L^M(\theta)$  are the standard associated Legendre functions.

If we look at right angle (*i.e.* in the production plane of the K-meson), we find that for the special case of  $J = 2$  only the  $M = 2$  and  $M = -2$  substates then contribute to this effect and in opposite ways. We obtain

$$(19) \quad \frac{1}{2} \langle \sigma_b \rangle_{\pi/2} = \frac{m}{2E} \frac{\sqrt{\frac{3}{2}} (AB^* + BA^*)}{\frac{3}{2} |A|^2 + |B|^2} (P_2 - P_{-2}),$$

the  $\frac{3}{2}$  factor introduced is nothing but the ratio of the emission probabilities at right angle of the normalized waves corresponding respectively to  $\lambda = 0$  and  $\lambda = 1$ . With the values normally assumed for the K and the  $\mu$ -meson rest masses the ratio  $m/E$  turns out to be of the order of 0.39.

\* \* \*

The author is indebted to Dr. G. C. WICK for suggesting this problem and for his continued guidance.

### **Note added in proof.**

Since the completion of this work the author heard of similar calculations done by K. ITABASHY (*Progress of Theoretical Physics*, **19**, No. 4 (1958)) and L. DURAND, L. F. LANDOVITZ and J. LEITNER (*Physical Review*, to be published).

### RIASSUNTO (\*)

Si espongono considerazioni generali sul decadimento di una particella in due particelle di spin arbitrario e si derivano alcune formule. Il formalismo introdotto si adatta facilmente ai decadimenti non conservanti la parità. Si applicano i risultati ottenuti al decadimento  $K_{\mu 2}$  e si esegue il calcolo numerico per il caso speciale dello spin 2; si discute anche la polarizzazione del mesone  $\mu$  emesso.

(\*) Traduzione a cura della Redazione.

## Phenomenological Discussion of the Scattering and Absorption of K-Mesons by Protons.

J. D. JACKSON, D. G. RAVENHALL and H. W. WYLD jr.

*Physics Department, University of Illinois - Urbana, Illinois*

(ricevuto il 27 Maggio 1958)

**Summary.** — A simple phenomenological analysis of the scattering and absorption of low energy K-mesons by protons is presented. An effective range expansion is used to describe the complex phase shifts; *s*-wave interactions are assumed dominant; only the crudest approximation, that of zero effective range, is illustrated. The scattering and absorption of  $K^-$ -mesons by protons and the scattering of  $K^+$ -mesons by protons are consistent with this zero range approximation. The appreciable fall-off of the  $K^-$  elastic scattering cross-section with increasing energy as compared to the essential constancy of the  $K^+$  cross-section is attributable in large part to the presence of the absorption in flight for  $K^-$  mesons. The connection between the cross-sections for absorption in flight from states of definite angular momentum and the capture rates from the corresponding bound states is explicitly stated and the possibility of correlating the data from the two sources is discussed.

### 1. - Introduction.

Presently available data <sup>(1)</sup> on the scattering and absorption of negative K-mesons by free protons, while still meager, exhibit some rather simple broad features:

1) The elastic scattering cross section falls smoothly from a rather large value of  $\sim 70$  mb at zero energy to  $\sim 30$  mb at 100 MeV laboratory kinetic energy.

2) The angular distribution for elastic scattering averaged over this energy interval is consistent with an isotropic distribution, although there could be a moderate amount of angular variation within the statistics.

---

<sup>(1)</sup> See G. ASCOLI, R. D. HILL and T. S. YOON: *Nuovo Cimento*, **9**, 813 (1958), where some new data are presented and all published results are correlated.



3) The reaction cross section for the production of charged  $\Sigma$ -hyperons ( $K^- + p \rightarrow \Sigma^- + \pi^0$ ) increases rapidly with *decreasing* K-meson energy, being of the order of 10 mb at 100 MeV and rising to of the order of 60 mb at 15 MeV. The energy variation seems to be steeper than a  $(1/v)$  law.

4) The angular distribution of charged reaction products is again consistent with isotropy, although the statistics are sufficiently poor that appreciable contributions from  $p$ -waves or higher cannot be excluded.

The behavior of the negative K-meson scattering is to be compared with the positive K-meson-proton scattering<sup>(2)</sup> where the total cross section has a relatively small value of  $\sim 15$  mb essentially independent of energy up to 200 MeV, and the angular distribution seems isotropic.

Various attempts<sup>(3-6)</sup> have been made to treat the scattering of K-mesons by nucleons from a field theoretical point of view. Unfortunately such calculations are beset with severe difficulties and uncertainties—doubt about the parity of the K-meson, inability to handle strong virtual pion effects and baryon pair effects, etc. The usefulness of the static model, in which recoil effects and baryon pair effects are neglected, does not seem to carry over from the pion nucleon problem. For example, the dominant  $K^+$  nucleon interaction comes out attractive for either scalar or pseudoscalar K-mesons in the static model, whereas an optical model analysis of  $K^+$  scattering by nuclei in emulsions<sup>(7)</sup> indicates that the dominant interaction is repulsive. For  $K^-$  scattering the calculations are further complicated by the strong absorption processes.

The experimental evidence for both positive and negative K scattering at low energies strongly indicate that the dominant interaction is in  $s$ -states. Because of the uncertainties involved in a field theoretical treatment it is of interest to see whether a consistent description of these low energy scattering and absorption phenomena can be given in terms of non-relativistic quantum theory. We will show that a simple phenomenological analysis using an effective range expansion for  $s$ -state interactions can be used to correlate the data. The rather different behavior of the negative K scattering as compared to that of positive K-mesons appears mainly as a consequence of the strong

(2) J. E. LANNUTTI, S. GOLDBABER, G. GOLDBABER, W. W. CHUPP, S. GIAMBUZZI, C. MARCHI, G. QUARENI and A. WATAGHIN: *Phys. Rev.*, **109**, 2121 (1958).

(3) C. CEOLIN and L. TAFFARA: *Nuovo Cimento*, **5**, 435 (1957).

(4) D. AMATI and B. VITALE: *Nuovo Cimento*, **5**, 1533 (1957); **6**, 261 (1957); **6**, 1273 (1957); and subsequent papers.

(5) H. P. STAPP: *Phys. Rev.*, **106**, 134 (1957).

(6) P. T. MATTHEWS and A. SALAM: *Nuovo Cimento*, **7**, 789 (1958).

(7) G. IGO, D. G. RAVENHALL, J. J. TIEMANN, W. W. CHUPP, G. GOLDBABER, S. GOLDBABER, J. E. LANNUTTI and R. M. THALER: *Phys. Rev.*, **109**, 2133 (1958).

absorption accompanying the scattering. The problem of relating the reactions in flight to the capture from Bohr orbits is also discussed.

## 2. - Effective range analysis.

The problem of scattering and absorption of negative K-mesons by protons can be discussed in terms of complex phase shifts. At energies less than 100 MeV, non-relativistic approximations will be adequate. In the entrance channel the negative K-meson and proton can combine to give isotopic spin  $T=0$  and  $T=1$ . The corresponding complex phase shifts will be denoted by  $\delta_0$  and  $\delta_1$ :

The ordinary scattering, the charge exchange scattering, and the absorption cross section for  $K^-$ -mesons on protons are given by

$$(1) \quad \sigma_{\text{ord}} = \frac{\pi}{k^2} \left| \frac{1}{2} (1 - \exp[2i\delta_0]) + \frac{1}{2} (1 - \exp[2i\delta_1]) \right|^2,$$

$$(2) \quad \sigma_{\text{ex}} = \frac{\pi}{k^2} \left| \frac{1}{2} (1 - \exp[2i\delta_0]) - \frac{1}{2} (1 - \exp[2i\delta_1]) \right|^2,$$

$$(3) \quad \sigma_{\text{abs}} = \frac{1}{2}\sigma_{\text{abs}}^0 + \frac{1}{2}\sigma_{\text{abs}}^1,$$

where

$$(4) \quad \sigma_{\text{abs}}^T = \frac{\pi}{k^2} (1 - |\exp[2i\delta_T]|^2),$$

is the absorption cross section for the isotopic spin state  $T$ . In these expressions  $k$  is the wave number in the center of mass system ( $k \simeq (T_{\text{Klab}}(\text{MeV})/92)^{\frac{1}{2}} \cdot 10^{13} \text{ cm}^{-1}$ ). The absorption cross sections can be expressed in terms of the cross sections for the production of the various reaction products ( $\Lambda^0 + \pi^0$ ,  $\Sigma^0 + \pi^0$ ,  $\Sigma^- + \pi^+$ ,  $\Sigma^+ + \pi^-$ ). Thus we find

$$(5) \quad \begin{cases} \frac{1}{2}\sigma_{\text{abs}}^0 = 3\sigma(\Sigma^0 + \pi^0), \\ \frac{1}{2}\sigma_{\text{abs}}^1 = \sigma(\Sigma^- + \pi^+) + \sigma(\Sigma^+ + \pi^-) + \sigma(\Lambda^0 + \pi^0) - 2\sigma(\Sigma^0 + \pi^0). \end{cases}$$

If  $\Lambda^0$  production can be neglected <sup>(8)</sup> the observed cross section for production of charged  $\Sigma$ -hyperons is

$$(6) \quad \sigma(\Sigma^+ + \pi^-) + \sigma(\Sigma^- + \pi^+) \simeq \frac{1}{3}\sigma_{\text{abs}}^0 + \frac{1}{2}\sigma_{\text{abs}}^1.$$

These isotopic spin arguments are independent of the assumption of only

<sup>(8)</sup> As might be suspected in analogy with the observations on capture from bound orbits; see L. W. ALVAREZ, H. BRADNER, P. FALK-VAIRANT, J. D. GOW, A. H. ROSENFELD, F. T. SOLMITZ and R. D. TRIPP: *Nuovo Cimento*, **5**, 1026 (1957).

$s$ -wave interactions. Similar results can be written down for  $K^+$  interactions with neutrons, where only the  $T=1$  state enters.

So far we have used only the very general apparatus of scattering theory. The problem of course is to predict the behavior of the two complex phase shifts  $\delta_0$  and  $\delta_1$  as functions of the energy. Various phenomenological approaches are possible. We shall use here an effective range expansion. The expansion of  $k^{2l+1} \cot \delta$  in powers of  $k^2$  (or in relativistic problems  $(k^{2l+1}/c) \cot \delta$  in powers of  $c$ ) has been employed with considerable success in both low energy nucleon-nucleon scattering and in pion-nucleon scattering. In these problems there was no absorption. Consequently the phase shifts involved were real and the power series expansions involved only real coefficients. There is however no need for this restrictive assumption. For an  $s$ -wave process involving both scattering and absorption we may write

$$(7) \quad k \cot \delta = \frac{1}{A} + \frac{1}{2} R k^2 + \dots,$$

where the phase shift  $\delta$ , the scattering length  $A$ , and the effective range  $R$  are all complex numbers.

The usefulness of the effective range approximation in ordinary scattering problems lies in the fact that only two parameters are necessary to determine the scattering for each partial wave. For the  $K^-$ -meson problem there are two complex parameters for each isotopic spin state—eight parameters in all. The limited data available at present do not warrant the use of so many parameters. Accordingly we shall limit our discussion to the crudest approximation, that of zero effective range. In support of this we remark that, ignoring isotopic spin considerations, the zero energy elastic scattering cross section implies  $|A| \sim 0.7 \cdot 10^{-13}$  cm. If we assume that  $|R| \sim \hbar/m_K c = 0.4 \cdot 10^{-13}$  cm, the second term in Eq. (7) is only about 15% of the first term at 100 MeV. Neglected  $p$ -wave effects may well be of this same order at that energy.

If the scattering length for each isotopic spin state is written as  $A_T = a_T + ib_T$ , where  $a_T$  and  $b_T$  are real, the cross section formulas, Eqs. (1), (2), (3) in the zero range approximation become

$$(8) \quad \sigma_{\text{ord}} = \pi \left| \frac{a_0 + ib_0}{(1 + kb_0) - ika_0} + \frac{a_1 + ib_1}{(1 + kb_1) - ika_1} \right|^2,$$

$$(9) \quad \sigma_{\text{ex}} = \pi \left| \frac{a_0 + ib_0}{(1 + kb_0) - ika_0} - \frac{a_1 + ib_1}{(1 + kb_1) - ika_1} \right|^2,$$

$$(10) \quad \sigma_{\text{sc}} = \sigma_{\text{ord}} + \sigma_{\text{ex}} = 2\pi \left[ \frac{|A_0|^2}{1 + 2kb_0 + k^2|A_0|^2} + \frac{|A_1|^2}{1 + 2kb_1 + k^2|A_1|^2} \right],$$

$$(11) \quad \frac{1}{2} \sigma_{\text{abs}} = \frac{2\pi}{k} \frac{b_T}{1 + 2kb_T + k^2|A_T|^2}.$$

As can be seen from Eq. (11),  $b_0$  and  $b_1$  are necessarily positive. Perhaps the most interesting aspect of Eqs. (9)-(11) is the linear dependence on  $k$  which appears in the denominators (the terms  $kb_0$  and  $kb_1$ ). These terms appear only when absorptive processes are possible. They cause the scattering cross sections to fall off more rapidly with increasing energy than would be the case for pure scattering with no absorption. They also cause the absorption cross sections to fall off with energy more rapidly than a simple  $1/v$  law.

The formulas (8)-(11) have been used by ASCOLI, HILL, and YOON<sup>(1)</sup> to fit the data on  $K^-$  proton scattering. In spite of the drastic assumption of zero range the cross section formulas still involve four parameters. These are adequate to describe the experiments, but the limited data are such that a unique fit cannot be made, although some limitations can be placed on the parameters. Further information on the parameter  $a_1$  and  $b_1$  might be obtained from  $K^-$ -neutron scattering, as inferred from  $K^-$ -nucleus interactions, although the problems of interpretation are difficult.

The scattering of  $K^+$ -mesons by protons can be discussed in the same terms as the  $K^-$  scattering. The analysis is simpler because only the  $T=1$  isotopic spin state enters and there is no charge exchange or absorption. In the zero range approximation the scattering cross section is

$$(12) \quad \sigma_{sc} = \frac{4\pi a^2}{1 + k^2 a^2},$$

where  $a$  is a real scattering length. The observed low energy cross section<sup>(2)</sup> of  $\sim 15$  mb implies  $|a| \simeq 0.34 \cdot 10^{-13}$  cm. With this scattering length Eq. (12) predicts a very slow fall-off of the cross section with energy (13.3 mb at 100 MeV, 12.0 mb at 200 MeV), completely consistent with experiment, especially since at the higher energies higher partial waves will presumably contribute.

Finally we remark that in the absence of interference with some interaction of known sign there is an ambiguity in sign for the real part of the scattering length which cannot be determined within the limits of our phenomenological analysis.

### 3. - Bound state capture of $K^-$ by protons.

Another possibility for obtaining information about the parameters  $a_\tau$ ,  $b_\tau$  used to describe the  $K^-$ -nucleon interaction is the study of the capture by protons of  $K^-$ -mesons in bound states. Assuming that the capture is entirely from  $s$ -states and using the experimental branching ratios<sup>(3)</sup>  $\Sigma^- \pi^+ : \Sigma^+ \pi^- : \Sigma^0 \pi^0 : \Lambda^0 \pi^0 \simeq$



$\simeq 8:4:4:1$  one finds from Eqs. (5) and (11) that  $b_0 \simeq 3b_1$ . Unfortunately  $p$ -state capture cannot be excluded <sup>(9)</sup>.

To relate explicitly the bound state capture rates to the absorption cross sections we note that an effective range relation of the form

$$(13) \quad k^{2l+1} \cot \delta_l = \frac{1}{A_l} = \frac{1}{a_l + ib_l},$$

for the  $l$ -th partial wave gives for very low energies

$$(14) \quad \text{Im } \delta_l \rightarrow k^{2l+1} b_l,$$

and implies an absorption cross section

$$(15) \quad \sigma_{\text{abs}}(l) \rightarrow \frac{4\pi}{k} (2l+1) k^{2l} b_l.$$

For simplicity spin and isotopic spin effects have been suppressed. With the idea in mind that the absorption is related to the square of the incident wave function for  $s$ -waves and derivatives of the wave function for higher partial waves we can write the absorption cross sections for  $l=0$  and  $l=1$  in the suggestive forms:

$$(16) \quad \begin{cases} \sigma_{\text{abs}}(l=0) \rightarrow \frac{4\pi}{k} b_0 |\psi(0)|^2, \\ \sigma_{\text{abs}}(l=1) \rightarrow \frac{12\pi}{k} b_1 |\nabla \psi(0)|^2, \end{cases}$$

where  $\psi$  is the incident plane wave <sup>(10)</sup>. The absorption rates are obtained by multiplying by  $v$ , the incident flux.

With the assumption <sup>(11)</sup> that the absorption is strictly proportional to the particle density (or its derivatives) at the origin, the absorption rates for a bound  $K^-$  are then

$$(17) \quad \begin{cases} \Gamma_s = \frac{4\pi\hbar}{\mu} b_0 |\psi(0)|^2, \\ \Gamma_v = \frac{12\pi\hbar}{\mu} b_1 |\nabla \psi(0)|^2, \end{cases}$$

<sup>(9)</sup> Rough estimates of the possibility of capture from other than  $s$ -states have been made by J. M. BLATT and S. T. BUTLER: *Nuovo Cimento*, **3**, 409 (1956) and R. GATTO: *Nuovo Cimento*, **3**, 1142 (1956).

<sup>(10)</sup> We ignore Coulomb effects for the reactions in flight. These will be important only for incident energies less than  $\sim 5$  MeV.

<sup>(11)</sup> K. A. BRUECKNER, R. SERBER and K. M. WATSON: *Phys. Rev.*, **81**, 575 (1951); **84**, 258 (1951); S. DESER, M. L. GOLDBERGER, K. BAUMANN and W. THIRRING: *Phys. Rev.*, **96**, 774 (1954).

where  $\mu$  is the reduced mass of the K-meson-proton system and the wave functions are now appropriate to hydrogenic bound states. The connection between the  $\text{Im } \delta_l$ , Eq. (14), and the capture rates (17) can be shown to hold generally in the approximation that the difference in energy between the continuum and the bound state does not affect the capture process and that the complex energy shift of the bound state eigenvalue due to the absorption is small compared to the eigenvalue itself.

To determine whether  $p$ -state capture is important we must compare the  $p$ -state rate given by (17) with the  $(2p \rightarrow 1s)$  radiative transition rate<sup>(12)</sup>. Since we do not have separate experimental data on the  $p$ -wave absorption in flight, we will reverse the argument and determine what  $p$ -wave absorption cross section is implied by a bound  $p$ -state capture rate equal to the  $(2p \rightarrow 1s)$  radiative rate *i.e.* 50%  $p$ -state capture. The radiative rate is easily found to be  $\Gamma_\gamma(2p \rightarrow 1s) = 4.0 \cdot 10^{11} \text{ s}^{-1}$ . By equating this to the absorption rate (Eq. (17)), we find  $b_1 \simeq 2.4 \cdot 10^{-2} (10^{-13} \text{ cm})^3$ . Barring a  $p$ -wave resonance at low energies, the  $p$ -wave absorption cross section can be estimated from its low energy limit, Eq. (15). The calculated value of  $b_1$  implies a cross section of the order of  $9(T_K(\text{MeV})/92)^{1/2} \text{ mb}$ . The experimental total absorption cross section is about 10 mb at 100 MeV, and is predominantly  $s$ -wave at lower energies. Hence it is perhaps reasonable to argue that the  $p$ -wave contribution is not more than one-half of the total at 100 MeV. This means that in the bound states  $p$ -wave absorption is perhaps not more than  $\sim 30\%$  of the total absorption. Unfortunately this is sufficiently large that the evidence from bound state capture cannot be used reliably to give information on the  $s$ -state absorption in flight. This conclusion is perhaps borne out by preliminary results<sup>(13)</sup> for  $(K^- + p)$  reactions at  $\sim 30 \text{ MeV}$  where the  $\Sigma^-/\Sigma^+$  ratio is of order unity, compared to a value of about two for capture at rest.

#### 4. - Discussion.

The approach to K-meson scattering and absorption presented here is frankly phenomenological. The aim has been to describe the low energy phenomena by a limited number of parameters which have some intuitive meaning and which one hopes will eventually emerge from a fundamental field theoretic treatment.

As ASCOLI, HILL and YOON<sup>(1)</sup> show, the zero range formulas (8)-(11) are capable of fitting the data on K<sup>-</sup>-proton scattering and absorption. The pre-

<sup>(12)</sup> In the cascading down from higher orbits the K meson travels predominantly through the states of highest angular momentum for a given principal quantum number. Hence the crucial stage is the  $2p \rightarrow 1s$  transition.

<sup>(13)</sup> Private communication from G. GOLDBABER on Berkeley bubble chamber work.

sence of two isotopic spin states means, however, that unique values of the four parameters  $a_T$ ,  $b_T$  cannot be determined. There is just the indication (<sup>1</sup>), based on use of the optical theorem, that a mixture of  $T=0$  and  $T=1$  amplitudes is necessary. It is clear that more detailed information on angular distributions will clarify the contributions of higher partial waves neglected here and will perhaps allow a correlation between the bound state capture process and reactions in flight.

Perhaps the most interesting although elementary point is that the monotonic decrease of the elastic  $K^-$ -proton scattering cross sections by a factor of two from zero energy to 100 MeV and the essential constancy of the  $K^-$ -proton scattering cross section up to 200 MeV are both consistent with a zero range approximation for the scattering. The decrease in the  $K^-$  cross-section is due in large part to the presence of appreciable absorption in flight.

\* \* \*

The authors wish to thank Drs. G. ASCOLI and R. D. HILL for many stimulating conversations.

### *Note added in proof.*

The zero formulas (8)–(11) have been employed by R. H. DALITZ at the 1958 Annual International Conference on High Energy Physics at CERN, June 30–July 5, 1958, in a discussion of the latest  $K^-$  proton scattering data. These newer data are quite consistent with the energy dependence of the zero range formulas. The reader may refer to the Proceedings of the conference for details, such as the possible solutions for the complex amplitudes  $A_T$ .

### RIASSUNTO (\*)

Si espone una semplice analisi fenomenologica dello scattering e dell'assorbimento di mesoni  $K$  di bassa energia da parte di protoni. Si ricorre ad uno sviluppo in serie in termini del range effettivo per descrivere gli spostamenti di fase complessi; si presuppone dominanti le interazioni delle onde  $s$ ; si descrive solo l'approssimazione più grossolana; quella in termini del range effettivo zero. Lo scattering e l'assorbimento dei mesoni  $K^-$  da parte di protoni e lo scattering dei  $K^+$  sui protoni sono compatibili con tale approssimazione. L'apprezzabile diminuzione della sezione d'urto per lo scattering elastico dei  $K^-$  al crescere dell'energia in confronto dell'essenziale costanza della sezione d'urto dei  $K^+$  è da attribuirsi in gran parte all'assorbimento in volo dei  $K^-$ . Si stabilisce esplicitamente la connessione tra le sezioni d'urto per l'assorbimento in volo da parte di stati con momento angolare definito e i tassi di cattura da parte dei corrispondenti stati legati e si discute la possibilità di una correlazione fra i dati ricavati dalle due sorgenti.

(\*) Traduzione a cura della Redazione.

## The $\Lambda$ -Hyperon-Nucleon Problem from Meson Theory (\*).

F. FERRARI and L. FONDA

*Istituto di Fisica dell'Università - Padova*

*Istituto di Fisica dell'Università - Trieste*

*Istituto Nazionale di Fisica Nucleare - Sezione di Padova*

*Istituto Nazionale di Fisica Nucleare - Sottosezione di Trieste*

(ricevuto il 30 Maggio 1958)

**Summary.** — A discussion of the implications of the meson theory with regard to the binding of the  $\Lambda$ -hyperon in nuclear matter is carried out taking explicitly into account the phenomenological results of DALITZ and DOWNS. The interactions through pions and K-mesons are analyzed, considering all possible combinations of the parity of the  $\Sigma$ -hyperon and the K-meson. Particular attention is devoted to the case of a universal pion-baryon interaction. In this case one is led to the conclusion that the K-meson is pseudoscalar. Another solution to the problem can be obtained assuming that the  $\Sigma$ -hyperon has different parity from that of the  $\Lambda$ -hyperon. This implies that the K-meson contribution to the  $\Lambda$ -nucleon potential is of the same order of magnitude as that of the pion field. It is argued that no other solutions can be given. In particular the interaction through the K-meson field only is not able to give agreement with experiment. The stability of the ( $\Xi$ , nucleon) and ( $\Sigma$ , nucleon) systems are also briefly discussed.

### 1. — Introduction.

For some time it has been known that the  $\Lambda$ -hyperon may be bound in nuclear matter and give rise to the formation of hyperfragments. Moreover, an event found in Padua seems to indicate that the  $\Lambda$ -hyperon can also give

---

(\*) The results relative to the case in which the  $\Sigma$ -hyperon has the same parity as the  $\Lambda$ -hyperon, have been communicated at the Padua-Venice Conference. See F. FERRARI and L. FONDA: *Binding energy of light hyperfragments and nucleon-hyperon forces*, in *Proceedings of the International Conference on Mesons and Recently Discovered Particles*, Padua-Venice, September 1957.



stable compounds with nucleons (\*). The information deducible from these experiments, and in particular from the rather well established ones concerning the binding energy of the lightest hypernuclei, shows that the hyperon interacts strongly with the nucleons. The relative strength seems smaller than that of the nucleon-nucleon interactions, but of the same order of magnitude.

Now, two alternative approaches are available for calculating the binding energy of the hyperfragments. One can follow a phenomenological pattern, *i.e.* just schematizing the interactions with selected potentials (generally with holes) whose parameters are determined by fitting the experimental data (<sup>1</sup>). On the other hand, one can assume certain elementary interactions between particles, and on the basis of a consistent field-theoretical treatment evaluate the binding energy of the hyperfragments (<sup>2</sup>). Unfortunately, the present experimental data are mainly concerned with the binding energy, a quantity from which no sure evidence about the nature and type of interactions between the particles can be obtained. Therefore, one could think that a detailed calculation involving particular choices for the elementary interactions, is premature because the same information can also be deduced in a simpler way by making use of phenomenological potentials. However, the field-theoretical point of view has the advantage of revealing some special features of the hyperon-nucleon interactions. Along these lines we shall discuss the possibility that  $\pi$  or/and K-mesons constitute the field quanta of the baryonic (nucleonic or hyperonic) field (<sup>3</sup>). It will be seen that certain properties of the strange particles  $\Lambda$ ,  $\Sigma$  and K will be determined and that a unique choice of the mesonic parameters will explain completely all the binding energies of the lightest hyperfragments.

Let us take as basic the following elementary interactions for the  $\Lambda$ -hyperon-nucleon forces:

$$(1) \quad \Lambda \rightarrow \Sigma + \pi, \quad \Sigma \rightarrow \Lambda + \pi, \quad N \rightarrow N + \pi,$$

and/or

$$(2) \quad \Lambda \rightarrow N + \bar{K}, \quad \Sigma \rightarrow N + \bar{K}, \quad N \rightarrow \begin{cases} \Lambda + K, \\ \Sigma + K. \end{cases}$$

(\*) W. F. FRY *et al.*: *Evidence for a  $(\Sigma^+, p)$  compound*. Padua-Venice Conf. (1957).

(<sup>1</sup>) R. H. DALITZ: *Proc. Rochester Conf.*, **6**, 40 (1956); *Rep. Prog. Phys.*, **20**, 163 (1957); *Phys. Rev.*, **99**, 1475 (1955); L. M. BROWN and M. POSHKIN: *Phys. Rev.*, **107**, 272 (1957); D. B. LICHTENBERG and M. ROSS (in press).

(<sup>2</sup>) D. B. LICHTENBERG and M. ROSS: *Phys. Rev.*, **103**, 1131 (1956); G. WENTZEL: *Phys. Rev.*, **101**, 835 (1956); N. DALLAPORTA and F. FERRARI: *Nuovo Cimento*, **5**, 111 (1957) (in this paper there are unfortunately some errors in the expressions of the potentials and in Table I); F. FERRARI and L. FONDA: *Nuovo Cimento*, **6**, 1027 (1957).

(<sup>3</sup>) D. B. LICHTENBERG and M. ROSS have also considered the effects of exchange of pions and K-mesons: Padua-Venice Conference, 1957: *K-meson contribution to forces between baryons* (in press).

These interactions take place with conservation of the total isotopic spin and strangeness (mathematically equivalent to writing down the interaction Lagrangians responsible for these processes in a form invariant under rotations and reflections in isotopic spin space). The only supposition we have to make is the one relative to the spin of the particles. There is much experimental evidence of spin  $\frac{1}{2}$  for the  $\Lambda$ -hyperon and spin 0 for the K-meson. A spin  $\frac{1}{2}$  for the  $\Sigma$ -hyperon is also compatible with present experimental data. We shall assume then spin  $\frac{1}{2}$  for all the baryons and spin 0 for all the mesons. As for the parities of the particles involved in the processes, it is seen from reactions (1.1) and (1.2) that the only combinations in which nucleons, hyperons and mesons appear are (\*)

$$\bar{N}N\pi, \quad \Lambda\Sigma\pi, \quad \bar{N}\Lambda K \quad \text{and} \quad N\Sigma K.$$

By assuming the same parity for the  $\Lambda$ -hyperon and for the nucleon, one has only to specify the parity of the  $\Sigma$ -hyperon and the parity of the K-meson separately with respect to the  $\Lambda$ . We shall discuss all these possibilities and see the consequences of each choice (+).

A further remark concerns the choice of the various coupling constants. It has been emphasized by Wigner, Gell-Mann and Schwinger that the conservation of the total number of baryons in any physical process must be connected with the equality of all the pion-baryon coupling constants, just as in electrodynamics it is possible to deduce a conservation theorem for the total charge, by supposing that the electromagnetic coupling is always the same, that is  $e$ . Following this line of thought we shall consider in detail the case in which all the pion-baryon coupling constants are equal. In this way we shall reduce the number of parameters in the theory by identifying part of them with the rather well known pion-nucleon parameters.

Finally, it is to be pointed out that our approach to the hyperon-nucleon problem is meaningful only if the methods of the field theory are also applicable to the description of the strange particles. Inasmuch as there exist serious suspicions for this, it has seemed worthwhile to examine the consequences of the meson theories of baryon forces to see to what extent the results are in agreement with the actual experimental data.

In Sect. 2 we give a brief account of the formal derivation of the hyperon-nucleon potential and the general implicit expressions for the  $\pi$ -meson, K-meson and the mixed  $\pi$  and K-meson contributions to the potentials. The explicit expressions for these contributions are then given for any choice of the

(\*) A combination of the type  $\Sigma\Sigma\pi$  has no effect in our approach to the  $\Lambda$ -nucleon problem.

(+) In what follows, we shall refer as scalar to a particle whose parity is that of the nucleon, as pseudoscalar when its parity is different.

parities of  $\Sigma$ -hyperon and K-meson. Qualitative considerations along with some preliminary indications of the nature (scalar or pseudoscalar) of  $\Sigma$  and K particles, are found in Sect. 3. Detailed calculations, quantitative results and comparison with experiment are given in Sect. 4. A concluding discussion is made in the same section.

## 2. - Construction of the hyperon nucleon potential.

2.1. *Formal derivation.* - The hyperon-nucleon potential will be obtained by following a non-relativistic perturbation theory similar to that used by many authors on the two-nucleon problem<sup>(3)</sup>. We summarize briefly here the usual derivation, extending the method to the case in which two mesonic fields are present.

In order to obtain the stationary states of  $\pi$  and K-mesons interacting with the baryon field, we have to solve the Schrödinger equation:

$$(2.1) \quad (H_0 + H_I)|P\rangle = E|P\rangle.$$

If the interaction hamiltonian is linear in the two meson fields, it can be splitted into the sum

$$(2.2) \quad H_I = H^+ + H^-,$$

where  $H^+ = H_\pi^+ + H_K^+$  creates one  $\pi$  and one K-meson, and  $H^- = H_\pi^- + H_K^-$  annihilates one  $\pi$ -meson and one K-meson.

The state  $|P\rangle$  can be expanded in a complete orthogonal set of eigenstates  $|\varphi_{m,n}\rangle$  of  $H_0$  containing only one hyperon and a given number of nucleons:

$$(2.3) \quad |P\rangle = \sum_{m,n} |\varphi_{m,n}\rangle \langle \varphi_{m,n} | P \rangle \equiv \sum_{m,n} |\psi_{m,n}\rangle,$$

$|\varphi_{m,n}\rangle$  are specified as follows:

$ \varphi_{0,0}\rangle$	(no mesons)
$ \varphi_{1,0}\rangle,  \varphi_{0,1}\rangle$	(one $\pi$ -meson, one K-meson)
$ \varphi_{2,0}\rangle,  \varphi_{1,1}\rangle,  \varphi_{0,2}\rangle$	(two $\pi$ -mesons, one $\pi$ -meson and one K-meson, two K-mesons)
. . . . .	

Neglecting the terms containing more than two mesons (*i.e.* terms with  $m+n \geq 2$ ) in the expansion of the state  $|P\rangle$ , with the usual procedure one obtains the

<sup>(3)</sup> K. A. BRUECKNER and K. W. WATSON: *Phys. Rev.*, **92**, 1023 (1953); M. LÉVY: *Phys. Rev.*, **88**, 725 (1952); A. KLEIN: *Phys. Rev.*, **94**, 195 (1954).

following equation for  $|\psi_{0,0}\rangle$ :

$$(2.4) \quad (E - H_0)|\psi_{0,0}\rangle = H^- G_0 G_1 |\psi_{0,0}\rangle,$$

where  $G_0 = (E - H_0)^{-1}$ ;  $G_1$  satisfies the integral equation:

$$(2.5) \quad G_1 = H^+ + H^- G_0 H^+ G_0 G_1.$$

Solving this integral equation for  $G_1$ , equation (2.4) becomes:

$$(2.6) \quad (E - H_0)|\psi_{0,0}\rangle = H^- G_0 (1 - H^- G_0 H^+ G_0)^{-1} H^+ |\psi_{0,0}\rangle.$$

If we expand the operator  $(1 - H^- G_0 H^+ G_0)^{-1}$  and retain only the first and second term (the method employed avoids consideration of the so-called «ladder correction terms»), the hyperon-nucleon potential reads as follows:

$$(2.7) \quad V_{\text{YN}} = \text{D.P.} (H^- G_0 H^+ + H^- G_0 H^- G_0 H^+ G_0 H^+).$$

By D.P. we mean that one has to take the diagonal part of the above expression with respect to  $\pi$ -meson, K-meson, nucleon and hyperon occupation numbers.

We point out that the potential (2.7) is reliable in the non-relativistic region only. The interaction at short distances ( $r \leq 0.5\hbar/\mu_{\pi}c$ ) will be arbitrarily replaced by an infinite repulsive core as usually made in the two-nucleon problem<sup>(3)</sup>.

Considering the structure of the interaction hamiltonians responsible for the elementary reactions (1.1) and (1.2), we see that the only  $\pi$ -meson contribution to the  $\Lambda$ -nucleon potential (2.7) is the fourth order term

$$(2.8) \quad V_{\pi} = \text{D.P.} (H_{\pi}^- G_0 H_{\pi}^- G_0 H_{\pi}^+ G_0 H_{\pi}^+),$$

where  $H_{\pi}$  specifies the emission or the absorption of one  $\pi$ -meson either by the nucleon or by the hyperon.

The K-meson contribution is given by:

$$(2.9) \quad V_{\text{K}} = \text{D.P.} (H_{\text{K}}^- G_0 H_{\text{K}}^+ + H_{\text{K}}^- G_0 H_{\text{K}}^- G_0 H_{\text{K}}^+ G_0 H_{\text{K}}^+).$$

There exists obviously a term which takes into account the  $\pi$ -meson and K-meson mixed contribution, *viz.*

$$(2.10) \quad V_{\pi\text{K}} = \text{D.P.} (H_{\text{K}}^- G_0 H_{\pi}^- G_0 H_{\text{K}}^+ G_0 H_{\pi}^+ + H_{\text{K}}^- G_0 H_{\pi}^- G_0 H_{\pi}^+ G_0 H_{\text{K}}^+ + H_{\pi}^- G_0 H_{\text{K}}^- G_0 H_{\text{K}}^+ G_0 H_{\pi}^+ + H_{\pi}^- G_0 H_{\text{K}}^- G_0 H_{\pi}^+ G_0 H_{\text{K}}^+).$$

Terms odd in  $H_{\pi}$  and  $H_{\text{K}}$  or bilinear in  $H_{\pi}^{-(+)}$  and  $H_{\text{K}}^{+(-)}$  give no contribution to the potential (2.10).

The quantum-mechanical potentials (2.8), (2.9) and (2.10) are useful in the evaluation of two-body and three-body forces between  $\Lambda$ -hyperon and nucleons. In the next section we give the explicit expressions of such forces



for the case of two-body interaction. Three-body forces will not be considered in this paper. By such a statement, however, we do not mean that the contribution from three-body forces is negligible. In fact, as we shall see, the largest contribution to the two-body hyperon-nucleon potential comes from the exchange of two mesons and consequently one can expect that also three-body forces contribute to the binding of the hypernuclei <sup>(4)</sup>. However, it seems convenient for simplicity to discuss the hyperfragment data on the basis of only two-body interaction as in the case of nucleon-nucleon interaction in nuclei.

2'2. *Explicit expressions of the potentials.* — In the application of the potentials, given in the previous paragraph, to the evaluation of the binding energy of the light hyperfragments, it will be sufficient to consider the static approximation (fixed baryon sources). It is to be noted that this is a good approximation when pion-baryon reactions are considered, but is not satisfactory when K-meson-baryon reactions are taken into account. However, it is to be expected that the qualitative features of the interaction will also be respected in this simpler formulation. Analogously, in the energy denominators of the various terms, the energy dependence and the mass differences  $M_\Sigma - M_\Lambda$  and  $M_{\Sigma,\Lambda} - M_n$  will be neglected. In addition the non relativistic approximation for the various  $\gamma_5$ -couplings (Dyson-Foldy transformation) will be used, dropping all the terms but the gradient one.

The interaction hamiltonian density which is responsible of the  $\Lambda$ -nucleon forces, can be written in general as:

$$(2.11) \quad \mathcal{H}_I = \mathcal{H}_I^{nn} + \mathcal{H}_I^{\Lambda\pi} + \mathcal{H}_I^{\Lambda K} + \mathcal{H}_I^{\Sigma K},$$

where

$$\begin{aligned} \mathcal{H}_I^{nn} &= ig_{n\pi} \bar{n} \gamma_5 (\boldsymbol{\pi} \cdot \boldsymbol{\tau}) n \\ \mathcal{H}_I^{\Lambda\pi} &= \begin{cases} ig_{\Lambda\pi}^{\text{ps}} \bar{\Lambda} \gamma_5 \boldsymbol{\pi} \cdot \boldsymbol{\Sigma} & + \text{h.c.} & \text{for } \Sigma^+, \\ g_{\Lambda\pi}^s \bar{\Lambda} \boldsymbol{\pi} \cdot \boldsymbol{\Sigma} & + \text{h.c.} & \text{for } \Sigma^-, \end{cases} \\ \mathcal{H}_I^{\Lambda K} &= \begin{cases} g_{\Lambda K}^s \bar{\Lambda} \Lambda K & + \text{h.c.} & \text{for } K^+, \\ ig_{\Lambda K}^{\text{ps}} \bar{n} \gamma_5 \Lambda K & + \text{h.c.} & \text{for } K^-, \end{cases} \\ \mathcal{H}_I^{\Sigma K} &= \begin{cases} g_{\Sigma K}^s \bar{\Sigma} (\boldsymbol{\Sigma} \cdot \boldsymbol{\tau}) K & + \text{h.c.} & \text{for } K^+ \Sigma^+ \text{ and } K^- \Sigma^-, \\ ig_{\Sigma K}^{\text{ps}} \bar{n} \gamma_5 (\boldsymbol{\Sigma} \cdot \boldsymbol{\tau}) K & + \text{h.c.} & \text{for } K^+ \Sigma^- \text{ and } K^- \Sigma^+. \end{cases} \end{aligned}$$

With  $\psi^+(\psi^-)$  we mean that the field  $\psi$  is scalar (pseudoscalar).

<sup>(4)</sup> R. SPITZER has considered the contribution of three-body forces in the hypertriton (in press).

From the structure of the hamiltonian density (2.11), one deduces that all the different spinor fields  $n$ ,  $\Lambda$  and  $\Sigma$  must anticommute one another <sup>(5)</sup> in order that the equations of motions for all field operators be uniquely determined from the principle of stationary action.

In what follows we shall give the explicit expressions of the  $\Lambda$ -nucleon potentials relative to the various cases considered. The singlet  $V_s$  and triplet  $V_T$  central potentials as well as the ratio  $V_s/V_T$  are arranged in Tables I to VIII as functions of the parameters  $x = \mu_{\pi} r$ . The potentials given in Tables I, II, III, and IV are in units  $(g_{\Lambda\pi})^2/4\pi = 13.3$ .

TABLE I. -  $V_{\pi\pi}^{\Lambda\pi}$  in  $\text{MeV} \cdot (g_{\Lambda\pi}^s)^2/4\pi$ .

$x$	Singlet	Triplet	$V_s/V_T$
0.4	-49.09	-18.68	2.63
0.5	-18.05	-7.62	2.37
0.6	-5.40	-2.39	2.26
0.7	-2.42	-1.08	2.24
0.8	-1.18	-0.53	2.23
0.9	-0.71	-0.32	2.23
1.0	-0.33	-0.15	2.23
1.2	-0.12	-0.054	2.23
1.4	-0.051	-0.023	2.23
1.6	-0.022	-0.010	2.22

TABLE II. -  $V_{\pi\pi}^{\Sigma}$  in  $\text{MeV} \cdot (g_{\Lambda\pi}^s)^2/4\pi$ .

Singlet=Triplet	$V_s/V_T$
-253.18	+1
-108.65	+1
-62.46	+1
-36.07	+1
-21.39	+1
-13.94	+1
-8.71	+1
-3.93	+1
-1.91	+1
-0.96	+1

TABLE III.

$V_{K^+}$ in $\text{MeV} \cdot (g_{\Lambda K}^s)^2/4\pi \langle P_X \rangle$			in $\text{MeV} \cdot (g_{\Lambda K}^s)^2/4\pi \langle P_X \rangle$			$V_{K^+} + V_{\pi K^+}$ in $\text{MeV} \cdot (g_{\Lambda K}^s)^2/4\pi \langle P_X \rangle$			
$x$	Singlet	Triplet	$V_s/V_T$	Singlet	Triplet	$V_s/V_T$	Singlet	Triplet	$V_s/V_T$
0.4	-81.76	+81.76	-1	+17.18	+5.73	+3	-64.58	+87.49	-0.74
0.5	-43.81	+43.81	-1	+4.72	+1.57	+3	-39.09	+45.38	-0.86
0.6	-26.74	+26.74	-1	+1.16	+0.39	+3	-25.58	+27.13	-0.94
0.7	-16.73	+16.73	-1	+0.31	+0.10	+3	-16.42	+16.83	-0.97
0.8	-9.66	+9.66	-1	+0.04	+0.01	+3	-9.62	+9.67	-0.99
0.9	-5.35	+5.35	-1	+0.01	+0.00	+3	-5.34	+5.35	-0.99
1.0	-2.42	+2.42	-1	+0.00	+0.00	+3	-2.42	+2.42	-1.00

<sup>(5)</sup> T. KINOSHITA: *Phys. Rev.*, **96**, 199 (1954). We are indebted to Prof. G. MORPURGO for a discussion on this point.

TABLE IV.

$V_{K^-}$ in $\text{MeV} \cdot (g_{\Lambda K}^{\text{ps}})^2 / 4\pi \langle P_X \rangle$				$V_{\pi K^-}$ in $\text{MeV} \cdot (g_{\Lambda K}^{\text{ps}})^2 / 4\pi \langle P_X \rangle$				$V_{K^-} + V_{\pi K^-}$ in $\text{MeV} \cdot (g_{\Lambda K}^{\text{ps}})^2 / 4\pi \langle P_X \rangle$			
$x$	Singlet	Triplet	$V_S/V_T$	Singlet	Triplet	$V_S/V_T$	Singlet	Triplet	$V_S/V_T$		
0.4	-4.74	-1.58	+3	-45.08	+15.53	-2.90	-49.82	+13.95		-3.57	
0.5	-2.54	-0.85	+3	-11.50	+3.88	-2.96	-14.04	+3.03		-4.63	
0.6	-1.55	-0.52	+3	-4.21	+1.41	-2.98	-5.76	+0.89		-6.47	
0.7	-0.97	-0.32	+3	-1.95	+0.65	-3.00	-2.92	+0.33		-8.85	
0.8	-0.56	-0.19	+3	-0.64	+0.21	-3.00	-1.20	+0.02		-60.00	
0.9	-0.31	-0.10	+3	-0.23	+0.07	-3.00	-0.54	-0.03		+21.50	
1.0	-0.14	-0.05	+3	-0.00	+0.00	-3.00	-0.14	-0.05		+2.80	

2.2.1. Interaction by means of the pion field only. — The potential (2.8) only is effective. The relative processes are of the type sketched in Fig. 1. One finds respectively:

Scalar  $\Sigma$ -hyperon

$$V_{\pi\pi}^{\Sigma^+} = -\beta \frac{(g_{\Lambda\pi}^{\text{ps}})^2}{4\pi} \left( \frac{\mu_\pi}{M_\Sigma + M_\Lambda} \right)^2 \frac{1}{x^3} \frac{6}{\pi} \left\{ \exp[-x] \cdot \right.$$

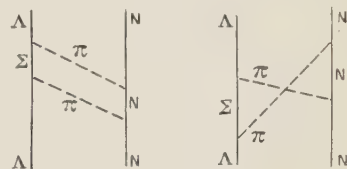


Fig. 1.

$$\begin{aligned} & \left[ \frac{4+4x+x^2}{x} K_1(x) + (2+2x+x^2) K_0(x) \right] + \frac{2}{3} (\sigma_1 \cdot \sigma_2) \left[ (1+x) K_0(x) \exp[-x] - \right. \\ & \left. + \frac{2+2x+x^2}{x} K_1(x) \exp[-x] - 6K_0(2x) - \frac{6+4x^2}{x} K_1(2x) \right] + \frac{1}{3} S_{12} \left[ 12K_0(2x) + \right. \\ & \left. + \frac{15+4x^2}{x} K_1(2x) - (1+x) K_0(x) \exp[-x] - \frac{5+5x+x^2}{x} K_1(x) \exp[-x] \right] \Big\} . \end{aligned}$$

$$x = \mu_\pi r, \quad \beta = \mu_\pi \left( \frac{\mu_\pi}{2M_\Lambda} \right)^2 \frac{g_{\Lambda\pi}^2}{4\pi} .$$

Note that this potential is expressed by the same formula as the Brueckner-Watson nucleon-nucleon potential<sup>(3)</sup> putting  $\tau_1 \cdot \tau_2 = 0$  and assuming  $m_\Sigma = m_\Lambda = m_n$  and  $g_{\Lambda\pi}^{\text{ps}} = (g_{n\pi})^2$ .

Pseudoscalar  $\Sigma$ -hyperon

$$V_{\pi\pi}^{\Sigma^-} = -\beta \frac{(g_{\Lambda\pi}^{\text{ps}})^2}{4\pi} \frac{6}{\pi} \left( 1 + \frac{1}{x} \right) \frac{K_1(x)}{x} \exp[-x] .$$

2.2.2. Interaction by means of K-mesons only. — In this case the hyperon does not interact directly with the pion field ( $\mathcal{H}_I^{\Lambda\pi} = 0$ ). The contribution to the potentials (2.9) and (2.10) arises from graphs of the type

shown in Fig. 2. The potentials relative to processes in which two K-mesons are exchanged between nucleon and hyperon are very short ranged. With the selected K-baryon coupling constants (see Sects. 3 and 4) these potentials are effective in the hard core region only and will not be considered explicitly. We have  $(y = \mu_K r)^{(*)}$ :

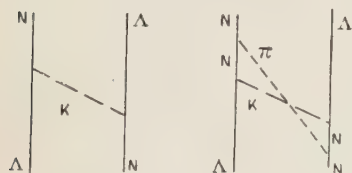


Fig. 2.

*Scalar K-meson*

$$V_{K^-} = \frac{(g_{\Lambda K}^s)^2}{4\pi} \cdot \mu_K \frac{\exp[-y]}{y} P_x P_\sigma,$$

$$\begin{aligned} V_{\pi K^+} = & \frac{g_{n\pi}^2}{4\pi} \frac{(g_{\Lambda K}^s)^2}{4\pi} \left( \frac{\mu_\pi}{2M_n} \right)^2 \mu_\pi \frac{1}{\pi} P_x P_\sigma \frac{1}{x} \cdot \\ & \cdot \left\{ (\boldsymbol{\sigma}_1 \cdot \boldsymbol{\sigma}_2) \left[ -K_0(y) \exp[-x] + \left( \frac{K_1(x)}{x} - K_0(x) \right) \right. \right. \\ & \cdot \left( \exp[-y] - \frac{2}{\pi} \frac{\mu_K}{\mu_\pi + \mu_K} x K_0(y) \right) \left. \right] - S_{12} \left[ K_0(y) \exp[-x] \frac{3 + 3x + x^2}{x^2} + \right. \\ & \left. \left. + \left( 2 \frac{K_1(x)}{x} + K_0(x) \right) \left( \exp[-y] - \frac{2}{\pi} \frac{\mu_K}{\mu_\pi + \mu_K} x K_0(y) \right) \right] \right\}. \end{aligned}$$

*Pseudoscalar K-meson*

$$V_{K^-} = -\frac{1}{3} \frac{(g_{\Lambda K}^{ps})^2}{4\pi} \left( \frac{\mu_K}{M_n - M_\Lambda} \right)^2 \mu_K P_x P_\sigma \left[ (\boldsymbol{\sigma}_1 \cdot \boldsymbol{\sigma}_2) + \frac{3 + 3y + y^2}{y^3} S_{12} \right] \frac{\exp[-y]}{y},$$

$$\begin{aligned} V_{\pi K^+} = & \frac{g_{n\pi}^2}{4\pi} \frac{(g_{\Lambda K}^{ps})^2}{4\pi} \left( \frac{\mu_\pi}{2M_n} \right)^2 \left( \frac{\mu_\pi}{M_n + M_\Lambda} \right)^2 \mu_\pi \frac{3}{\pi} P_x P_\sigma \cdot \\ & \cdot \left\langle \frac{\exp[-y]}{x^3} \left\{ K_0(x)(2 + 2y + y^2) + \frac{K_1(x)}{x} (4 + 4y + y^2) - \right. \right. \\ & - \frac{2}{3} (\boldsymbol{\sigma}_1 \cdot \boldsymbol{\sigma}_2) \left[ K_0(x)(1 + y) + \frac{K_1(x)}{x} (2 + 2y + y^2) \right] + \\ & + \frac{1}{3} S_{12} \left[ K_0(x)(1 + y) + \frac{K_1(x)}{x} (5 + 5y + y^2) \right] \left. \right\} + \\ & + \text{the same expression with } x \leftrightarrow y \text{ times } \left( \frac{\mu_K}{\mu_\pi} \right)^5 + \end{aligned}$$

(\*) In evaluating the potentials in which a factor  $\mu_\pi \mu_K / (\mu_\pi + \mu_K)$  appears, the following approximation has been used.

$$\frac{\omega \Omega'}{\omega + \Omega'} \sim \frac{\mu_\pi \mu_K}{\mu_\pi + \mu_K}.$$



$$\begin{aligned}
& + \frac{\mu_K^3}{\mu_\pi^2(\mu_\pi + \mu_K)} \frac{2}{3\pi} \left\{ 2(\sigma_1 \sigma_2) \left[ \frac{K_1(x)}{x} \frac{K_1(y)}{y} + K_0(x) \frac{K_1(y)}{y} + K_0(y) \frac{K_1(x)}{x} \right] - \right. \\
& - S_{12} \left[ 4 \frac{K_1(x)}{x} \frac{K_1(y)}{y} + K_0(x) \frac{K_1(y)}{y} + K_0(y) \frac{K_1(x)}{x} \right] \left. \right\} + \\
& + \frac{\mu_K^3}{\mu_\pi^2(\mu_\pi + \mu_K)} \frac{1}{\pi} \left\{ \left( \frac{K_1(x)}{x} - K_0(x) \right) \left( \frac{K_1(y)}{y} - K_0(y) \right) - \right. \\
& - 2 \left( \frac{K_1(x)}{x} - K_0(x) \right) \frac{K_1(y)}{y} - 2 \left( \frac{K_1(y)}{y} - K_0(y) \right) \frac{K_1(x)}{x} + \\
& \left. + 3 \left( \frac{K_1(x)}{x} + K_0(x) \right) \left( \frac{K_1(y)}{y} + K_0(y) \right) \right\} \rangle.
\end{aligned}$$

### 2.2.3. Interaction by means of both pions and K-mesons. —

Besides the processes sketched in Figs. 1 and 2, one has to look upon graphs of the kind shown in Fig. 3. Then, in addition to the potentials  $V_{K^\pm} + V_{\pi K^\pm}$  and  $V_{\pi\pi}^{\pm\pm}$ , four other potentials, corresponding to the possibilities  $\Sigma^+K^+$ ,  $\Sigma^+K^-$ ,  $\Sigma^-K^+$  and  $\Sigma^-K^-$ , are to be considered:

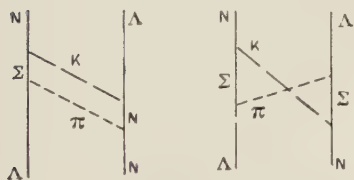


Fig. 3.

*Scalar  $\Sigma$ -hyperon, scalar K-meson*

$$\begin{aligned}
V_{\pi K^-}^{\Sigma^-} = & (g_{\Sigma K}^s)^2 \left( \frac{g_{\Lambda\pi}^{ps}}{M_\Sigma + M_\Lambda} \right)^2 \left[ (g_{\Lambda K}^s)^2 \left( \frac{g_{\pi\pi}^s}{2M_n} \right)^2 \right]^{-1} V_{\pi K^+} + \\
& + \frac{g_{n\pi} g_{\Lambda\pi}^{ps} g_{\Lambda K}^s g_{\Sigma K}^s}{4\pi \cdot 4\pi} \frac{\mu_\pi^2}{2M_n(M_\Sigma + M_\Lambda)} \frac{\mu_\pi \mu_K}{\mu_\pi + \mu_K} \frac{4}{\pi^2} P_x P_\sigma \cdot \\
& \cdot K_0(y) \left[ (\sigma_1 \sigma_2) \left( \frac{K_1(x)}{x} - K_0(x) \right) - S_{12} \left( 2 \frac{K_1(x)}{x} + K_0(x) \right) \right].
\end{aligned}$$

TABLE V.

$x$	$V_{\pi K^+}^{\Sigma^+}(1)$ in MeV $\cdot \frac{(g_{\Lambda\pi}^{ps})^2}{4\pi} \frac{(g_{\Sigma K}^s)^2}{4\pi} \langle P_x \rangle$			$V_{\pi K^-}^{\Sigma^-}(2)$ in MeV $\cdot \frac{g_{n\pi} g_{\Lambda\pi}^{ps} g_{\Lambda K}^s g_{\Sigma K}^s}{4\pi \cdot 4\pi} \langle P_x \rangle$		
	Singlet	Triplet	$V_s/V_T$	Singlet	Triplet	$V_s/V_T$
0.4	+ 0.859	+ 0.286	+ 3	+ 0.560	+ 0.187	+ 3
0.5	+ 0.236	+ 0.079	+ 3	+ 0.165	+ 0.055	+ 3
0.6	+ 0.058	+ 0.019	+ 3	+ 0.077	+ 0.026	+ 3
0.7	+ 0.015	+ 0.005	+ 3	+ 0.033	+ 0.011	+ 3
0.8	+ 0.002	+ 0.001	+ 3	+ 0.012	+ 0.004	+ 3
0.9	+ 0.000	+ 0.000	+ 3	+ 0.005	+ 0.002	+ 3
1.0	+ 0.000	+ 0.000	+ 3	+ 0.000	+ 0.000	+ 3

*Scalar  $\Sigma$ -hyperon, pseudoscalar K-meson*

$$\begin{aligned}
 V_{\pi K^-}^{\Sigma^+} = & \frac{(g_{\Lambda\pi}^{\text{ps}})^2}{(M_\Sigma + M_\Lambda)^2} \left( \frac{g_{\Sigma K}^{\text{ps}}}{M_\Sigma + M_\Lambda} \right)^2 \left[ \left( \frac{g_{n\pi}}{2M_n} \right)^2 \left( \frac{g_{\Lambda K}^{\text{ps}}}{M_\Lambda + M_n} \right)^2 \right]^{-1} V_{\pi K^-} - \\
 & + \frac{g_{n\pi} g_{\Lambda\pi}^{\text{ps}} g_{\Lambda K}^{\text{ps}} g_{\Sigma K}^{\text{ps}}}{4\pi \cdot 4\pi} \left( \frac{\mu_\pi}{M_\Sigma + M_\Lambda} \right)^2 \frac{\mu_K^2}{2M_n(M_\Lambda + M_n)} \frac{\mu_\pi \mu_K}{\mu_\pi + \mu_K} \frac{2}{\pi^2} P_x P_\sigma \cdot \\
 & \cdot \left\{ 4(\sigma_1 \cdot \sigma_2) \left( \frac{K_1(x)}{x} \frac{K_1(y)}{y} + K_0(x) \frac{K_1(y)}{y} + K_0(y) \frac{K_1(x)}{x} \right) - \right. \\
 & 2S_{12} \left( 4 \frac{K_1(x)}{x} \frac{K_1(y)}{y} + K_0(x) \frac{K_1(y)}{y} + K_0(y) \frac{K_1(x)}{x} \right) - \\
 & - 3 \left[ \left( \frac{K_1(x)}{x} - K_0(x) \right) \left( \frac{K_1(y)}{y} - K_0(y) \right) - 2 \left( \frac{K_1(x)}{x} - K_0(x) \right) \frac{K_1(y)}{y} - \right. \\
 & \left. \left. - 2 \left( \frac{K_1(y)}{y} - K_0(y) \right) \frac{K_1(x)}{x} + 3 \left( \frac{K_1(x)}{x} + K_0(x) \right) \left( \frac{K_1(y)}{y} - K_0(y) \right) \right] \right\}.
 \end{aligned}$$

TABLE VI.

$x$	$V_{\pi K^-}^{\Sigma^+}(1)$ in MeV $\cdot \frac{(g_{\Lambda\pi}^{\text{ps}})^2}{4\pi} \frac{(g_{\Sigma K}^{\text{ps}})^2}{4\pi} \langle P_x \rangle$			$V_{\pi K^-}^{\Sigma^+}(2)$ in MeV $\cdot \frac{g_{n\pi} g_{\Lambda\pi}^{\text{ps}} g_{\Lambda K}^{\text{ps}} g_{\Sigma K}^{\text{ps}}}{4\pi \cdot 4\pi} P_x$		
	Singlet	Triplet	$V_s/V_T$	Singlet	Triplet	$V_s/V_T$
0.4	-1.920	+0.662	-2.90	+0.253	-0.051	-4.96
0.5	-0.490	+0.165	-2.96	+0.105	-0.025	-4.20
0.6	-0.179	+0.060	-2.98	+0.042	-0.012	-3.50
0.7	-0.083	+0.028	-3.00	+0.020	-0.007	-2.96
0.8	-0.027	+0.009	-3.00	+0.008	-0.003	-2.67
0.9	-0.010	+0.003	-3.00	+0.004	-0.002	-2.00
1.0	-0.000	+0.000	-3.00	+0.002	-0.001	-1.65

*Pseudoscalar  $\Sigma$ -hyperon, scalar K-meson*

$$\begin{aligned}
 V_{\Sigma^-}^{\pi K^+} = & (g_{\Lambda\pi}^s)^2 \frac{(g_{\Sigma K}^{\text{ps}})^2}{(M_n + M_\Sigma)^2} \left[ \left( \frac{g_{n\pi}}{2M_n} \right)^2 (g_{\Lambda K}^s)^2 \right]^{-1} V_{\pi K^+} \text{ (with } \mu_\pi \leftrightarrow \mu_K) + \\
 & - \frac{g_{n\pi} g_{\Lambda\pi}^s g_{\Lambda K}^s g_{\Sigma K}^{\text{ps}}}{4\pi \cdot 4\pi} \left( \frac{\mu_\pi}{2M_n} \right) \left( \frac{\mu_K}{M_n + M_\Sigma} \right) \frac{\mu_\pi \mu_K}{\mu_\pi + \mu_K} \frac{4}{\pi^2} P_x P_\sigma (\sigma_1 \sigma_2 + S_{12}) K_1(x) K_1(y).
 \end{aligned}$$

TABLE VII.

$x$	$V_{\pi K^+}^{\Sigma^-}(1)$ in MeV $\cdot \frac{(g_{\Lambda\pi}^s)^2}{4\pi} \frac{(g_{\Sigma\pi}^{ps})^2}{4\pi} \langle P_x \rangle$			$V_{\pi K^+}^{\Sigma^-}(2)$ in MeV $\cdot \frac{g_{n\pi}^s g_{\Lambda\pi}^s g_{\Lambda K}^s g_{\Sigma K}^{ps}}{4\pi \cdot 4\pi} \langle P_x \rangle$		
	Singlet	Triplet	$V_s/V_T$	Singlet	Triplet	$V_s/V_T$
0.4	-64.74	-21.58	+3	+18.38	+6.13	+3
0.5	-29.44	-9.81	+3	+9.28	+3.09	+3
0.6	-16.82	-5.61	+3	+4.44	+1.48	+3
0.7	-9.52	-3.17	+3	+2.18	+0.73	+3
0.8	-4.73	-1.58	+3	+1.20	+0.40	+3
0.9	-2.05	-0.68	+3	+0.74	+0.25	+3
1.0	-0.91	-0.30	+3	+0.46	+0.15	+3

*Pseudoscalar  $\Sigma$ -hyperon, pseudoscalar K-meson*

$$V_{\pi K^+}^{\Sigma^-} = \frac{(g_{\Lambda\pi}^s)^2}{4\pi} \frac{(g_{\Sigma\pi}^{ps})^2}{4\pi} \frac{3}{\pi} P_x P_\sigma \cdot$$

$$\cdot \left\{ \mu_\pi \frac{\exp[-x]}{x} K_0(y) + \mu_K \frac{\exp[-y]}{y} K_0(x) - \frac{\mu_\pi \mu_K}{\mu_\pi + \mu_K} \frac{2}{\pi} K_0(x) K_0(y) \right\} +$$

$$+ \frac{g_{n\pi}^s g_{\Lambda\pi}^s g_{\Lambda K}^s g_{\Sigma K}^{ps}}{4\pi \cdot 4\pi} \left( \frac{\mu_\pi}{2M_n} \right) \left( \frac{\mu_K}{M_n + M_\Lambda} \right) \frac{\mu_\pi \mu_K}{\mu_\pi + \mu_K} \frac{12}{\pi^2} P_x P_\sigma K_1(x) K_1(y).$$

TABLE VIII.

$x$	$V_{\pi K^+}^{\Sigma^-}(1)$ in MeV $\cdot \frac{(g_{\Lambda\pi}^s)^2}{4\pi} \frac{(g_{\Sigma\pi}^{ps})^2}{4\pi} \langle P_x \rangle$			$V_{\pi K^+}^{\Sigma^-}(2)$ in MeV $\cdot \frac{g_{n\pi}^s g_{\Lambda\pi}^s g_{\Lambda K}^s g_{\Sigma K}^{ps}}{4\pi \cdot 4\pi} \langle P_x \rangle$		
	Singlet	Triplet	$V_s/V_T$	Singlet	Triplet	$V_s/V_T$
0.4	-119.33	+119.33	-1	-1.43	+1.43	-1
0.5	-51.52	+51.52	-1	-0.75	+0.75	-1
0.6	-26.41	+26.41	-1	-0.35	+0.35	-1
0.7	-14.28	+14.28	-1	-0.18	+0.18	-1
0.8	-6.70	+6.70	-1	-0.09	+0.09	-1
0.9	-2.75	+2.75	-1	-0.03	+0.03	-1
1.0	-0.98	+0.98	-0	-0.01	+0.01	-1

### 3. - Qualitative considerations.

From a phenomenological analysis of the binding energy of the light hyperfragments in terms of a two-body  $\Lambda$ -nucleon interaction, DALITZ and DOWNS (\*)

(\*) R. DALITZ and B. W. DOWNS: *Hypernuclear binding energies and the  $\Lambda$ -nucleon interaction* (in press). In the following quoted as D.D.

have recently established that the  $\Lambda$ -nucleon potential must be spin-dependent. In particular if the singlet  $\Lambda$ -nucleon potential is more attractive than the triplet, the triplet is also attractive but only between one-half to one-third as strong. On the other hand, if the triplet interaction is more attractive than the singlet, then the singlet interaction has to be repulsive and is between one-fourth to three-fourths as strong. In details, the volume integrals are given by D.D. as follows:

TABLE IX.

Range	Singlet favored ( $\text{MeV} \cdot 10^{-39} \text{ cm}^3$ )		Triplet favored ( $\text{MeV} \cdot 10^{-39} \text{ cm}^3$ )	
	$(\mu_K)^{-1}$	$(2\mu_\pi)^{-1}$	$(\mu_K)^{-1}$	$(2\mu_\pi)^{-1}$
$V_s$	-290	-475	+ 60	+ 270
$V_T$	-133	-143	-250	-393
$V_s/V_T$	+ 2,18	+ 3,32	- 0,24	- 0,69

Following this line of thought, it is therefore consistent to select from our potentials given in Sect. 2 only those cases (or combinations) which are able to reproduce these conditions.

We will not consider explicitly the effect of tensor forces. This is a good approximation because the contribution of tensor forces to the binding is effective only if their range is longer than that of the central forces. For the  $\Lambda$ -hyperon-nucleon potentials the range of the tensor forces is shorter than that of the central ones (<sup>6</sup>).

Let us consider the following possibilities:

3'1. *Interaction by means of pion field only.* - From Tables I and II we see that only the case in which the  $\Sigma$ -hyperon has the same parity of the  $\Lambda$  gives rise to a spin dependent  $\Lambda$ -nucleon potential. In particular, while it is never possible to obtain the second D.D. condition, the first one is very well reproduced: the singlet potential is two to three times more attractive than the triplet one. Consequently the total spin of the system  ${}^3\text{H}_\Lambda$  will be  $\frac{1}{2}$ , that of the systems  ${}^4\text{H}_\Lambda$  and  ${}^4\text{He}_\Lambda$  will be zero. This is particularly interesting in consideration of the fact that from observations of  ${}^4\text{H}_\Lambda$  decay D.D. argue that the  ${}^4\text{H}_\Lambda$ ,  ${}^4\text{He}_\Lambda$  doublet has effectively spin zero thus giving experimental support to a singlet  $\Lambda$ -nucleon potential deeper than the triplet one.

On the contrary, the case in which the  $\Sigma$ -hyperon has parity different from that of the  $\Lambda$ -hyperon is excluded, because the  $\Lambda$ -nucleon potential here is not spin dependent.

(<sup>6</sup>) R. L. PEASE and H. FESHBACH: *Phys. Rev.*, **88**, 945 (1952).

3'2. *Interaction by means of K-mesons only.* — We point out that, even if the hyperon does not interact, in this case, directly with the pion field ( $\mathcal{H}_I^{\Lambda\pi} = 0$ ), exchanges of pions are allowed in any way between nucleon states and, further, that these mixed processes give rise to a large contribution to the  $\Lambda$ -nucleon potential for pseudoscalar K-mesons.

From inspection of Tables III and IV we realize that the potentials  $V_{K\pm} + V_{\pi K\pm}$ , do not reproduce the D.D. conditions either for scalar or for pseudoscalar K-mesons. It should be emphasized that for pseudoscalar K-mesons the potential  $V_K$  (alone) would give agreement with the first D.D. alternative, but the contribution from  $V_{\pi K}$  potential, which is predominant in this case, destroys this agreement. Concluding, the interaction through K-mesons only is excluded.

Therefore, we can say that the hyperon must interact directly with the pion field and, in addition, that the pion contribution to the  $\Lambda$ -nucleon potential probably has to be predominant with respect to the K-meson contribution.

### 3'3 *Interaction by means of both pions and K-mesons.*

Let us now discuss the general case in which both pions and K-mesons interact directly with the hyperon.

The discussion will be divided into two parts:

3'3.1. The  $\Sigma$ -hyperon is scalar. — In order to reproduce the first D.D. alternative (the second can never be approximated), the largest contribution to the  $\Lambda$ -nucleon potential allowed from K-meson field is about 10% for scalar K-mesons, and 20% for pseudoscalar K-mesons. If the contribution from K-meson field exceeds these limits, no agreement with the D.D. conditions can be obtained. It is to be noted that these limits are independent of the choice of the pion-hyperon and K-baryon coupling constants, but impose a limitation on them. For instance, if  $(g_{\Lambda\pi}^{\pi})^2$  is fixed, then the K-baryon coupling constants are automatically determined.

Therefore, the pion contribution to the  $\Lambda$ -nucleon potential is predominant ( $\geq 80\%$ ) with respect to the K-meson contribution. Unfortunately, this analysis gives no sufficient support for a selection between scalar and pseudoscalar K-mesons. However, an indication can be obtained by taking for  $(g_{\Lambda\pi}^{\pi})^2/4\pi$  a fixed value. If, in the spirit of a universal pion-baryon interaction (<sup>7</sup>), one chooses  $(g_{\Lambda\pi}^{\pi})^2/4\pi = (g_{\pi\pi})^2/4\pi$  then (see Sect. 4) a contribution of about 15% to the  $\Lambda$ -nucleon forces has to come from K-mesons. This determines the magnitudes of the K-baryon coupling constants which turn out to be of the order of unity in agreement with photoproduction of K-mesons as well as

(<sup>7</sup>) E. WIGNER: *Nat. Acad. Sci. U.S.*, **38**, 449 (1952); J. SCHWINGER: *Seventh Rochester Conf.*, 1957; M. GELL-MANN: *Phys. Rev.*, **106**, 1296 (1957).



with K-nucleon scattering. As a consequence, a very satisfactory agreement with the first D.D. alternative is obtained for pseudoscalar K-mesons, while the agreement is not very satisfactory for scalar K-mesons (see Sect. 4).

Before concluding, we want to emphasize that, in the same hypothesis of a universal pion-baryon interaction, the systems  $(\Xi^-, \text{neutron})$  and  $(\Xi^0, \text{proton})$  are not stable. This comes from the fact that these systems are identical with the virtual singlet state of the deuteron but with a potential less effective by a factor  $(M_n/M_\Xi)^2 = 0.5$ . For the same reason also the systems  $(\Sigma^+, \text{proton})$  and  $(\Sigma^-, \text{neutron})$  should not be bound, but in these cases contributions from one K-meson exchange (and of course, one K-meson + one  $\pi$ -meson exchange) are allowed, thus being able to give binding (\*) (see ref. (8)). It is to be pointed out that for the systems  $(\Xi, \text{nucleon})$  only two K-meson exchanges are allowed which gives a contribution that is effective in the hard core region only. Furthermore, calculations made with the method of Omura, Morita and Yamada (9) show that the systems  $(\Sigma^+, \text{proton, proton})$  and  $(\Sigma^-, \text{neutron, neutron})$  are not bound (the potentials used are those of ref. (8)). This is again a consequence of the fact that the singlet hyperon-nucleon potentials is more attractive than the triplet.

3'3.2. The  $\Sigma$ -hyperon is pseudoscalar. — The problem here becomes somewhat more involved and one does not obtain a very clear panorama of the situation as for the case in which the  $\Sigma$ -hyperon has the same parity of the  $\Lambda$ . As before, it is again impossible to approximate the second D.D. condition: the first condition can be reproduced provided that the K-meson field contribution is of the same order of magnitude as that of the pion field.

The magnitudes of the pion-hyperon and K-baryon coupling constants have been determined by following a variational calculation with the imposed conditions that the system  $(\Lambda, \text{nucleon})$  is not bound and the system  ${}^5\text{He}_\Lambda$  has the correct binding energy (the core radius has been chosen to be  $r_c = 0.33(\hbar/\mu_\pi c)$ ).

In particular, for scalar K-mesons (supposing the positive sign of the product  $g_{n\pi}g_{\Lambda\pi}^s g_{\Lambda K}^s g_{\Sigma K}^s$ ) the contribution from K-meson field is about 35%.

(\*) In order evaluate the potential for the systems  $(\Xi, \text{nucleon})$  and  $(\Sigma, \text{nucleon})$  one has to add to the hamiltonian (2.11) the following terms

$$-ig_{\Sigma\pi}^{\text{ps}}(\Sigma\gamma_5 \times \Sigma) \cdot \pi + ig_{\Xi\pi}^{\text{ps}}\bar{\Xi}\gamma_5(\pi \cdot \tau)\Xi + \mathcal{H}_I^{\Xi K}.$$

Universal pion-baryon interaction means that:

$$(g_{n\pi})^2 = (g_{\Lambda\pi}^{\text{ps}})^2 = (g_{\Sigma\pi}^{\text{ps}})^2 = (g_{\Xi\pi}^{\text{ps}})^2.$$

(8) F. FERRARI and L. FONDA: *Nuovo Cimento*, **6**, 1027 (1957).

(9) T. OHMURA, M. MORITA and M. YAMADA: *Prog. Theor. Phys.*, **17**, 326 (1957).

The values of the coupling constants are as follows:

$$\begin{aligned} \frac{(g_{\Lambda K}^s)^2}{4\pi} &\gtrsim 0.6, \\ \frac{(g_{\Lambda\pi}^s)^2}{4\pi} &= 0.55, \end{aligned} \quad \boxed{\Sigma^- K^+ \quad g_{n\pi} g_{\Lambda\pi}^s g_{\Lambda K}^s g_{\Sigma K}^{ps} > 0.}$$

This result is practically independent of the value of the pseudoscalar coupling constant  $(g_{\Sigma K}^{ps})^2/4\pi$  which can vary between zero and three.

On the other hand, if the product  $g_{n\pi} g_{\Lambda\pi}^s g_{\Lambda K}^s g_{\Sigma K}^{ps}$  is negative, one obtains:

$$\begin{aligned} \frac{(g_{\Lambda K}^s)^2}{4\pi} &\gtrsim 0.45, \\ \frac{(g_{\Lambda\pi}^s)^2}{4\pi} &= 0.4, \end{aligned} \quad \boxed{\Sigma^- K^+ \quad g_{n\pi} g_{\Lambda\pi}^s g_{\Lambda K}^s g_{\Sigma K}^{ps} < 0.}$$

The contribution from K-mesons is about 50 %. The above result is also largely independent of the value of  $(g_{\Sigma K}^{ps})^2/4\pi$  which can vary between zero and three.

Finally, for pseudoscalar K-mesons we have:

$$\begin{aligned} \frac{(g_{\Sigma K}^s)^2}{4\pi} &\gtrsim 0.8, \\ \frac{(g_{\Lambda\pi}^s)^2}{4\pi} &= 0.5, \end{aligned} \quad \boxed{\Sigma^- K^- \quad g_{n\pi} g_{\Lambda\pi}^s g_{\Lambda K}^{ps} g_{\Sigma K}^s \gtrsim 0.}$$

The contribution from the K-meson field is about 40 %. The sign of the product  $g_{n\pi} g_{\Lambda\pi}^s g_{\Lambda K}^{ps} g_{\Sigma K}^s$  is here unimportant, and the above results are independent of the value of the pseudoscalar coupling constant  $(g_{\Lambda K}^{ps})^2/4\pi$  which can be between zero and three.

In conclusion, these values of the scalar K-baryon coupling constants  $(g_{\Lambda K}^s)^2/4\pi$  and  $(g_{\Sigma K}^s)^2/4\pi$  seem in agreement with those values required to fit the low energy  $K^+$ -proton scattering and the photoproduction of K-mesons <sup>(10)</sup>. Notwithstanding, we are led to the suspicion that this solution, involving pseudoscalar  $\Sigma$ -hyperon is somewhat questionable.

Detailed calculations about the binding energy of the lightest hypernuclei will be carried out on the hypothesis of scalar  $\Sigma$ -hyperon only.

#### 4. - Quantitative results and conclusions.

From the qualitative considerations given in Sect. 3, one can draw a first indication relative to the possible properties of the strange particles  $\Lambda$ ,  $\Sigma$  and K.

<sup>(10)</sup> P. T. MATTHEWS and A. SALAM: *Nuovo Cimento*, **6**, 789 (1957).

As has been seen, only certain cases can give agreement with the experimental data. In particular, should the pion forces be predominant with respect to the K forces, the  $\Sigma$ -hyperon must have the same parity as the  $\Lambda$ -hyperon. In this case one is naturally led to the suggested theoretical idea of a universal pion-baryon interaction (<sup>7</sup>). In order to test this scheme, let us consider explicitly the binding energy of the lightest hyperfragments.

It is known experimentally that the  $\Lambda$ -hyperon gives rise to the formation of hyperfragments only with those nuclei which are intrinsically stable (<sup>1</sup>). Therefore, since the hyperon-nucleon interaction is of shorter range and weaker than the nucleon-nucleon one, we can assume that the nuclear core of the hyperfragment is only weakly deformed as a result of the hyperon-nucleon forces. In addition, we shall suppose that the reduction of the total  $\Lambda$ -nucleus potential to a sum of two-body potentials is valid. The resulting  $\Lambda$ -nucleus potential can then be written as:

$$(4.1) \quad V_{\Lambda}(r) = \sum_{i=1}^A \int V_{\Lambda n i}(\mathbf{r} - \mathbf{r}_i) \varrho(r_i) f^2(\mathbf{r} - \mathbf{r}_i) d^3 r_i.$$

In this expression the nuclear density  $\varrho(r)$  is defined by

$$\varrho(r) = \varrho_0 \exp\left(-\frac{r^2}{R^2}\right),$$

where  $R$  is determined from Hofstadter's data on high energy electron-nucleus scattering (<sup>11</sup>) (see Table X)

TABLE X.

	r.m.s. $10^{13}$ cm	$R \cdot 10^{13}$ cm
He <sup>4</sup>	1.61	1.32
He <sup>3</sup>	1.83	1.50
H <sup>3</sup>	1.83	1.50
D	1.73	1.42

Further, it has to be emphasized that our quantum-mechanical potentials exhibit repulsive cores at short distances. Therefore, it is necessary to introduce a correlation  $f(\mathbf{r} - \mathbf{r}_i)$  to take into account that the wave function

(<sup>11</sup>) R. HOFSTADTER: *Proc. Fifth Rochester Conf.*, 1955; *Proc. Seventh Rochester Conf.*, 1957.

vanishes <sup>(12)</sup> for  $|\mathbf{r} - \mathbf{r}_i| = r_c$  ( $\mathbf{r} - \mathbf{r}_i$  specifies the distance between the  $\Lambda$  and the  $i$ -th nucleon). For simplicity, this function has been chosen as follows:

$$(4.2) \quad f(\mathbf{r} - \mathbf{r}_i) = \begin{cases} 1 - \exp[-\beta(|\mathbf{r} - \mathbf{r}_i| - r_c)] & \text{for } |\mathbf{r} - \mathbf{r}_i| > r_c, \\ 0 & \text{otherwise.} \end{cases}$$

As far as the choice of the phenomenological cores is concerned, we have no criterion for establishing their radii. In the two nucleon problem, the core and the pion-nucleon coupling constant cannot be regarded as completely unspecified, since the analysis of the pion-nucleon scattering indicates that  $g_{\pi\pi}^2/4\pi \simeq 14$ , the core radius is consequently determined by fitting the low-energy nucleon-nucleon experimental data <sup>(3)</sup>. At present, it is not possible to find any similar connection for the hyperon-nucleon problem. On the other hand, it seems rather difficult to see a physical link between the nucleon-nucleon and the hyperon-nucleon systems respectively. Therefore, for mathematical convenience only, we shall suppose that the hyperon-nucleon core is the same as in the nucleon-nucleon case, *i.e.*  $r_c = 0.33\hbar/\mu_\pi c$  without giving any physical meaning to this statement.

Now, assuming the pion-baryon coupling constant equal, *i.e.*  $g_{\pi\pi}^2 = (g_{\Lambda\pi}^{ps})^2$ , the only free parameters are the K-baryon coupling constants  $(g_{\Lambda K}^s)^2$  and  $(g_{\Sigma K}^s)^2$  in the case of scalar K-mesons, and  $(g_{\Lambda K}^{ps})^2$  and  $(g_{\Sigma K}^{ps})^2$  in the case of the pseudoscalar K-mesons. These constants must be determined to reproduce the experimental data relative to the binding of the  $\Lambda$ -hyperon in nuclear matter. In this connection, a contribution is required of about 15% arising from K-mesons exchange, because, being the pion-baryon coupling constants equal, the  $\Lambda$ -nucleus potential due to pion field only is not sufficient to reproduce the experimental data (see Tables XII, XIII, XIV). As will be seen below, the K-mesons must then be pseudoscalar, since scalar K-mesons would give a negative contribution to the binding.

In order to analyze in detail this point, let us consider the expressions for the K-meson potentials writing the spin-dependent part in an explicit form. We have:

*Scalar K-meson* (see Tables III, V)

$$(4.3) \quad V_{K^+} + V_{\pi K^+} + V_{\pi K^+}^{\Sigma^+} = P_x P_\sigma |F_0(x)| + P_x P_\sigma (\boldsymbol{\sigma}_1 \cdot \boldsymbol{\sigma}_2) |F_1(x)|.$$

*Pseudoscalar K-meson* (see Tables IV, VI)

$$(4.4) \quad V_{K^-} + V_{\pi K^-} + V_{\pi K^-}^{\Sigma^+} = P_x P_\sigma |G_0(x)| - P_x P_\sigma (\boldsymbol{\sigma}_1 \cdot \boldsymbol{\sigma}_2) |G_1(x)|.$$

<sup>(12)</sup> T. D. LEE and C. N. YANG: *Phys. Rev.*, **105**, 1119 (1957); K. HUANG and C. N. YANG: *Phys. Rev.*, **105**, 767 (1957); P. MARTIN and C. DE DOMINICIS: *Phys. Rev.*, **105**, 1417 (1957).

The functions  $F_0(x)$ ,  $F_1(x)$ ,  $G_0(x)$  and  $G_1(x)$  are linear combinations of the spatial part of the potentials given in Sect. 3. In particular  $G_0(x)$  is about two times larger than  $G_1(x)$ .

The expectation values of the operators  $P_\sigma$  and  $P_\sigma(\sigma_1 \cdot \sigma_2)$  for the states describing the systems  $(\Lambda, \text{nucleon})$ ,  ${}^3\text{H}_\Lambda$ ,  ${}^4\text{H}_\Lambda$ ,  ${}^4\text{He}_\Lambda$  and  ${}^5\text{He}_\Lambda$  are given in Table XI

TABLE XI.

	Spin	$P_\sigma$	$P_\sigma(\sigma_1 \cdot \sigma_2)$
$(\Lambda, \text{n})$	0 (*)	- 1	+ 3
	1	+ 1	+ 1
${}^3\text{H}_\Lambda$	$\frac{1}{2}$ (*)	- 1	+ 5
	$\frac{3}{2}$	+ 2	+ 2
${}^4\text{H}_\Lambda$	0 (*)	0	+ 6
${}^4\text{He}_\Lambda$	1	+ 2	+ 4
${}^5\text{He}_\Lambda$	$\frac{1}{2}$ (*)	+ 2	+ 6

(\*) Only these values of the total spin are of interest in our problem, because the singlet potential is more attractive than the triplet one.

From these values of  $P_\sigma$  and  $P_\sigma(\sigma_1 \cdot \sigma_2)$ , and taking into account formulae (4.3) and (4.4), one concludes that pseudoscalar K-mesons enhance the binding, while scalar K-mesons reduce it. This implies that scalar K-mesons must be excluded in the case of a universal pion-baryon interaction even if this does not prevent agreement with the D.D. conditions (see Sect. 3). This result does not change if the core radius of the hyperon-nucleon system is reduced by (10 ÷ 20%).

The calculated values for the kinetic energy and the potential energy have been evaluated using the customary variational method, assuming the trial wave function: (\*)

$$(4.5) \quad u = c\{\exp[-\alpha r] - \exp[-8\alpha r]\}.$$

The values, in MeV, of the kinetic energy (row *a*), of the potential energy due to the pion field only (row *b*), and of the potential energy arising from K-mesons and  $\pi$ -mesons exchange (see (4.4)) (row *c*) are arranged in Tables XII, XIII and XIV. The units  $(g_{\pi\pi})^2/4\pi = (g_{\Lambda\pi\pi}^{\text{is}})^2/4\pi = 13.3$  and  $(g_{\Lambda K}^{\text{ps}})^2/4\pi =$

(\*) The evaluation of the binding energies of the  $\Lambda$ -hyperon has been carried out by following a method similar to that used by S. D. DRELL and K. HUANG: *Phys. Rev.*, **91**, 1527 (1953).



$= (g_{\Sigma K}^{\nu s})^2 / 4\pi = 1$  have been used. Due to the variational method used, the values for the binding energies are not accurate to better than 5 or 10 percent.

TABLE XII.

System ${}^3\text{H}_\Lambda$					
$\beta \backslash \alpha$	0.05	0.10	0.15	0.20	
2	2.35	6.02	10.68	15.83	(a)
	2.09	3.71	5.38	6.74	(b)
	0.11	0.21	0.32	0.44	(c)
4	2.81	6.65	11.47	16.77	(a)
	2.73	5.03	7.13	7.13	(b)
	0.15	0.31	0.48	0.64	(c)
6	3.23	7.31	12.20	17.62	(a)
	3.18	5.82	8.27	10.50	(b)
	0.20	0.42	0.64	0.85	(c)
8	3.69	7.73	12.66	18.48	(a)
	3.55	6.59	9.33	11.80	(b)
	0.24	0.52	0.75	0.99	(c)

TABLE XIII.

Systems ${}^4\text{He}_\Lambda$ and ${}^4\text{H}_\Lambda$ .					
$\beta \backslash \alpha$	0.50	0.10	0.15	0.20	
2	2.24	5.40	8.92	13.15	(a)
	1.95	3.92	5.95	7.88	(b)
	0.19	0.38	0.59	0.78	(c)
4	8.30	5.59	9.31	14.09	(a)
	2.29	4.73	7.15	9.55	(b)
	0.29	0.57	0.87	1.15	(c)
6	2.39	5.84	9.85	14.80	(a)
	2.81	5.40	8.18	10.96	(b)
	0.38	0.72	1.09	1.45	(c)
8	2.40	6.16	11.02	15.15	(a)
	2.91	6.01	8.88	12.20	(b)
	0.42	0.83	1.25	1.66	(c)

TABLE XIV.

System ${}^5\text{He}_\Lambda$ .					
$\beta \backslash \alpha$	0.05	0.10	0.15	0.20	
2	3.63	8.11	13.95	19.97	(a)
	2.61	4.82	6.85	8.76	(b)
	0.23	0.49	0.84	1.18	(c)
4	3.46	7.92	13.43	19.15	(a)
	3.50	6.40	9.00	11.40	(b)
	0.34	0.74	1.20	2.12	(c)
6	3.25	7.73	13.05	18.47	(a)
	4.13	7.38	10.31	12.97	(b)
	0.50	0.93	1.49	2.12	(c)
8	3.07	7.50	12.68	17.73	(a)
	4.61	8.17	11.40	14.25	(b)
	0.50	1.07	1.71	2.43	(c)

From inspection of Tables XII, XIII and XIV we see that good agreement with experimental data (see Table XV) and with the first D.D. condition is obtained by choosing  $(g_{\Lambda K}^{\text{D}\pi})^2/4\pi = (g_{\Sigma K}^{\text{D}\pi})^2/4\pi = 1.6$ .

TABLE XV.

	${}^3\text{H}_\Lambda$	${}^4\text{H}_\Lambda$	${}^4\text{He}_\Lambda$	${}^5\text{He}_\Lambda$
Experimental B. E. $({}^{13})$ (MeV)	0.25	1.44	1.77	2.56
Calculated B. E. (MeV) (K- and $\pi$ -fields) $(g_K^{\text{D}\pi})^2/4\pi = 1.6$ (universal pion-baryon interaction)	0.27	1.18	1.18	2.56
Calculated B. E. (MeV) ( $\pi$ -field only) $(g_{\Lambda\pi}^{\text{D}\pi})^2/4\pi = 16.1$	0.66	1.19	1.19	2.56

$({}^{13})$  V. L. TELEGDI: *Proc. Seventh Rochester Conf.*, 1957.

It is interesting to note that this value of the K-baryon coupling constant is in agreement also with photoproduction of K-mesons and with K-nucleon scattering <sup>(10)</sup>.

Furthermore; the experimental data can also be fitted disregarding the contribution from the K-meson field to the  $\Lambda$ -nucleon potential ( $\mathcal{H}_I^{\Lambda K} = \mathcal{H}_I^{\Sigma K} = 0$ ). This implies obviously (assuming  $(g_{\pi\pi})^2/4\pi = 13.3$  and  $r_c = 0.33\hbar/\mu_\pi c$ ) a value for the pion-hyperon coupling constant larger than that of the pion-nucleon interaction (see Table XV), *viz.*

$$\frac{(g_{\Lambda\pi}^{\text{ps}})^2}{4\pi} = 16.1.$$

In conclusion, the analysis carried out in this paper does not allow a unique theoretical picture of the  $\Lambda$ -nucleon problem. However, we have essentially two solutions, which are strictly connected with the relative contributions of the pion and K-meson fields respectively.

If one believes that the pion contribution is predominant ( $\geq 80\%$  or eventually the only one which comes into play), the  $\Sigma$  and the  $\Lambda$  hyperons have to be of the same parity. In particular, if a universal pion-baryon interaction is considered, the K-meson is pseudoscalar.

On the other hand, if the contribution from the pion-field and from the K-meson field are of the same order of magnitude ( $(35 \div 50)\%$ ) the parity of the  $\Sigma$ -hyperon has to be opposite to that of the  $\Lambda$ -hyperon.

Finally, no agreement with experiment can be obtain if the  $\Lambda$ -nucleon interaction is essentially due to the exchange of K-mesons (scalar or pseudo-scalar).

\* \* \*

The authors should like to thank Prof. N. DALLAPORTA for his kind interest. Many thanks also to Mr. PINORI and Mr. DONADONI for numerical calculations.

## RIASSUNTO

Si discute l'energia di legame della  $\Lambda$  in materia nucleare tenendo conto esplicito dei risultati fenomenologici di DALITZ e DOWNS. Si analizzano tutte le possibili combinazioni delle parità del mesone K e dell'iperone  $\Sigma$  nei vari processi di interazione con scambio di pioni e di mesoni K. La soluzione più probabile risulta quella in cui l'iperone  $\Sigma$  ha la stessa parità dell'iperone  $\Lambda$ . In questo caso il contributo del campo pionico è prevalente rispetto a quello del campo K. Si discute anche la stabilità dei sistemi ( $\Xi$ , nucleone) e ( $\Sigma$ , nucleone).

## Nuclear Interactions of Neutral K-Mesons of Long Lifetime.

V. BISI, R. CESTER, A. DEBENEDETTI, C. M. GARELLI,  
B. QUASSIATI, L. TALLONE and M. VIGONE

*Istituto di Fisica dell'Università - Torino*  
*Istituto Nazionale di Fisica Nucleare - Sezione di Torino*

(ricevuto il 31 Maggio 1958)

**Summary.** — An emulsion stack was exposed at the Berkeley Bevatron, to a neutral beam emitted at  $45^\circ$  with the internal beam entering a Be target. The total distance between stack and target was 6 meters. 9  $K^+$ , 8 particles of strangeness  $-1$  and 4 hyperfragments, all outcoming from stars in emulsion, were found scanning for interaction products of long lived neutral K. From the relative frequency of particles with different strangeness, we deduced the composition of the  $\theta_2^0$  beam entering the stack. The experimental result is compatible with a strangeness mixture of the type proposed by GELL-MANN and PAIS.

### 1. — Introduction.

In the last year some experiments <sup>(1-5)</sup> have been carried out in order to prove the existence of the  $\theta_2^0$  meson, as predicted by the Gell-Mann and Pais scheme <sup>(6)</sup>. The mode of interaction of the  $\bar{\theta}^0$  component of the long lived neutral K particles has also been studied in detail.

In this work both  $\theta^0$  and  $\bar{\theta}^0$  interaction modes were studied in emulsion. This allows us to give a rough estimate of the relative proportion of the

(1) K. LANDE, E. T. BOOTH, I. IMPEDUGLIA, L. M. LEDERMAN and W. CHINOWSKI: *Phys. Rev.*, **103**, 1901 (1956); K. LANDE, L. M. LEDERMAN and W. CHINOWSKI: *Phys. Rev.*, **105**, 1925 (1957).

(2) W. F. FRY, J. SCHNEPS and M. S. SWAMI: *Phys. Rev.*, **103**, 1904 (1956).

(3) M. BALDO CEOLIN, C. C. DILWORTH, W. F. FRY, W. D. B. GREENING, H. HUZITA, S. LIMENTANI and A. E. SICHIOLO: *Nuovo Cimento*, **6**, 130 (1957).

(4) R. AMMAR, J. I. FRIEDMAN, R. LEVI-SETTI and V. L. TELEGGI: *Proc. VII-th Rochester Conference* (1957).

(5) W. K. H. PANOFSKI, V. L. FITCH, R. M. MOTLEY and W. G. CHESNUT: *Phys. Rev.*, **109**, 1353 (1958).

(6) M. GELL-MANN and A. PAIS: *Phys. Rev.*, **47**, 1387 (1955).

particles of different strangeness in the  $\theta_2^0$  beam. This is found to be in good agreement with a mixture of the Gell-Mann and Pais type.

## 2. - Exposure details.

The stack was exposed to a neutral beam coming from a Berillium target in the Bevatron, at an angle of  $45^\circ$  with the 6.3 GeV proton beam.

A 20000 G magnet to sweep out the charged particles, and a Pb  $\gamma$ -rays converter, one inch thick, were set in the path between target and stack.

The total distance between target and stack was of 6 m.

Following the calculations of BLOCK *et al.* <sup>(7)</sup> one can obtain the energy

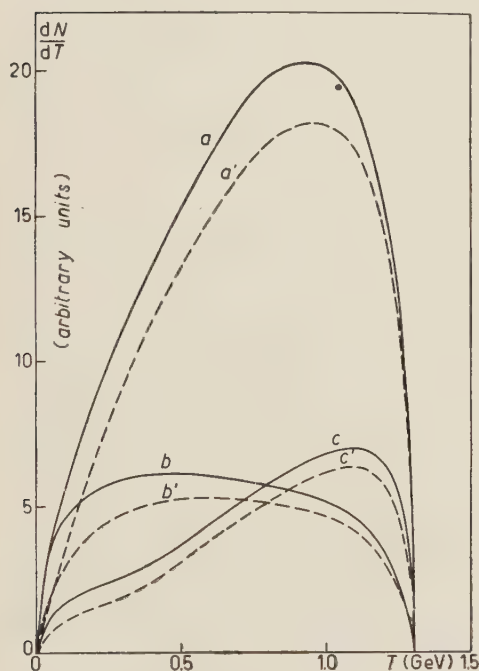


Fig. 1.

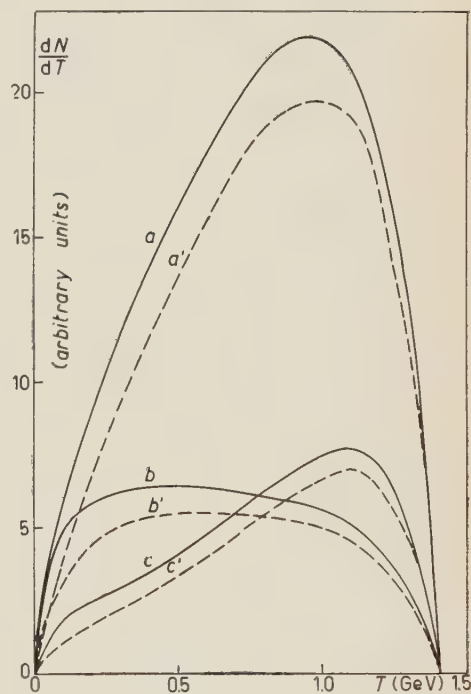


Fig. 2.

Fig. 1. - Energy distribution in the laboratory system of the particles produced at  $45^\circ$  with the 6.3 GeV proton beam in the reaction  $p + \bar{K} \rightarrow \Sigma + \theta_2^0 + \bar{K}$ . Three different hypotheses for the matrix element of production have been considered: isotropic and energy independent (curves *a*), dependent on  $\cos^2 \bar{\theta}$  (curves *b*), dependent on  $\bar{p}^2 \cos^2 \bar{\theta}$  (curves *c*). The dashed lines represent the same cross-section when a value of  $7 \cdot 10^{-8}$  s for the mean life of the  $\theta_2^0$  particles is taken into account.

Fig. 2. In this figure are plotted the same curves of Fig. 1, calculated for the reaction  $p + \bar{K} \rightarrow \Lambda^0 + \theta^0 + \bar{K}$ .

(7) M. M. BLOCK, E. M. HARTH and R. M. STERNHEIMER: *Phys. Rev.*, **100**, 324 (1955).



distribution in the laboratory system for the  $\theta^0$  particles produced at  $45^\circ$  with the proton beam, when the energy of the incident protons is 6.3 GeV. We made this calculation for three different hypotheses for the matrix element of production in the centre of mass system: isotropic and energy independent, dependent on  $\cos^2 \bar{\theta}$ , dependent on  $\bar{p}^2 \cos^2 \bar{\theta}$  (the barred quantities refer to the centre of mass system) (\*). We introduced the simplifying hypothesis that the struck nucleon is at rest, and we took into consideration the two possible reactions for production of  $\theta^0$  particles:

$$p + \pi^- \rightarrow \Sigma + \theta^0 + \pi^-,$$

$$p + \pi^- \rightarrow \Lambda^0 + \theta^0 + \pi^-.$$

The results are represented in Fig. 1 and 2, where the values of the cross section per MeV per steradian are given in arbitrary units.

The curves of Fig. 1 and 2 give for the mean energy of the  $\theta^0$  produced a value that ranges between 620 MeV and 820 MeV.

### 3. - Neutrons' contamination.

We tried to evaluate the contribution of energetic neutrons to the production of strange particles with a special study on the stars observed in our stack.

We scanned very carefully ( $55 \times$  (oil)  $10 \times$  magnification) an additional volume of  $0.7 \text{ cm}^3$ , looking for stars with at least one light prong (ionization equal to or lower than 1.2 minimum). We found a total of 88 stars with one light prong and 9 stars with two light prongs. We assume that all these stars have neutral primary even if it cannot be excluded that in some cases the light prong is the primary of the star.

According to the results obtained by FOWLER *et al.* (\*), the stars produced by neutrons of energy  $\geq 1.2 \text{ GeV}$  have two relativistic prongs in 50% of the cases. Therefore, in our stack, the number of stars produced by neutrons of energy  $\geq 1.2 \text{ GeV}$  is:  $(9/0.7) \cdot 2 = 25/\text{cm}^3$ . This figure corresponds to a total of 212 fast neutron interactions in the volume of  $8.5 \text{ cm}^3$  scanned in the present experiment. If we assume that in each neutron interaction one  $\pi^+$  is emitted, from the known value of the ratio  $\pi^+/K^+$  we can deduce the number of  $K^+$  produced by neutrons. The ratio  $\pi^+/K^+$  has been studied in several experiments <sup>(9,10)</sup>

(\*) Calculations of this type have been originally performed by G. WATAGHIN (*An. Ac. Bras. de Ciências; Symposium*, 1941).

(8) W. B. FOWLER, G. MAENCHEN, W. M. POWEL, G. SHAPHIR and R. W. WRIGHT: *Phys. Rev.*, **101**, 911 (1956).

(9) S. J. LINDENBAUM and C. L. YUAN: *Phys. Rev.*, **105**, 1931 (1957).

(10) P. BAUMEL, G. HARRIS, J. OREAR and S. TAYLOR: *Nevis 52* (October 1957).

and the results, though not in perfect agreement, range from 100 to 300. Consequently in the volume considered in this experiment 1 or 2  $K^+$  can be produced by neutrons.

We would like to point out that all the assumptions made in the preceding evaluation result in an overestimation of the neutron contribution.

#### 4. - Scanning method.

A volume of 8.5 cm<sup>3</sup> of emulsion has been scanned in order to find the strange particles produced in the interactions of the  $\theta_2^0$  particles. The scanning has been made looking for the following events:

- a)  $K^+$  decays at rest;
- b)  $K^-$  captures at rest;
- c)  $\Sigma^\pm$  decays at rest and in flight;
- d)  $\Sigma^-$  captures at rest;
- e) Hyperfragments.

The scanning has been made under  $30\times$  (oil)  $10\times$  magnification.

The scanned volume is situated in the central region of a stack of 40 plates Ilford G5, 600  $\mu$ m thick, at a mean distance of 15 cm from the top and lateral edges.

For events of type a) the scanning losses are mainly due to the lack of observation of minimum secondary tracks emitted with a bad geometry. From the analysis of our data it appears that all minimum secondary tracks with dip angle larger than  $45^\circ$  have been missed. We estimated therefore that 30% of events were lost in the scanning.

As it has already been done by other authors, we estimate the scanning loss of events of type b) in the following way: from the analysis of  $K^-$ -capture stars <sup>(11,12)</sup> we know that certainly we do not detect 18% of the events: 14% of  $K^-$ -captures giving nothing ( $K_p$ ) and 4% of  $K^-$ -captures giving very large stars; taking an 80% scanning efficiency for all the other types of  $K^-$ -captures, it follows that the scanning loss for  $K^-$  at rest is 35%.

To detect the events of type c), all the stars with two prongs and no visible recoil have been collected in the scanning. In a second time, all the two prongs events with at least one prong of  $\beta \leq 0.5$  have been analysed. In this way we can detect the decays in flight of the  $\Sigma^\pm$  with kinetic energy lower than 200 MeV. The scanning losses in this case, as in the case of  $\Sigma^+$  at rest, are very difficult to evaluate

<sup>(11)</sup> W. ALLES, N. N. BISWAS, M. CECCARELLI and J. CRUSSARD: *Nuovo Cimento*, **6**, 571 (1957).

<sup>(12)</sup> C. BESSON, J. CRUSSARD, V. FOUCHÉ, J. HENNESSY, G. KAYAS, V. R. PARIKH and G. TRILLING: *Nuovo Cimento*, **6**, 1168 (1957).

We estimate the scanning loss for events of type *d*) in the same manner as for events of type *b*): 30 % of  $\Sigma^-$  at rest are absorbed giving nothing ( $\Sigma_p$ )<sup>(13)</sup>; taking an 80 % scanning efficiency for all the other types of captures, we calculate a 44 % scanning loss for  $\Sigma^-$ -captures at rest.

All the double stars noticed in the scanned volume have been studied in order to look for the decays of hyperfragments produced in the interaction of a  $\bar{\theta}^0$  with the nucleus:  $\bar{\theta}^0 + (A, Z) \rightarrow \Lambda^0 + (A - 1, Z)$ . The selection criteria were the following: all the double stars whose connecting track was not at the end of its range, or had  $\delta$ -rays in vicinity to the secondary star, or had a charge lower than the total charge of the secondary star, have been rejected.

## 5. - Experimental results.

In the scanned volume of 8.5 cm<sup>3</sup>, we found the following strange particles originating inside the stack from stars with neutral primary:

- 9  $K^+$  decaying at rest;
- 1  $K^-$  giving a  $\sigma$ -star at rest;
- 3 events that can be interpreted as  $\Sigma^+$  decaying in flight into a proton;
- 3  $\Sigma^-$  giving a  $\sigma$ -star at rest;
- 1  $\Sigma$  interacting in flight;
- 4 hyperfragments;
- 4 double stars whose connecting track could not be positively identified (GOKS).

In the same volume 5  $K^-$ -capture stars, 1  $\Sigma^-$  coming from a  $K^-$ -capture, 1  $\tau$  decaying in flight have been found, all of these mesons entering the stack from outside. In addition one case of  $\Lambda^0 \rightarrow p + \pi + 37$  MeV has been observed.

The features of the events that originate in the stack are given in Tables I-A and I-B.

All the prongs of the stars from which the  $K^+$  mesons originate have been accurately analysed in order to exclude the presence of other charged strange particles. The events collected in Table I-A can be interpreted as inelastic scattering with charge exchange of the  $\theta^0$  particles. The possible contribution of the incident neutrons to the production of  $K^+$  mesons has been discussed in Sect. 3.

The first four events of Table I-A are compatible with the hypothesis of a charge exchange of the  $\theta^0$ . In fact, the measured energies and angles are in agreement with the kinematics of the reaction:  $\theta^0 + p \rightarrow K^+ + n$ , where  $p$  can

<sup>(13)</sup> W. F. FRY, J. SCHNEPS, G. A. SNOW, M. S. SWAMI and D. C. WOLD: *Phys. Rev.*, **107**, 257 (1957).

be either a H nucleus of the emulsion or a peripheral proton of an emulsion nucleus. The calculated kinetic energy of the  $\theta^0$  is given in column 7 of Table I-A.

TABLE I-A. - *Particles of strangeness +1.*

Event no.	Strange particle produced	Parent star		Strange particle		Calculated kinetic energy of $\theta^0$ from reaction $\theta^0 + p \rightarrow \rightarrow K^+ + n$ MeV	Remarks
		no. of prongs	Total visible kinetic energy MeV	Angle in the L.S. with the $\theta^0$ beam	Kinetic energy MeV		
1	$K^+$	1	85	$43^\circ$	85	130	
2	$\tau^+$	4	65	$46^\circ$	41	95	
3	$K^+$	1	74	$163^\circ$	74	300	
4	$K^+$	1	28	$70^\circ$	28	70	
5	$K^+$	5	130	$142^\circ$	48		One fast proton of kinetic energy of 72 MeV is emitted from the parent star
6	$\tau^+$	4	324	$179^\circ$	48		One fast proton of kinetic energy of 254 MeV is emitted from the parent star
7	$K^+$	8	323	$65^\circ$	6		One fast proton of kinetic energy of 195 MeV is emitted from the parent star
8	$K^+$	6	547	$139^\circ$	58		One fast proton of kinetic energy of 440 MeV is emitted from the parent star
9	$K^+$	9	180	$7^\circ$	41		One stopping $\pi^-$ of 34 MeV and a proton of 71 MeV are emitted from the parent star

The events 5, 6, 7, 8 are characterized by the presence, among the prongs of the parent star, of an energetic proton that is responsible for almost all the visible energy of the star. These four events can be due to a double interaction of the  $\theta^0$  inside the nucleus (inelastic scattering and charge exchange).

In the event no. 9 a  $\pi^-$  meson is emitted from the parent star of the  $K^+$ -meson. This event can be interpreted as due to a reaction of the type:  $\theta^0 + p \rightarrow \pi^- + p + K^+$ ; the incident  $\theta^0$  has an energy larger than 400 MeV and has suffered inside the nucleus a scattering of  $50^\circ$  before exchanging its charge.

TABLE IB., - *Particles of strangeness - 1.*

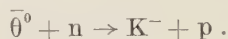
Event no.	Strange particle produced	Parent star			Strange particle						Remarks
		no. of prongs	Total visible kinetic energy (MeV)	Emission of a $\pi$	Kinetic energy (MeV)	Track length ( $\mu\text{m}$ )	Angle in L.S. with the $\theta^0$ beam	Capture star or decay mode			
								no. of prongs	Visible energy (MeV)	Mode of decay	
1	$K^-$ (at rest)	8	118		41	10 500	127°	2	23		From capture star one $\pi^+$ of 22 MeV of kinetic energy is emitted
2	$\Sigma^-$ (at rest)	5	102	no	65	12 400	53°	2			Auger electron visible in the capture star
3	$\Sigma^-$ (at rest)	10	246	no	4	110	158°	4	6		
4	$\Sigma^-$ (at rest)	7	73	no	5	135	83°	1	10		
5	$\Sigma^+$ (decay-ing in flight)	1	134	no	134	29 200	75°			$\Sigma^+ \rightarrow p + \pi^0$	
6	$\Sigma^+$ (decay-ing in flight)	1	72	no	72	1 880	32°			$\Sigma^+ \rightarrow p + \pi^0$	
7	$\Sigma^+$ (decay-ing in flight)	2	155	no	137	19 900	160°			$\Sigma^+ \rightarrow p + \pi^0$	





The events collected in Table I-B can be interpreted as  $\bar{\theta}^0$  interactions since in all of them there is evidence of a particle of strangeness  $-1$  being produced.

Event no. 1 was interpreted as a charge exchange process of the type:



The  $K^-$  outcoming from the interaction star was captured at rest with emission of a  $\pi^+$ . Ionization and scattering measurements made on the strange particle track lead to a positive identification of the  $K^-$  particle.

Events from no. 2 to no. 7 were interpreted as  $\theta^0$  interactions of the type:



The identification of the  $\Sigma$  particles was based on the following considerations:

Event no. 2: On the 1.2 cm long track ionization and scattering measurements were made and the mass was found to be  $(2360 \pm 200) m_e$ .

Event no. 3: The existence of an Auger electron outcoming from the capture star was taken as a definite indication of the particle being a  $\Sigma^-$ . Also profile measurements were made on the 110  $\mu\text{m}$  long track, and the results were found to be in agreement with what would be expected for a  $\Sigma$  hyperon track.

Event no. 4: In this case as well the particle track was rather short (140  $\mu\text{m}$ ) and the mass identification had to rely completely on profile measurements. This event can be interpreted as:

- 1) capture star of a  $\pi^-$ -meson;
- 2) capture star of a  $K^-$ -meson;
- 3) capture star of a  $\Sigma^-$ -hyperon;

4) hyperfragment of charge  $Z \geq 4$ , since the capture star is a four prong star.

The results of profile measurements are given in the following table:

	Dip angle	Profile width (arbitrary units)
Studied track	$29^\circ$	$11.1 \pm 1.0$
Proton tracks in the same region of emulsion	$\sim 29^\circ$	$8.6 \pm 0.5$
Li track outcoming from the parent star of the studied track	$24^\circ$	$12.5 \pm 1.5$

This seems to rule out the hypotheses 1), 2) and 4).

Events no. 5, no. 6, no. 7: For these events the kinematics is in agreement with the decay in flight  $\Sigma^+ \rightarrow p + \pi^0$  and the time of flight is compatible with the  $\Sigma$  mean life; however, we cannot rule out the possibility that these events are scattering of slow protons. The mass values, obtained from scattering and ionization measurements, are:  $(2600 \pm 400) m_e$  for event no. 5 and  $(2140 \pm 300) m_e$  for event no. 7. No attempt has been made to do mass measurements in event no. 6, owing to the short range of the track.

Event no. 8 has been interpreted as the interaction in flight of a  $\Sigma$  hyperon. Since both stars connected by the 2.2 mm long track have an energy larger than the kinetic energy of the connecting track, this track must be due to an unstable particle. From scattering and ionization measurements the particle mass results  $(2360_{-800}^{+1000}) m_e$ , in good agreement with that of a  $\Sigma$  particle. Ionization measurements allow us to establish the sense of motion of the  $\Sigma$  particle interacting in flight.

Four double stars (events no. 9, no. 10, no. 11, no. 12) could be studied in detail and interpreted as hyperfragments. This was done mainly by profile measurements, which, in all the four cases, gave a value for the charge of the fragment compatible with the sum of the charges emitted from the secondary star. In event no. 10 the kinematics of the hyperfragment decay was studied and was found to be in agreement with the reaction:  ${}^4\text{He}_\Lambda \rightarrow 2p + 2n$ .

## 6. - $\theta^0$ flux as deduced from charge exchange process.

From the number of  $K^+$  decaying at rest in the scanned volume, and interpreted as charge exchange of the  $\theta^0$  particles in emulsion, it is possible to evaluate the incident flux of  $\theta^0$ . In this evaluation we assume that  $\theta^0$  particles behave as  $K^+$  and therefore we use the available experimental information on  $K^+$  interactions <sup>(14-16)</sup>.

The number of  $K^+$  decaying at rest in the scanned volume (see Table I-A), corrected for scanning losses (see Sect. 4) is 12. This number must also be corrected for geometrical losses, due to the finite size of the stack; in fact, owing to the position of the scanned volume in the stack, we cannot detect  $K^+$  of energy higher than 200 MeV; the fraction of  $K^+$  of energy  $\leq 200$  MeV stopping in the scanned volume is roughly given by:  $\sin d/R$ , where  $d$  is half the thickness of the stack and  $R$  is the residual range of the emitted  $K^+$ . The efficiency of detection is then a function of the energy of the incident  $\theta^0$ .

<sup>(14)</sup> B. SECHI ZORN and G. T. ZORN: *Phys. Rev.*, **108**, 1098 (1957).

<sup>(15)</sup> M. BALDO CEOLIN, M. CRESTI, N. DALLAPORTA, M. GRILLI, L. GUERRIERO, M. MERLIN, G. A. SALANDIN and G. ZAGO: *Nuovo Cimento*, **5**, 402 (1957).

<sup>(16)</sup> M. GRILLI, L. GUERRIERO, M. MERLIN, O'FRIEL and G. A. SALANDIN: to be published.

Using the data of the Padua group <sup>(16)</sup>, we have estimated for the average energy loss  $\Delta T/T$  a mean value of 40% for charge exchange processes, and a mean value of 80% for double scattering processes. We assume that the probability of a double scattering inside the nucleus increases with increasing energy and reaches a value of 40% for energies higher than 300 MeV <sup>(17)</sup>. From the preceding considerations and for the  $\theta^0$  energy distribution of Fig. 1, curve  $b'$ , we found that the efficiency of detection for charge exchanges, integrated over the whole range of incident energy, is 11%.

The actual number of  $K^+$  produced in a volume of 8.5 cm<sup>3</sup> is then  $12/0.11 = 109$ . To this number a correction must be made for  $K^+$  directly produced by neutrons; the number of these has been estimated in Sect. 3 to be  $\leq 2$ .

The available data on  $K^+$  <sup>(14-16)</sup> indicate that the cross section for charge exchange in emulsion rapidly increases with energy; we calculated a weighted mean of the charge exchange cross section taking into account the incident energy distribution (Fig. 1, curve  $b'$ ) and the geometrical efficiency of detection. This calculation gives a value of 120 mb, corresponding to an effective mean free path for charge exchange detectable in our experiment of 170 cm.

The  $\theta^0$  incident flux, integrated over the time of exposure, has then the value:

$$\varphi_{\theta^0} = \frac{107}{8.5} \cdot 170 = 2130 \text{ particles/cm}^2.$$

## 7. - $\bar{\theta}^0$ flux as deduced from the number of hyperfragments (H.F.).

The first assumption that we have to make, in order to evaluate the incident flux of  $\bar{\theta}^0$ , is that the  $\bar{\theta}^0$  particles behave as  $K^-$ -mesons. In this case we met some difficulties owing to the lack of experimental data on the production of strange particles by  $K^-$ -mesons that are not at rest.

The interaction products of the  $\bar{\theta}^0$  that are observed in the present experiment are: H.F.,  $K^-$  and  $\Sigma$  hyperons. We started our analysis of the  $\theta^0$  flux from the number of H.F. which were found in the scanned volume and could be interpreted as due to  $\Lambda^0$  produced by  $\theta^+$  of the beam. The other strange particles produced in the  $\theta^0$  interactions could not be used for the same analysis since:

- the  $K^-$  charge exchange cross section is completely unknown at all energies;
- the scanning losses in detecting  $\Sigma$  hyperons are very hard to evaluate, as we already pointed out in Sect. 4.

Under our scanning conditions the scanning loss for H.F. must be very small, and we take it to be  $= 0$ . The cross section for H.F. production at

<sup>(17)</sup> K. A. BRUECKNER, R. SERBER and K. M. WATSON: *Phys. Rev.*, **84**, 258 (1951).

the energies we are dealing with, is not known and we have to make the following assumptions:

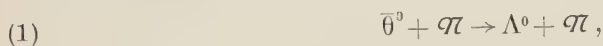
1)  $\bar{\theta}^0$  particles have the same cross section as  $K^-$ -mesons for the production of hyperons and for charge exchange (this should be the case since the reactions we are dealing with are charge symmetric of the  $K^-$ -nucleon reactions).

2) The total inelastic cross section of  $K^-$  is not strongly dependent on energy and the value found experimentally in the study of the  $K^-$  beam of energy up to 150 MeV <sup>(18)</sup> can be used for our  $\bar{\theta}^0$  energy spectrum.

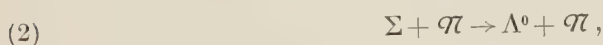
3) The ratio  $\Lambda^0/\Sigma$  directly produced does not depend on energy and the results found for  $K^-$  captures can be used in our analysis:  $\Lambda^0/\Sigma = 0.22$  <sup>(19)</sup>.

4) K re-emission with or without charge exchange is still rather low in our energy interval: of the order of 10% <sup>(19)</sup>.

These assumptions are not sufficient to completely solve the problem, since, as many authors pointed out,  $\Lambda^0$  can be produced in emulsion both directly in the reaction:



and indirectly as a secondary product from the reaction:



occurring inside the nucleus.

The existence of reaction (2) had to be assumed in order to explain the small number of  $\Sigma$  emitted from the interaction of  $K^-$  in nuclei as compared to the large number emitted in the collision of  $K^-$  with hydrogen <sup>(19,20)</sup>.

The contribution of reactions (1) and (2) in the production of H.F. has been studied with an analysis similar to that made in reference <sup>(19)</sup> using an optical model for the nucleus with a 15 MeV potential well for the  $\Lambda^0$  and a tentatively chosen 35 MeV potential well for  $\Sigma$  hyperons.

H.F. production is due:

i) to the low energy  $\Lambda^0$  produced in reaction (1) ( $T_{\Lambda^0} \leq 15$  MeV) and trapped inside the nucleus;

<sup>(18)</sup> E. LOHRMANN, M. NIKOLIĆ, M. SCHNEEBERGER, P. WALOSCHEK and H. WINZELER: *Nuovo Cimento*, **7**, 163 (1958); Y. EISENBERG, W. KOCH, E. LOHRMANN, M. NIKOLIĆ, M. SCHNEEBERGER and H. WINZELER (to be published).

<sup>(19)</sup> J. HORNBOSTEL and G. T. ZORN: *Phys. Rev.*, **109**, 165 (1958).

<sup>(20)</sup> L. W. ALVAREZ, H. BRADNER, P. FALK VAIRANT, J. D. GOW, A. H. ROSENFELD, F. T. SOLMITZ and R. D. TRIPP: *Nuovo Cimento*, **5**, 1026 (1957).



ii) to the low energy  $\Sigma$  hyperons ( $T_{\Sigma} \leq 35$  MeV) trapped in the nucleus and converted by reaction (2) into slow  $\Lambda^0$ ;

iii) to fast  $\Sigma$  hyperons ( $T_{\Sigma} > 35$  MeV) producing, by reaction (2), slow  $\Lambda^0$  in nuclear matter.

The contribution of process i) to the number of  $\Lambda^0$  particles trapped inside the nucleus, has been evaluated in the following way: Starting from the calculated  $\theta^0$  spectrum (Fig. 1, curve  $b'$ ) we have estimated the energy distribution of the  $\Lambda^0$  particles produced in the reaction (1) when the nucleon is bound in a nucleus of the emulsion. The fraction of  $\Lambda^0$  particles trapped inside the nucleus has been taken as equal to the percentage of  $\Lambda^0$  particles of energy  $\leq 15$  MeV and is found to be 0.7%. From assumptions 3) and 4) it follows that the reaction (1) occurs in about 16% of the total number of  $\bar{\theta}^0$  interactions; it therefore results that the events in which a  $\Lambda^0$  particle, directly produced by reaction (1), is trapped in a nucleus are 0.1% of all  $\bar{\theta}^0$  interactions.

Since the cross section inside the nucleus for reaction (2) is not known, the contribution of  $\Lambda^0$  produced in this reaction cannot be exactly estimated. For this reason we evaluated the contribution of processes ii) and iii) in two different cases:

- case *a*: the reaction (2) takes place mainly for trapped  $\Sigma$  hyperons (absorption mean free path:  $\lambda_a = 10$  times the geometrical mean free path) *i.e.* the contribution of process iii) is = 0.
- case *b*: the contribution of fast  $\Sigma$  hyperons in producing  $\Lambda^0$  is comparatively large ( $\lambda_a = 1$  geometrical mean free path) *i.e.* 80% of fast  $\Sigma$  hyperons gives rise to process iii).

We have calculated the energy distribution of  $\Sigma$  hyperons produced in the reaction  $\bar{\theta}^0 + \mathcal{N} \rightarrow \Sigma + \pi$  and we found that only 2.2% of them have an energy  $\leq 35$  MeV. As we know, from assumptions 3) and 4), that  $\Sigma$  hyperons are produced in 74% of  $\bar{\theta}^0$  interactions, we deduce that  $0.74 \cdot 2.2\% = 1.6\%$  of all  $\bar{\theta}^0$  interactions produce  $\Sigma$  hyperons trapped inside the nucleus.

The fast  $\Sigma$  hyperons result to be 72% of all  $\bar{\theta}^0$  interactions; in case *a*, these hyperons do not contribute to the production of  $\Lambda^0$  particles, but in case *b*, a percentage of 80% of these fast  $\Sigma$  hyperons gives rise to  $\Lambda^0$  particles. We calculated the energy spectrum of  $\Lambda^0$  produced by fast  $\Sigma$  hyperons in the reaction (2) and we obtained the fraction of  $\Lambda^0$  having an energy  $\leq 15$  MeV to be 0.7%.

The fraction of slow  $\Lambda^0$  due to process iii) is then

$$0.80 \cdot 0.72 \cdot 0.007 = 0.4\%,$$

of all  $\bar{\theta}^0$  interactions.

Therefore the percentage of  $\Lambda^0$  trapped inside the nucleus is in case *a* 1.7% and in case *b* 2.1% of all  $\bar{\theta}^0$  interactions.

Only a fraction of the trapped  $\Lambda^0$  particles gives rise to excited fragments of range detectable in emulsion. A value of  $\frac{1}{3}$  for this fraction has been derived by HORNBOSTEL and ZORN<sup>(19)</sup>.

The  $\bar{\theta}^0$  flux was derived for cases *a* and *b*:

— case *a*: number of H.F./cm<sup>3</sup> = 0.47.

Total  $\bar{\theta}^0$  interactions/cm<sup>3</sup> = 0.47/0.006 = 78

$$\varphi_{\bar{\theta}^0} = 78 \cdot 27.5 = 2150 \text{ particles/cm}^2.$$

— case *b*: number of H.F./cm<sup>3</sup> = 0.47.

Total  $\bar{\theta}^0$  interactions/cm<sup>3</sup> = 0.47/0.007 = 67

$$\varphi_{\bar{\theta}^0} = 67 \cdot 27.5 = 1850 \text{ particles/cm}^2.$$

The calculated value of the  $\theta^0$  flux appears to be not very sensitive to the choice of the mean free path for reaction (2) of  $\Sigma$  hyperons in nuclear matter.

The value that we obtained for  $\varphi_{\bar{\theta}^0}$  is of the same order of magnitude as the  $\theta^0$  flux calculated for the  $K^+$  produced in charge exchange; this fact seems to be an indication that  $\theta_2^0$  particles are a mixture of different strangeness particles, of the type proposed by GELL-MANN and PAIS<sup>(6)</sup>.

### 8. — $\theta_2^0$ flux incident on our stack.

In order to prove the consistence of the results, we compare the flux values deduced in Sect. 7 with the calculated value of the  $\theta_2^0$  flux emitted from a 6 in. Be target at an angle of 45° with the 6 GeV proton beam.

The total proton number entering the target was, in our experiment,  $N_p = 5 \cdot 10^{12}$ . We suppose that the total cross section for  $\theta^0$  production is of the same order of magnitude as that for  $K^+$ . We derived the value of the total cross section for  $K^+$  production by 6 GeV protons on Be ( $\sim 2.2$  mb) from the value found by BAUMEL *et al.*<sup>(10)</sup> for 3 GeV protons on Li and Cu, and we made the hypothesis that the production matrix element is a constant.

For the long lived  $\theta_2^0$  incident on our stack, we obtained the flux value:

$$\varphi_{\theta_2^0} = 3260/\text{cm}^2.$$

This value is in very good agreement, as order of magnitude, with  $\theta^0$  and  $\bar{\theta}^0$  fluxes found in Sect. 7 and 8.

## 9. - Hyperon production.

The number of hyperons emitted from a  $\theta^0$  interaction with the nuclei of the emulsion is a very sensitive function of the value assumed for the mean free path  $\lambda_a$  of  $\Sigma$  in nuclear matter.

If we assume  $\lambda_a$  to be of the order of 10 times the geometrical mean free path. (case *a*, Sect. 7) charged  $\Sigma$  are calculated (under assumptions 3) and 4), Sect. 7) to be emitted from  $\bar{\theta}^0$  interactions in 39% of the cases; this leads to a total number of  $\Sigma$  produced in the scanned volume of 263. If instead we assume  $\lambda_a$  to be of the order of the geometrical mean free path (case *b* Sect. 7) charged  $\Sigma$  can be emitted in 10% of  $\theta^0$  interactions and the total number of  $\Sigma$  to be found in the scanned volume is 42.

Only charged  $\Sigma$  of energy  $\leq 200$  MeV could be detected in our experiment. This represents 29% of the  $\Sigma$  produced by  $\theta^0$  having the energy distribution plotted in Fig. 1, curve *b'*.

It results that, in case *a* we should have observed 72  $\Sigma$  hyperons decaying or interacting at rest or in flight in the scanned volume; in case *b* this number should have been 12.

The total number of  $\Sigma$  observed in this experiment is 7; this number, though it should still be corrected for scanning loss which, as it has already been mentioned, is very difficult to evaluate, seems to rule out the hypothesis of case *a*. Some experiments of other authors (<sup>18,19</sup>) give an analogous indication.

## 10. - $K^-$ production.

One  $K^-$  star was found in the scanned volume, originating from a star that can be interpreted as charge exchange of  $\bar{\theta}^0$  in emulsion.

Owing to the extremely low statistics, no attempt was made to give an estimate of the charge exchange cross section for the  $\theta^0$ , though this appears to be not negligible at the energies we are dealing with.

## 11. - Conclusions.

Our results lead to the following conclusions:

1) Further evidence is added to the existence of a long lived  $\theta_2^0$  component.

2) The number of interactions of  $\theta^0$  and  $\bar{\theta}^0$  detected in our experiment is compatible with a strangeness mixture of the type proposed by Gell-Mann

and Pais, if we assume that the cross sections for the various processes of the  $\theta^0$  and  $\bar{\theta}^0$  are the same as those for the charge symmetric reactions of  $K^+$  and  $K^-$ .

3) A tentative calculation of the incident flux of  $\theta_2^0$ , taking into account the production process at the target, gives a results which agrees, as an order of magnitude, with the flux values deduced from interactions of  $\theta_2^0$ . This can be taken as an indication of the correctness of our assumptions on the production and interaction cross sections.

\* \* \*

We are glad to express our thanks to Prof. G. WATAGHIN, who planned and carried out the exposure at the Berkeley Bevatron and helped us with constant interest during this work.

We are grateful to Dr. E. LOFGREN for his valuable advice and co-operation, and to Dr. CHUPP and Dr. GOLDBABER for help during the exposure.

Thanks are also due to Dr. M. BALDO CEOLIN and to Dr. W. F. FRY for many stimulating discussions.

We express our appreciation to Mr. V. BORRELLI, Mr. M. GRECO and Mr. P. TROSSERO for their accuracy in the difficult task of scanning the plates.

## RIASSUNTO

Uno stack di emulsioni è stato esposto, al bevatrone di Berkeley, al fascio neutro emesso a  $45^\circ$  rispetto al beam interno incidente su un bersaglio di berillio. La distanza totale delle lastre dal bersaglio era di 6 metri. Nel corso di una esplorazione fatta per cercare i prodotti delle interazioni dei K neutri a vita lunga, sono stati trovati 9  $K^+$ . 8 particelle di stranezza — 1 e 4 iperframmenti, tutti emessi da stelle nell'emulsione. Dalla frequenza relativa di particelle di diversa stranezza si è determinata la composizione del fascio di  $\theta_2^0$  che entrano nell'emulsione. Il risultato sperimentale è compatibile con la composizione prevista dallo schema di Gell-Mann e Pais.

## Observation in Quantum Mechanics.

H. S. GREEN (\*)

*Dublin Institute for Advanced Studies*

(ricevuto il 9 Giugno 1958)

**Summary.** — This paper gives an explanation of how the indeterminacy of a quantum-mechanical observable is removed by the process of measurement. It is pointed out that the observation of an individual micro-system is possible only by means of its interaction with a macroscopic system in a metastable state. An interaction of this kind is studied quantum-mechanically. The model consists of a particle with two spin states which are split and brought into interaction with separate detectors. Each detector comprises two set of oscillators at different temperatures, which become coupled by interaction with the particle, so that the latter can be detected by a temperature change. It is found that states in which the spin is indeterminate cannot affect either detector, and that they are rapidly suppressed when the interaction is « switched on ». After the interaction, the state of the particle is no longer pure, and can no longer be represented by a single wave-function. There is no discontinuity in the transition.

### 1. — Introduction.

Recent discussion on the physical interpretation of quantum mechanics (KÖRNER <sup>(1)</sup>) has revealed that there is still a surprising variety of opinion on this subject. There are, of course, those who, following PLANCK <sup>(2)</sup>, EINSTEIN <sup>(3)</sup>, DE BROGLIE <sup>(4)</sup> and SCHRÖDINGER <sup>(5)</sup>, dislike the metaphysical im-

(\*) On leave from the University of Adelaide.

(<sup>1</sup>) S. KÖRNER: *Observation and Interpretation* (London, 1957).

(<sup>2</sup>) M. PLANCK: *Scientific Autobiography* (London, 1950), pp. 121-150.

(<sup>3</sup>) A. EINSTEIN: *Out of My Later Years* (New York, 1950), pp. 85-93 and 106-110.

(<sup>4</sup>) L. DE BROGLIE: *Nuovo Cimento*, **1**, 37 (1955).

(<sup>5</sup>) E. SCHRÖDINGER: *Nuovo Cimento*, **1**, 5 (1955).



plications of Born's statistical interpretation, and some, such as BOPP <sup>(6)</sup>, BOHM <sup>(7)</sup> and VIGIER <sup>(8)</sup>, who are actively trying to supply a new alternative. But even among those who hold the orthodox view, one finds important differences concerning the theory of observation.

Especially notable are contrasting attitudes to a sort of paradox which is frequently produced by the critics of the statistical interpretation. A simple example of such a paradox is provided by the radio-active nucleus which, in the instant of its decay, causes a record of the decay to be made in a photographic plate. It is sometimes supposed that the orthodox theory requires such an event to remain indeterminate, until the photographic plate is processed and scrutinized by the observer. Thus it becomes a purely subjective question whether the decay has actually occurred. While such a view is probably unacceptable to the majority of physicists, it is not contradicted by most accounts of the interpretation of quantum theory, and is in fact consistent with not only those which talk of quantum «jumps», but with more sophisticated versions such as EVERETT III's <sup>(9)</sup>.

The antidote to such a subjective view of quantum-mechanical transitions is to observe a distinction between the properties of micro-systems and the apparatus by means of which they are observed. Obviously only macro-objects are accessible to direct observation, and though these are not immune to the indeterminacy principle, they are affected to only a completely unnoticeable extent. Thus, at the instant when the micro-system interacts with the macroscopic measuring device, the indeterminacy associated with the measured property must disappear. There is, however, no detailed account of the mechanism responsible for this process, and it is not even clear that it would be consistent with the quantum-mechanical laws and their conventional interpretation. It may be contended that, though quantum mechanics provides a self-consistent theory of the behaviour of micro-systems, this does not embrace the processes by which such systems are observed.

Attention has been drawn to the survival of such an important problem recently by FEYERABEND <sup>(10)</sup> and DURAND III <sup>(11)</sup>. They both reject the subjective account, and DURAND III also criticizes the assumption of von NEUMANN <sup>(12)</sup> and others that the act of measurement leaves the microsystem in

<sup>(6)</sup> F. BOPP: *Ann. Inst. Poincaré*, **15**, 113 (1956).

<sup>(7)</sup> D. BOHM: *Phys. Rev.*, **85**, 166 (1952).

<sup>(8)</sup> J. P. VIGIER and D. BOHM: *Phys. Rev.*, **96**, 208 (1954).

<sup>(9)</sup> H. EVERETT III: *Rev. Mod. Phys.*, **29**, 454 (1957).

<sup>(10)</sup> I. FEYERABEND: *Zeits. f. Phys.*, **148**, 551 (1957).

<sup>(11)</sup> L. DURAND III: *On the Theory and Interpretation of Measurement in Quantum Mechanical Systems* (preprint) (1958).

<sup>(12)</sup> J. VON NEUMANN: *Mathematical Foundations of Quantum Mechanics* (Princeton, 1955).

an eigenstate of the measured observable. He points out that the apparatus by which the measurement is made is always in an impure state (in the quantum-mechanical sense) and must be represented by a statistical matrix rather than a wave-function. It is quite true that quantum mechanics in the past has been unduly preoccupied with pure states, and this may have been an important though unrecognized source of dissatisfaction to those who were unable to accept it. It may also have been a serious obstacle to the development of an adequate theory of measurement.

It is well known that the statistical matrix is an important tool for the description of macroscopic states. But, alone, it does not help to explain how properties of micro-systems can be made manifest at the macroscopic level. That is the task which will be undertaken in this paper. A rudimentary theory of measuring systems will be proposed, and illustrated by means of a particular model. The result will vindicate the orthodox interpretation of quantum mechanics without offending the objectivist. At the same time it will suggest the need for a more thorough study of systems not in a pure state.

## 2. - Theory of observation.

It will be *assumed*, for the purposes of this discussion, that basically every observation is concerned with a single micro-system, though for statistical purposes it may be desirable to collate observations on a large number of similar systems, and convenient to make them in the same experiment. The apparatus will generally have two distinct functions. The first of these is to effect a spectral resolution of the observable whose measurement is desired. Some part of the apparatus is therefore devoted to a physical separation of micro-systems, whereby any system characterized by a particular eigenvalue or range of eigenvalues of the measured observable is diverted into a particular channel. The importance of this function varies widely with the degree to which the experiment is controlled. There is, however, in any case no difficulty in describing the process in purely quantum-mechanical terms; it corresponds to splitting the wave-function into components corresponding to the eigenvalues or range of eigenvalues of the observable. The spatial separation of the components is effected, if necessary, by an interaction whose magnitude depends on the eigenvalue concerned.

The second function of the apparatus, and the essential one, is the detection of a micro-system by signalling at a macroscopic level the arrival of the system in one of the eigenvalue channels, which are, of course, often contiguous. Concerning the detector, it must obviously be of a macroscopic nature, and must have a definite state of equilibrium which is undisturbed except by the micro-system. In order that the disturbance created by the micro-system

should be observable, it is further necessary that this equilibrium state of the detector should be *metastable*, in the sense that even a small perturbation of the right kind is sufficient to precipitate a change of state readily observable on a macroscopic scale. Cloud chambers and bubble chambers contain matter which is literally in a metastable state: photographic emulsions and electron multipliers are easily seen to be metastable in a closely related sense.

The essential problem to be faced, therefore, concerns the detector. It has to be explained how the *probability amplitude* for the arrival of a micro-system in one of two or more channels gets converted into a *probability* for the transition between the metastable and stable states of a particular detector. In mathematical terms, let  $\psi = \sum_a \psi_a$  be the wave function of the micro-system, resolved into the eigenstates  $\psi_a$  of an observable, and let  $\varrho_D$  be the statistical matrix of the undisturbed detecting system. Then it has to be shown that the effect of the interaction is to cause a transition from the initial combined state with statistical matrix  $P_i = \sum_{a,b} \psi_a \varrho_D \psi_b^*$  to a final state with a statistical matrix of the form  $P = \sum_a P_a$ . The indeterminacy of the observable of the micro-system is associated with the terms  $\psi_a \varrho_D \psi_b^*$  with  $b \neq a$  of  $P_i$ , and it is these which must be annihilated by the interaction.

This problem will be investigated by means of a simple model. Little is yet known about the quantum-mechanical specification of the metastable states of super-saturated vapours or superheated liquids. The model adopted for the detector is therefore the mathematically simpler one provided by a system of harmonic oscillators, in a thermodynamically metastable state. It will be imagined that certain of the normal modes (called the *x*-modes) of this system are in the state of thermal equilibrium corresponding to the temperature  $T$ , and that the others (called the *y*-modes) in a different state of thermal equilibrium, corresponding to the temperature  $T_0$  (taken as absolute zero for simplicity). When this system is perturbed by the micro-system, the *x*- and *y*-modes are coupled, and there is an irreversible transition in the direction of stable equilibrium.

For the micro-system, a charged particle with two spin states ( $\pm \frac{1}{2}$ ) will be considered, for maximum simplicity. A spectral resolution of the two spin states is supposed to have been achieved by a magnetic field, the wave function being split, thus:

$$(1) \quad \psi = \psi_+ + \psi_-, \quad (\sigma\psi_+ = \psi_+; \quad \sigma\psi_- = -\psi_-),$$

so that  $\psi_+$  and  $\psi_-$  are the different eigenstates of the spin  $\frac{1}{2}\sigma$ , and are also spatially separated, so that  $\psi_+$  becomes coupled to the statistical matrix  $\varrho_+$  of the detector  $D_+$ , and  $\psi_-$  becomes coupled to the statistical matrix  $\varrho_-$  of the detector  $D_-$ .

Again for simplicity, and not of course as a matter of necessity, it will be assumed that the coupling energy  $\hbar V$  commutes with the unperturbed Hamiltonian, and that

$$(2) \quad V\psi_+ = V_+\psi_+; \quad V\psi_- = V_-\psi_-,$$

where  $V_+$  involves only co-ordinates of  $D_+$  and  $V_-$  only co-ordinates of  $D_-$ . The statistical matrix of the coupled system at time  $t$  after the interaction is «switched on» is

$$(3) \quad P = \exp[-iVt]\varrho_+\varrho_-\psi^* \exp[iVt].$$

Because of (1) and (2), one can also write

$$(4) \quad \left\{ \begin{array}{l} P = P_+ + P_- + P_{\pm}, \\ P_+ = \exp[-iV_+t]\varrho_+\varrho_-\psi^* \exp[iV_+t]\varrho_-, \\ P_- = \exp[-iV_-t]\varrho_-\varrho_-\psi^* \exp[iV_-t]\varrho_+, \\ P_{\pm} = \exp[-iV_+t]\varrho_+\varrho_+\varrho_-\psi^* \exp[iV_-t] + \\ \quad + \exp[-iV_-t]\varrho_-\varrho_+\varrho_+\psi^* \exp[iV_+t]. \end{array} \right.$$

Of special interest will be the behaviour of the term  $P_{\pm}$ , which measures the indeterminacy of the spin, after the particle has interacted with the measuring device for time  $t$ . To make the calculation, it will be necessary first to obtain the explicit form of  $\varrho_+$  and  $\varrho_-$ .

### 3. — Quantum statistical mechanics of the detector.

The detector consists of a large number of oscillators, such as one has to describe the molecular motion in a crystal. The Hamiltonian of such a system may be written in the form

$$-\frac{\hbar^2}{2md^2} \sum_i \frac{\partial^2}{\partial x_i^2} + U_0 + \sum_{i,j} U_{ij} x_i x_j,$$

where  $m$  is the particle mass and  $d$  any convenient unit of length, chosen here so that  $2md^2 = \hbar^2$ . The statistical matrix  $\varrho$  for such a system has the form

$$(5) \quad \varrho = \exp[\beta E] \sigma(\beta; x, x')$$



in the co-ordinate representation. where  $\beta$  is inversely proportional to the absolute temperature,  $F$  is the free energy, and  $\sigma$  satisfies Bloch's equation

$$(6) \quad \frac{\partial \sigma}{\partial \beta} = \left\{ \sum_i \frac{\partial^2}{\partial x_i^2} - (U_0 + \sum_{i,j} U_{ij} x_i x_j) \right\} \sigma,$$

with the boundary condition

$$(7) \quad \sigma = \prod_i \delta(x_i - x'_i) \quad \text{when } \beta = 0.$$

It turns out that (6) is satisfied by a solution of the form

$$(8) \quad \sigma = \exp \left[ -A - \frac{1}{2} \sum_{ij} (B_{ij} x_i x_j - 2C_{ij} x_i x'_j + B'_{ij} x'_i x'_j) \right],$$

where  $B_{ij}$  and  $B'_{ij}$  are symmetric in  $i$  and  $j$ . In fact, direct substitution shows that (6) is fulfilled, provided

$$\begin{aligned} A_{,\beta} + \frac{1}{2} \sum_{ij} (B_{ij,\beta} x_i x_j - 2C_{ij,\beta} x_i x'_j + B'_{ij,\beta} x'_i x'_j) &= \\ &= \sum_i \{ B_{ii} - \sum_j (B_{ij} x_i - C_{ij} x'_j)^2 \} + U_0 + \sum_{ij} U_{ij} x_i x_j, \end{aligned}$$

where,  $\beta$  denotes differentiating with respect to  $\beta$ . So, if  $B$ ,  $C$ ,  $B'$ ,  $U$  denote the matrices with element  $B_{ij}$ ,  $C_{ij}$ ,  $B'_{ij}$ ,  $U_{ij}$ , and  $\text{tr}$  denotes the trace (sum of the diagonal elements),

$$(9) \quad \begin{cases} B_{,\beta} = 2(U - B^2); & C_{,\beta} = -2BC; \\ B'_{,\beta} = -2C^2; & A_{,\beta} = U_0 + \text{tr } B. \end{cases}$$

The matrix  $U$  must have exclusively positive eigenvalues, or the system would have no stationary states. Therefore it possesses a unique square root  $D$  (such that  $D^2 = U$ ) which is also positive definite. In terms of this matrix, the required solution of (9) is

$$(10) \quad \begin{cases} B = D \coth(2\beta D); & C = D \text{ cosech}(2\beta D); \\ B' = B; & A = \beta U_0 + \frac{1}{2} \text{tr} \log \{ 2\pi D^{-1} \sinh(2\beta D) \}. \end{cases}$$

The constants of integration have been chosen so that, for very small  $\beta$ ,

$$(11) \quad \sigma \sim \exp \left[ - \sum_i (x_i - x'_i)^2 / (4\beta) - \frac{1}{2} N \log(4\pi\beta) \right],$$

where  $N$  is the number of degrees of freedom: for this satisfies the boundary condition (7).



The free energy can be calculated from (5) using the normalizing condition

$$(12) \quad \exp [\beta F] \int \sigma(\beta; x, x) d^N x = 1.$$

On substitution from (8) and (10), this leads to

$$(13) \quad \beta F = \beta U_0 + \frac{1}{2} \text{tr} \log \{4 \sinh^2 (\beta D)\},$$

or, in case  $D$  is a diagonal matrix, with diagonal elements  $D_i$ ,

$$(14) \quad \beta F = \beta U_0 + \sum_i \log \{2 \sinh (\beta D_i)\}.$$

This result may be checked against that obtained by other methods [*e.g.* in §§ 15-16 of BORN and HUANG <sup>(13)</sup>].

Finally, if  $D$  is diagonal,

$$(15) \quad \varrho(x, x') = \prod_i \{(B_i - C_i)/\pi\}^{\frac{1}{2}} \exp \left[ -\left\{ \frac{1}{2} B_i (x_i^2 + x_i'^2) - C_i x_i x_i' \right\} \right],$$

$$\begin{cases} B_i = D_i \coth (2\beta D_i); \\ C_i = D_i \operatorname{cosech} (2\beta D_i). \end{cases}$$

At absolute zero ( $\beta = \infty$ ) this reduces to

$$(16) \quad \varrho_0(x, x') = \prod_i (D_i/\pi)^{\frac{1}{2}} \exp [-D_i(x_i^2 + x_i'^2)],$$

which is, of course, the statistical matrix for the oscillators in their ground-states. Even if  $D$  is not diagonal, the statistical matrix can be reduced to the form (15) or (16) by the choice of normal co-ordinates.

#### 4. - Operation of the model.

For the statistical matrices  $\varrho_+$  and  $\varrho_-$  of Sect. 2, in the co-ordinate representation the forms

$$(17) \quad \begin{cases} \varrho_+ = \varrho(x_+, x'_+) \varrho_0(y_+, y'_+), \\ \varrho_- = \varrho(x_-, x'_-) \varrho_0(y_-, y'_-), \end{cases}$$

are adopted, with  $\varrho(x, x')$  and  $\varrho_0(y, y')$  given by (15) and (16). It may be imagined that the  $x_{+i}$  and  $y_{+i}$  are the  $x$ - and  $y$ - co-ordinates of the same par-

<sup>(13)</sup> M. BORN and K. HUANG: *Dynamical Theory of Crystal Lattices* (Oxford, 1954).

ticle, so that the energy associated with the  $x$ -modes is what one would expect at temperature  $T$ , while the  $y$ -modes are all in their ground states. The interaction with the particle must be such as to couple the  $x$ - and  $y$ -modes; in particular one may take

$$(18) \quad \begin{cases} V_+ = -i \sum_i \omega_i \left( x_{+i} \frac{\partial}{\partial y_{+i}} - y_{+i} \frac{\partial}{\partial x_{+i}} \right) \\ V_- = i \sum_i \omega_i \left( x_{-i} \frac{\partial}{\partial y_{-i}} - y_{-i} \frac{\partial}{\partial x_{-i}} \right). \end{cases}$$

The spin of the particle is thus coupled to the angular momentum of each oscillator with which it interacts, causing it to rotate in the  $x$ - $y$  plane. The angular frequencies  $\omega_i$  measure the strength of the interaction, and might very well vary in magnitude and sign from oscillator to oscillator. As the oscillators rotate, the presence of the particle will be detected macroscopically by the rise in temperature associated with the  $y$ -modes.

For an arbitrary function  $f$ ,

$$(19) \quad \begin{cases} \exp [iV_{\pm} t] f(x_{\pm i}, y_{\pm i}) = f(\xi_{\pm i}, \eta_{\pm i}), \\ \xi_{\pm i} = x_{\pm i} \cos(\omega_i t) \pm y_{\pm i} \sin(\omega_i t); \\ \eta_{\pm i} = y_{\pm i} \cos(\omega_i t) \pm x_{\pm i} \sin(\omega_i t). \end{cases}$$

Hence one finds from (4) and (17)

$$(20) \quad \begin{cases} P_+ = \psi_+ \varrho(\xi_+, \xi'_+) \varrho_0(\eta_+, \eta'_+) \varrho(x_-, x'_-) \varrho_0(y_-, y'_-) \psi_+^* ; \\ P_- = \psi_- \varrho(x_+, x'_+) \varrho_0(y_+, y'_+) \varrho(\xi_-, \xi'_-) \varrho_0(\eta_-, \eta'_-) \psi_-^* ; \\ P_{\pm} = \psi_+ \varrho(\xi_+, x'_+) \varrho_0(\eta_+, y'_+) \varrho(x_-, \xi'_-) \varrho_0(y_-, \eta'_-) \psi_-^* + \\ \quad + \psi_- \varrho(x_+, \xi'_+) \varrho_0(y_+, \eta'_+) \varrho(\xi_-, x'_-) \varrho_0(\eta_-, y'_-) \psi_+^* . \end{cases}$$

The  $x$ -modes are no longer uncorrelated with the  $y$ -modes. To obtain a clearer picture of what has happened, an averaging operation will be performed by setting  $x'_{\pm} = x_{\pm}$  and  $y'_{\pm} = y_{\pm}$ , and integrating with respect to the  $x_{\pm i}$ . This yields, on substitution from (15) and (16)

$$(21) \quad \begin{cases} \langle P_+ \rangle = \psi_+ \prod_i \{ (A_i/\pi)^{\frac{1}{2}} \exp [-A_i y_{+i}^2] (D_i/\pi)^{\frac{1}{2}} \exp [-D_i y_{-i}^2] \} \psi_+^* , \\ A_i = \frac{(B_i - C_i) D_i}{(B_i - C_i) \cos^2 \omega_i t + D_i \sin^2 \omega_i t} , \\ \langle P_- \rangle = \psi_- \prod_i \{ (D_i/\pi)^{\frac{1}{2}} \exp [-D_i y_{+i}^2] (A_i/\pi)^{\frac{1}{2}} \exp [-A_i y_{-i}^2] \} \psi_-^* , \\ \langle P_{\pm} \rangle = (\psi_+ \psi_-^* + \psi_- \psi_+^*) \prod_i (\lambda_i E_i / \pi) \exp [-E_i (y_{+i}^2 + y_{-i}^2)] , \end{cases}$$

$$(21) \quad \begin{cases} E_i = \frac{2(B_i - C_i \cos \omega_i t) D_i + D_i (D_i - B_i) \sin^2 \omega_i t}{B_i (1 + \cos^2 \omega_i t) - 2C_i \cos \omega_i t + D_i \sin^2 \omega_i t}, \\ \lambda_i = \frac{B_i - C_i}{(B_i - C_i \cos \omega_i t) + \frac{1}{2} (D_i - B_i) \sin^2 \omega_i t}. \end{cases}$$

It is easily verified that, because  $B_i^2 = D_i^2 + C_i^2$ ,  $\lambda_i$  cannot be greater than 1; this could have been expected on the basis of an analogue of Schwartz's inequality. To form some idea of the relative magnitudes involved, assume that  $\beta D_i$  is small, as it must be if the change in temperature of the  $y$ -modes is to be readily observable. Then one can see from (15) that  $B_i \gg D_i$  and  $B_i - C_i \approx \frac{1}{2} D_i^2 / B_i \ll D_i$ . Thus, if  $\omega_i t$  is not near to zero (or an integral multiple of  $\pi$ ), the approximations

$$(22) \quad \begin{cases} A_i \approx (B_i - C_i) \operatorname{cosec}^2 \omega_i t; & E_i \approx D_i; \\ \lambda_i \approx D_i^3 / \{B_i (1 - \cos \omega_i t)\}^2, \end{cases}$$

may be used. The coefficients  $A_i$ ,  $E_i$ ,  $D_i$  are empirical temperatures on a descending scale, with  $D_i$  representing absolute zero and  $B_i - C_i$  the temperature originally associated with the  $x$ -modes. It will be seen that the part  $\langle P_+ \rangle$  of  $\langle P \rangle$  represents the possibility that the particle has spin  $+\frac{1}{2}$  and the detector  $D_+$  has functioned by exhibiting a rise in temperature of the  $y$ -modes. Similarly the part  $P_-$  of  $P$  represents the possibility that the particle has spin  $-\frac{1}{2}$  and the detector  $D_-$  has functioned. The part  $\langle P_\pm \rangle$ , on the other hand, represents the possibility that the spin of the particle has remained indeterminate and *neither detector has functioned*.

The statistical weight of this third possibility is, however, immeasurably small, as one sees by performing a further integration with respect to the  $y_{\pm i}$ . This additional averaging operation yields

$$(23) \quad \begin{cases} \ll P_+ \gg = \psi_+ \psi_+^*, \\ \ll P_- \gg = \psi_- \psi_-^*, \\ \ll P_\pm \gg = (\psi_+ \psi_-^* + \psi_- \psi_+^*) \prod_i \lambda_i. \end{cases}$$

As a result of interaction with the detector system, the part of the statistical matrix of the particle representing indeterminate spin has become multiplied by the factor  $\prod_i \lambda_i$ . As one sees from (22), the  $\lambda_i$  are usually small compared with 1, and they are never greater than 1. The number of  $\lambda_i$ 's is the number of degrees of freedom of the detector, and since the latter is a macroscopic object,  $\prod_i \lambda_i$  is effectively zero.

## 5. - Conclusion.

To draw a general conclusion from the foregoing, it is necessary to separate the essential and inessential features of the model. The essential features were (i) the physical separation of the components of the detector system corresponding to different eigenvalues of the micro-observable; (ii) the metastability of the detectors; (iii) the macroscopic nature of the detectors; and (iv) the quantum-mechanical nature of the interaction, which ensured  $\lambda_i < 1$  (via an analogue of Schwartz's inequality). The apparently inessential features were those designed to ensure mathematical simplicity: (i) the choice of an observable with only two eigenvalues; (ii) the choice of a system of harmonic oscillators to represent the detector; and (iii) the assumed particular form of interaction between the microsystem and the detector; all that was necessary was that this should trigger the detector mechanism.

If one is satisfied that these latter features were inessential, one must conclude that the theory of Sect. 2 should apply quite generally, and admit the following: whenever a micro-system interacts with an efficient measuring device, the indeterminacy associated with the observable measured disappears. When the measuring device has functioned, the state of the micro-system has become impure, and can no longer be represented by a single wave-function. Without inspecting the measuring device, one cannot tell what the result of the measurement was, but the uncertainty is due to incomplete information rather than quantum-mechanical indeterminism.

\* \* \*

This work was initiated as a result of discussions at the Dublin Institute for Advanced Studies, and the author gladly acknowledges his debt to the members of the Institute.

## RIASSUNTO (\*)

Il presente lavoro spiega come l'indeterminazione di un'osservabile quantum-meccanica sia eliminata dal processo di misurazione. Si pone in evidenza che l'osservazione di un microsistema individuale è possibile solo per mezzo della sua interazione con un sistema macroscopico in uno stato metastabile. Si studia sotto l'aspetto quantum-meccanico una interazione di questa specie. Il modello consiste di una particella con due stati di spin che si dividono e si portano a interagire con detettori separati. Ogni detettore comprende due serie di oscillatori a differenti temperature che, per interazione, si accoppiano alla particella cosicchè questa può esser rivelata da una variazione di temperatura. Si trova che gli stati in cui lo spin è indeterminato non possono influenzare nessuno dei detettori e che si estinguono rapidamente quando si « inserisce » l'interazione. Dopo l'interazione lo stato della particella non è più puro e non può più essere rappresentato da una sola funzione d'onda. Non c'è discontinuità nella transizione.

(\*) Traduzione a cura della Redazione.

## Representations of Symmetry Operators.

P. G. FEDERBUSH (\*) and M. T. GRISARU (+)

*Palmer Physical Laboratory, Princeton University - Princeton, New Jersey*

(ricevuto il 20 Giugno 1958)

**Summary.** — Explicit representations in terms of the field variables are given for the charge conjugation, space inversion, and time reversal operators, for the case of free fields. These expressions are generalized to the case of coupled fields.

The invariance transformations of field theory may be divided into two classes. Transformations of the first class form connected continuous groups such that any transformation may be obtained from the identity by exponentiation of an infinitesimal operator. Included in this class are all the operators of the restricted inhomogeneous Lorentz group, and phase and gauge transformations. The expression of these operators in terms of the field quantities is easily derived in the Lagrangian formalism. The symmetry operations such as space inversion, time reversal, and charge conjugation belong to the second class. We wish to construct an explicit representation of these operators in terms of the field variables for the free field case. Following this, we shall consider a generalization to the coupled field case.

It is well known that, while the charge conjugation and parity operators can be chosen to be unitary, the time reversal operator is anti-unitary. However, since the latter can be written in the form  $T=UK$ , where  $U$  is unitary and  $K$  is the complex conjugation operator, we need discuss only the unitary part  $U$ .

We consider an arbitrary free Bose or Fermi field which may be expressed in terms of a complete set of annihilation and creation operators  $a, a^*$  satisfying

(\*) National Science Foundation Predoctoral Fellow.

(+) Charlotte Elizabeth Procter Fellow.



the usual commutation or anti-commutation relations

$$\Phi = \sum_K (F_K a_K + g_K a_K^*).$$

The transformed field can be written

$$\Phi' = \sum_K (F_K a'_K + g_K a'^*_K),$$

where the  $a_K$  and  $a'_K$  are related as follows: Either

$$\begin{aligned} a'_K &= O a_K O^{-1} = \exp[i\theta] a_K \\ a'^*_K &= O a^*_K O^{-1} = \exp[-i\theta] a^*_K \end{aligned}$$

or, we may select pairs of operators  $a_{j_1} a_{j_2}$  and  $a'_{j_1} a'_{j_2}$  such that

$$(1) \quad \begin{cases} a'_{j_1} = O a_{j_1} O^{-1} = \exp[i\theta] a_{j_1}, & a'^*_{j_1} = O a^*_{j_1} O^{-1} = \exp[-i\theta] a^*_{j_1}, \\ a'_{j_2} = O a_{j_2} O^{-1} = \exp[-i\varphi] a_{j_2}, & a'^*_{j_2} = O a^*_{j_2} O^{-1} = \exp[i\varphi] a^*_{j_2}. \end{cases}$$

The first case is met, for instance, if  $\Phi'$  is a charge conjugate neutral scalar field. An example of the second possibility occurs if  $\Phi'$  is a charge conjugate Dirac field, in which case the pair  $a_{j_1} a_{j_2}$  consists of destruction operators for a particle and an anti-particle of the same momentum and spin; one may choose the phases of  $\Phi$  and  $\Phi'$  such that  $\theta = \varphi = 0$ . In general, by suitably choosing phases, it is possible to set  $\theta = \varphi$  (implying  $O^2 = 1$ ), and this will be done in what follows.

Since the first possibility is a special case of the second, we may restrict ourselves to the latter. Let us start by constructing the operator  $O_j$  which performs the transformation (1) on the pair  $a_{j_1} a_{j_2}$ , leaving all others unchanged. Let

$$(2) \quad A_j = a^*_{j_1} a_{j_1} + a^*_{j_2} a_{j_2} - \exp[-i\theta] a^*_{j_2} a_{j_1} - \exp[i\theta] a^*_{j_1} a_{j_2}.$$

The infinitesimal operator  $\exp[i\delta A_j]$  transforms the creation and annihilation operators in the following manner:

$$(3) \quad \begin{cases} a_{j_1} \rightarrow a_{j_1} - i\delta a_{j_1} + i\delta \exp[i\theta] a_{j_2}, \\ a_{j_2} \rightarrow a_{j_2} - i\delta a_{j_2} + i\delta \exp[-i\theta] a_{j_1}, \\ a^*_{j_1} \rightarrow a^*_{j_1} + i\delta a^*_{j_1} - i\delta \exp[-i\theta] a^*_{j_2}, \\ a^*_{j_2} \rightarrow a^*_{j_2} + i\delta a^*_{j_2} - i\delta \exp[i\theta] a^*_{j_1}. \end{cases}$$

In matrix notation

$$(4) \quad \begin{pmatrix} a_{j_1} \\ a_{j_2} \end{pmatrix} \rightarrow \left[ (1 - i\delta) \begin{pmatrix} 1 & 0 \\ 0 & 1 \end{pmatrix} + i\delta \begin{pmatrix} 0 & \exp[i\theta] \\ \exp[-i\theta] & 0 \end{pmatrix} \right] \begin{pmatrix} a_{j_1} \\ a_{j_2} \end{pmatrix}.$$

Therefore the finite transformation  $\exp[i\omega A_j]$  may be written as

$$\begin{aligned} (5) \quad \begin{pmatrix} a_{j_1} \\ a_{j_2} \end{pmatrix} &\rightarrow \exp[i\omega A_j] \begin{pmatrix} a_{j_1} \\ a_{j_2} \end{pmatrix} \exp[-i\omega A_j] = \\ &= \exp \left[ -i\omega \begin{pmatrix} 1 & 0 \\ 0 & 1 \end{pmatrix} + i\omega \begin{pmatrix} 0 & \exp[i\theta] \\ \exp[-i\theta] & 0 \end{pmatrix} \right] \begin{pmatrix} a_{j_1} \\ a_{j_2} \end{pmatrix} = \\ &= \exp[-i\omega] \left[ \cos \omega + i \begin{pmatrix} 0 & \exp[i\theta] \\ \exp[-i\theta] & 0 \end{pmatrix} \sin \omega \right] \begin{pmatrix} a_{j_1} \\ a_{j_2} \end{pmatrix}. \end{aligned}$$

Choosing  $\omega = \pi/2$  we arrive at

$$\begin{aligned} a_{j_1} &\rightarrow \exp[i\theta] a_{j_2} \\ a_{j_2} &\rightarrow \exp[-i\theta] a_{j_1} \end{aligned}$$

and the corresponding relations for the creation operators. Note that the choice  $\omega = -\pi/2$  yields the same result and is equivalent to changing  $A_j$  into  $-A_j$ . Thus  $O_j = \exp[i(\pi/2)A_j]$  operates correctly on the pair  $a_{j_1} a_{j_2}$  and leaves all other operators unchanged.

We obtain the operator  $O$  by forming the product

$$O = \prod_j O_j = \exp \left[ i \frac{\pi}{2} \sum_j A_j \right],$$

with

$$\begin{aligned} (6) \quad \sum_j A_j &= \sum_j (a_{j_1}^* a_{j_1} + a_{j_2}^* a_{j_2} - \exp[-i\theta] a_{j_2}^* a_{j_1} - \exp[i\theta] a_{j_1}^* a_{j_2}) = \\ &= \sum_K (a_K^* a_K - a_K'^* a_K') = \sum_K (a_K^* a_K - a_K^* a_K'), \end{aligned}$$

where the summation in the last two forms extends over all operators rather than over pairs. The first term is simply the number operator. Special cases of this formula have been given before <sup>(1)</sup>.

<sup>(1)</sup> L. WOLFENSTEIN and D. G. RAVENHALL: *Phys. Rev.*, **88**, 279 (1953); S. WATANABE: *Rev. Mod. Phys.*, **27**, 40 (1955).

We finally exhibit the expression for the symmetry operator in terms of the field variables, in a theory containing a Dirac field  $\Psi$ , a charged scalar field  $\Phi$ , and a neutral scalar field  $\Phi_0$ .

$$(7) \quad O = \exp \left[ i \frac{\pi}{2} \int d^3x \left[ \bar{\Psi} i \gamma_4 \Psi - \frac{1}{2} \bar{\Psi}' i \gamma_4 \Psi - \frac{1}{2} \bar{\Psi} i \gamma_4 \Psi' + i \Phi^{*} \frac{\overleftrightarrow{\partial}}{\partial t} \Phi - \right. \right. \\ \left. \left. - \frac{i}{2} \Phi^{*} \frac{\overleftrightarrow{\partial}}{\partial t} \Phi' - \frac{i}{2} \Phi^{*'} \frac{\overleftrightarrow{\partial}}{\partial t} \Phi + \frac{1}{2} i \Phi_0^0 \frac{\overleftrightarrow{\partial}}{\partial t} \Phi_0 - \frac{i}{2} \Phi_0' \frac{\overleftrightarrow{\partial}}{\partial t} \Phi_0 \right]_{\tilde{N}} \right].$$

The symbol  $\tilde{N}$  (number-ordering) implies that creation operators appearing to the right of annihilation operators should be moved to the left and multiplied with minus one for the Boson case, and a plus one for the Fermion case. This sign convention is opposite to that used in normal-ordering. One may extend the above formula in an obvious manner, if more than one field of a given type appears. Vector fields, such as the electromagnetic field, may be included as well (by treating each component as a scalar field).

The time reversal operator can be written, as previously remarked, in the form  $T = UK$ .  $U$  is given by (7) with the understanding that  $\Phi' = U \Phi U^{-1}$ .

We wish to investigate the possibility of generalizing (7) to the case of coupled fields. As it stands, this expression is meaningless for this case, since the number-ordering is not defined. We begin by remarking that the symmetry operators are time-independent, even for the coupled fields, if the theory is invariant under the symmetry. For space inversion and charge conjugation we may express the operators at time  $t = -\infty$  in terms of the «in» fields, for which we have no difficulty in defining the number-ordering. Since the operator in (7), when expressed in terms of the «in» fields, is independent of time and correct at  $t = -\infty$ , it is correct at all times.

It would of course be more satisfying to be able to define the symmetry operators directly in terms of the coupled fields. This is possible if no neutral boson fields are present, and if we restrict ourselves to space inversion or time reversal. In this case, the number-ordering operation in (7) may be replaced by normal-ordering. Indeed, this would have the effect of replacing a term like

$$\int d^3x (\bar{\Psi} i \gamma_4 \Psi)_{\tilde{N}} = \text{number of particles} + \text{number of anti-particles},$$

with

$$\int d^3x (\bar{\Psi} i \gamma_4 \Psi)_N = \text{number of particles} - \text{number of anti-particles}.$$

However, since time or space inversion does not interchange particles and anti-particles (or positive and negative charge), and since the replacement

of  $A_j$  by  $-A_j$  for any  $j$  is permissible, the resulting operator is equal to the original one. Furthermore, in this case, one may insert in (7) the coupled fields, since the required properties are the same for the free and coupled fields at a given instant of time. If one uses renormalized coupled fields, the usual renormalization constant should be included. Thus, with the exception of theories that include uncharged Boson fields, it is possible to express both space and time inversion operators directly in terms of the coupled field.

#### RIASSUNTO (\*)

Per il caso di campi liberi si danno rappresentazioni esplicite in termini delle variabili di campo per gli operatori di coniugazione della carica, inversione dello spazio e inversione del tempo. Si generalizzano queste espressioni per il caso di campi accoppiati.

---

(\*) *Traduzione a cura della Redazione.*

## On a Possible Test of Symmetry in Pion-Baryon Interactions.

D. AMATI

*Istituto di Fisica dell'Università - Roma*  
*Istituto Nazionale di Fisica Nucleare - Sezione di Roma*

B. VITALE

*Istituto di Fisica Teorica dell'Università - Napoli*  
*Scuola di Perfezionamento in Fisica Teorica e Nucleare del C.N.R.N. - Napoli*

(ricevuto il 23 Giugno 1958)

**Summary.** — It is shown that the study of the branching ratios from absorption of low energy  $K^-$  on protons (from the continuum) can give a good insight about the symmetries in strong interactions. The possibility of deriving the K-H relative parity from the analysis of high energy absorption processes is also discussed.

### 1. — Introduction.

Several efforts have been devoted recently <sup>(1-5)</sup> to the possibility of systematizing strong interactions by studying the symmetries which they can present.

GELL-MANN <sup>(1)</sup> and SCHWINGER <sup>(2)</sup> proposed at first a universal pion-baryon interaction; PAIS <sup>(4)</sup> and SALAM <sup>(5)</sup> introduced also definite relations among the K-coupling constants. In this latter case, the particular symmetries of the whole Hamiltonian allow for conclusions which are independent of perturbation theory. These conclusions are however incompatible with the results

---

<sup>(1)</sup> M. GELL-MANN: *Phys. Rev.*, **106**, 1297 (1957).

<sup>(2)</sup> J. SCHWINGER: *Ann. of Phys.*, **2**, 407 (1957).

<sup>(3)</sup> J. TIOMNO: *Rochester Conference* (1957).

<sup>(4)</sup> A. PAIS: *Remarks on the Symmetry of the Strong Interactions* (preprint).

<sup>(5)</sup> A. SALAM: *On Symmetries of Strong Interactions* (preprint).



of associated production experiments. A very high symmetry therefore seems not to be allowed by the experimental evidence: SALAM concludes that these results indicate most probably that K-couplings are different, while  $\pi$ -couplings may be identical in agreement with the ideas of GELL-MANN and SCHWINGER. Then, since we have no global symmetries for the whole Hamiltonian, no general arguments (completely free from perturbative considerations) can be used. The only way we will be permitted to draw some conclusion would be such that the unsymmetrical K-coupling (MS interactions in the Gell-Mann model, responsible for the difference in mass and behaviour of baryons) shall be sufficiently weak so that their effects will not obscure completely the symmetry of  $\pi$ -couplings (VS interactions). The consequence of these symmetries are studied in this paper by analyzing the absorption of K on nucleons. It is shown that it will be possible to get a useful insight into this problem, as soon as the branching ratios for the four absorption reactions originated by low energy K on proton will be known. It is also discussed how an analysis of high energy absorption can give rise to a useful way of deriving the K-H relative parity, in the framework of  $\pi$ -baryon symmetry.

## 2. - Pion hyperon system.

Let us disregard for the moment MS interactions, and fix our attention upon the interaction of pions with  $\Lambda$  and  $\Sigma$  hyperons. Under the assumptions of spin  $\frac{1}{2}$  hyperons, equal parity of  $\Lambda$  and  $\Sigma$  and charge independence, the  $\pi$ -H interaction Hamiltonian (H stands for  $\Lambda$  or  $\Sigma$ ) is (1)

$$(1) \quad \mathcal{H}_{\pi H} = ig_{\pi\Lambda} [\bar{A}\gamma_5 \Sigma \cdot \pi + \bar{\Sigma}\gamma_5 A \cdot \pi] + g_{\pi\Sigma} [\bar{\Sigma}\gamma_5 \times \Sigma \cdot \pi].$$

The Hamiltonian given in (1) conserves the total isotopic spin  $T$  of the  $\pi$ -H system; it can be 0, 1 or 2 for  $\pi\Sigma$  (states  $\varphi_0$ ,  $\varphi_1$  and  $\varphi_2$ ) and 1 for  $\pi\Lambda$  ( $\psi_1$ ). GELL-MANN noted that if  $g_{\pi\Lambda} = g_{\pi\Sigma}$ , then  $\mathcal{H}_{\pi H}$  can be written as

$$(2) \quad \mathcal{H}_{\pi H} = ig_{\pi H} [\bar{Y}\gamma_5 \tau Y \cdot \pi + \bar{Z}\gamma_5 \tau Z \cdot \pi],$$

where  $Y$  and  $Z$  stand for the isotopic spin doublets:

$$(3) \quad Y = \begin{pmatrix} \Sigma^+ \\ Y^0 \end{pmatrix}, \quad Z = \begin{pmatrix} Z^0 \\ \Sigma^- \end{pmatrix},$$

with

$$(4) \quad Y^0 = \frac{\Lambda^0 - \Sigma^0}{\sqrt{2}}, \quad Z^0 = \frac{\Lambda^0 + \Sigma^0}{\sqrt{2}}.$$

From (2), it is easy to see that  $\mathcal{H}_{\pi H}$  also conserves the isotopic spin  $I$  of the  $\pi$ -Y or  $\pi$ -Z systems ( $I = \frac{1}{2}$  or  $\frac{3}{2}$ ). We can then define two scattering amplitudes  $a_{\frac{1}{2}}$  and  $a_{\frac{3}{2}}$ , in terms of which both the scattering  $\pi$ -Y and  $\pi$ -Z will be described.

In order to express in terms of  $a_{\frac{1}{2}}$  and  $a_{\frac{3}{2}}$  the scattering from eigenstates of  $T$ , we can develop the states  $q_0$ ,  $q_1$ ,  $q_2$  and  $\psi_1$  in eigenstates of  $I$ . It is then easy to find

$$(5) \quad \begin{cases} \langle \varphi_0 | S_0 | \varphi_0 \rangle = a_{\frac{1}{2}}; & \langle \varphi_1 | S_0 | \varphi_1 \rangle = \frac{2}{3}a_{\frac{1}{2}} + \frac{1}{3}a_{\frac{3}{2}}; & \langle \varphi_2 | S_0 | \varphi_2 \rangle = a_{\frac{3}{2}}; \\ \langle \varphi_1 | S_0 | \psi_1 \rangle = \frac{\sqrt{2}}{3}a_{\frac{1}{2}} - \frac{\sqrt{2}}{3}a_{\frac{3}{2}}; & \langle \psi_1 | S_0 | \psi_1 \rangle = \frac{1}{3}a_{\frac{1}{2}} + \frac{2}{3}a_{\frac{3}{2}}, \end{cases}$$

where  $S_0$  indicates the scattering matrix for VS interactions. These relations are of course independent of  $T_z$ .

It is evident that, owing to the existence of two hyperons,  $q_1$  and  $\psi_1$  do not diagonalize the  $S_0$  matrix. We form then the two linear combinations

$$(6) \quad \begin{cases} \eta_1 = \sqrt{\frac{2}{3}}q_1 + \sqrt{\frac{1}{3}}\psi_1, \\ \xi_1 = \sqrt{\frac{1}{3}}q_1 - \sqrt{\frac{2}{3}}\psi_1. \end{cases}$$

and note that from (5) we have

$$(7) \quad \langle \eta_1 | S_0 | \xi_1 \rangle = 0, \quad \langle \eta_1 | S_0 | \eta_1 \rangle = a_{\frac{1}{2}}, \quad \langle \xi_1 | S_0 | \xi_1 \rangle = a_{\frac{3}{2}}.$$

That the complete set  $q_0$ ,  $\eta_1$ ,  $\xi_1$ ,  $q_2$  of eigenstates of  $T$ , diagonalize the pion-hyperon scattering matrix for VS interactions when  $g_{\pi\Lambda} = g_{\pi\Sigma}$ .

### 3. - $\bar{K}$ absorption processes.

Let us now consider the processes

$$(8) \quad \bar{K} + N \rightarrow \Sigma + \pi, \quad \bar{K} + N \rightarrow \Lambda + \pi.$$

The initial states can have isotopic spin 0 or 1, (states  $\chi_0$ ,  $\chi_1$ ). Owing to the conservation of isotopic spin the processes (8) will be completely described by three transition matrix elements

$$(9) \quad A = \langle \chi_0 | S | \varphi_0 \rangle; \quad B = \langle \chi_1 | S | \eta_1 \rangle; \quad C = \langle \chi_1 | S | \xi_1 \rangle,$$

$A$ ,  $B$  and  $C$  will be complex numbers, independent of the third component of isotopic spin;  $S$  is the scattering matrix for all strong interactions.

By using the usual decomposition of physical states in eigenstates of  $T$ , we can describe all the transition amplitudes for reactions (8) in terms of  $A$ ,  $B$  and  $C$ . For instance for the reactions

$$(10) \quad \left\{ \begin{array}{l} K^- p \rightarrow \Sigma^0 \pi^0 \\ \quad \rightarrow \Sigma^+ \pi^- \\ \quad \rightarrow \Sigma^- \pi^+ \\ \quad \rightarrow \Lambda^0 \pi^0 \end{array} \right.$$

we have

$$(11) \quad \left\{ \begin{array}{l} \langle K^- p | S | \Sigma^0 \pi^0 \rangle = \frac{1}{\sqrt{6}} A; \quad \langle K^- p | S | \Sigma^- \pi^+ \rangle = \frac{1}{\sqrt{6}} \left( A - B - \frac{1}{\sqrt{2}} C \right), \\ \langle K^- p | S | \Sigma^+ \pi^- \rangle = \frac{1}{\sqrt{6}} \left( A + B + \frac{1}{\sqrt{2}} C \right); \quad \langle K^- p | S | \Lambda^0 \pi^0 \rangle = \frac{1}{\sqrt{6}} \left( B - \sqrt{2} C \right). \end{array} \right.$$

3'1. *Low energy absorption.* — We shall now concentrate our attention on the absorption of  $\bar{K}$  mesons from the continuum, but at rather small energy (let us say, smaller than 30 MeV). In this case the initial state will be in  $S$ -wave; the final state will be a  $P_{\frac{1}{2}}$  if the parity of the heavy meson relative to the hyperon is  $+1$ , and  $S_{\frac{1}{2}}$  if that parity is  $-1$ . We now make use of the hypothesis that the  $MS$  interactions are rather weaker than the  $VS$  ones by disregarding processes that involve  $MS$  interactions at an order higher than the first <sup>(6)</sup>. From the unitarity of the  $S$  matrix and invariance under time reversal <sup>(7)</sup>

$$(12) \quad A = i|A|\exp[i\alpha_{\frac{1}{2}}], \quad B = i|B|\exp[i\alpha_{\frac{1}{2}}], \quad C = i|C|\exp[i\alpha_{\frac{3}{2}}],$$

where  $\alpha_{\frac{1}{2}}$  and  $\alpha_{\frac{3}{2}}$  are the phase shifts for pion-hyperon scattering, for  $I = \frac{1}{2}$  and  $I = \frac{3}{2}$  respectively, in the  $P_{\frac{1}{2}}$  wave ( $S_{\frac{1}{2}}$ ) if the  $K$ - $H$  relative parity is plus

<sup>(6)</sup> We note that this approach is not a perturbative one in the common sense. We disregard physical processes of higher order or, which is the same, we take into account only the first power in the renormalized  $K$ -coupling constant. A direct test of this assumption of  $MS$  interactions weak with respect to  $VS$  ones will be the comparison of the  $K^-N$  scattering and absorption cross sections. The results of ALVAREZ *et al.* (Rochester Conference, 1957) give rather high values for the elastic and inelastic  $K^-$ -proton interaction (large with respect to the  $K^-N$  scattering cross sections), the elastic part being perhaps justifiable to a large extent by the shadow scattering. The results of the Bologna group (private communication from M. CECCARELLI) indicate instead a low cross section for absorption in flight (rather smaller than the elastic cross section); this would be roughly an indication for rather similar values for the  $\pi$ -hyperon couplings and  $K$ -couplings.

<sup>(7)</sup> See for instance K. WATSON: *Phys. Rev.*, **95**, 228 (1954).

(minus). It seems impossible, at present, to obtain a direct evaluation of these phase shifts from  $\pi$ -H scattering.

By normalizing to 1 the cross-section for the first reaction in (10) we have:

$$(13) \quad \begin{cases} \sigma_{\Sigma^0 \pi^0} = 1, \\ \sigma_{\Sigma^+ \pi^-} = 1 + b^2 + 2b + (c^2/2) + \sqrt{2}(1+b)c \cos(\alpha_{\frac{3}{2}} - \alpha_{\frac{1}{2}}), \\ \sigma_{\Sigma^- \pi^+} = 1 + b^2 - 2b + (c^2/2) - \sqrt{2}(1-b)c \cos(\alpha_{\frac{3}{2}} - \alpha_{\frac{1}{2}}), \\ \sigma_{\Lambda^0 \pi^0} = b^2 + 2c^2 - 2\sqrt{2}bc \cos(\alpha_{\frac{3}{2}} - \alpha_{\frac{1}{2}}), \end{cases}$$

where  $b$  and  $c$  are real numbers that could be evaluated together with  $\cos(\alpha_{\frac{3}{2}} - \alpha_{\frac{1}{2}})$  from (13). All we need are the branching ratios for the processes (10).

The system (13) will be solvable only if the branching ratios will satisfy some well definite relations. One of the simplest of them is the following one:

$$(14) \quad (W_{\Sigma^+ \pi^-} + W_{\Sigma^- \pi^+} - 4W_{\Sigma^0 \pi^0})^2 + 4W_{\Sigma^0 \pi^0} W_{\Lambda^0 \pi^0} \geq 4W_{\Sigma^+ \pi^-} W_{\Sigma^- \pi^+},$$

where the  $W$ 's are the branching ratios for the various processes (10) in arbitrary units<sup>(8)</sup>.

The branching ratios for the  $K^-$  absorption at low energy will be soon available; it will be then easy to see whether (13) has solutions. If this will not be the case we should infer that the symmetry of  $\pi$ -H interaction is of no use: either because the elementary interactions are different (for instance because of different  $\Lambda$  and  $\Sigma$  parity) or because the MS interactions are large enough to hide the symmetry.

If the system (13) can be solved, we shall be able to find from it the value of  $\cos(\alpha_{\frac{3}{2}} - \alpha_{\frac{1}{2}})$  in terms of the branching ratios.

We note now that in the Gell-Mann model, because of the complete symmetry of all VS interactions, the value of  $\cos(\alpha_{\frac{3}{2}} - \alpha_{\frac{1}{2}})$  would be expected to be very near that of  $\cos(\delta_{31} - \delta_{11})$  if the relative  $K$ -H parity is  $+1$ , and to that of  $\cos(\delta_3 - \delta_1)$  if the relative parity is  $-1$  (the  $\delta$ 's are the phase shifts for  $\pi$ -N scattering in the usual notations).

Even if it is not completely clear at what energy these phase shifts should have to be compared, because of the rather large mass difference between nucleons and hyperons, when  $K^-$  absorption occurs at very low energy the relative  $\pi$ -H energy is nearly that of resonance for the  $\pi$ -N system. At those energies  $\cos(\delta_3 - \delta_1)$  and  $\cos(\delta_{31} - \delta_{11})$  are very near, as numerical values: if their value would turn out to be near the value of  $\cos(\alpha_{\frac{3}{2}} - \alpha_{\frac{1}{2}})$  calculated

<sup>(8)</sup> The quantities  $W$  are essentially proportional to the modulus' square of the matrix elements (11). Owing to the difference in mass between  $\Lambda$  and  $\Sigma$  one must take into account the different kinematics, that give rise to different phase space factors, when comparison with experiment will be made.

from (13) we should have got a good support to the hypothesis of symmetrical  $\pi$ -barion interactions.

We have discussed here only the reactions given in (10), that are obviously the easiest to be studied experimentally. There are however other processes that will be soon investigated experimentally, for instance the low energy absorption of long lived neutral heavy mesons  $\theta_2$  in Hydrogen and the  $K^-$ -neutron interaction by means of deuterium bubble chambers. We can easily derive for all those processes, from (9) and (12), the expressions for the cross-sections as functions of the same quantities  $b$ ,  $c$  and  $\cos(\alpha_{\frac{3}{2}} - \alpha_{\frac{1}{2}})$ , which appear in (13). For instance:

$$(15) \quad \begin{cases} \sigma_{K^-n \rightarrow \Sigma^- \pi^0} = \sigma_{K^-n \rightarrow \Sigma^0 \pi^-} = 2\sigma_{\theta_2 p \rightarrow \Sigma^+ \pi^0} = \frac{1}{3}b^2 + \frac{1}{6}c^2 + \frac{\sqrt{2}}{3}bc \cos(\alpha_{\frac{3}{2}} - \alpha_{\frac{1}{2}}); \\ \sigma_{K^-n \rightarrow \Lambda^0 \pi^-} = 2\sigma_{\theta_2 p \rightarrow \Lambda^0 \pi^+} = \frac{1}{3}b^2 + \frac{2}{3}c^2 - \frac{2}{3}\sqrt{2}bc \cos(\alpha_{\frac{3}{2}} - \alpha_{\frac{1}{2}}). \end{cases}$$

The conclusions reached by the discussion of (13) could therefore be further supplemented by the conditions (15) when the corresponding experimental results will be available.

We note that the results reached so far can be applied to all absorption processes taking place from states with definite  $l$  and  $J$ ; in such cases,  $\alpha_{\frac{3}{2}}$  and  $\alpha_{\frac{1}{2}}$  will be the phase shifts for  $I = \frac{1}{2}$  and  $T = \frac{3}{2}$  for those particular values of  $l$  and  $J$ .

**3.2. Absorption from bound states.** — The results obtained in the preceeding section are valid also for absorption at rest, if the process takes place from a definite orbital. In the possible case of competition among more orbitals, there will be contributions to the branching ratios that will add up incoherently. Nevertheless in the equations analogous to ((13) and (15)) there will be a greater number of parameters like  $b$ ,  $c$  and the  $\alpha$ 's. Relation (14), in such a case, does not necessarily hold, as it is easily seen by its non linearity. Some very preliminar data on  $K^-$  absorption on protons from bound states (absorption at rest) indicate <sup>(9)</sup>:

$$(16) \quad W_{\Sigma^0 \pi^0} : W_{\Sigma^+ \pi^-} : W_{\Sigma^- \pi^+} : W_{\Lambda^0 \pi^0} :: 1 : 1 : 2 : \frac{1}{4}.$$

These values do not satisfy the condition (14). This disagreement, if confirmed by more precise experimental data, would indicate (always in the framework of equal  $\pi$ -hyperon couplings with small  $K$ -couplings) that the absorption for  $K^-$  takes place from more than one initial orbital state. Then, the symmetry of the theory, that could be checked from  $K^-$  absorption from the continuum can allow the use of the branching ratios measured in  $K^-$  absorption

<sup>(9)</sup> L. W. ALVAREZ *et al.*: UCRL 3775 (1957).



at rest on protons to have a good insight into the mechanism of absorption in  $K^-$ -atoms <sup>(10)</sup>.

**3.3. High energy absorption.** — An analysis similar to that developed in the previous paragraphs can be performed also when more than one coherent partial wave is present in the initial  $K$ - $N$  state. In this case we shall obviously have a greater number of real amplitudes. They could be determined however not only from the branching ratios, but also from the angular distributions and polarizations of the final hyperons <sup>(11)</sup>. Let us think in terms of symmetric  $\pi$ -baryon coupling. At energies such that we can take into account only  $S$  and  $P$  waves in the initial state, the final  $\pi$ -hyperon system can involve the  $(\frac{3}{2}, \frac{3}{2})$  resonance only if the heavy meson is pseudoscalar (with respect to the hyperons). This will give rise to qualitatively different behaviour of the cross-sections (energy dependence, polarization, etc.) for scalar or pseudoscalar  $K$ : for instance the hyperon polarization, that depends on the sinus of the phase shift differences, will be appreciable if the  $K$  is pseudoscalar while it would practically vanish if the  $K$  were scalar.

The possibility of checking the hypothesis of  $\pi$ -baryon symmetry from low energy absorption processes (where the conclusions are rather independent of the  $K$  parity), will therefore provide a good tool for the study of the  $K$ - $H$  relative parity, by the analysis of high energy absorption of  $\bar{K}$ , and of the polarization of the emitted hyperon.

\* \* \*

We are grateful to Prof. M. CINI for his kind interest and enlightening discussions. We want also to thank Prof. S. FUBINI for a useful conversation.

<sup>(10)</sup> A. FUJII and R. MARSHAK (*Nuovo Cimento*, **8**, 643 (1958)) have performed a calculation perturbative in both  $g_\pi$  and  $g_K$  (under the hypothesis of global symmetry) in order to find the theoretical values for the branching ratios in absorption of  $K^-$  from  $1s$  and  $2p$  states.

<sup>(11)</sup> An analysis similar to that proposed here was performed in the case of associated production (D. AMATI and B. VITALE: *Nuovo Cimento*, **9**, 340 (1958)). The possibility of measuring the hyperon polarization by its decay is discussed by T. D. LEE, J. STEINBERGER, G. GREIBER, P. K. KABIR and C. Y. YANG: *Phys. Rev.*, **106**, 1367 (1957).

## RIASSUNTO

Si studiano le conseguenze della ipotesi di simmetrie nelle interazioni dei pioni con i barioni, sui rapporti tra le sezioni d'urto per i processi di assorbimento dei  $K$  su protoni. Si discute anche della possibilità di ottenere informazioni sulla parità relativa  $K$ - $H$  dall'analisi dei dati sperimentali sull'assorbimento dei  $K$  ad alta energia.

## The Height of the Barrier Hindering Rotation in Nitrosodimethylamine.

M. SIMONETTA and S. CARRÀ

*Department of Physical Chemistry - University of Milan (Italy)*

(ricevuto il 27 Giugno 1958)

**Summary.** — The height of the barrier hindering rotation in nitrosodimethylamine has been calculated by a simple molecular orbital treatment, in its  $\pi$  electrons approximation.  $\sigma$  bond energies and non bonding-forces are also evaluated. Fair agreement with experimental results is obtained.

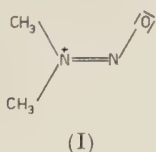
The height of the barrier hindering rotation in dimethylnitrosoamine was determined by an analysis of its nuclear magnetic resonance by E. LOONEY, W. D. PHILLIPS and E. L. REILLY (<sup>1</sup>). The value reported by these authors is 23 kcal/mole. After comparison with values of rotation around single bonds in different molecules, they suggested that the high value found for dimethylnitrosamine might be due to partial double bond character of the N-N bond in this molecule.

To test this explanation we performed a theoretical calculation of the height of the barrier and the results are reported in the present paper.

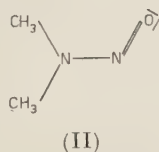
The method of calculation adopted by us was as following:  $\pi$ -electrons energy,  $\sigma$  bond energy and non-bonding energy were calculated for  $\varphi = 0^\circ$ ,  $30^\circ$ ,  $60^\circ$  and  $90^\circ$ ,  $\varphi$  being the angle between N—N=O and CNC planes. The difference between the total energy  $E_T = E_\pi + E_\sigma + E_{N.B.}$  for  $\varphi = 0^\circ$  and  $\varphi = 90^\circ$  was taken as a measure of the height of the barrier. The major part of this difference was expected to be due to differences in  $\pi$  electron energy. In fact

(<sup>1</sup>) C. E. LOONEY, W. D. PHILLIPS and E. L. REILLY: *J.A.C.S.*, **79**, 6136 (1957).

the planar (except for the hydrogen atoms) molecule can be described as resonating between the forms:



and



but after a rotation of  $90^\circ$  the molecule is essentially in form (I).

Calculation of the  $\pi$  energy was performed according to the standard molecular orbital method, in its LCAO approximation. The  $\pi$  electron system contains four electrons which occupy the two lowest of molecular orbitals formed by combination of three atomic orbitals centered on the two nitrogen and the oxygen atoms. The prescriptions followed in the calculation of the energies of the relevant molecular orbitals are similar to those given by ITO, SHIMADA, KURAISHI and MIZUSHIMA <sup>(2)</sup>:

1) All the overlap integrals are neglected and all the exchange integrals except between neighbouring atoms are neglected.

2) The Coulomb integral of each atom with zero formal charge is assumed to be approximatively measured by its first ionization potential in an appropriate valence state when the atom contributes one electron to the  $\pi$  system and by its second ionization potential plus the value of the integral ( $aa/aa$ ) (for details of the symbolism used in the present paper see reference <sup>(3)</sup>) when the atom contributes two electrons to the  $\pi$  system.

3) Variation of the Coulomb integral of each atom due to formal charge is taken care of, by the formula  $\alpha = \alpha_0(x/x_0)$ , where  $\alpha_0$  and  $x_0$  are the Coulomb integral and the electronegativity of the unchanged atom,  $\alpha$  and  $x$  are the same quantities in the atom with formal charge  $e_f$ .

4) Formal charges are evaluated according to the following definition:

Formal charge of atom  $i$  ( $e_f$ ) = atomic number — number of electrons non concerned in chemical binding —  $\frac{1}{2}$  number of  $\sigma$  bonds emanating from atom  $i$  —  $\sum_k (\mu_{ik}/r_{ik})$  —  $\pi$  electron density on atom  $i$ .

$\mu_{ik}$  and  $r_{ik}$  are  $\sigma$  bond moment and length of  $i$ - $k$  bond, and summation is made over all  $\sigma$  bonds emanating from atom  $i$ .

<sup>(2)</sup> M. KO, R. SHIMADA, T. KURAISHI and W. MIZUSHIMA: *Journ. Chem. Phys.*, **26**, 1508 (1957).

<sup>(3)</sup> M. SIMONETTA, G. FAVINI and S. CARRÀ: *Molecular Physics*, **1**, 181 (1958).

5) Variation of electronegativity  $\Delta x = x - x_0$  due to formal charge is evaluated as suggested by PAULING <sup>(4)</sup>:  $\Delta x = \Delta e_f/3$ .

6) Exchange integrals were evaluated by the formula:

$$\beta_{ab} = -S_{ab}(\alpha_a^0 + \alpha_b^0)/2,$$

where  $\alpha_a^0$  is the Coulomb integral of the uncharged atom  $i$ , as defined in prescription 2).

7) Overlap integrals  $S_{ab}$  were obtained from the tables given by MULLIKEN, RIECKE, ORLOFF and ORLOFF <sup>(5)</sup>, with the necessary atomic distances calculated in the following way <sup>(6)</sup>:

$$R_{NO}^2 = \frac{4.98}{N + 1.45}, \quad R_{NN}^2 = \frac{5.28}{N + 1.41},$$

where  $N$  is the total bond order.

8) Starting with an assumed  $\pi$  electron distribution, and the relevant Coulomb integrals,  $\pi$ -orbital energies  $\pi$  charge distribution and bond orders were calculated. With the recalculated values of Coulomb and exchange integrals the calculation repeated until the final value of the Coulomb integral of each atom, and hence the coefficients of atomic orbitals in molecular orbitals converges to a constant value (the values of exchange integrals as defined in prescription 6) converge much faster owing to the rapid convergence of calculated distances).

We shall note that our definitions of Coulomb and exchange integrals involve the assumption that all penetration integrals can be disregarded. In the case of the molecule with the configuration corresponding to  $\varphi = 90^\circ$  the assumption 6) involves  $\beta_{NN} = 0$ , which was found to be incorrect <sup>(4)</sup>: however  $\beta_{NN \varphi=90^\circ}$  was kept equal to zero for consistency in all our assumptions. For the evaluation of  $\alpha_{N+}^0$  the integral  $(aa/aa)$  is to be evaluated. In the case of a neutral atom it is well known that, for this integral both theoretical and semiempirical values are available. The theoretical value is given <sup>(8)</sup> by  $(aa/aa) = 5.323Z = 20.76 \text{ eV}$  ( $Z = 3.90$ ) <sup>(9)</sup>, while the semiempirical value is <sup>(10)</sup>:

<sup>(4)</sup> L. PAULING: *The Nature of the Chemical Bond* (Ithaca, N.Y., 1948), p. 66.

( ) R. S. MULLIKEN, C. A. RIECKE, D. ORLOFF and H. ORLOFF: *Journ. Chem. Phys.*, **17**, 1248 (1949).

<sup>(6)</sup> W. GORDY: *Journ. Chem. Phys.*, **15**, 305 (1947).

<sup>(7)</sup> R. S. MULLIKEN and C. C. J. Roothaan: *Chem. Rev.*, **41**, 219 (1947).

<sup>(8)</sup> R. G. PARR and B. L. CRAWFORD: *Journ. Chem. Phys.*, **16**, 1049 (1948).

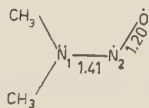
<sup>(9)</sup> J. C. SLATER: *Phys. Rev.*, **36**, 57 (1930).

<sup>(10)</sup> R. PARISER and R. G. PARR: *Journ. Chem. Phys.*, **21**, 767 (1953).

$(aa/aa) = I_N - A_N = 10.68$  eV ( $I = 12.26$  and  $A = 1.58$  <sup>(11)</sup> for the N atom in  $sp^3V_3$  state). According to DEWAR and PAOLONI <sup>(12)</sup> the value of  $(aa/aa)$  for a nitrogen atom with plus charge one should be given by  $I_{N^+} + A_{N^+} = I_{N^+} - I_N$  with these quantities calculated for the  $sp^3V_3$  and  $sp^4V_3$  states. Their calculation was repeated by us using modern values <sup>(11)</sup> for valence state energies instead of their old Mulliken's values <sup>(13)</sup> and give  $(aa/aa) = 14.36$  eV with an increase of the order of about 40% of the value for the neutral atom. On the other hand the theoretical ratio between the two integrals is  $Z'/Z = 4.25/3.90 = 1.090$  and the increase is in the order of ten per cent. Recently PAOLONI <sup>(14)</sup> found a new empirical relation to calculate  $(aa/aa)$  values:  $(aa/aa) = 3.294Z$  which gives 12.85 and 14.00 eV for N and  $N^+$  respectively.

We decided rather arbitrarily to use the 10.68 eV value but we checked that a reasonable change in the value adopted for this integral does not influence sensibly the final results.

For the case of  $\varphi = 90^\circ$  we started with the following electron distribution and bond lengths:



that is we assumed an N—N single bond and N—O double bond, to start with. The  $\alpha^0$  values adopted by us were:

$$\alpha_{N_1}^0 = -18.17 \text{ eV}, \quad \alpha_{N_2}^0 = -14.16 \text{ eV}, \quad \alpha_O^0 = -17.28 \text{ eV}.$$

$\alpha_{N_2}^0$  is the value calculated by BROWN and PENFOLD <sup>(15)</sup> for the nitrogen atom in the  $s^1p^3$  configuration,  $\alpha_O^0$  was given by SKINNER and PRITCHARD <sup>(11)</sup> for the  $s^2p^4$  state.  $\alpha_{N_1}^0$  was obtained by  $-28.85 + 10.68$  where  $-28.85$  is given by:

$$N^+ s^2p^2 {}^3P \rightarrow N^{++} s^2p^2 {}^2P - 29.60 \text{ eV} \quad (16),$$

$$N^+ s^2p^2 {}^3P \rightarrow N^+ sp^3V_4 - 11.95 \text{ eV} \quad (11),$$

$$N^{++} s^2p^2 {}^2P \rightarrow N^{++} sp^3V_3 - 11.20 \text{ eV} \quad (11).$$

<sup>(11)</sup> H. A. SKINNER and M. O. PRITCHARD: *Chem. Rev.*, **49**, 745 (1955).

<sup>(12)</sup> M. J. S. DEWAR and L. PAOLONI: *Trans. Far. Soc.*, **53**, 261 (1957).

<sup>(13)</sup> R. S. MULLIKEN: *Journ. Chem. Phys.*, **2**, 782 (1934).

<sup>(14)</sup> L. PAOLONI: *Nuovo Cimento*, **4**, 410 (1956).

<sup>(15)</sup> A. D. BROWN and A. PENFOLD: *Trans. Far. Soc.*, **53**, 397 (1957).

<sup>(16)</sup> C. E. MOORE: *Atomic Energy Levels* (Washington D. C., 1949).



$\sigma$  bonds moments were assumed to be equal to difference of Pauling's electronegativity values:  $\mu_{\text{NO}} = 0.5 D$ ,  $\mu_{\text{CN}} = 0.5 D$ . At this point all the necessary parameters were available to start the iterative process.

For  $\varphi = 30^\circ$  and  $60^\circ$  the calculations followed the same lines. For  $\varphi = 90^\circ$  the secular equation split in a first degree and a second degree determinants as  $\beta_{\text{NN}} = 0$ . The results are reported in Table I.

TABLE I.

$\varphi$	$E$ (eV)	$E$ (kcal)	$e_{\text{N}_1}$	$e_{\text{N}_2}$	$e_{\text{O}}$	$r_{\text{NN}}$ (Å)	$r_{\text{NO}}$ (Å)
0	82.7674	32.362	1.87044	0.75890	1.37064	1.367	1.225
30	82.4360	24.720	1.89790	0.75946	1.34620	1.382	1.219
60	81.8644	11.539	1.96672	0.77006	1.26324	1.422	1.210
90	81.3640	—	2.00000	0.79256	1.20724	1.480	1.205

For  $\varphi = 0^\circ$  the calculated dipole moment is  $\varphi = 3.82 D$ , in close agreement with the experimental value  $3.98 D$  <sup>(17)</sup>.

The energy for  $\sigma$  bond stretching was roughly evaluated with the elastic

potential formula, as given by PAULING <sup>(18)</sup>, with  $k$  constant taken from GORDY <sup>(19)</sup>. Results are summarized in Table II.

Non-bonding forces between the oxygen atom and the two methyl groups vary with rotation of the N—O bond around the N—N axis, owing to different distances between oxygen and carbon and hydrogen atom. The difference of non bonding energy between spatial configurations with  $\varphi = 90^\circ$  and  $\varphi = 0^\circ$  was roughly evaluated by the method suggested by DE LA MARE <sup>(20)</sup> and others and was found to be

smaller than 1.0 kcal/mole. Fig. 1 shows the curve  $E_\pi + E_\sigma$  as function of  $\varphi$ .

The calculated variation of the total energy was  $E_{\tau_{90}} - E_{\tau_{00}} = 30.3$  kcal/mole,

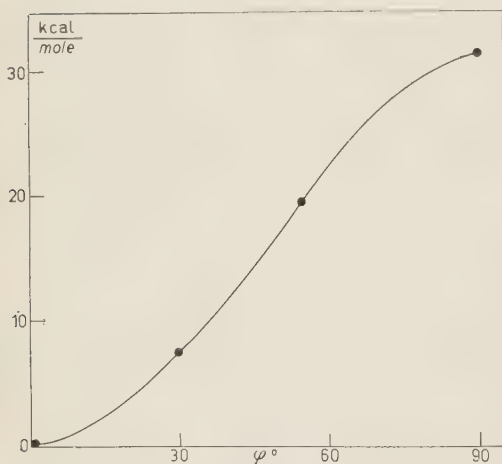


Fig. 1.

<sup>(17)</sup> E. G. COWLEY and J. R. PARTINGTON: *Journ. Chem. Soc.*, 1255 (1933).

<sup>(18)</sup> Ref. <sup>(4)</sup>, p. 175.

<sup>(19)</sup> W. GORDY: *Journ. Chem. Phys.*, **14**, 305 (1956).

<sup>(20)</sup> P. B. D. DE LA MARE, L. FOWDEN, E. D. HUGHES, C. K. INGOLD and J. D. H. MACKIE: *Journ. Chem. Soc.*, 3169 (1955).

TABLE II.

$\varphi$	$E_{\text{NN}}$ (kcal/mole)	$E_{\text{NO}}$ (kcal/mole)	$E_{\sigma}$ (kcal/mole)	$\Delta E_{\sigma}$ (kcal/mole)
0	6.250	25.230	31.480	—
30	4.697	26.760	31.457	— 0.023
60	1.272	29.140	30.412	— 1.068
90	—	30.501	30.501	— 0.970

in reasonable agreement with the experimental value 23 kcal/mole of the height of the barrier: the N—N bond order for the planar form is 1.42 so that our theoretical investigation supports the justification for the height of the barrier suggested by LOONEY, PHILLIPS and REILLY.

## RIASSUNTO

È stata calcolata l'altezza della barriera di rotazione interna della nitrosodimetilammina con una trattazione semplificata della teoria degli orbitali molecolari nell'approssimazione  $\pi$ . Abbiamo anche calcolato le energie dei legami  $\sigma$  e quelle relative alle forze di non legame. I risultati ottenuti risultano in buon accordo con quelli sperimentali.

## Absorption Cross Sections of Carbon, Iron and Lead for 1.5 GeV Negative Pions and 2.8 GeV Protons (\*) (+).

T. BOWEN (+), M. DI CORATO (×), W. H. MOORE, (†)  
and G. TAGLIAFERRI (+)

(+) *Palmer Physical Laboratory, Princeton University - Princeton, N.J.*

(×) *Istituto di Scienze Fisiche dell'Università - Milano*

and

*Istituto Nazionale di Fisica Nucleare - Sezione di Milano*

(†) *Brookhaven National Laboratory - Upton, N.Y.*

(ricevuto il 28 Giugno 1958)

**Summary.** — Absorption cross-sections of Carbon, Iron and Lead for high energy negative pions and protons have been measured with a multiple expansion cloud chamber exposed to beams from the Brookhaven Cosmotron. The results are compared to an optical model computation assuming a nuclear potential distribution with the form of the charge density distribution indicated by electron scattering experiments. The measured cross-sections appear to agree with the ones deduced using this model from the known values of the free pion-nucleon and proton-nucleon total cross-sections.

### 1. — Introduction.

A large multiple plate expansion cloud chamber has been exposed to the negative pion and proton beams from the Brookhaven Cosmotron to study the production of  $\Lambda^0$  and  $\theta^0$  particles in various nuclei<sup>(1)</sup>. At the

---

(\*) A summary of this work has been presented at the International Conference on Mesons, Padua-Venice, 1957.

(+) Supported in part by the joint program of the U.S. Office of Naval Research and the U.S. Atomic Energy Commission.

(1) T. BOWEN, F. COOKSON, G. TAGLIAFERRI, A. WERBROUCK and W. H. MOORE: *Bull. Am. Phys. Soc.*, **2**, 19 (1957); T. BOWEN, G. E. MASEK, GEO. T. REYNOLDS, L. SARTORI, G. TAGLIAFERRI, A. WERBROUCK and W. H. MOORE: *Bull. Am. Phys. Soc.*, **2**, 221 (1957).

time when the experiment was planned (early 1955), no accurate experimental information was available concerning the nuclear interaction cross-section of complex nuclei for pions and protons at Cosmotron energies. Since knowledge of such cross-sections seemed desirable for the interpretation of the results on strange particles production, we anticipated the need of obtaining from our own experiment some statistically significant information on the rates of interaction of high energy pions and protons with C, Fe and Pb nuclei. Consequently, while rough-scanning the material gathered, a certain number of photographs were selected on the basis of *a priori* criteria, and later used to measure nuclear interaction mean free paths.

The results of these measurements yielded absorption cross-sections, which, when compared to the optical model of the nucleus <sup>(2)</sup>, could be adequately represented by assuming that the nuclear potential distribution follows the charge density distribution deduced from the electron scattering experiments <sup>(3)</sup>. It was therefore thought of some interest to report our results in detail. It must be borne in mind, however, that the experiment was not primarily designed to measure absorption cross-sections.

## 2. - Experimental.

2'1. *Cloud chamber.* - The instrument used was a volume controlled expansion type cloud chamber, with inside dimensions 28 in.  $\times$  28 in.  $\times$  10 $\frac{1}{4}$  in. illuminated depth. Except for size, the chamber design, employing a rigid piston and two expansion valves, is entirely conventional. Stereoscopic pictures were taken with two cameras on 70 mm linagraph ortho film. The plate assemblies used inside the chamber were successively: 15 iron plates; 7 lead plates; a mixed assembly containing 7 carbon and 4 lead plates. All plates were  $\frac{1}{2}$  in. thick, covered on both sides with 20 mil aluminum foils. The chamber was surrounded by a concrete shielding 36 in. thick on the side facing the Cosmotron. Pictures were taken at a rate of 40  $\div$  45 an hour. Details on the operation of the cloud chamber at the Cosmotron will be published elsewhere.

2'2. *Beams.* - The proton beam was a « blow-up » beam of nominal kinetic energy 2.91 GeV. The beam was defined through the Cosmotron shielding wall by means of a channel 6 in. wide and 12 feet long. The protons were then magnetically deflected through an angle of about 4°, and thus directed into the cloud chamber. The mean value of the momentum selected was de-

---

<sup>(2)</sup> S. FERNBACH, R. SERBER and T. B. TAYLOR: *Phys. Rev.*, **75**, 1352 (1949); H. A. BETHE and R. R. WILSON: *Phys. Rev.*, **83**, 690 (1951).

<sup>(3)</sup> R. HOFSTADTER: *Rev. Mod. Phys.*, **28**, 214 (1956).

terminated by a current carrying wire measurement to be  $(3.60 \pm 5\%)$  GeV/c, corresponding to a proton kinetic energy of  $(2.78 \pm .17)$  GeV.

The negative pion beam was produced by 3 GeV protons striking an aluminum target in a quadrant of the Cosmotron. The negative pions emitted from the target in a forward direction were partially analyzed and deflected

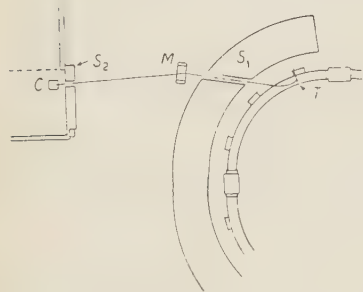


Fig. 1. - Schematic arrangement of the apparatus (not to scale): *T*, target; *S*<sub>1</sub> and *S*<sub>2</sub>, concrete shields; *M*, deflecting magnet; *C*, cloud chamber.

by the Cosmotron magnetic field into a channel about 6 in. high and 9 in. wide in the Cosmotron shield. After emerging from the shield, the pions were bent through an average angle of  $9^\circ$  by a deflecting magnet. The distance from the target to the chamber was 23 m. A schematic diagram of the experimental arrangement for the pion beam is shown in Fig. 1. The momenta of the negative pions entering the chamber were determined by plotting of the allowable trajectories. The «central ray» of the pion beam was found to correspond to a momentum of 1.67 GeV/c; however, the «extreme rays» correspond to momenta of 1.35 and 2.62 GeV/c respectively. To evaluate the momentum distribution of the pions entering the chamber one should also know the production spectrum at the target.

This spectrum was estimated in two ways: by extrapolating the experimental results of COOL *et al.* <sup>(4)</sup>, and by using the theoretical prediction of the «isobar model» of LINDENBAUM and STERNHEIMER <sup>(5)</sup>. The resultant spectra are very much alike. The pion momentum distribution at the chamber, in the case of the isobar model calculation, is plotted in Fig. 2. For this distribution, the weighted average pion momentum is 1.65 GeV/c (1.51 GeV kinetic energy).

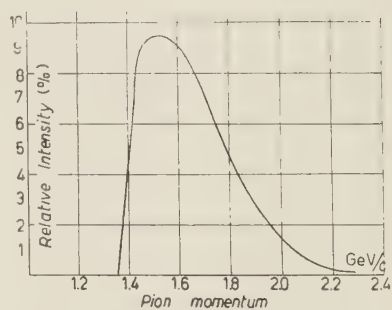


Fig. 2. - Momentum distribution of the pions entering the chamber.

**2.3. Scanning procedure.** - Pictures were selected on the basis of the following *a priori* criteria: the number of beam particles entering the chamber was lower than a given figure (ranging from 10 to 15 according to the plate assembly used); and the quality of the tracks throughout the chamber

<sup>(4)</sup> R. COOL, J. W. CRONIN and A. ABASHIAN: private communication.

<sup>(5)</sup> S. J. LINDENBAUM and R. M. STERNHEIMER: *Phys. Rev.*, **105**, 1874 (1957).



was judged satisfactory. The track count was determined at the exit of the first plate of the assembly. To be accepted as produced by a beam particle, a track was to be near-minimum ionizing and within an angular spread of  $\pm 5^\circ$  (orthogonally projected angle) with respect to the average beam direction.

Each accepted track was then followed and classified as either leaving the chamber or interacting. This experiment should thus provide a direct measurement of the interaction cross-sections from the number of interactions observed and the pion or proton path length.

**2'4. Selection of interactions.** — The following types of events were accepted as interactions:

*a)* All cases where the beam particle appears to suffer an energy loss in a plate, as evidenced by the production of secondary particles (other than knock-on electrons), or by a change in ionization.

*b)* Large angle scatterings of beam particles in traversing a single plate.

*c)* Disappearances of beam particles inside a plate.

The distinction between these three types of events is a purely phenomenological one, and the assignment of one event to a particular type is primarily a consequence of the plate material and thickness used. For nearly all the events in classes *a)* and *b)*, the depth inside the plate at which the event took place was measured to an accuracy of  $\frac{1}{5}$  of the plate thickness. Whenever the origin of the event could not be located, and for the events in class *c)*, an arbitrary depth of production of  $\frac{1}{2}$  the plate thickness was assumed. The scattering events considered in class *b)* are the ones where the orthogonally projected angle is not smaller than  $7^\circ$  in at least one of the pair of stereoscopic photographs. The events considered in class *c)* were carefully checked to make sure that the disappearing beam particle would not have left the illuminated region of the chamber while crossing the plate concerned.

Events produced in the first and the last two plates of the Fe-plate assembly, and in the first and last plate of the other assemblies, were excluded from the statistics, as were the crossings of beam particles in the same plates. Since the chamber was considerably larger than the spread of the beam, there is no need to exclude side particles or interactions.

**2'5. Beam contamination.** — The only contamination expected to be of importance for the purpose of the present work is the muon contamination in the pion beam. That a considerable number of muons should be present among the pions reaching the chamber is to be anticipated both from the decay properties of the pion and from the geometry of the experiment as well as from

the results of previous research performed under rather similar conditions <sup>(6)</sup>. An accurate estimate of the fraction  $f$  of muons in the pion beam is however made difficult in our case because the geometrical configuration of target, channels, magnet and chamber allowed a wide interval of particle momenta to be accepted. Therefore we limited ourselves to an approximate calculation of  $f$  along the following lines. First, we evaluated the probability for a pion to decay while traveling from target to chamber, assuming the pion momentum distribution reported in Fig. 2. Second, we attempted to estimate the probability for the muon produced from the decaying pion to remain in the beam and thus reach the chamber. Subject to two simplifying assumptions, *viz.* (i) that the angular distribution of the pions emitted from the target be isotropic within a small forward solid angle of .004 steradians, and (ii) that the distribution of the  $\pi \rightarrow \mu$  decay angles be symmetrical around the direction of the decaying pion, the probability of loss of muons from the beam turned out to be negligible (of the order of  $(1 \div 2)\%$ ). Accordingly, we obtained  $f \cong 21\%$  of the total number of particles in the pion beam.

Since the pions are strongly absorbed by nuclei, whereas muons are not, a statistical analysis of the pion beam attenuation curves observed in the chamber could be based on the hypothesis that the experimental curves result from the superposition of an exponentially absorbed pion component plus a non-interacting muon component. The analysis should then yield both  $f$  and  $\lambda_{\text{att}}$ , the pion attenuation mean free path. Unfortunately, only one of the plate assemblies we used was thick enough to allow the trend of the attenuation curve to be detected. This was the iron assembly, where the useful number of plates in the chamber was 12, giving a total thickness of  $124.8 \text{ g/cm}^2$ . The iron attenuation curve is plotted in semi-logarithmic co-ordinates

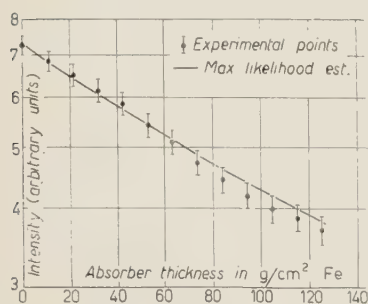


Fig. 3. — The attenuation of the pion beam in iron.

on Fig. 3. With the data of this figure, a maximum likelihood estimation gave  $f = (24^{+8}_{-10})\%$  and  $\lambda_{\text{att}} = (127^{+31}_{-21}) \text{ g/cm}^2$  of iron. Due to the large statistical error, the experimental determination of  $f$  does not help to check the value found by calculation; however, there is no indication of inconsistency between the two.

In the following, we shall use for the muon contamination the calculated value of .21, which we shall consider to be accurate within  $\pm .02$  (unless the assumptions made are invalid).

<sup>(6)</sup> Cfr. *e.g.*: R. COOL, O. PICCIONI and D. CLARK: *Phys. Rev.*, **103**, 1082 (1956).

### 3. - Results.

The experimental results are reported in Table I. Columns 1*a*, 1*b* and 1*c* give the observed pion and proton path lengths in C, Fe and Pb respectively: the numbers shown are corrected for the presence of the aluminum foils covering the plates, and increased by 1.5% to take into account the average inclination of the beam particles with respect to the normals to the plates. The pion paths are also corrected for a 21% muon contamination. Columns 2*a*, 2*b* and 2*c* give the numbers of interactions observed in the path lengths shown. Columns 3*a*, 3*b* and 3*c* give the attenuation cross-sections

TABLE I. - *Attenuation cross-sections of Carbon, Iron and Lead for 1.5 GeV negative pions and 2.8 GeV protons.*

Element	Carbon			Iron			Lead		
	1 <i>a</i> g/cm <sup>2</sup>	2 <i>a</i>	3 <i>a</i> mb	1 <i>b</i> g/cm <sup>2</sup>	2 <i>b</i>	3 <i>b</i> mb	1 <i>c</i> g/cm <sup>2</sup>	2 <i>c</i>	3 <i>c</i> mb
Pions	31681	348	219 ± 11	46638	333	662 ± 32	92431	420	1563 ± 67
Protons	34782	352	202 ± 10	131332	877	619 ± 21	86988	376	1487 ± 67

resulting from the figures of the previous columns; the errors quoted include the statistical probable error on the number of interactions, and a 1% uncertainty in the path length arising from the errors within which the thicknesses of the plate assemblies were known. The pion cross-sections are also affected by the error attached to the determination of the muon contamination. In this connection, it should be noticed that since beam conditions were the same for every material used, any error in the estimate of the muon fraction would affect the reported cross-sections by quantities of the same sign, and of magnitude dependent only upon the plate assembly used. Actually, a change in the assumed *f* value from .21 to .22 would increase the carbon, iron and lead cross-sections by 1.4%, 1.9% and 1.5% respectively.

The breakdown of the observed interactions into the three categories of Sect. 2'4 is shown in Table II. It is seen that the fraction of events pertaining

TABLE II. - *Breakdown of interactions.*

	Category (a)	Category (b)	Category (c)
Pions on Carbon . . .	(60.9 ± 4.2) %	(28.5 ± 2.9) %	(10.6 ± 1.7) %
Pions on Iron . . . .	(51.4 ± 3.9) %	(37.5 ± 3.4) %	(11.1 ± 1.8) %
Pions on Lead . . . .	(55.2 ± 3.6) %	(32.4 ± 2.8) %	(12.4 ± 1.7) %
Protons on Carbon . .	(81.0 ± 3.6) %	(16.2 ± 2.2) %	( 2.8 ± 0.9) %
Protons on Iron . . .	(77.0 ± 3.2) %	(18.3 ± 1.5) %	( 4.7 ± 0.8) %
Protons on Lead . . .	(81.1 ± 6.4) %	(17.4 ± 3.0) %	( 1.5 ± 0.9) %

to each category remains practically unchanged with all absorbers both for pions and protons. It should be remarked, however, that due to the phenomenological character of our classification the good agreement of the results for light and heavy elements is likely to be fortuitous.

#### 4. - Corrections.

The raw results of Table I must be corrected in order to obtain the absorption cross-sections  $\sigma_a$ . We shall discuss the following sources of error: 1) Scanning efficiency; 2) Spurious events; 3) Multiple Coulomb scattering; 4) Diffraction scattering; 5) Loss of nuclear scattering events. It will be seen that the cumulative effect of the applicable corrections will be an increase over the cross-sections of Table I by amounts always less than 15%.

**4.1. Scanning efficiency.** - Re-scanning was carried out by different observers for some 10% of the pictures. As expected, since the scanning had been done by an «along the track» method, very few events appeared to have been overlooked. The scanning efficiency was estimated to reach about 97%, and accordingly a small correction of 3% was applied to the observed cross-sections.

**4.2. Spurious events.** - Under this heading, we discuss whether events due to electrons possibly present in the beams, and knock-on showers produced by beam particles, might have been included in the statistics. It should be remarked that the examination of our pictures shows that the proportion of fast electrons in the proton and pion beams was not appreciable.

Consider now the results with the Pb and Fe plate assemblies, where the thickness of one single plate is equal to at least one shower unit. It is very probable that the greatest part of any electrons in the beam would have interacted in the first plate of the assembly. Since interactions in this plate were not counted (cfr. Sect. 2.4), practically all electrons would in effect have been removed from the beam. Thus we are left only with the knock-on showers produced by pions, muons and protons. However, such cases can be nearly always recognized because the beam particle continues with very little scattering in the plate where the knock-on shower was produced. These events were therefore excluded from the statistics.

In the plate assemblies containing carbon plates, beam particles pass through several of the carbon plates before reaching the first lead plate, raising the possibility of spurious interactions in these carbon plates due to electrons. However, if electrons were present in the beam, most of them would interact in the first lead plate they encounter. A comparison of the numbers and types



of events found in this first lead plate and subsequent lead plates indicates a negligible contribution due to electrons.

Summing up, we are confident that very few, if any, of the spurious events considered here have been included in the statistics, making it unnecessary to correct the observed cross-sections.

**4.3. Multiple Coulomb scattering.** — The scattering events chosen are the ones showing the trajectory of a beam particle to be deflected through an angle of not less than  $7^\circ$  in projection. This limitation was in fact introduced because with our  $\frac{1}{2}$  in. plates the multiple Coulomb scattering would have been responsible for a great many scattering events at smaller angles in the heavy absorbers. The probability of a projected angle  $\geq 7^\circ$  in one Pb-plate crossing is  $\sim 10^{-3}$  for pions with  $p\beta c = 1.6$  GeV; whereas it is not greater than  $3 \cdot 10^{-4}$  for the other combinations of plates and beams. Hence only the cross-section of Pb for pions might warrant a small correction. This was estimated to be a decrease of about 2% (including the contribution due to the muons) in the value of Table I.

**4.4. Diffraction scattering.** — Diffraction scattering can be responsible for a few scatterings of pions through angles  $\geq 7^\circ$  (in projection), but for practically none of protons. The expected contributions were estimated from the diffraction of an equivalent black disk of radius  $R = 1.30 \cdot 10^{-13} A^{\frac{1}{3}}$  cm. Diffraction cross-sections of 80, 360 and 1300 mb were assumed for C, Fe and Pb respectively. In order to estimate the corrections to our data, the projected distribution was calculated from the spatial distribution of the diffraction scattering angles, which showed that the pion cross-sections of Table I should be decreased by about 4%, whereas for protons the corrections amounted to less than 1%, and were therefore ignored.

**4.5. Loss of nuclear scattering events.** — The cut-off of the scatterings at  $7^\circ$  projected angle excludes from the statistics an unknown number of inelastic events. To evaluate the corrections to be applied, the observed differential distributions of scattering angles were linearly extrapolated beyond  $7^\circ$ . The procedure, although crude, appears adequate for our purpose, since the fast secondaries from inelastic processes at Cosmotron energies are expected to give rise to fairly broad angular distributions. Therefore, the corrections considered should represent minor contributions to the absorption cross-sections. Actually, our projected angular distributions could be reasonably well approximated, within the experimental errors by straight lines up to  $35^\circ$  at least (considerably more for the pions-on-iron and pions-on-lead cases, cfr. Fig. 4). The corrections, evaluated by least squares fittings for the interval  $7^\circ \div 35^\circ$ , raise the cross-sections of Table I by amounts between 10% (protons on carbon) and 4.5% (pions on lead).



The cross sections, corrected as described above, are now assumed to represent the absorption cross-sections of the elements investigated. Their values

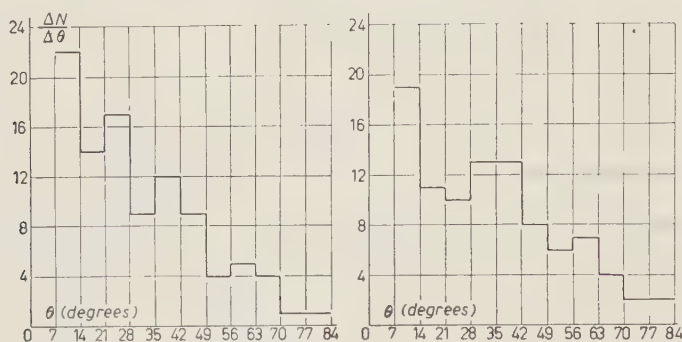


Fig. 4. — Differential projected angle distributions of inelastic scatterings.  
Left: Pions on iron. Right: Pions on lead.

are given in the columns 1 and 3 of Table III. The errors quoted are the sum of the errors reported in Table I, plus the standard errors of the estimated corrections for the loss of inelastic scatterings.

TABLE III. — *The absorption cross-sections (mb) of Carbon, Iron and Lead for 1.5 GeV negative pions and 2.8 GeV protons.*

Element	Pions		Protons	
	Measured	Calculated	Measured	Calculated
	1	2	3	4
Carbon . . . . .	$240 \pm 14$	224 (205)	$230 \pm 12$	258 (237)
Iron . . . . .	$705 \pm 37$	661	$690 \pm 28$	755
Lead . . . . .	$1600 \pm 95$	1580	$1630 \pm 75$	1665

## 5. — Discussion and comparison with other work.

The square well optical model of FERNBACH, SERBER and TAYLOR <sup>(2)</sup>, or one of its later modifications, have been used by several authors to interpret the results of measurements of total and absorption cross-sections <sup>(7)</sup>. We

<sup>(7)</sup> A. E. TAYLOR: *Reports on Progress in Physics*, **20**, 86 (1957).

may first analyze our  $\sigma_a$ 's employing the uniform square well model. Values of radii,  $R$ , and opacities,  $\sigma_a/\pi R^2$ , resulting from this analysis are reported in Table IV. The free proton-nucleon and pion-nucleon cross-sections used in the computation were taken from the works of CHEN, LEAVITT and SHAPIRO <sup>(8)</sup> and of COOL, PICCIONI and CLARK <sup>(6)</sup>, respectively.

TABLE IV. — *Uniform model analysis of the cross-sections reported in columns 1 and 3 of Table III.*

Element	Pions		Protons	
	$R \cdot 10^{13}$ (cm)	$\sigma_a/\pi R^2$	$R \cdot 10^{13}$ (cm)	$\sigma_a/\pi R^2$
Carbon . . . . .	$3.72 \pm 0.28$	0.55	$3.13 \pm 0.14$	0.75
Iron . . . . .	$5.21 \pm 0.21$	0.83	$4.95 \pm 0.13$	0.90
Lead . . . . .	$7.37 \pm 0.25$	0.94	$7.35 \pm 0.18$	0.96

When  $R$  is plotted *vs.*  $A^{1/3}$ , the straight lines giving the best fit to the points for the three elements would not pass through the origin:  $R = (1.39 + 1.01A^{1/3}) \cdot 10^{-13}$  cm from the pion data, and  $R = (0.48 + 1.16A^{1/3}) \cdot 10^{-13}$  cm from the proton ones. Although the errors affecting the empirical  $R$  values of Table IV prevent any conclusion in the proton case, it is suggested at least for pions that it would be difficult to fit the shape of the experimental points with a law of the form  $R = r_0 A^{1/3}$  and a single value for  $r_0$ . This result would not by itself rule out the uniform optical model, whose main difficulty remains however that there seems to be little correlation between radii obtained with different beams and energies.

The uniform model will not be considered further, since it is now generally held that the assumption of a square potential well is unrealistic <sup>(9)</sup>. In fact, measurements of electron scattering by complex nuclei <sup>(3)</sup> have shown that the charge density distribution is not uniform but smoothed out, and can be represented by a Fermi type function. It is tempting therefore to assume an optical model nuclear potential following the same distribution, and compare the cross-sections thus computed with the measured ones. This procedure has been employed in a recent work by CRONIN, COOL and ABASHIAN <sup>(10)</sup> to analyse results obtained with 970 MeV negative pions:

<sup>(8)</sup> F. F. CHEN, C. P. LEAVITT and A. M. SHAPIRO: *Phys. Rev.*, **103**, 211 (1956).

<sup>(9)</sup> Cfr. *e.g.* R. W. WILLIAMS: *Phys. Rev.*, **98**, 1387 (1955).

<sup>(10)</sup> J. W. CRONIN, R. COOL and A. ABASHIAN: *Phys. Rev.*, **107**, 1121 (1957).

a « Fermi tapered » model computation, using a single radial parameter, provided values in excellent agreement with the absorption cross-sections observed in the experiment. In this work the authors examined also some results for 825 MeV protons, and concluded that the assumption of the same optical model parameters as those used in the pion case is satisfactory. Other results for protons of energies from 650 to 900 MeV are considered by BOOTH, HUTCHINSON and LEDLEY<sup>(11)</sup> who likewise find that the optical model with a nuclear potential having the shape of the charge distribution indicated by electron scattering can account for the measured absorption cross-sections.

The comparison of the  $\sigma_a$ 's obtained in the present experiment with the predictions of the above model is shown in Table III, where the « calculated » cross-sections of columns 2 and 4 have been deduced following the procedure of CRONIN, COOL and ABASHIAN. The values quoted are for the Fermi-type density distribution  $\varrho(r)/\varrho_0 = 1 + \exp[(r - cA^{1/3})/a]$ , with  $a = 0.53 \cdot 10^{-13}$  cm and  $c = 1.08 \cdot 10^{-13}$  cm. The values for carbon reported in brackets are for the modified gaussian distribution  $\varrho(r)/\varrho_0 = (1 + \frac{4}{3}(r^2/a^2)) \exp[-r^2/a^2]$  with  $a = 1.635 \cdot 10^{-13}$  cm. For  $\bar{\sigma}$ , the average pion-nucleon or proton-nucleon cross-section, we have taken 30.5 and 39 mb, respectively<sup>(6,8)</sup>.

It is seen that for pions there is agreement, within practically the quoted errors of the experimental results, between measured and calculated cross-sections. A higher value of the radial parameter  $c$ , e.g.  $c = 1.14 \cdot 10^{-13}$  cm as suggested by CRONIN, COOL and ABASHIAN, would be equally acceptable. For protons, Table III shows that the calculated cross-sections of carbon and iron are greater than the measured ones by 2.3 times the errors quoted. Thus a  $c = 1.14 \cdot 10^{-13}$  cm would be uncalled for, even if  $\bar{\sigma}$  were reduced by several percent to correct for the Pauli exclusion principle<sup>(10)</sup>.

We might further remark that a better agreement for the  $\text{proton} \rightarrow \text{C}$  cross-section is found by assuming in the computation the modified gaussian distribution, whereas the opposite seems to be the case for the  $\text{pion} \rightarrow \text{C}$  cross-section.

Summing up, our results support the conclusion already reached by counter measurements at lower energies<sup>(10,11)</sup>: namely, that the absorption cross-sections of complex nuclei for high energy negative pions and protons can be accounted for by the optical model with the assumption of a nuclear potential distribution not far different from the charge density distribution. Whether the choice of a single radial parameter in the potential distribution is satisfactory for every combination of target nucleus, bombarding particle and incident energy, cannot be decided as yet.

(11) N. E. BOOTH, G. W. HUTCHINSON and B. LEDLEY: *Proc. Phys. Soc.*, **71**, 293 (1958).

\* \* \*

The assistance and co-operation of the Cosmotron staff at the Brookhaven National Laboratory is gratefully acknowledged. In the setting up and operation of this experiment we were greatly assisted by others in the Princeton Elementary Particles Laboratory. One of the authors (G.T.) took part in this work while on leave from the University of Milan.

### RIASSUNTO

Con una camera di Wilson a molti piatti esposta a fasci di particelle ottenuti dal Cosmotrone di Brookhaven, si sono misurate le sezioni di assorbimento nucleare del carbonio, del ferro e del piombo per pioni negativi da 1.5 GeV e protoni da 2.8 GeV di energia cinetica. I risultati sperimentali vengono confrontati con i valori previsti dal modello ottico del nucleo, assumendo che la distribuzione del potenziale nucleare abbia la stessa forma della distribuzione di densità di carica elettrica dedotta dagli esperimenti sullo scattering degli elettroni nei nuclei complessi. Con i valori attualmente noti delle sezioni d'urto elementari pione-nucleone e protone-nucleone, l'accordo tra i risultati del calcolo e quelli sperimentali è soddisfacente.

# LETTERE ALLA REDAZIONE

(La responsabilità scientifica degli scritti inseriti in questa rubrica è completamente lasciata dalla Direzione del periodico ai singoli autori).

## A New Representation for Baryonic Fields and Strong Interactions.

B. D'ESPAGNAT

CERN - Geneva

(ricevuto il 6 Giugno 1958)

Several authors have stressed the interest of splitting the strong interaction into two parts, the very strong (VS) and medium strong (MS) interactions. This split may be done through several somewhat different recipes<sup>(1-3)</sup> but the guiding principle always remains that the VS should exhibit more symmetries than the MS.

The purpose of the present letter is to point out a very general and somewhat striking formal analogy between this kind of split and the familiar distinction between parity conserving and parity non-conserving interaction terms: to that end a change of representation is introduced, by means of which the VS and MS interaction Lagrangian are brought into expressions that differ from each other by the presence of a supplementary  $\gamma_5$ . Of course the new kind of « parity » thus introduced has nothing to do with parity in the true sense. The formal parallelism is, however, noteworthy in that it may serve to derive new results concerning these interactions through the simple use of old and familiar concepts.

For the sake of greater simplicity, let us first consider the very simple example of  $NN\pi + \Xi\Xi\pi$  interactions, and let us, temporarily, assume that these are p.v. interactions. In the ordinary representation these interactions, provided that they are invariant in the isotopic spin space ( $I^+$  space) can be written as

$$(1) \quad L_1 = i[f(\bar{N}\gamma_\mu\gamma_5\boldsymbol{\tau}N + \bar{\Xi}\gamma_\mu\gamma_5\boldsymbol{\tau}\Xi) + f'(\bar{N}\gamma_\mu\gamma_5\boldsymbol{\tau}N - \bar{\Xi}\gamma_\mu\gamma_5\boldsymbol{\tau}\Xi)]\frac{\partial\pi}{\partial x_\mu},$$

where  $N = \begin{pmatrix} p \\ n \end{pmatrix}$ ,  $\Xi = \begin{pmatrix} \Xi^0 \\ \Xi^- \end{pmatrix}$  and where  $f = (g_{N\pi} + g_{\Xi\pi})/2$ ;  $f' = (g_{N\pi} - g_{\Xi\pi})/2$ .

As is obvious and well known, the  $f$  terms are also invariant under rotation in another isospace, the  $I^-$  space, where  $\begin{pmatrix} N \\ \Xi \end{pmatrix}$  is considered as a spinor and  $\pi$  as a scalar. This is not the case for the  $f'$  terms: this is why the  $f$  terms are in some

(<sup>1</sup>) M. GELL-MANN: *Phys. Rev.*, **106**, 1296 (1957).

(<sup>2</sup>) J. C. POLKINGHORNE: *Nuovo Cimento*, **6**, 864 (1957).

(<sup>3</sup>) B. D'ESPAGNAT, J. PRENTKI and A. SALAM: *Nuclear Physics*, **5**, 447 (1958).



schemes considered as being very strong and the  $f'$  terms as being medium strong (other schemes make the hypothesis  $f' = 0$ : MS interactions are then assumed to be identical with K interactions).

Now let us make the following change of representation (already considered <sup>(4)</sup> in another context)

$$\begin{cases} \chi = \alpha N + \beta i\tau_2 \Xi^c, \\ \tilde{\chi} = \beta N + \alpha i\tau_2 \Xi^c, \end{cases}$$

with

$$\alpha = \frac{1}{2}(1 + \gamma_5); \quad \beta = \frac{1}{2}(1 - \gamma_5); \quad \gamma_5^+ = \gamma_5$$

it then turns out that

$$L_1 = i\bar{\chi}\gamma_\mu \tau(f + f'\gamma_5)\chi \frac{\partial \pi}{\partial x_\mu} - i\tilde{\chi}\gamma_\mu \tau(f - f'\gamma_5)\tilde{\chi} \frac{\partial \pi}{\partial x_\mu},$$

which verifies the above statement that in the new representation the (VS)  $f$  terms involve no  $\gamma_5$  while the (MS)  $f'$  terms involve one  $\gamma_5$ .

Let us now give a proof for the most general case, with the well-known eight independent coupling constants for  $\pi$  and K interactions. There is then an unambiguous way, quite similar to (1), of splitting this Lagrangian into two parts, one of which is invariant both in  $I^+$  and in  $I^-$  spaces ( $f$  terms or, if one so postulates, VS terms) while the other one is not ( $f'$  terms, or MS). In  $I^-$  space  $\begin{pmatrix} N \\ \Xi \end{pmatrix}$  and  $\begin{pmatrix} K \\ i\tau_2 K^* \end{pmatrix}$  are then spinors while all other fields are scalars. In the new representation both  $X = \begin{pmatrix} \chi \\ i\tau_2 \chi^c \end{pmatrix}$  and  $\mathcal{X} = \begin{pmatrix} K \\ i\tau_2 K^* \end{pmatrix}$  are spinors in  $I^+$  space. The  $\Lambda$  and  $\Sigma$  fields are analogously introduced by means of the combinations

$$\sigma = \alpha \Sigma^+ + \beta \Sigma^{-c}$$

$$\sigma_0 = \alpha \Sigma^0 + \beta \Sigma^{0c} = \sigma_0^c$$

$$\lambda = \alpha \Lambda - \beta \Lambda^c = -\lambda^c$$

together with  $\tilde{\sigma}$ ,  $\tilde{\sigma}_0$ ,  $\tilde{\lambda}$  ( $\chi^c = C^{-1}\gamma_4\chi^*$ , etc.).

In  $I^+$ ,  $\sigma = ((\sigma^c + \sigma)/\sqrt{2}, (\sigma^c - \sigma)/i\sqrt{2}, \sigma_0)$  is then a vector and  $\lambda$  is a scalar; in  $I^-$  they are all scalars.

Let us then consider the product of 180° rotations around the 2-nd axes in  $I^+$  and in  $I^-$  spaces, i.e. the product  $R$  of

$$R^+: \quad \begin{cases} \chi \rightarrow i\tau_2 \chi, & K \rightarrow i\tau_2 K, & \sigma \rightarrow -\sigma^c, & \sigma_0 \rightarrow -\sigma_0^c, \\ \lambda \rightarrow -\lambda^c, & \pi^+ \rightarrow -\pi^{+*}, & \pi^0 \rightarrow -\pi^0. \end{cases}$$

by

$$R^-: \quad X \rightarrow i\zeta_2 X, \quad \mathcal{X} \rightarrow i\zeta_2 \mathcal{X}, \quad \sigma \rightarrow \sigma, \quad \lambda \rightarrow \lambda, \quad \pi \rightarrow \pi$$

(4) B. D'ESPAGNAT: *Nuovo Cimento*, **8**, 894 (1958).

one gets easily

$$R: \quad \begin{cases} \chi \rightarrow -\chi^c, & \sigma \rightarrow -\sigma^c, & \sigma_0 \rightarrow -\sigma_0^c, & \lambda \rightarrow -\lambda^c, \\ \pi^+ \rightarrow -\pi^{+*}, & \pi^0 \rightarrow -\pi^0, & K^+ \rightarrow -K^{+*}, & K_0 \rightarrow -K_0^*, \end{cases}$$

$f$  terms are thus invariant under  $R$ . On the other hand, they are, we assume, invariant under  $C$  and  $P$  and therefore under  $CP$ . Choosing for space parity  $N \rightarrow i\gamma_4 N$  etc., the  $CP$  transformation turns out to be

$$CP: \quad \begin{cases} \chi \rightarrow i\gamma_4 \chi^c, & \sigma \rightarrow i\gamma_4 \sigma^c, & \sigma_0 \rightarrow i\gamma_4 \sigma_0^c, & \lambda \rightarrow i\gamma_4 \lambda^c, & \pi^+ \rightarrow -\pi^{+*}, \\ \pi^0 \rightarrow -\pi^0, & K^+ \rightarrow \eta K^{+*}, & K_0 \rightarrow \eta K_0^{*}; & x_k \rightarrow -x_k, \end{cases}$$

$\eta = +1$  if  $K$  scalar,  $\eta = -1$  if  $K$  pseudoscalar.

$f$  terms being invariant both under  $R$  and under  $CP$  are invariant under their product, i.e. under «paraparity»  $P'$

$$P': \quad \begin{cases} \chi \rightarrow -i\gamma_4 \chi, & \sigma \rightarrow -i\gamma_4 \sigma, & \sigma_0 \rightarrow -i\gamma_4 \sigma_0, & \lambda \rightarrow -i\gamma_4 \lambda, \\ \pi^+ \rightarrow \pi^+, & \pi^0 \rightarrow \pi^0, & K^+ \rightarrow -\eta K^+, & K^0 \rightarrow -\eta K^0; & x_k \rightarrow -x_k. \end{cases}$$

This clearly means, if  $K$  is pseudoscalar, that the ( $I^-$  invariant)  $f$  terms do not involve a  $\gamma_5$ , and consequently that  $f'$  terms involve one  $\gamma_5$ . If  $K$  turned out to be a scalar, obvious changes should be made to this conclusion: the ( $I^-$  invariant)  $f$  terms of  $K$  interactions would involve a  $\gamma_5$  while the  $f'$  terms would not.

The conclusion is general, as  $\tilde{\chi}$  behaves in all these transformations in just the same way as  $\chi$ : it does not matter therefore whether the interactions are of the pseudoscalar or pseudovector types. It may be noticed that  $P$  and  $C$  invariance were not made use of separately in the proof.

In order to show the possible interest of the new representation, we mention briefly simple examples of application of the formal analogy between  $P'$  and parity. In the new representation the  $N$ ,  $\Xi$  mass difference shall manifest itself through the expression

$$(2) \quad M[\tilde{\chi}(a + b\gamma_5)\chi + \bar{\chi}(a - b\gamma_5)\tilde{\chi}]$$

for the mass term, with  $M_N = M(a+b)$ ,  $M_\Xi = M(a-b)$ . If we want this mass difference to be of dynamical origin (due to the interactions) then it is obviously impossible to take all  $\pi$  interactions of the same type (with or without  $\gamma_5$ ) and simultaneously all  $K$  interactions of the same type (same or opposite to the  $\pi$  type), for there would then be some assignments of «paraparity» under which  $L_{\text{int}}$  would be invariant while (2) would not be. Therefore such choices as e.g.:  $g_1 = g_4$ ,  $g_5 = -g_7$ ,  $g_6 = -g_8$  are incompatible with the hypothesis of  $M_\Xi - M_\pi$  being of dynamical origin.

If  $g_3 = 0$  the same holds for  $g_1/g_4 = -1$ ,  $g_5/g_7 = -g_6/g_8 = \pm 1$ . If  $g_2 = 0$  it holds for  $g_1/g_4 = 1$ ,  $g_5/g_7 = -g_6/g_8 = \pm 1$  and if  $g_2 = g_3 = 0$  for the remaining simple choices  $g_2/g_4 = -1$ ,  $g_5/g_6 = g_7/g_8 = \pm 1$  as easily shown by similar arguments. It thus looks as if the  $\Sigma\Delta\pi$ ,  $\Sigma\Sigma\pi$  interactions should contribute decisively to the  $N\Xi$  mass-splitting. As «paraparity» assignments correspond to  $N \rightarrow \pm\gamma_4\tau_2\Xi^c$ ,  $\pi \rightarrow \pm\pi$  etc.,  $x_k \rightarrow -x_k$  in the usual representation, all the results above could

of course be obtained using such substitutions and, much more simply <sup>(5)</sup>, using substitutions such as  $N \rightarrow \pm \Xi$ ,  $\pi \rightarrow \pm \pi$ ,  $K \rightarrow \pm K$ ,  $\Lambda \rightarrow \pm \Lambda$ ,  $\Sigma \rightarrow \pm \Sigma$ , which are products of  $P'$ ,  $P$ ,  $C$  and  $180^\circ$  rotations around  $I_2$ .

Concluding we would like to stress that the new representation derives, in our opinion, what interest it may have from three main reasons:

- a) conservation of  $\mathbf{I}$ ,  $U$  and  $N$  are simply expressed:  $\mathbf{I}$  in the usual way,  $U$  through  $\chi \rightarrow e^{i\theta}\chi$ ,  $K \rightarrow e^{i\theta}K$ ,  $N$  through  $\chi \rightarrow e^{i\theta\gamma_5}\chi$ ,  $\sigma \rightarrow e^{i\theta\gamma_5}\sigma$ ,  $\sigma_0 \rightarrow e^{i\theta\gamma_5}\sigma_0$ ,  $\lambda \rightarrow e^{i\theta\gamma_5}\lambda$ .
- b) the formal analogy between the (VS, MS) split and the (no  $\gamma_5$ ,  $\gamma_5$ ) split can be exploited as shown,
- c) it may give a clue <sup>(4)</sup> to a general description of weak interactions.

It may be finally pointed out <sup>(6)</sup> that for the free fields the Dirac equation is replaced by

$$\gamma_\mu \partial_\mu \chi - M(a - b\gamma_5)\bar{\chi} = 0,$$

$$\gamma_\mu \partial_\mu \bar{\chi} - M(a + b\gamma_5)\chi = 0.$$

<sup>(5)</sup> We are indebted to Dr. PRENTKI for this remark.

<sup>(6)</sup> Compare for instance: H. UMEZAWA and A. VISCONTI: *Nuclear Physics*, **4**, 224 (1957).



## LIBRI RICEVUTI E RECENSIONI

*Handbuch der Physik* — Band 21:  
*Elektronenemission. Gasentladungen I.* 378 Figure; 683 pag., in 8°;  
Springer editore, 1956, 132 D.M.  
Band 22: *Elektronenemission. Gasentladungen II.* 337 figure;  
652 pag., in 8°; Springer editore, 1956; 128 D.M.

Su un soggetto come quello delle scariche elettriche nei gas molto è stato scritto e da molto tempo. Ciò nonostante le nostre conoscenze di questo fenomeno sono ancora imperfette e le spiegazioni che sappiamo darci dei suoi vari aspetti sono largamente insoddisfacenti.

I due volumi editi da Springer come Band 21 e Band 22 dell'*Handbuch der Physik* sul detto argomento riflettono questo stato di cose. Suddivisi in 9 capitoli il primo (Band 21) ed in 7 il secondo, raccolgono la parte più interessante di quell'enorme materiale che è stato raccolto da fisici di tutto il mondo in più di mezzo secolo di paziente lavoro; ed ampio spazio è lasciato alle teorie classiche su cui si sono basate le interpreta-

zioni dei vari fenomeni associati alle scariche nei gas. Cito — ad esempio le teorie di Townsend discusse nel capitolo « Ionization growth and breakdown » (Band 22), le teorie classiche della diffusione delle particelle cariche nel capitolo « Motion of Ions and Electrons » (Band 21) e teorie ed esperimenti riguardanti l'emissione termoionica nel capitolo « Thermoionic Emission » (Band 21).

Accanto a questa raccolta, completa e molto chiara, di fatti ed idee note, hanno trovato posto sia le questioni venute alla luce recentemente sia i dati aggiornati e perfezionati dagli ultimi progressi tecnici. Particolarmente interessanti le pagine relative alla microscopia ionica, la moderna interpretazione delle scintille, gli ultimi risultati nello studio della propagazione delle medesime in campi uniformi e non uniformi, in gas omogenei e non omogenei. Numerose tabelle di valori numerici delle varie costanti fisiche via via considerate sono aggiunte al testo.

CARLO FRANZINETTI

PROPRIETÀ LETTERARIA RISERVATA

Direttore responsabile: G. POLVANI

Tipografia Compositori - Bologna

Questo fascicolo è stato licenziato dai torchi il 10-IX-1958